
**MOLECULAR MECHANISMS OF THE
CTBP1-S/BARS-DEPENDENT
MEMBRANE FISSION PROCESSES
INVOLVED IN MEMBRANE
TRAFFICKING AND IN MITOSIS**

Lucia Laura Giordano

Dottorato in Scienze Biotechologiche – XXVII ciclo
Indirizzo Biotecnologie Industriali e Molecolari
Università di Napoli Federico II



Dottorato in Scienze Biotechologiche –XXVII ciclo
Indirizzo Biotecnologie Industriali e Molecolari
Università di Napoli Federico II



**MOLECULAR MECHANISMS OF THE
CTBP1-S/BARS-DEPENDENT
MEMBRANE FISSION PROCESSES
INVOLVED IN MEMBRANE
TRAFFICKING AND IN MITOSIS**

Lucia Laura Giordano

Dottorando: Lucia Laura Giordano

Relatore: Daniela Corda

Coordinatore: Prof.re Giovanni Sannia

Ai miei genitori.

*Soltanto l'ardente pazienza
porterà al raggiungimento
di una splendida felicità.
"Lentamente muore"
Pablo Neruda*

TABLE OF CONTENTS

Table of contents	pag. 1
List of figures/tables	pag. 5
Abbreviations	pag. 7
Riassunto	pag.11
Abstract	pag.19
CHAPTER 1:	pag.21
Introduction	pag.21
1.1 The Golgi complex	pag.21
1.1.1 The Golgi: discovery and structure.....	pag.21
1.1.2 The <i>trans</i> -Golgi network.....	pag.22
1.2 Membrane trafficking at the TGN	pag.23
1.3 Membrane fission	pag.26
1.3.1 The role of lipids.....	pag.27
1.3.1.1 The role of phosphatidic acid in membrane fission.....	pag.28
1.3.1.2 The role of DAG in membrane fission.....	pag.30
1.3.2 The role of proteins in membrane fission.....	pag.32
1.3.2.1 Protein kinase D.....	pag.32
1.3.2.2 CtBP1-S/BARS.....	pag.32
1.4 Structure and regulation of BARS	pag.34
1.5 The role of BARS in membrane fission	pag.37
1.5.1 PGC formation.....	pag.37
1.5.2 Macropynocytosis.....	pag.37
1.5.3 COPI-coated vesicle formation.....	pag.37
1.5.4 Fluid-phase endocytosis.....	pag.38
1.5.5 Golgi fragmentation during mitosis.....	pag.38
1.6 Golgi behaviour during mitosis	pag.39
1.7 The role of proteins in Golgi partitioning during mitosis	pag.42
1.7.1 GRASP65.....	pag.44
1.7.2 GRASP55.....	pag.45
1.7.3 BARS.....	pag.45
1.7.4 PKD.....	pag.46
CHAPTER 2	pag.47
Materials and methods	pag.47

2.1 Materials	pag.47
2.2 Solutions	pag.47
2.3 Subcloning and mutation of DNA	pag.47
2.3.1 Materials.....	pag.47
2.3.2 Solutions and media.....	pag.47
2.3.3 DNA agarose gels.....	pag.47
2.3.4 PCR amplification of DNA inserts.....	pag.48
2.3.5 Restriction and ligation.....	pag.48
2.3.6 DNA mutagenesis.....	pag.48
2.3.7 Transformation of bacteria.....	pag.48
2.3.8 Small-scale preparation of plasmid DNA (minipreps).....	pag.49
2.3.9 Large-scale preparation of plasmid DNA (maxipreps).....	pag.49
2.4 Expression and purification of recombinant proteins	pag.49
2.4.1 Solutions.....	pag.49
2.4.2 Expression and purification of GST-tagged proteins.....	pag.49
2.4.3 Expression and purification of His-tagged proteins.....	pag.49
2.5 General biochemical procedures	pag.49
2.5.1 Materials.....	pag.49
2.5.2 Solutions.....	pag.50
2.5.2.1 Assembly of polyacrylamide gel.....	pag.50
2.5.2.2 Evaluation of protein concentration.....	pag.50
2.5.2.3 Sample preparation and running.....	pag.50
2.5.3 Western blotting.....	pag.51
2.5.3.1 Protein transport onto nitrocellulose.....	pag.51
2.5.3.2 Probing the nitrocellulose with specific antibodies.....	pag.51
2.6 Cell culture	pag.51
2.6.1 Materials.....	pag.51
2.6.2 Cell growth conditions.....	pag.52
2.7 Immunoprecipitation and pull-down experiments	pag.52
2.7.1 Immunoprecipitation procedures.....	pag.52
2.7.1.1 Solutions.....	pag.52
2.7.1.2 Immunoprecipitation.....	pag.53
2.7.2 GST and His pull-down assay.....	pag.54
2.7.2.1 Solutions.....	pag.54
2.7.2.2 GST pull-down.....	pag.54

2.7.2.3 Histidine pull-down.....	pag.55
2.8 Cell transfection.....	pag.55
2.8.1 Plasmids, chemicals and recombinant proteins.....	pag.55
2.8.2 TransIT-LT1-Reagent based cell transfection.....	pag.56
2.8.3 Lipofectamine LTX-based cell transfection.....	pag.56
2.8.4 siRNA transfection.....	pag.56
2.8.4.1 Materials.....	pag.56
2.8.4.2 Procedure.....	pag.56
2.9 Cell infection with vesicular stomatitis virus.....	pag.57
2.9.1 Materials.....	pag.57
2.9.2 Procedure.....	pag.57
2.10 Electron Microscopy.....	pag.57
2.11 Transport assays.....	pag.57
2.11.1 VSVG transport from the TGN to the PM.....	pag.57
2.12 Drug treatments.....	pag.58
2.12.1 Ro3306 treatment.....	pag.58
2.12.2 CI-976 treatment.....	pag.58
2.13 LPAAT <i>in vitro</i> assays.....	pag.58
2.13.1 Materials	pag.58
2.13.2 LPAAT <i>in vitro</i> assays on BARS.....	pag.58
2.13.2.1 Solutions.....	pag.58
2.13.2.2 Preparation of oleoylLPA.....	pag.59
2.13.2.3 Procedure.....	pag.59
2.13.3 LPAAT δ <i>in vitro</i> assay.....	pag.59
2.13.3.1 Solutions.....	pag.59
2.13.3.2 Preparation of oleoylLPA.....	pag.59
2.13.3.3 Procedure.....	pag.59
2.14 Immunofluorescence.....	pag.60
2.14.1 Materials.....	pag.60
2.14.2 Solutions.....	pag.60
2.14.3 Sample preparation.....	pag.60
2.14.4 Light and immunofluorescence analysis.....	pag.61
2.14.5 Fluorescence lifetime imaging microscopy measurements.....	pag.61
2.15 Cell cycle synchronization.....	pag.61
2.15.1 Materials.....	pag.61

2.15.2 HeLa cell synchronization.....	pag.61
2.15.3 Preparation of mitotic and interphase extracts.....	pag.62
CHAPTER 3.....	pag.63
RESULTS	pag.63
3.1 Role of BARS in membrane trafficking.....	pag.63
3.1.1 Introduction.....	pag.63
3.1.2 Results (Pagliuso et al., Manuscript under revision).....	pag.64
3.1.2.1 BARS interacts with a Golgi localized protein, LPAAT δ	pag.64
3.1.2.2 <i>Escherichia coli</i> LPAAT binds to the fission-active BARS conformation and competes with LPAAT δ for BARS binding.....	pag.68
3.1.2.3 LPAAT δ is required for post-Golgi carrier fission.....	pag.70
3.1.2.4 The enzymatic activity of LPAAT δ is needed for post-Golgi carrier fission.....	pag.72
3.1.2.5 BARS activates LPAAT δ and this activation is required for carrier fission.....	pag.75
3.1.2.6 The BARS-LPAAT δ interaction occurs at the Golgi complex in live cells.....	pag.79
3.2 Role of BARS in mitosis.....	pag.82
3.2.1 Introduction.....	pag.82
3.2.2 Results.....	pag.82
CHAPTER 4.....	pag.87
DISCUSSION.....	pag.87
CHAPTER 5.....	pag.89
CONCLUSIONS.....	pag.89
REFERENCES.....	pag.91
AKNOWLEDGMENTS.....	pag.101
Appendix.....	pag.103

LIST OF FIGURES/TABLES

Figure 1.1 The structure of the Golgi apparatus	pag.22
Figure 1.2 Membrane trafficking at the TGN.....	pag.24
Figure 1.3 Two possible mechanisms of cargo export from the Golgi complex.....	pag.25
Figure 1.4 Schematic representation of the steps leading to the formation of intracellular transport carriers.....	pag.26
Figure 1.5 Lipid organisation at the fission site.....	pag.28
Figure 1.6 Pathways of glycerophospholipids biosynthesis.....	pag.30
Figure 1.7 Possible mechanisms regulating the levels of diacylglycerol (DAG) at theTGN.....	pag.31
Figure 1.8 The CtBP family proteins.....	pag.33
Figure 1.9 Structure of BARS.....	pag.35
Figure 1.10 CtBP1/BARS: mechanisms of its functional switch.....	pag.36
Figure 1.11 BARS-activated membrane fission in different pathways..	pag.38
Figure 1.12 Golgi fragmentation begins during the G2 phase of the cell cycle.....	pag.41
Figure 1.13 Golgi ribbon partitioning begins in G2, with the severing of the Golgi ribbon into isolated groups of stacks.....	pag.42
Figure 1.14 Model of mitotic Golgi cisternal unstacking.....	pag.43
Figure 1.15 Schematic representation of the GRASP65 sequence.....	pag.44
Figure 3.1 BARS interacts with the <i>trans</i> -Golgi localized LPAAT δ	pag.66
Figure 3.2 Localization of LPAAT β and LPAAT ϵ	pag.68
Figure 3.3 BARS binds <i>Escherichia coli</i> LPAAT in a conformation-dependent fashion.....	pag.69
Figure 3.4 LPAAT δ is required for the fission of basolaterally directed carriers.....	pag.71
Figure 3.5 LPAAT δ is a canonical LPAAT and its activity is required for post-Golgi carrier formation.....	pag.74
Figure 3.6 BARS activates LPAAT δ and this activation is required for post-Golgi carrier formation.....	pag.77
Figure 3.7 14-3-3 γ , but not other 14-3-3 isoforms, is required for	

LPAATδ activity.....	pag.78
Figure 3.8 BARS colocalizes with 14-3-3γ and PI4KIIIβ at the TGN and in carrier precursors, and interacts with LPAATδ at the Golgi.....	pag.80
Figure 3.9 BARS interacts with GRASP55 but not with GRASP65.....	pag.83
Figure 3.10 BARS localises at the Golgi complex in a PI4P dependent manner.....	pag.85

Tables:

Table 2.1 List of antibodies used in Western blot experiments.....	pag.52
Table 2.2 List of antibodies used in immunofluorescence experiments.	pag.61

ABBREVIATIONS

3D	Three-dimensional
aa	Aminoacids
acyl-CoA	Acyl-coenzyme A
ADP	Adenosine diphosphate
APS	Ammonium persulphate
ARF	ADP-ribosylation factor
ATP	Adenosine triphosphate
BFA	Brefeldin A
BSA	Bovine serum albumin
Cdk	Cyclin-dependent kinase
cDNA	Complementary DNA
CGN	<i>cis</i> -Golgi network
CFP	Cyan fluorescence protein
COP	Coat protein complex
COS	<i>Cercopithecus aethiops</i>
CtBP1-S/BARS	C-terminal binding protein1-short form /Brefeldin A- dependent ADP-ribosylation substrate
DAG	Diacylglycerol
DGK	Diacylglycerol kinase
DMEM	Dulbecco's modified Eagle's medium
DMSO	Dimethylsulfoxide
DTT	DL-dithiothreitol
EDTA	Ethylenediaminetetraacetic acid
EGTA	Ethylene glycolbis(beta-aminoethyl ether)-N,N,N',N'- tetraacetic acid
EM	Electron microscopy
ER	Endoplasmic reticulum
ERK	Extracellular regulated MAP kinase
FBS	Fetal bovine serum
FCS	Fetal calf serum
FITC	Fluorescein isothiocyanate

FL	Full lenght
GAP	GTP-ase activating protein
GAPDH	Glyceraldehyde-3-phosphate dehydrogenase
GDP	Guanosine diphosphate
GED	GTP-ase effector domain
GEF	Guanine nucleotide exchange factor
GFP	Green fluorescence protein
GRASP	Golgi ReAssembly Stacking
GST	Glutathione S-transferase
GTP	Guanosine triphosphate
h	Hours
HEPES	4-(2-Hydroxy-ethyl)-piperazine-1-ethane-sulfonic acid
IF	Immunofluorescence
IgGs	Immunoglobulins G
IPTG	Isopropyl-C-D-1-thiogalactopyranoside
LB	Luria-Bertani broth
LPA	Lysophosphatidic acid
LPAAT	Lysophosphatidic acid acyl-transferases
LPI	Lysophosphatidilinositol
MAPK	Mitogen-activated kinase
MAPKK	Mitogen-activated kinase kinase
MEK1	Mitogen-activated kinase kinase1
MEM	Minimum Essential Medium
MEFs	Mouse embryonic fibroblasts
min	Minutes
mM	Millimolar
NAD	Nicotinamide-adenine dinucleotide
NBD	Nucleotide-binding domain
NLS	Nuclear localization signal
O/N	Overnight
PA	Phosphatidic acid
Pak1	The p21-activated kinase
PBS	Phosphate buffered saline
pCoA	Palmitoyl-coenzyme ACoA

PCR	Polymerase chain reaction
PGC	Post-Golgi carrier
PKC	Protein kinase C
PKD	Protein kinase D
PH	Pleckstrin-homology
PI	Phosphatidyl-inositol
PI4K	Phosphoinositide-4 kinase
PLA ₂	Phospholipase A2
PLC	Phospholipase C
PLD	Phospholipase D
PM	Plasma membrane
RT	Room temperature
SBD	Substrate-binding domain
SD	Standard deviation
SDS	Sodium dodecyl sulphate
SDS-PAGE electrophoresis	Sodium dodecyl sulphate-polyacrylamide gel
shRNA	Short hairpin RNA
siRNAs	Short interference RNA
SUMO	Small ubiquitin-like modifier
TAE	Tris-acetate EDTA
TEMED	N,N,N',N'-tetramethylethylenediamine
TGN	<i>Trans</i> -Golgi network
Tris	Tris[Hydroxymethyl]aminomethane
Tween-20	Polyoxyethylenesorbitan monolaurate
ts	Temperature sensitive
v/v	Volume/volume
w/v	Weight/volume
VSV	Vesicular stomatitis virus
VSV-G	Vesicular stomatitis virus glycoprotein
YFP	Yellow fluorescence protein

Riassunto

L'argomento della mia tesi di dottorato è stato lo studio del ruolo funzionale della proteina CtBP1-S/BARS (C-terminal binding protein 1-short form/ brefeldin A ADP-ribosylation substrate; chiamata BARS per semplicità) nei processi di fissione delle membrane intracellulari. La fissione delle membrane è un processo richiesto sia durante la formazione delle vescicole di trasporto sia durante la divisione cellulare. Il complesso del Golgi rappresenta uno degli organelli cellulari con maggior numero di processi di fissione delle membrane ed è quindi usato come modello per studiare tale processo.

Il complesso di Golgi è stato scoperto nel 1898 dall'italiano Camillo Golgi mentre era alla ricerca di un metodo per colorare il tessuto nervoso, (Golgi C.1898). La sua reale esistenza è stata dibattuta per anni, fino agli anni '50 quando è stata introdotta la microscopia elettronica nella ricerca biologica, che ha risolto tale controversia (Dalton and Felix, 1954).

Il complesso di Golgi è un organello costituito da cisterne membranose appiattite impilate l'una sull'altra e connesse tra loro da tubuli. Funzionalmente può essere suddiviso in tre compartimenti principali: il cis, il medial e il trans (Farquar and Palade 1981). E' un organello essenziale per la biosintesi dei lipidi e per il processamento e lo smistamento di proteine; rappresenta, infatti, la stazione centrale lungo il pathway secretorio. Riceve proteine neo sintetizzate dal reticolo endoplasmatico (RE) e le ridistribuisce verso le loro destinazioni finali come ad esempio la membrana plasmatica, gli endosomi o i lisosomi, svolgendo quindi un ruolo centrale nel traffico intracellulare (Keller and Simons, 1997).

Il traffico intracellulare è quel processo per cui a partire da una membrana di un organello si formano, per fissione, vescicole che contengono proteine e/o lipidi (carga) diretti verso i compartimenti cellulari dove svolgeranno le loro funzioni. Il processo di fissione, nello specifico, è basato sulla formazione delle suddette vescicole di trasporto, contenenti cargo, a partire da una membrana appiattita, la quale va incontro a budding o gemmazione, elongazione, costrizione ed infine fissione con il rilascio delle vescicole di trasporto libere. La fissione delle membrane è quindi un processo cellulare fondamentale alla base sia del traffico intracellulare che della frammentazione delle membrane del Golgi in mitosi, uno step fondamentale per la regolazione del ciclo cellulare.

Nel laboratorio della Dr.ssa Daniela Corda, dove ho svolto il mio progetto di dottorato, è stato dimostrato il ruolo della proteina BARS in diversi processi di fissione cellulare, in particolare nella macropinocitosi (Liberali et al., 2008), nella pinocitosi, durante la formazione di vescicole di trasporto dal *trans*-Golgi network (TGN) dirette verso la membrana plasmatica basolaterale (chiamate post-Golgi carriers, PGCs; Bonazzi et al., 2005, Valente et al., 2012), durante la formazione di vescicole ricoperte di COPI dirette dal cis-Golgi verso il RE (Yang et al., 2005) ed infine nella ripartizione dell'apparato di Golgi tra le due cellule figlie durante la fase G2 del ciclo cellulare (Hidalgo Carcedo et al., 2004, Colanzi et al., 2007).

BARS appartiene alla famiglia delle C-terminal binding proteins (CtBPs).

Le CtBPs sono proteine aventi due funzioni ben definite: co-repressori della trascrizione nel nucleo, e regolatori della fissione delle membrane.

BARS infatti è coinvolta sia in processi di fissione, nel citoplasma, sia nell'espressione di geni coinvolti in apoptosi e nella trasformazione di cellule da

epiteliali a mesenchimali (Corda et al., 2006; Nardini et al., 2003; Chinnadurai, 2009; Grootclaes et al., 2003).

La fissione delle membrane è regolata da diversi meccanismi, molti dei quali sono stati ampiamente studiati e caratterizzati a livello molecolare.

Il meccanismo meglio studiato e caratterizzato è quello regolato dalla proteina dinamina, una GTPasi che si assembla nel sito di costrizione della vescicola durante la fase di gemmazione per poi, in seguito all'idrolisi del GTP subire un cambio conformazionale tale da indurre la fissione e il successivo rilascio della vescicola (Hinshaw et al., 2000).

Altri processi di fissione sono indotti dall'inserimento in membrana di porzioni idrofobiche di proteine contenenti α -eliche anfipatiche. L'inserimento di queste porzioni idrofobiche nel doppio strato lipidico induce una curvatura di membrana seguita da fissione. Esempi di proteine che agiscono attraverso questo meccanismo sono Arf1 e Sar1, proteine implicate nella fissione di vescicole di trasporto ricoperte da COPI e COPII, rispettivamente (Boucrot et al., 2012; Lee et al., 2005; Godi et al., 1999).

Il meccanismo di fissione regolato da BARS meglio caratterizzato a livello molecolare è quello richiesto durante la formazione di vescicole di trasporto dal TGN e dirette verso la membrana basolaterale, chiamate vescicole post-Golgi (post-Golgi carriers; PGCs) (Bonazzi et al., 2005, Valente et al., 2012).

Nel laboratorio della Dr.ssa Corda è stato identificato il complesso multiproteico in cui BARS agisce per indurre la fissione. Tale complesso comprende BARS e la phosphatidylinositol 4-chinasi tipo III β (PI4KIII β) legate tra di loro attraverso la proteina 14-3-3 γ . Questo complesso si assembla e disassembla dinamicamente sotto il controllo di altre due chinasi, PKD che fosforila PI4KIII β e PAK che fosforila BARS. Questi due eventi di fosforilazione stabilizzano la formazione di questo complesso, attivandolo durante la formazione dei PGCs sulle membrane del TGN (Valente et al. 2012). Questo complesso induce fissione delle membrane attraverso il reclutamento e l'attivazione di una classe di enzimi capace di modificare la composizione lipidica nel sito di fissione.

Durante il dottorato ho contribuito ad identificare una specifica classe di enzimi, aciltransferasi dell'acido lisofosfatidico (lysophosphatidic acid acyltransferase; LPAAT) come componente enzimatico essenziale del complesso proteico regolato da BARS per indurre la fissione delle membrane del TGN. La famiglia delle LPAAT comprende 11 isoforme (Yamashita et al., 2014; Shindou et al., 2013). Io ho contribuito a identificare l'isoforma delta come quella capace specificamente di legare BARS e di essere attivata enzimaticamente da BARS quando è in complesso con PI4KIII β e 14-3-3 γ .

LPAAT δ è un enzima capace di catalizzare l'incorporazione di un gruppo acilico dall'Acil-Coenzyme A (acilCoA) all'acido lisofosfatidico per formare acido fosfatidico (phosphatidic acid; PA). La sintesi di acido lisofosfatidico (LPA) nel lato citosolico del doppio strato lipidico delle membrane attraverso la sua forma a cuneo è stato proposto facilitare il processo di gemmazione/ tubulazione, viceversa, la sintesi di PA attraverso la sua forma conica, destabilizza tali tubuli promuovendone la loro fissione in vescicole di trasporto.

Durante il mio dottorato ho contribuito a studiare il ruolo funzionale dell'interazione tra BARS e la LPAAT δ nei processi di fissione delle membrane di Golgi regolate da BARS.

Nella prima parte della mia tesi riassumo i dati ottenuti sullo studio del legame, a livello molecolare, tra BARS e LPAAT δ e di come questo legame sia importante per

la formazione di vescicole di trasporto dirette specificamente verso la membrana basolaterale e non verso quella apicale. Nello specifico, l'attività enzimatica di LPAAT δ è importante nel processo di fissione. Infatti, l'inibizione della sua attività enzimatica genera lunghi tubuli che originano dalle membrane del TGN per gemmazione ma che sono incapaci di fissionare e generare vescicole di trasporto. BARS, nel complesso proteico in precedenza identificato (Valente et al., 2012) stimola l'attività enzimatica di LPAAT δ . Tale stimolazione induce un aumento della sintesi di PA a livello del TGN (dove tutto il complesso proteico localizza) promuovendo la fissione dei PGCs diretti verso la membrana basolaterale.

Nella seconda parte della mia tesi, mi focalizzo sulla fissione delle membrane del Golgi regolata da BARS in mitosi (Hidalgo Carcedo et al., 2004; Colanzi et al., 2007). La mitosi o divisione cellulare richiede un'accurata duplicazione e segregazione del contenuto cellulare, che include non solo il genoma, ma anche gli organelli intracellulari.

Nel laboratorio della Dr.ssa Corda è stato dimostrato come la corretta ripartizione dell'apparato di Golgi sia una fase cruciale nella divisione cellulare. La prima fase della frammentazione del Golgi avviene in G2 e prevede la rottura dei tubuli che tengono unite le diverse pile di cisterne (stacks) del Golgi tra di loro, in modo da generare stacks isolati dispersi nel citoplasma. Questo processo è necessario per la transizione dalla fase G2 alla fase M del ciclo cellulare ed è regolata dalla fissione delle membrane del Golgi mediato da BARS. L'inibizione di BARS causa un potente e prolungato blocco del ciclo cellulare in fase G2. Come BARS regola e coordina la transizione G2-M non è noto, per tale motivo l'identificazione molecolare del suo meccanismo d'azione è fondamentale per il controllo del ciclo cellulare.

Una delle caratteristiche principali delle cellule tumorali è la loro incontrollata proliferazione. Diversi sono gli agenti chemioterapici agenti sui processi regolatori della mitosi attualmente usati. Tuttavia per ovviare alla citotossicità e alla farmacoresistenza di alcuni di questi trattamenti è importante identificare nuovi possibili bersagli molecolari. L'identificazione di composti/ molecole capaci di modulare l'attività di BARS o di un suo interattore/i rilevante/i in fissione potrebbe essere usato per regolare la proliferazione delle cellule cancerose.

Tale approccio potrebbe quindi essere alla base di una nuova strategia antitumorale.

Ruolo di CtBP1-S/BARS nella fissione delle vescicole di trasporto dal Golgi verso la membrana basolaterale (PGCs).

Nel laboratorio della Dott.ssa Corda è stato precedentemente dimostrato che: a) le membrane di Golgi isolate da fegato di ratto contengono un'attività aciltransferasica capace di trasferire un gruppo acile dall'AcilCoenzima A all'acido lisofosfatidico (LPA) per generare acido fosfatidico (PA), tale attività è una aciltransferasi dell'acido lisofosfatidico (LPAAT) (Weigert et al., 1999); b) l'aggiunta della proteina BARS purificata a membrane di Golgi stimola sia la produzione di PA che la fissione delle membrane di Golgi (Weigert et al., 1999); c) i trattamenti che bloccano BARS in una conformazione dimerica, incapace di indurre la fissione delle membrane, inibiscono anche l'attività aciltransferasica (Weigert et al., 1999; Yang et al., 2005; Colanzi et al., 2013); e d) BARS purificata non è un' aciltransferasi bensì è associata ad un'attività aciltransferasica (Gallop et al., 2005).

Diversi laboratori hanno dimostrato il ruolo del PA in fissione e questi dati insieme ai nostri, sopra elencati, ci hanno portato ad analizzare una possibile interazione tra BARS e una LPAAT endogena capace di indurre fissione delle membrane.

Il genoma umano codifica per 11 diverse LPLAT (lysophospholipids acyltransferases), quattro delle quali sono state clonate e caratterizzate come LPAAT, cioè capaci specificamente di produrre PA a partire da LPA. Queste LPAAT sono; LPAAT α , β , γ e δ .

Nel laboratorio della Dott.ssa Corda è stato dimostrato che tra le 11 diverse LPLAT, le LPAAT γ , LPAAT δ e LPAAT η localizzano, almeno in parte, nel complesso di Golgi, il compartimento cellulare dove agisce il complesso molecolare di fissione regolato da BARS.

Partendo quindi da questi dati e con l'obiettivo di identificare una LPAAT che potesse essere coinvolta nella fissione delle membrane mediata da BARS, ho co-overespresso, in cellule COS7, BARS con ognuna di queste tre LPAAT (γ , δ e η) legate ad un tag flag (sequenza di riconoscimento). Attraverso approcci biochimici come ad esempio esperimenti di immunoprecipitazione ho dimostrato che BARS co-immunoprecipita con LPAAT γ e LPAAT δ e viceversa ma non con LPAAT η . Contemporaneamente, Brown ed i suoi colleghi hanno dimostrato che LPAAT γ localizza nel *cis*-Golgi ed è importante per il corretto mantenimento della struttura del Golgi. In seguito, il laboratorio della Dott.ssa Corda attraverso una collaborazione con quello del Dr. Victor Hsu (Harvard Medical School, Boston) ha dimostrato che la produzione di PA mediata da LPAAT γ promuove la fissione delle vescicole ricoperte di COPI dipendente da BARS.

Per quanto riguarda LPAAT δ , è stata dimostrata la sua attività LPAAT nel cervello, ma non è noto il suo ruolo funzionale nelle membrane di Golgi. Quindi, ho focalizzato i miei studi sull'interazione tra LPAAT δ e BARS e sul ruolo funzionale di tale interazione nelle membrane del Golgi, nello specifico durante la formazione dei PGCs.

Dal punto di vista strutturale BARS è simile alle D-hydroxyacid deidrogenasi (Nardini et al., 2005). Infatti, contiene un dominio di legame al NAD/H chiamato dominio di legame ai nucleotidi (Nucleotide binding domain; NBD) responsabile della conformazione di BARS; il legame a NBD del NAD/H induce una conformazione dimerica di BARS incompatibile con la sua attività di fissione (ma compatibile con quella trascrizionale). Al contrario, il legame a NBD di AcilCoA induce una conformazione monomerica compatibile con la sua attività di fissione (ma incompatibile con quella trascrizionale; Nardini et al., 2005; Liberali et al., 2008; Valente et al., 2013; Birts et al., 2013). Un altro importante ligando di BARS è BAC (brefeldin A ADP ribosilated conjugate), un metabolita della brefeldina A che blocca BARS nella sua forma dimerica e quindi inattiva in fissione (Colanzi et al., 2013). Quindi, con lo scopo di definire se LPAAT δ interagisce selettivamente con la forma monomerica di BARS attiva in fissione, ho analizzato attraverso esperimenti di co-immunoprecipitazione e di pull-down come questi cofattori di BARS ne influenzano la sua interazione con LPAAT δ . Ho dimostrato che il legame di BARS a BAC ed in particolare l'ADP ribosilazione di BARS, abolisce quasi completamente l'interazione tra BARS e LPAAT δ , indicando che BARS lega LPAAT δ nella sua forma monomerica attiva in fissione.

In seguito, ho analizzato il ruolo funzionale di questa interazione durante la formazione dei PGCs dipendente da BARS utilizzando un saggio ben caratterizzato nel laboratorio della Dott.ssa Corda. Tale saggio prevede l'utilizzo, come marker del traffico, di un mutante temperatura sensibile della glicoproteina del virus della

stomatite vescicolare (VSVG). Tale proteina dopo essere stata sintetizzata nel RE è trasportata nel Golgi e successivamente viene incorporata nei PGCs che dal TGN sono diretti verso la membrana basolaterale. Questi diversi steps di trasporto possono essere sincronizzati attraverso specifici blocchi di temperatura: la VSVG a 40°C è bloccata nel RE, a 20°C è bloccata nel TGN e a 32°C viene incorporata nei PGCs e diretta verso la membrana plasmatica (PM). Attraverso l'utilizzo della microscopia a fluorescenza tale traffico di VSVG all'interno della cellula può essere visualizzato e quantificato.

Con il fine di analizzare il ruolo di LPAAT δ nel traffico di PGCs diretti verso la PM (step di trasporto mediato da BARS) ho utilizzato diversi approcci.

Inizialmente ho inibito cronicamente LPAAT δ attraverso uno specifico pool di piccole sequenze di RNA (small interfering RNA; siRNAs) capace di inibire la sintesi proteica di LPAAT δ . Le cellule COS7 così deplete di LPAAT δ sono state sottoposte al traffico della VSVG. Ho dimostrato che la deplezione di LPAAT δ non ha effetto sul traffico di VSVG dal RE al Golgi, bensì nel traffico dal TGN verso la PM. Infatti la formazione dei PGCs è ridotta del 50% rispetto alle cellule controllo (contenenti livelli endogeni di LPAAT δ).

Inoltre, per determinare quale fase durante la formazione dei PGCs è regolata dall'attività di LPAAT δ (formazione o fissione delle vescicole di trasporto), abbiamo analizzato la formazione di questi PGCs mediante video-microscopia, in cellule che esprimono GFP-VSVG. In oltre il 30% delle cellule deplete per LPAAT δ si formano lunghe vescicole di trasporto di forma tubulari contenenti VSVG a partire dalle membrane di Golgi incapaci di andare incontro a fissione e quindi di generare PGCs diretti verso la PM. Questi risultati indicano che il processo di fissione dei PGCs, e non di formazione, è compromesso in cellule deplete per LPAAT δ .

Sulla base di questi dati ho successivamente analizzato se LPAAT δ , come BARS, è coinvolta solo nel trasporto basolaterale e non in quello apicale. Ho prima analizzato il ruolo di LPAAT δ nel trasporto di un cargo apicale (p75) e poi ho usato un altro cargo basolaterale, l' LDLr. Il trasporto di LDLr, ma non quello di p75, risente della deplezione di LPAAT δ indicando che questo enzima è coinvolto, come BARS, solo nel trasporto basolaterale e non in quello apicale.

In parallelo, la Dott.ssa Carmen Valente ha studiato l'attività enzimatica di LPAAT δ attraverso un saggio specifico per le aciltransferasi che prevede l'utilizzo di estratti cellulari, ed in particolare di surnatanti post-nucleari incubati con il [1-¹⁴C]-oleoil-CoA e l'oleoil-LPA al fine di seguire la formazione del di-oleoil [1-¹⁴C]-PA. Tale prodotto di reazione viene estratto e separato attraverso una cromatografia su strato sottile (TLC) e successivamente quantificato attraverso uno strumento capace di quantificare la radioattività, e quindi il prodotto PA, formato in ogni campione del saggio. L'attività specifica di LPAAT δ è stata determinata attraverso questo saggio utilizzando surnatanti post-nucleari preparati da cellule overesprimenti LPAAT δ , o deplete della LPAAT δ o overesprimenti un mutante cataliticamente inattivo della LPAAT δ (perché incapace di legare il substrato LPA). Estratti ottenuti a partire da cellule deplete per LPAAT δ con specifici siRNAs o trattati con specifici anticorpi contro LPAAT δ mostrano una riduzione dell'attività aciltrasferasica mentre estratti ottenuti dall'overespressione di LPAAT δ mostrano un aumento dell'attività aciltrasferasica, aumento che è completamente inibito dall' anticorpo specifico contro LPAAT δ .

Parallelamente, con lo scopo di capire se è l'attività catalitica di LPAAT δ importante per la formazione dei PGCs, la Dott.ssa Valente ha effettuato esperimenti di rescue utilizzando LPAAT δ^{wt} o un suo mutante LPAAT δ^{H96V} cataliticamente inattivo perché

incapace di legare il substrato LPA. Cellule deplete per LPAAT δ , e poi trasfettate in modo da indurre l'espressione o della LPAAT δ^{wt} o della LPAAT δ^{H96V} , mostrano che solo la proteina wild-type ripristina la formazione di PGCs ma non il mutante LPAAT δ^{H96V} cataliticamente inattivo. Questo esperimento indica che è l'attività catalitica di LPAAT δ , e non la proteina per sé, rilevante nella fissione dei PGCs.

La Dott.ssa Valente ha poi analizzato se BARS, legandosi a LPAAT δ , è capace di modularne la sua attività enzimatica, e se questa eventuale regolazione è coinvolta nella fissione dei PGCs. Sia la deplezione di BARS che la sua inibizione (attraverso un anticorpo specifico contro BARS) comportano una riduzione dell'attività enzimatica di LPAAT δ e parallelamente inibiscono la fissione dei PGCs. Risultati simili sono stati ottenuti anche bloccando BARS nella sua forma dimerica attraverso il suo legame a BAC indicando che è la forma monomerica di BARS, attiva in fissione, capace di legare e regolare l'attività catalitica di LPAAT δ . A conferma di questo, l'overespressione di mutanti di BARS inattivi in fissione risultano inibire l'attività enzimatica di LPAAT δ .

BARS, ha un ruolo in fissione in complesso con la 14-3-3 γ e con la PI4KIII β . Quindi, è stato analizzato anche il ruolo di queste due proteine nella regolazione dell'attività di LPAAT δ . La loro deplezione o la loro inibizione riducono l'attività di LPAAT δ , indicando che la formazione del complesso BARS-14-3-3 γ -PI4KIII β stabilizza BARS nella sua conformazione necessaria al legame con la LPAAT δ e quindi di conseguenza alla fissione attraverso l'attivazione dell' LPAAT δ e produzione di PA.

Gli effetti che BARS e LPAAT δ hanno sulla fissione dei PGCs che si formano a partire dalle membrane del Golgi ci hanno poi portato a pensare che la loro interazione avviene specificamente a livello di questo organello. Per confermare quindi questa idea abbiamo analizzato la localizzazione di BARS e degli altri componenti del suo complesso, LPAAT δ , 14-3-3 γ e PI4KIII β con tecniche di immunofluorescenza. Attraverso analisi con microscopia confocale abbiamo dimostrato che LPAAT δ , 14-3-3 γ e PI4KIII β localizzano con BARS nei tubuli che contengono VSVG e che si formano a partire dal TGN. Infine per dimostrare che l'interazione tra BARS e LPAAT δ si verifica nelle membrane di Golgi, ho utilizzato esperimenti di FRET che rivelano la presenza di due proteine a una distanza inferiore o uguale a 8nm, utilizzando CFP-LPAAT δ e BARS-YFP. Un segnale di FRET, indicatore della loro interazione, aumenta durante il trasporto di VSVG dal Golgi verso la PM confermando quindi l'idea che l'interazione tra LPAAT δ e BARS avviene sul Golgi durante la formazione dei PGCs.

Ruolo di CtBP1-S/BARS nella frammentazione del complesso di Golgi in mitosi.

Nei mammiferi l'apparato di Golgi è composto da 40-100 diverse pile di cisterne (stacks) connesse tra loro da tubuli membranosi, questo porta alla formazione del Golgi ribbon localizzato nella zona perinucleare della cellula (Dalton and Felix, 1954). Un aspetto interessante di questo organello è il suo meccanismo di ereditarietà durante la mitosi. Il Golgi in mitosi, infatti, va incontro ad una progressiva e reversibile riorganizzazione del ribbon. Il primo step di questa riorganizzazione è la fissione dei tubuli che interconnettono gli stacks al fine di raggiungere una corretta suddivisione delle membrane del Golgi tra le due cellule figlie. I meccanismi molecolari alla base di questo processo sono parzialmente conosciuti e alcune delle diverse molecole coinvolte sono state identificate. Tra queste la proteina BARS (Hidalgo Carcedo et al., 2004), le proteine strutturali di membrana GRASP65 (Sutterlin et al., 2002) e GRASP55 (Duran et al., 2008), le chinasi Raf, MEK1, Erk

(Acharya et al., 1998), PKD (Kienzle et al., 2012), Cdk1 e Plk1 (Sutterlin et al., 2002). Quale sia il meccanismo molecolare di BARS in mitosi non è noto. E' stato proposto che la sua fosforilazione può portare a reclutare proteine/ enzimi importanti per il processo di fissione. Meglio conosciuti in mitosi sono i meccanismi di GRASP65 e della proteina strutturalmente correlata GRASP55. Queste proteine sono importanti nella formazione e nel mantenimento dei tubuli che interconnettono gli stacks all'interno del Golgi ribbon. La fosforilazione di GRASP65 in mitosi ne impedisce la sua oligomerizzazione, necessaria per il linking delle membrane di Golgi (Wang et al., 2005; Wang et al., 2003). L'espressione della porzione C-terminale di GRASP65 incapace di essere fosforilata causa un ritardo nell'entrata in mitosi, dimostrando quindi l'importanza della fosforilazione di GRASP65 per la mitosi. Similmente è stato dimostrato che GRASP55 possiede numerosi siti che possono essere fosforilati da parte delle chinasi MEK e Erk, fosforilazioni richieste nel processo di frammentazione e quindi nella progressione mitotica (Duran et al., 2008). Le chinasi Raf, MEK, ed Erk sono state dimostrate essere coinvolte nella frammentazione mitotica del complesso di Golgi. In particolare, nella transizione G2/M del ciclo cellulare queste tre chinasi sono attivate in modo consequenziale. La deplezione di MEK1 (attraverso specifici siRNA) o la sua inibizione attraverso l'uso di specifici inibitori chimici causano un ritardo nell'entrata in mitosi (Acharya et al., 1998). Inoltre, recentemente è stato dimostrato che PKD, proteina appartenente alla famiglia delle serin/treonin chinasi è richiesta per l'entrata delle cellule in mitosi favorendo la rottura delle connessioni tra gli stacks nella fase G2 del ciclo cellulare attraverso l'attivazione sequenziale di Raf1, MEK e GRASP55 (Kienzle et al., 2012).

Nella seconda parte della mia tesi ho quindi analizzato il ruolo dei singoli componenti del complesso multiproteico di cui BARS fa parte (identificato durante la formazione dei PGCs) nella frammentazione del Golgi in mitosi.

Ho dimostrato, che la deplezione di 14-3-3 γ , PI4KIII β , LPAAT γ e LPAAT δ porta al blocco dell'entrata delle cellule in mitosi regolata da BARS.

Inoltre, attraverso approcci biochimici, ho analizzato l'eventuale interazione tra BARS e GRASP65 e/o GRASP55 in Interfase e in cellule sincronizzate in fase G2 e fase M del ciclo cellulare. Ho dimostrando che BARS interagisce con GRASP55 ma non con GRASP65. Successivamente, attraverso esperimenti di immunofluorescenza ho dimostrato che la localizzazione di BARS sulle membrane di Golgi non dipende da GRASP55 o da GRASP65 bensì da PKD (chinasi responsabile dell'attivazione di GRASP55). Infatti, in cellule deplete di GRASP55 o di GRASP65, BARS localizza nel Golgi come in cellule controllo, mentre in cellule deplete di PKD, BARS si ridistribuisce in parte dal Golgi al citosol.

Questi dati preliminari suggeriscono che BARS, in mitosi, è coinvolta nel pathway che porta all'attivazione di GRASP55.

Studi futuri sull'identificazione del meccanismo molecolare di BARS nella regolazione della divisione dell'apparato di Golgi tra le due cellule figlie in mitosi e quindi l'entrata delle cellule in mitosi saranno fondamentali per le importanti conseguenze fisiologiche e farmacologiche. Infatti, la sintesi di composti chimici in grado di modulare l'attività di BARS o di un suo interattore/i rilevante/i in fissione durante la mitosi potrebbe essere usato per regolare la proliferazione delle cellule cancerose (caratterizzate da una incontrollata proliferazione cellulare).

Tale approccio potrebbe quindi essere alla base di una nuova strategia antitumorale.

Abstract

This thesis is focused on the role of CtBP1-S/BARS (C-terminal binding protein 1-short form/ brefeldin A ADP-ribosylation substrate; BARS), in membrane fission, a process that is involved in both intracellular membrane trafficking and Golgi partitioning during mitosis.

The Golgi complex is the organelle that was initially described in 1898 by the Italian Camillo Golgi, although the real existence of this organelle was debated for decades, until the introduction of electron microscopy in the 1950s, which solved the controversy. Nowadays, it is well known that the Golgi complex is a cell organelle that is involved in many cellular functions, such as intracellular trafficking, post-translational modification of proteins and lipids, cell partitioning during mitosis, and membrane curvature and fission.

Golgi membrane curvature and the membrane fission that follows is integral to many cell functions, such as membrane trafficking and cell partitioning. They are required for the formation of intracellular transport carriers, and are controlled by cooperative contributions of both lipids and proteins. Membrane fission appears to rely on multiple mechanisms, and many of these are mediated by BARS.

BARS is a dual-function protein that acts as a co-repressor of transcription in the nucleus and as a regulator of membrane fission in the cytoplasm. In our laboratory, it has been demonstrated that BARS is required in the following processes: macropinocytosis, fluid-phase endocytosis, membrane transport from the trans-Golgi network (TGN) to the basolateral plasma membrane (PM), COPI vesicle formation, and Golgi partitioning that occurs during the G2 phase of the cell cycle (a step that controls cell entry into mitosis).

In the first part of my project, I focused my studies on the fission-inducing property of BARS that is required during the formation of basolaterally directed post-Golgi carriers. Here, the fission-driving property of BARS is associated with a lysophosphatidic acid acyltransferase (LPAAT) activity. I have shown that BARS specifically binds LPAAT δ , a Golgi-resident enzyme that our laboratory has characterised as an LPAAT enzyme that can incorporate acyl-coenzyme A (acylCoA) into lysophosphatidic acid (LPA), to form phosphatidic acid (PA). This LPAAT δ activity is required at the fission step during post-Golgi carrier formation, as shown by long tubular carrier precursors that emanate from the Golgi mass but cannot undergo fission under LPAAT δ inhibition.

In the second part of my project, I focused on the fission-inducing property of BARS in Golgi partitioning during mitosis. Mitosis, or cell division, requires accurate duplication and segregation of the cell contents, which includes not only the genome, but also the intracellular organelles. Correct inheritance of the Golgi complex is crucial for cell division. The Golgi complex is composed of individual stacks of cisternae that are laterally connected by tubules, and the cleavage of these tubules in G2 phase leads to the break-up of the Golgi ribbon into separate stacks. Treatments that block the fission-inducing activity of BARS inhibit the cleavage of these tubules, which results in potent and prolonged cell-cycle block in G2 phase.

With the aim to better understand and define the molecular mechanisms underlying this BARS-mediated Golgi-ribbon unlinking process, I analysed: (i) the role of the LPAAT δ enzyme, a BARS interactor, in this process; and (ii) whether the BARS-driven fission machinery interface with the other well-known signalling pathways is required for Golgi fragmentation in mitosis.

CHAPTER 1

INTRODUCTION

1.1 The Golgi complex

1.1.1 The Golgi: discovery and structure

In 1898, at the Medico-Surgical Society of Pavia, Camillo Golgi announced the discovery of a new cell organelle, now known as the 'Golgi apparatus' or the 'Golgi complex', or simply, 'the Golgi'. He defined this organelle as an "internal reticular apparatus", which was based on its 'net-like' structure and intracellular location. In 1873, he developed the so-called "*reazione nera*" or 'black reaction', based on the use of silver nitrate to stain the nervous tissue and allowed the view of the Golgi, which he defined as a "fine and elegant reticulum within the cell body" (Figure 1.1, A) (Golgi, 1898). After that, it became clear that this new structure was present in a variety of cell types and not only in nervous tissue cells. However, the existence of the Golgi as an organ was debated for decades, until the controversy was finally resolved by the introduction of electron microscopy (EM) in 1954, when the Golgi complex became accepted as a cell organelle (Dalton and Felix, 1954).

Nowadays, it is well known that the Golgi complex performs essential functions for growth, homeostasis and division of eukaryotic cells. It is the central station along the secretory pathway, and as such, it receives proteins and lipids synthesised in the endoplasmic reticulum (ER) and redistributes them to their final destinations, such as lysosomes, endosomes or the plasma membrane (PM). The Golgi complex is also important for post-translational modifications, and in particular, the glycosylation of proteins and lipids, as they move through the secretory pathway; indeed the Golgi has been defined as a 'carbohydrate factory' (Farquhar and Palade, 1981).

In addition, the Golgi recycles selected components back to the ER. The Golgi thus serves both as a processing station for newly synthesised glycoproteins and glycolipids derived from the ER, and as a filtering system, to separate proteins and lipids destined to the PM from those retained in the ER. In mammalian cells, the Golgi is typically located around the centrosome, where it remains due to a microtubule (MT)-dependent mechanism. The Golgi complex undergoes fragmentation when MTs are depolymerised by specific drugs (e.g., nocodazole). Schematically, the Golgi consists of flat cisternae that are grouped into several stacks (the 'compact zones') that are interconnected by tubular networks (the 'non-compact zones'), which together form a continuous membranous ribbon (the 'Golgi ribbon'; Figure 1.1, B) that is collected into the pericentriolar space.

The Golgi is composed of three main compartments: the *cis*-, medial and *trans*-Golgi (Mellman and Simons, 1992). At the *cis*-side of the Golgi stacks, there is a tubular network that is known as the *cis*-Golgi network (CGN), which is composed of branching tubules that are connected with the *cis*-most cisterna. The CGN is followed by the stack of flat cisternae. Finally, at the *trans*-side of the stacks, there is another structure that appears as a network of branching tubules, the *trans*-Golgi network (TGN). Newly synthesised membrane and secretory proteins coming from the ER enter the Golgi through the *cis*-face, traverse across the stack, and leave via the *trans*-face. The reticulum of tubules that emanate from the *trans*-most cisterna, which are collectively referred to as the TGN, reflects the actual sites of exit (Figure 1.1, C).

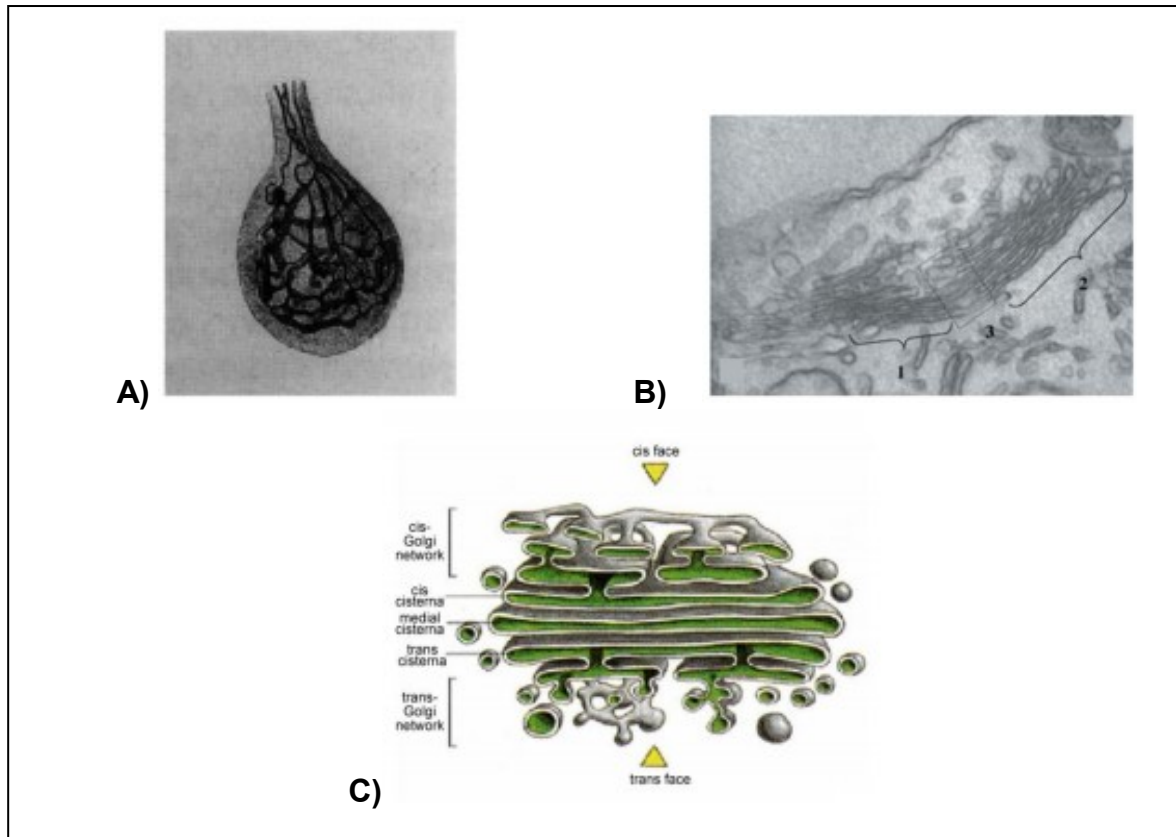


Figure 1.1. The structure of the Golgi apparatus.

A. Camillo Golgi's historical image of the "*apparato reticolare interno*" of a Purkinje cell [taken from (Golgi, 1898)]. **B.** Micrograph from NRK cells illustrating a Golgi ribbon portion that is comprised of two stacks (1, 2) connected through a non-compact zone (3) (taken from Polishchuk, 2004). **C.** Schematic representation of a polarised Golgi stack and its sub-compartments (modified from Alberts et al., 2007).

1.1.2 The trans-Golgi network

The TGN is the main sorting station along the secretory pathway, it receives the proteins that are processed within the Golgi complex, and it is responsible for their sorting into specialised carriers that derive from the TGN membranes, and for their delivery to their final destinations (Figure 1.1, C). In this specific compartment, the terminal glycosylation of proteins takes place, and the cargo are also packaged into membrane carriers that are directed to the PM or to the endosomes or lysosomes. The TGN has been considered to be the *trans*-most cisterna of the Golgi, which was also seen to continue into a large tubular network (Griffiths et al., 1989; Clermont et al., 1995). In contrast, some reports have considered the TGN as an independent organelle (Geuze and Morre, 1991; Reaves and Banting, 1992). Indeed, in some cell types, the tubulated TGN is positioned at some distance from the *trans* aspect of the Golgi ribbon.

Analyses in different mammalian cell types have revealed that the TGN can be different in both size and composition (Clermont et al., 1995). Indeed, the morphology and the size of the TGN depends on the type and amount of cargo proteins that depart from the Golgi complex. This indicates that the structure of the

TGN varies from one cell type to another, and that the TGN is not a static compartment of the Golgi, but is constantly undergoing renewal.

1.2 Membrane trafficking at the TGN

Membrane trafficking is the process by which specific compartments and their protein contents (the 'cargo') move between and within the intracellular sub-compartments. This intracellular process involves three main pathways:

- (i) The biosynthetic pathway, by which newly synthesised proteins (with the concurrent movement of membrane lipids) destined for secretion are transported from the ER to their final destinations (e.g., the PM, endosomes). This pathway can be further subdivided into three steps: ER-to-Golgi transport; intra-Golgi transport; and TGN-to-PM transport (Lippincott-Schwartz et al., 2001).
- (ii) The endocytic pathway, by which fluid-phase solutes and membrane-bound proteins are internalised within membrane-bounded carriers from the extracellular environment (Cossart and Sansonetti, 2004; Mellman et al., 1996; Pelkmans and Helenius, 2003).
- (iii) The retrograde transport pathway, by which viruses and bacteria enter cells, and also for the retrieval of various proteins and lipids to the organelles involved in the secretory pathway (Cossart et al., 2004; Pelkmans and Helenius, 2003) (Figure 1.2).

The main traffic carriers that operate in these different trafficking pathways can be classified into two groups: small round vesicles, and large pleiomorphic carriers (LPCs). The first class comprises COPI, COPII and clathrin-dependent vesicles (which indicates their protein coat), and they are characterised by a regular spherical shape and a diameter of <100 nm (Rothman JE, 2002). LPCs are much larger and are more variable in shape than vesicles, whereby the smallest LPCs usually have a size of 300 nm to 400 nm, while some of the largest ones can reach several microns in length. Many of these carriers appear globular, but they can also be tubular in shape during their translocation through the cytosol. Thus LPCs are frequently termed as 'pleiomorphic' structures.

Among the LPCs, the best characterised are those that are involved in TGN-to-PM transport, and are thus known as post-Golgi carriers (PGCs). The life cycle of these PGCs can be schematised in three stages: (1) their formation; (2) their transition through the cytosol; and (3) their docking and fusion with the PM (Polishchuk et al., 2000). The most critical issue regarding PGCs is their formation. The common belief was that they result from the budding and release of many small vesicles that then undergo homotypic fusion to form large PGCs (Bannykh et al., 1997). However, more recently it has become clear that they emerge *en bloc* from a donor membrane, potentially through the aid of a pulling force that is supplied by microtubule-based motors (Polishchuk et al., 2003) (Figure 1.3).

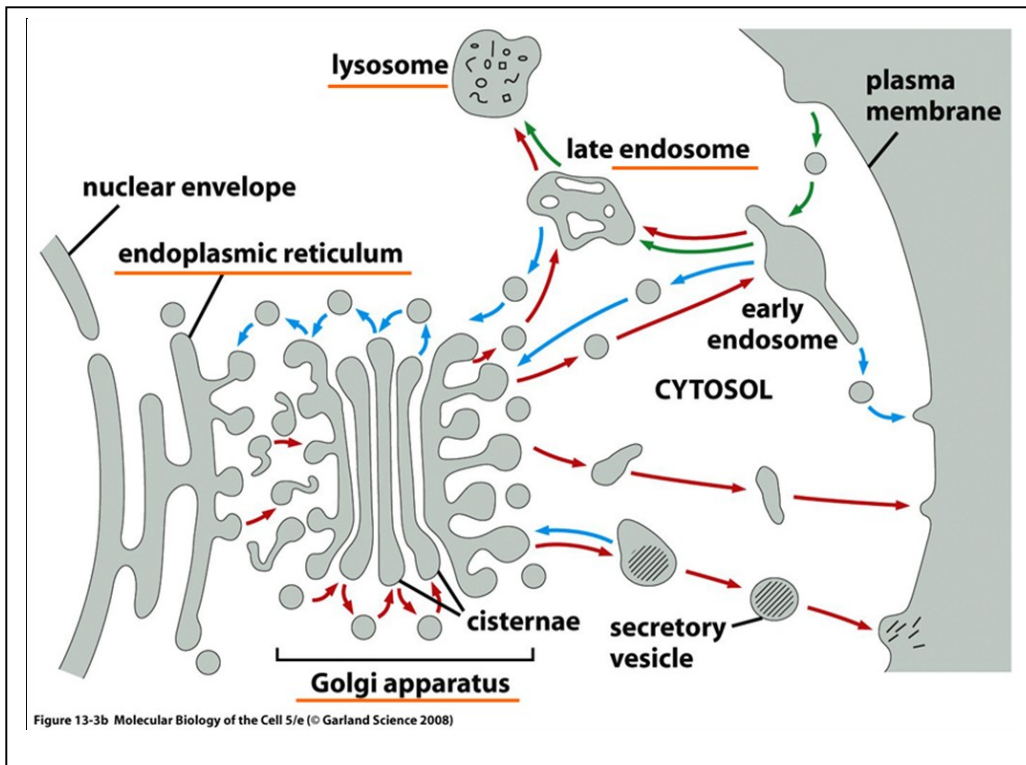


Figure 1.2 Membrane trafficking at the TGN.

The major organelles involved in intracellular membrane trafficking are represented. Red and blue arrows, membrane movement along the biosynthetic-secretory pathway, for anterograde and retrograde transport, respectively; green arrows, membrane movements along the endocytic pathway (modified from Alberts et al. 2007).

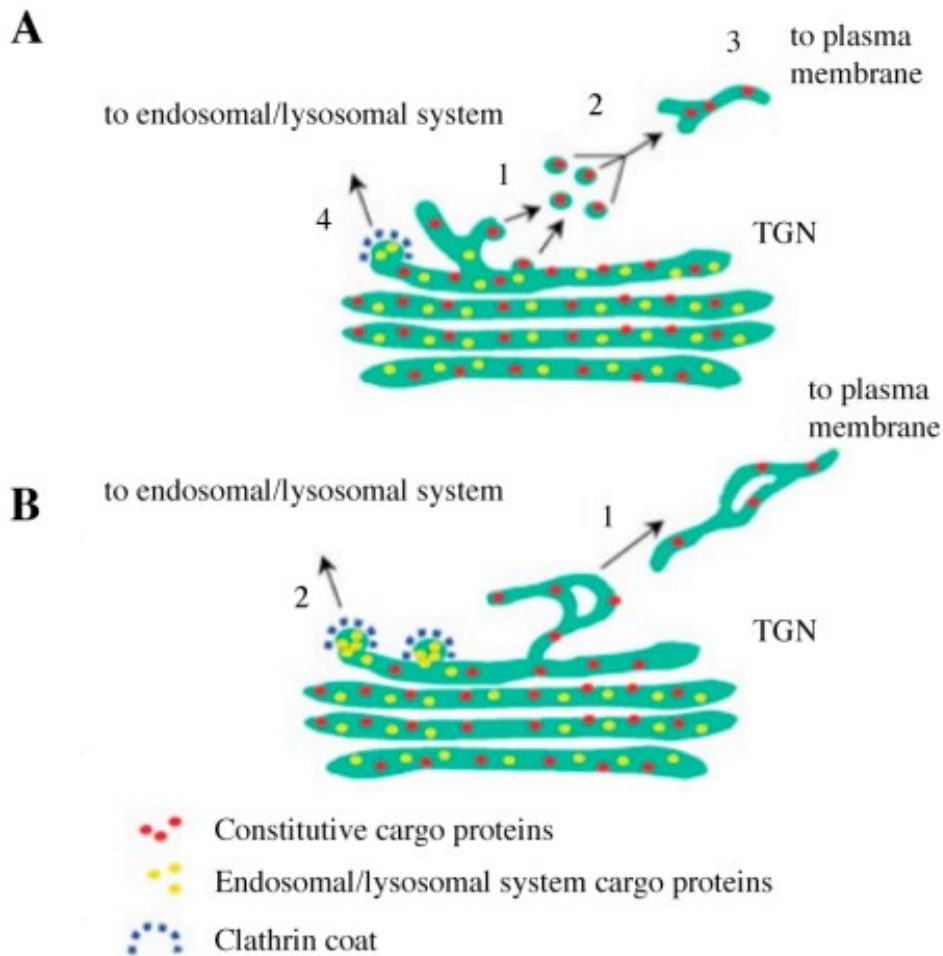


Figure 1.3 Two possible mechanisms of cargo export from the Golgi complex.

A. Constitutive cargo proteins exit the TGN within small vesicles (1), which undergo homotypic fusion (2) into large cargo containers (3), which can then move off to the plasma membrane. Cargo directed to the endosomal-lysosomal system is sorted at the TGN into clathrin-coated domains and carriers (4). **B.** Constitutive cargo proteins remain in the bulk of the TGN membranes, and then exit from the Golgi through the fission of complex tubular-reticular domains from the rest of the TGN (1). Cargo directed to the endosomal-lysosomal system is again sorted at the TGN into clathrin-coated domains and carriers (2) (modified from Polishchuk et al., 2004).

1.3 Membrane fission

Membrane fission is an essential cellular process by which one membrane divides into two separate ones. It is required for the formation of transport vesicles during membrane traffic, organelle partitioning, and cell division (Corda et al., 2002; McNiven and Thompson, 2006). Fission of the membranes of the PM generates endocytic vesicles, which transport proteins from the outside medium into the cell cytoplasm (Schmid et al., 1997), while fission of ER or Golgi membranes leads to the production of carriers for intracellular transport between these organelles, or directed to the PM. (Griffiths et al., 2000; Lippincott-Schwartz et al., 2001; Mironov et al., 1997).

Membrane curvature followed by membrane fission are the essential steps in the formation of all of these transport carriers (Corda et al., 2002) (Figure 1.4). These require local distortion and remodelling of the lipid bilayer to create a separate membrane-bound compartment, without compromising the integrity of the maternal bilayer. The evolution of the initial intact bilayer into two separate membranes must proceed via a pathway of intermediate structures (Kozlovsky and Kozlov, 2003). This requires both deformation of the membrane monolayers and their transient disruption. The deformation is necessary at the early stages of the process, where the membrane site adopts a typical neck-like shape, and then at the later stages of the formation of the non-bilayer intermediates. The perturbation of membrane integrity is an extremely thermodynamically unfavourable event, and thus it most probably accompanies the transition from one intermediate structure to another. The forces required to drive membrane fission are provided by the protein machinery within the cell, and by the lipid composition of the membranes (Chernomordik and Kozlov, 2003; Kozlovsky and Kozlov, 2003).

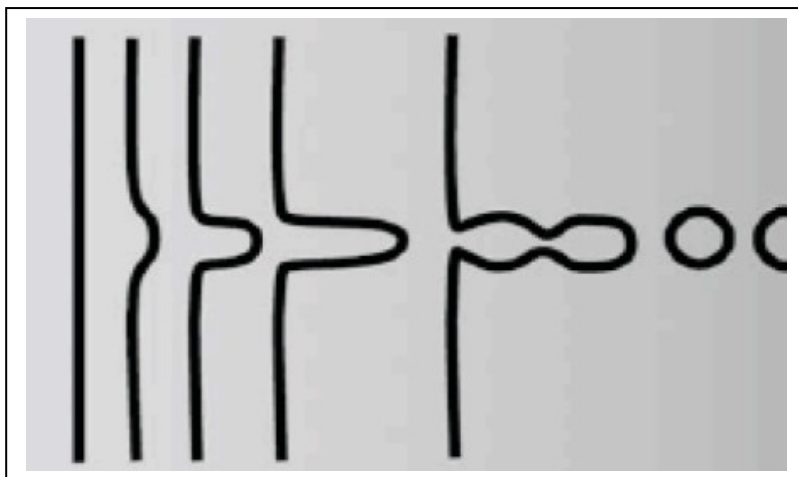


Figure 1.4 Schematic representations of the steps leading to the formation of intracellular transport carriers.

Buds can be generated from flat membranes, which can then be elongated into tubules, and subsequently undergo constriction and fission (from Corda et al., 2002).

1.3.1 The role of lipids

Lipids are both structural components of the membrane bilayer and also signalling molecules and protein cofactors, the actions of which are exerted in different cell compartments. In the secretory pathway, phospholipids represent most of the lipids that are synthesised at the ER, and these are then transported to their final destinations via the Golgi complex (De Matteis et al., 2002; Kent and Carman, 1999). The lipid composition of cell membranes is not homogeneous, and this heterogeneity can affect the shape and geometry of the bilayer, which will be involved in protein segregation and sorting, as well as in membrane fission (Burger et al., 2000; Chernomordik et al., 1995). Moreover, the bilayer is characterised by an asymmetry in lipid composition between the internal and external leaflets that can also have a role in fission.

Biological lipids can be classified in three main groups based on their molecular shapes and structures: cylindrical (phosphatidylcholine [PC] or other phospholipids), conical (or type II; diacylglycerol [DAG], cholesterol), or inverted cones (or type I; lysophospholipids) (Figure 1.5, A). When the cytoplasmic leaflet is enriched in cone-shaped lipids or the luminal/ external leaflet is enriched in inverted-cone lipids, the bilayer acquires negative spontaneous curvature. On the other hand, when the cytoplasmic monolayer is enriched in inverted-cone-shaped lipids or the luminal external monolayer is enriched in cone-shaped lipids, the membrane acquires positive spontaneous curvature (Chernomordik and Zimmerberg, 1995; Corda et al., 2002). For a flat bilayer, most of the lipids will be cylindrical, as this conformation allows optimal packing and minimises the free energy. If non-bilayer lipids are introduced into a flat bilayer, some deformation is expected, which will generate a bending moment and lead to curvature in the bilayer (Figure 1.5, B).

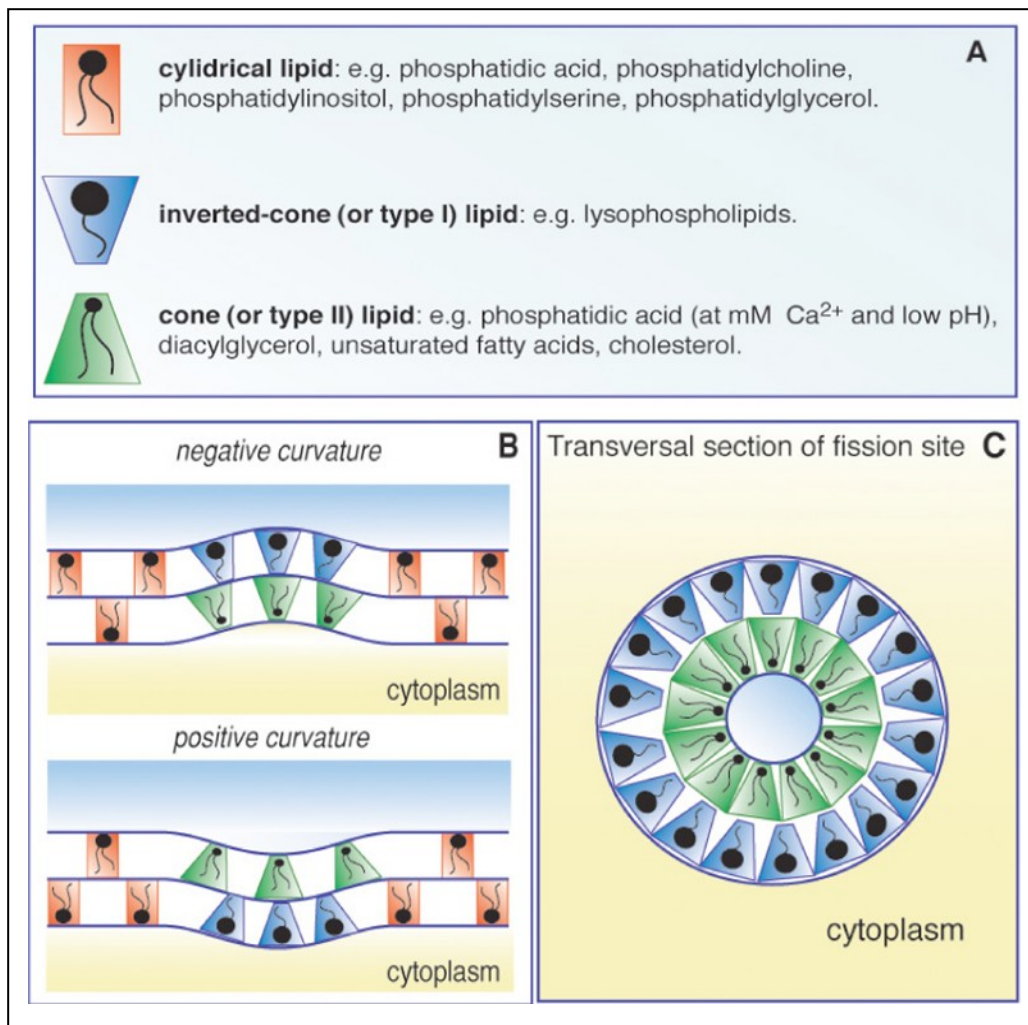


Figure 1.5 Lipid organisation at the fission site.

A. Schematic representation of the three classes of lipids. Examples of biologically relevant lipids classified on the basis of their molecular shapes. **B.** Schematic representation of spontaneous membrane curvature and bending. When the cytoplasmic leaflet is enriched in cone-shaped lipids and/ or the lumenal/ external leaflet is enriched in inverted-cone lipids, the bilayer acquires negative spontaneous curvature and bends towards the organelle lumen or the extracellular space. Conversely, when the cytoplasmic leaflet is enriched in inverted-cone lipids and/ or the lumenal/ external leaflet is enriched in cone-shaped lipids, the membrane acquires positive spontaneous curvature and bends towards the cytoplasm. **C.** Transverse section of the fission site. In transverse section, the geometry of the fission site shows positive curvature that better accommodates cone-shaped lipids in the lumenal/ external layer and inverted-cone lipids in the cytoplasmic layer (from Corda et al., 2002).

1.3.1.1 The role of phosphatidic acid in membrane fission

Phosphatidic acid is an important lipid in membrane fission. It only consists of two acyl chains, a phosphate, and glycerol. PA can bind to different proteins, and it is involved in several cellular processes (Tigyi and Parrill, 2003; Testerink and Munnik, 2005). PA is a cone-shaped lipid that can induce negative spontaneous curvature,

and its lipid headgroup charge is important in the molecular shape of PA, but also influences interactions with other lipids and PA-binding proteins. PA is involved in membrane fission because it allows interactions of a membrane-destabilising protein with the membrane and can facilitate membrane bending.

There are three alternative biosynthetic pathways that can lead to the formation of PA: (i) phosphorylation of DAG by DAG-kinase; (ii) hydrolysis of phospholipids by phospholipase D (PLD); and (iii) acylation of lyso-PA (LPA) by LPA-acyltransferases (LPAATs). PA can be also formed by the sequential action of phospholipase C (PLC), which forms DAG, and DAG kinase (DGK), which converts DAG to PA. Moreover, PA can be dephosphorylated by PA-phosphatases, to form DAG (Corda et al., 2002). PA and DAG have been shown to be in dynamic equilibrium, and this mechanism can affect the composition and curvature of both of the leaflets of the bilayer (Brindley and Waggoner, 1998). PA is also formed by the breakdown of other phospholipids, and in particular by the activity of phosphatidylcholine (PC)-specific phospholipase D (PLD). It has been reported that PLD-induced increases in PA levels can stimulate the release of transport carriers from both the TGN and the *cis*-Golgi (Chen et al., 1997; Ktistakis et al., 1996; Yang et al., 2008). Conversely, when the activity of PLD is inhibited by primary alcohols (e.g., 1-butanol), the intracellular PA levels are reduced and the release of carriers is inhibited (Siddhanta et al., 2000; Yang et al., 2008).

As mentioned above, LPA can be converted to PA by LPAATs (Figure 1.6). PA is a central phospholipid because it can be metabolised into DAG, then converted into triacylglycerol, phosphatidylcholine and phosphatidylethanolamine, and some of these are finally changed into phosphatidylserine (Figure 1.6). The other glycerol derivative is cytidine diphosphate DAG, which is modified to form PtdIns, phosphatidylglycerol, cardiolipin or phosphatidylserine (Figure 1.6).

There is evidence that LPAATs are involved in membrane trafficking events, because the small-molecule antagonist 2,2-methyl-N-(2,4,6-trimethoxyphenyl)dodecanamide (CI-976) was shown to inhibit a Golgi-associated LPAAT activity (Chambers et al., 2004; Drecktrah et al., 2003). LPAAT inhibition by CI-976 induces Golgi membrane tubulation, and this in turn results in enhanced retrograde trafficking to the ER (Chambers et al., 2004). The tubulation effect on Golgi membranes after CI-976 treatment might be explained by the inhibition of an unidentified LPAAT, the activity of which contributes to vesicle fission through the production of negative curvature, via local PA production (or secondarily, DAG).

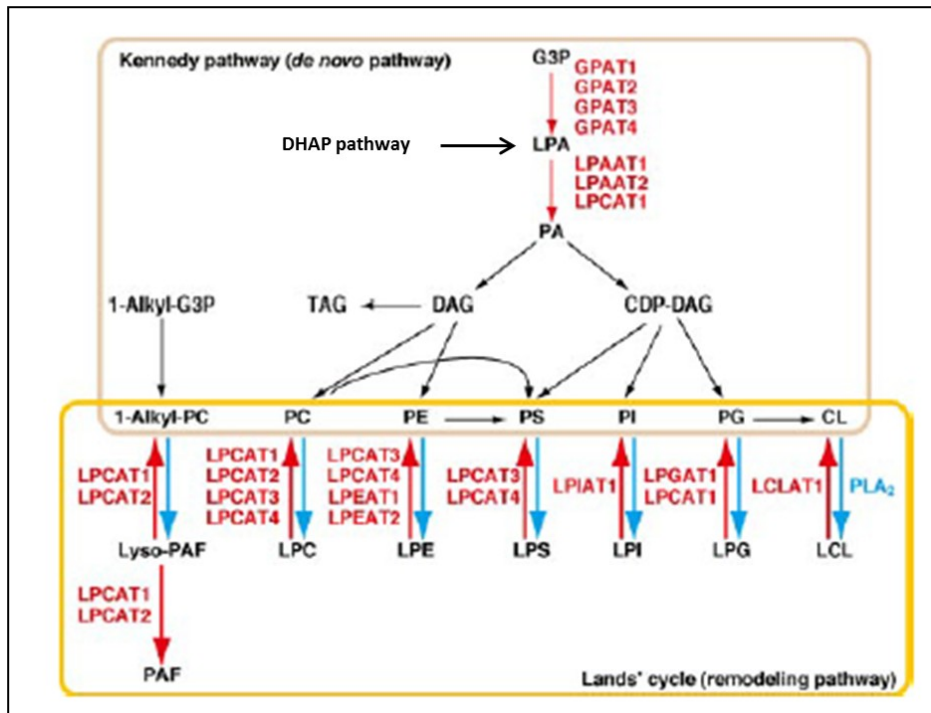


Figure 1.6 Pathways of glycerophospholipid biosynthesis.

Glycerophospholipids are first synthesised through the *de-novo* pathway (the Kennedy pathway), and then modified through the remodelling pathway (Lands' cycle). Red and blue arrows, acyltransferases and PLA₂s, respectively. G3P, glycerol 3-phosphate; LPC, LPE, LPS, LPI, LPG, and LCL, lyso-PC, lyso-PE, lyso-PS, lyso-PI, lyso-PG, and lyso-CL, respectively; CDP-DAG, cytidine diphospho-DAG (modified from Shindou and Shimizu, 2009).

1.3.1.2 The role of diacylglycerol in membrane fission

Diacylglycerol is also involved in the regulation of membrane fission processes. It is a conical lipid that can induce negative membrane curvature (Goni and Alonso, 1999; Burger et al., 2000; Shemesh et al., 2003). The enzymes that lead to the production of DAG are located on the cytoplasmic face of the cell membranes, so the accumulation of DAG bends the membrane towards the lumen. The generation of a DAG-enriched domain in the outer leaflet of the TGN might be the relevant event in PGC formation.

Diacylglycerol can be produced at the TGN by three possible mechanisms: (i) from PC by sphingomyelin synthase, which transfers PC to ceramide, to produce sphingomyelin and release DAG (Ichikawa and Hirabayashi, 1998); (ii) from PtdIns4P or phosphatidylinositol 4,5-bisphosphate (PtdIns4,5P₂), that can be converted into DAG and inositol bisphosphate or trisphosphate via a phosphoinositide-specific phospholipase C (PI-PLC) (Rhee et al., 2001) and; (iii) from phospholipase D (PLD) which converts PC into PA, then dephosphorylated by lipid phosphate phosphatase (LPP), thus generating DAG (Brindley and Waggoner, 1998; Pyne et al., 2004). (Figure 1.7).

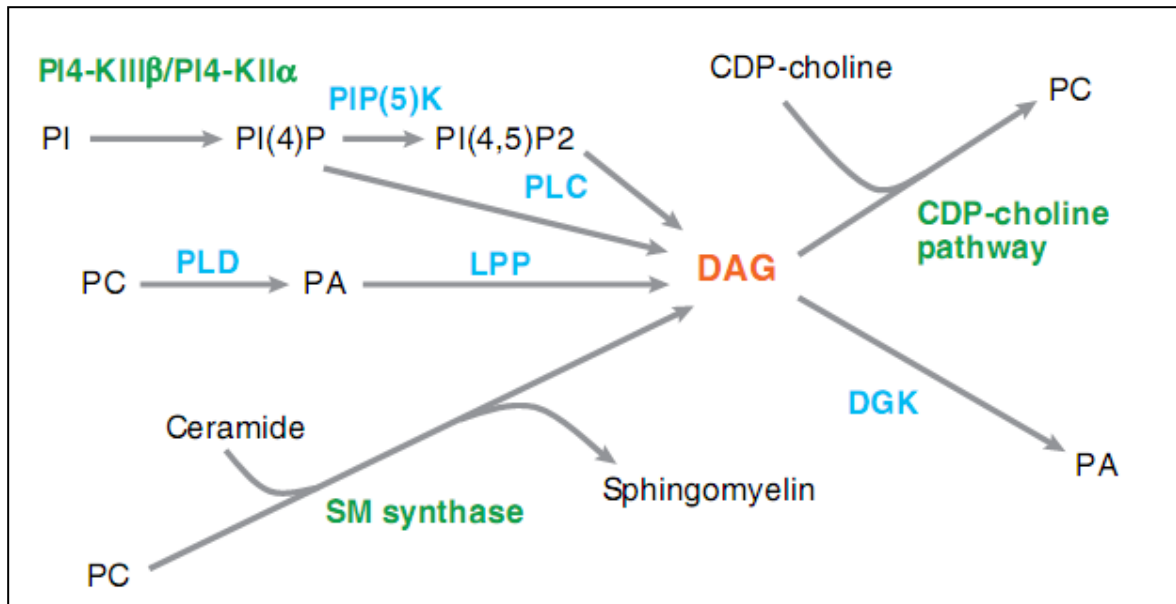


Figure 1.7 Possible mechanisms regulating the levels of diacylglycerol (DAG) at the TGN.

Diacylglycerol is generated transiently in biological membranes. The possible sources of DAG at the TGN are shown. The enzymes thus far localised to the Golgi membranes are shown in green. Other enzymes that have roles in DAG metabolism and for which the Golgi localisation is controversial are shown in blue. DGK, DAG kinase; LPP, lipid phosphate phosphatase; PA, phosphatidic acid; PC, phosphatidylcholine; PI, phosphatidylinositol; PI(4)P, phosphatidylinositol 4-phosphate; PIP5-K, phosphatidylinositol 4-phosphate 5-kinase; PI(4,5)P2, phosphatidylinositol 4,5-bisphosphate; PLC, phospholipase C; PLD, phospholipase D; SM synthase, sphingomyelin synthase (from Bard and Malhotra, 2006).

1.3.2 The role of proteins in membrane fission

The role of lipids is not sufficient to drive membrane fission; indeed, proteins can cooperate with lipids to trigger the severing of membranes. Here I analyse the roles of two relevant proteins: PKD and CtBP1-S/BARS.

1.3.2.1 Protein kinase D

Protein kinase D is a serine/ threonine-specific family of enzymes that consists of three isoforms; PKD1/PKC μ , PKD2 and PKD3/PKC ν . These contain: (i) zinc-finger-like cysteine-rich motifs that are involved in recruitment of PKD to the membrane; (ii) a PH domain that has an inhibitory role in the regulation of catalytic activity; and (iii) a C-terminal catalytic domain.

It has been demonstrated that PKD is required to form PGCs at the TGN (Baron and Malhotra, 2002, Yeaman et al., 2004). The expression of a kinase-inactive form of PKD, or of PKD-specific chemical inhibitors, blocks protein transport from the TGN to the PM. Under these conditions, there is tubulation of the TGN, and these tubules contain cargo that are specifically destined to the PM. It appears that when PKD is not active, the cell-surface cargo is sorted into budding transport carriers, but they cannot detach from the TGN; thus, there is the formation of tubules. Thus PKD is required for fission of transport carriers from the TGN.

All three PKDs are involved in the transport of proteins that contain basolateral sorting signals. The role of PKD on basolaterally directed PGCs fission can be explained on the basis that PKD can recruit a generic pool of DAG to the TGN, which can induce fission. After the arrival of the PM-destined cargo and its sorting in the TGN, a signalling cascade is activated, through which a PKD-dependent reaction increases the local concentration of DAG. The cargo activates a trimeric G-protein through a G-protein-coupled receptor. The activated G-protein subunits, β/γ , activate PLC, which hydrolyses PtdIns4P to make DAG at the TGN. The generated DAG activates TGN-associated PKC η , which then phosphorylates and activates PKD. PKD activates PI4-KIII β to generate PtdIns4P from PtdIns. The PtdIns4P is hydrolysed to produce DAG. This feedback loop increases the local concentration of DAG. DAG is prevented from premature consumption, and upon reaching a critical concentration, it catalyses membrane fission.

1.3.2.2 CtBP1-S/BARS

The C-terminal-binding protein/brefeldin A ADP-ribosylated substrate (CtBP1-S/BARS) is a member of the CtBP family of proteins (Chinnadurai, 2002). Mammals have two CtBP-encoding genes: *CtBP1* and *CtBP2*. The *CtBP1* gene encodes two splice variant proteins: CtBP1-L (long) and CtBP1-S (short) (Corda et al., 2006), which are different because CtBP1-S lacks the first 11 N-terminal amino acids. CtBP1-L was identified as a protein that can bind the C-terminal region of the adenovirus E1A oncoprotein (Boyd et al., 1993), while CtBP1-S was identified as a substrate of the ADP ribosylation induced by the fungal toxin BFA, and for this reason was named as brefeldin A ADP-ribosylated substrate (BARS) (De Matteis et al., 1994).

CtBP2 has three splice variants: CtBP2-L (Katsanis and Fisher, 1998), CtBP2-S and RIBEYE. CtBP2-S lacks the N-terminal nuclear localisation signal (NLS) of CtBP2-L. RIBEYE contains a large N-terminal domain unrelated to CtBPs. Moreover, CtBP2-L is the only isoform that contains a NLS (Verger et al., 2006) (Figure 1.8).

The CtBP1-L and BARS isoforms localise into the nucleus and in the cytosol. CtBP2-L has a predominantly nuclear localisation, while CtBP2-S has a cytosolic localisation

(Verger et al., 2006). CtBP1-L and CtBP2-L were characterised as important transcriptional corepressors (Chinnadurai, 2002), while RIBEYE was identified independently and cloned on the basis of its localisation in synaptic ribbons (Schmitz et al., 2000).

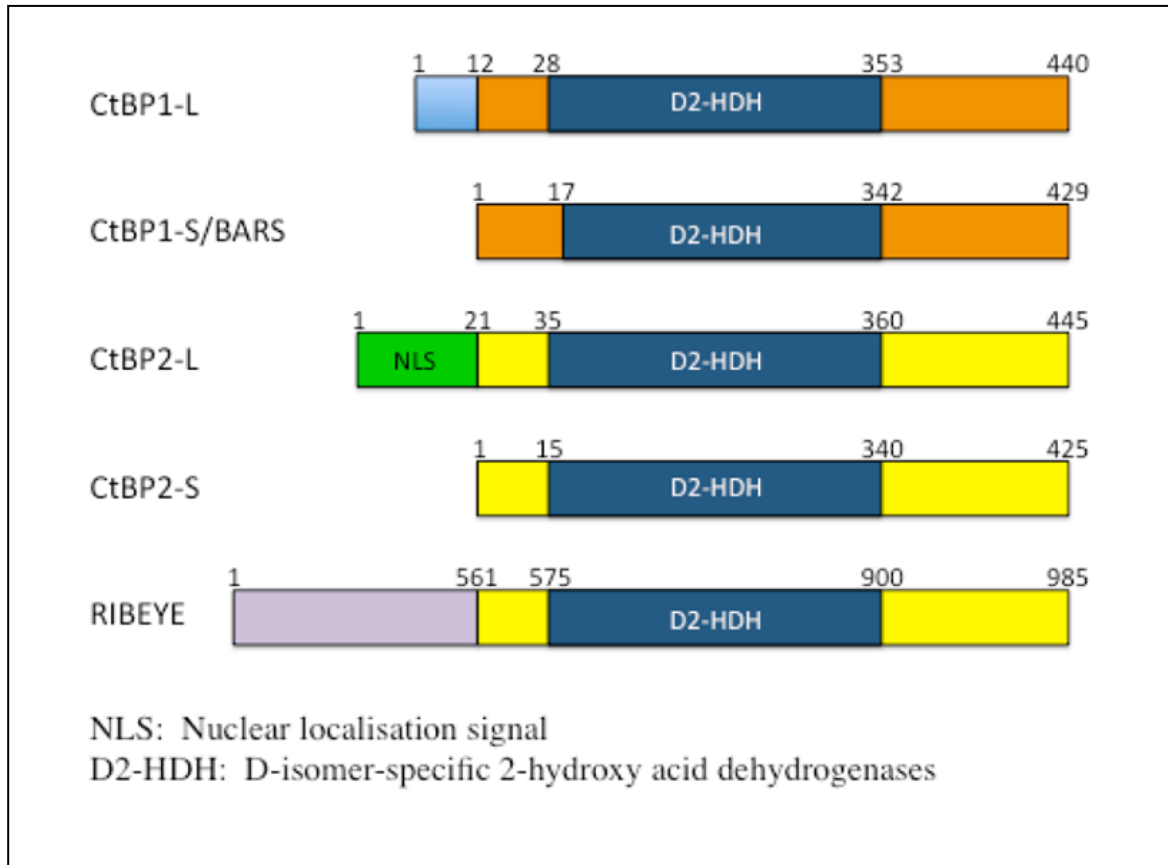


Figure 1.8 The CtBP family proteins.

Schematic representation of the sequences of the CtBP family of proteins. CtBP1-L and CtBP1-S/BARS are the alternative splice variants of the *CtBP1* gene; CtBP2-L, CtBP2-S and Ribeye are alternative splice variants of the *CtBP2* gene. The region conserved in all of the CtBPs is shown in dark blue. This includes a dehydrogenase homology region (D2-HDH) that has weak but significant similarity to the D-stereoisomer-specific 2-hydroxyacid NAD dependent dehydrogenases (Nardini et al., 2003). CtBP2-L is the only isoform of the CtBPs that has a nuclear localisation signal (NLS; green) (Verger et al., 2006).

1.4 Structure and regulation of BARS

The truncated form of the rat protein BARS (Figure 1.9 B), has been crystallised with NAD(H) (Nardini et al., 2003). Its structure is similar to that of the D-stereoisomer-specific-2-hydroxyacid NAD-dehydrogenases (Kumar et al., 2002; Nardini et al., 2003).

The BARS:NAD(H) complex forms an homodimer, where each BARS monomer consists of two domains, the nucleotide-binding domain (NBD; residues 113-308) and the substrate-binding domain (SBD; residues 1-112 and 309-350) (Figure 1.9, A). The NBD contains the residues for NAD⁺ binding, while the SBD is able to bind the PxDLS sequence (Nardini et al., 2003). Structural modelling and binding studies have shown that BARS can bind NAD(H) and long-chain acyl-CoAs in the same site. This analysis suggested that when BARS binds NAD(H) it is in a 'closed conformation/ dimerisation', while its binding with acyl-CoA induces an 'open conformation/ monomerisation' (Nardini et al., 2003; Nardini et al., 2009). This mechanism represents a switch between the two relevant roles of BARS: transcriptional corepressor in the nucleus and regulator of membrane fission in the cytoplasm.

Indeed, BARS can act both in transcription and in membrane fission and these activities are regulated by different co-factors. BARS can also shuttle between the nucleus and the cytoplasm, and the regulation of this movement can be due to post-translational modifications, protein binding, and/or the formation of multiprotein complexes (Figure 1.10).

The two cofactors, acyl-CoAs and NAD(H), can bind BARS in the same pocket (Nardini et al., 2003) and this induces the structural change that is connected to the change in BARS function. NAD(H) stabilises the dimer, and the interaction with PxDLS-containing proteins is increased. At the same time, the effect of NAD(H) is also to decrease the interaction between some non-PxDLS-containing proteins and BARS (Mirnezami et al., 2003). Acyl-CoAs favour the interactions between BARS and ARFGAP1, which promotes membrane fission, while NAD(H) inhibits this interaction.

Secondly, as mentioned above, BARS can be regulated by its interactions with other proteins, including CtBP2, transcription factors, and neuronal nitric oxide synthase (nNOS) (Figure 1.10). BARS and CtBP2 can homodimerise and heterodimerise, and it has been demonstrated that this influences the re-distribution of BARS from the cytosol to the nucleus (Verger et al., 2006).

Finally, BARS is regulated by post-translational modifications, and in particular by phosphorylation and SUMOylation (Figure 1.10). BARS can be phosphorylated on different residues by different kinases: at Ser422 by the homeodomain-interacting protein kinase-2 (HIPK2) and c-Jun NH2-terminal kinase 1 (JNK1), at the Thr176 by Akt1 (Merrill et al., 2010; Figure 1.10), at Ser158 by AMP-activated protein kinase (AMPK) (Kim et al., 2013; Figure 1.10), and at Ser147 by PAK1. All of these phosphorylation events have two important effects: they block BARS co-repressor activity (Barnes et al., 2003), and change its oligomerisation status, shifting it towards the monomeric state that is active in membrane fission (Liberali et al., 2008; Valente et al., 2012).

Conversely, the SUMOylation of BARS at Lys428, leads to nuclear retention and is critical for the corepressor activity of BARS (Kagey et al., 2003; Lin et al., 2003).

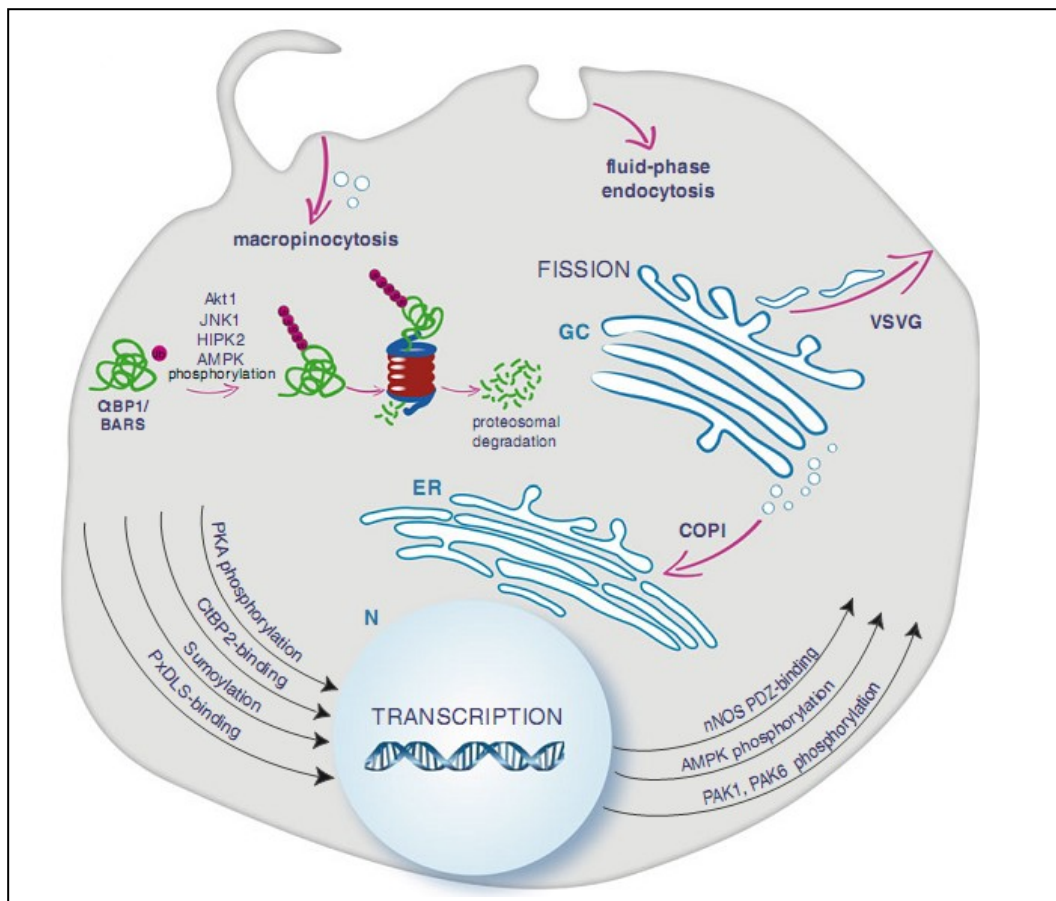


Figure 1.10 CtBP1/BARS: mechanisms of its functional switch.

Representative scheme of the CtBP1/BARS functions mediated by a change in its oligomerisation state, intracellular localisation, and post-translational modifications. In the cytoplasm, CtBP1/BARS drives membrane fission in several dynamin-independent trafficking steps (magenta arrows): fluid-phase endocytosis, macropinocytosis, trans-Golgi network (TGN) to basolateral-PM-directed VSVG cargo in epithelial cells, retrograde transport of the KDEL receptor to the ER by COPI-coated vesicles, fragmentation of the Golgi complex (GC) during mitosis (not shown in the scheme). Mechanisms for cytoplasm localisation of CtBP1/BARS might depend on binding to the PDZ domain of nNOS, and to AMPK, PAK1, and PAK6 phosphorylation (see black arrows on the lower right). In the nucleus (N), CtBP1/BARS functions in the assembly of multiprotein repressor complexes involved in the modulation of gene expression (not shown in the scheme). Mechanisms for nuclear localisation of CtBP1/BARS might depend on its oligomerisation with CtBP2, binding to transcription factors containing the PxDSL motif, PKA phosphorylation, and SUMOylation (see black arrows on the low left). CtBP1/BARS is targeted for ubiquitylation followed by proteasome-mediated degradation upon Akt1, JNK1, HIPK2, and AMPK phosphorylation (green protein) (from Valente et al, 2013).

1.5 The role of BARS in membrane fission

CtBP1/BARS has been shown to be involved in a number of fission processes, as described below.

1.5.1 PGC formation

During membrane trafficking from the TGN to the basolateral PM in epithelial cells, PGCs are first extruded, and then fission takes place, to form free carriers directed to the PM (Polishchuk et al., 2003). When BARS function is inhibited (e.g., by injection of dominant-negative mutants), these PGC tubular precursors do not detach from the Golgi complex, but elongate out and retract back into the Golgi mass. Thus the fission step of PGC formation is inhibited (Bonazzi et al., 2005; Valente et al., 2012) (Figure 1.11A).

There are several proteins involved in the formation of PGCs, including PI4KIII β and its product PtdIns4P (Bruns et al., 2002; Godi et al., 2004); Arf (Godi et al., 1999); neuronal calcium sensor-1 (NCS-1) (Haynes et al., 2005); the glycolipid-transfer protein FAPP2 (D'Angelo et al., 2007; Cao et al., 2009); and GOLPH3 (De Matteis and Luini, 2008; Kreitzer et al., 2000).

Instead, the proteins involved in the fission process are: PKD, which is recruited to the TGN by Arf and DAG (Pusapati et al., 2010); myosin II and Rab6 (Miserey-Lenkei et al., 2010); and BARS (Bonazzi et al., 2005; Valente et al., 2012).

In particular our laboratory has demonstrated the role of a novel and crucial protein in carrier formation, the 14-3-3 γ protein (Valente et al., 2012). This protein bridges between PI4KIII β and BARS, which together form the tripartite PI4KIII β –14-3-3 γ (x2)–BARS core complex, which is involved in BARS-mediated transport from the TGN to the PM.

Moreover, the two other BARS complex components, PKD and PAK1 kinases, can stabilise the tripartite complex by reversible phosphorylation, which leads to the assembly and disassembly of this dynamic complex (Valente et al., 2012). In particular, PKD phosphorylates PI4KIII β at Ser294, which stabilises the 14-3-3 γ binding to PI4KIII β (Hausser et al., 2006). The formation of this complex is crucial for PGC fission; indeed manipulations that impair the formation of this complex result in long VSVG-containing tubules that elongate out of the Golgi complex, but cannot undergo fission.

1.5.2 Macropinocytosis

This form of endocytosis results in the formation of large endocytic vesicles, called macropinosomes, which originate from actin ruffles at the PM. This ruffling is followed by PM invagination and formation of the macropinocytic cup, which then undergoes fission of its junction with the PM (Swanson and Watts, 1995). It has been demonstrated that the inhibition of BARS does not affect macropinocytic cup formation, but instead inhibits the membrane fission process required for macropinosome closure, again underlining the specific BARS role in membrane fission (Liberali et al., 2008) (Figure 1.11, B).

1.5.3 COPI-coated vesicle formation

COPI-coated vesicles mediate retrograde transport of the KDEL-receptor from the Golgi complex to the ER. When BARS function is inhibited, COPI-coated vesicles bud, but do not detach from Golgi cisternae both *in vivo* and *in vitro*, consistent with fission inhibition (Yang et al., 2005) (Figure 1.11, C).

1.5.4 Fluid-phase endocytosis

Constitutive fluid-phase endocytosis can be monitored by dextran uptake, and it is inhibited by BARS impairment (e.g., by injection or expression of a dominant-negative mutant or a blocking antibody, or by RNA interference) (Bonazzi et al., 2005).

1.5.5 Golgi fragmentation during mitosis

During the G2–mitosis transition, the Golgi ribbon is first fragmented into isolated stacks of cisternae, and then fragmented into tubulo-vesicular elements. These elements are separated into the two main pools that constitute the new Golgi complexes in the daughter cells. BARS is necessary for the first stage of this fragmentation. Immunodepletion of BARS (e.g., by a polyclonal antibody) results in inhibition of mitotic Golgi partitioning and arrest of the cell cycle at the G2 phase (Hidalgo Carcedo et al., 2004) (Figure 1.11, D).

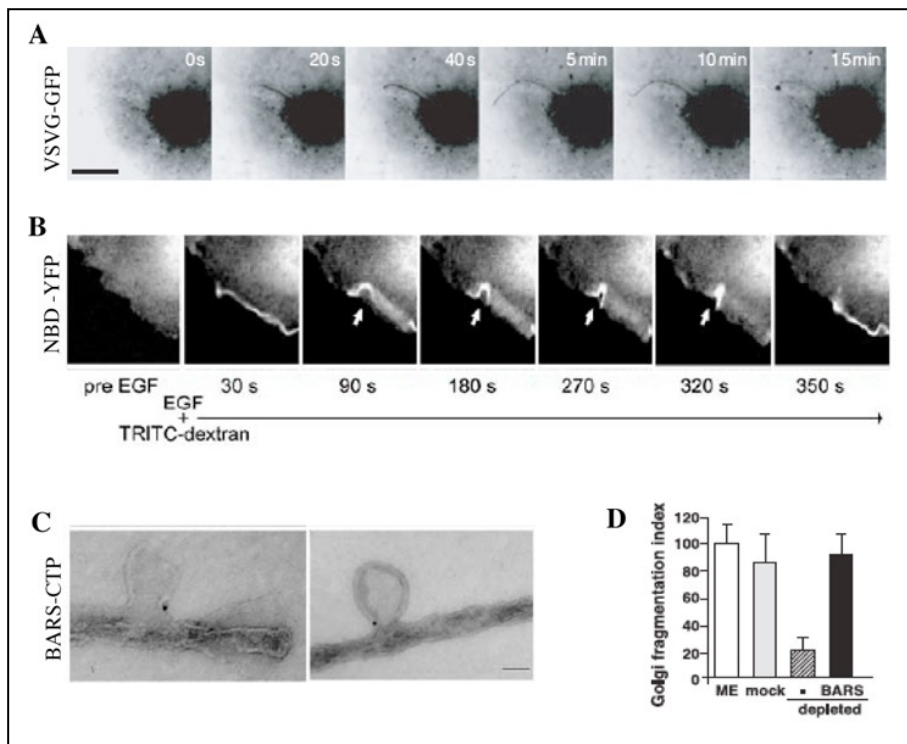


Figure 1.11 BARS-activated membrane fission in different pathways

A. Effects of BARS inhibition on post-Golgi transport of VSV-G, taken from Bonazzi et al. (2005). Representative frames of time-lapse imaging of COS7 cells expressing VSV-G-GFP and injected with BARS^{D355A}, a dominant-negative BARS mutant. In the VSV-G transport assay, the recombinant BARS^{D355A} mutant was injected during the 20 °C block (when the VSV-G was trapped on the Golgi complex), and images were acquired from 20 min after the shift to 32 °C (temperature block release, allowing exit of VSV-G from the Golgi). The images show the formation at and the elongation from the Golgi complex of a VSV-G-containing tubule that does not undergo fission. Scale bar: 5 µm. **B.** Effects of BARS inhibition on macropinocytosis, taken from Liberali et al. (2008). Representative frames of time-lapse imaging of epidermal growth factor (EGF)-induced macropinocytosis in BARS-NBD-YFP (NBD-YFP) expressing cells. To detect the newly formed macropinosomes, this stimulation was performed in the

presence of TRITC-dextran, as a probe of fluid-phase macropinocytosis. The arrows from 90 s to 320 s after EGF stimuli show the formed macropinosome that has not sealed. **C.** Effects of BARS inhibition in COPI vesicle formation, taken from Yang et al. (2005). Immunogold labelling of the C terminal inhibitory portion of BARS (BARS-CTP) show its localisation at the neck of the non-fissioned buds in a COPI vesicle reconstitution system using Golgi membranes. Scale bar: 50 nm. **D.** Effects of BARS immunodepletion in mitotic fragmentation of the Golgi complex, taken from Hidalgo Carcedo et al. (2004). Quantification of the Golgi fragmentation index in digitonin-permeabilised NRK cells incubated with mitotic extract (ME), mock-depleted mitotic extract (mock), or BARS-depleted mitotic extract without (-) or with 10 µg recombinant BARS (BARS).

1.6 Golgi behaviour during mitosis

As mentioned above, the Golgi apparatus is composed of individual stacks of flat cisternae, called 'compact zones' (Dalton and Felix, 1954). These compact zones are laterally connected with adjacent stacks by membranous tubular bridges, which are referred to as the 'non-compact zone' (Rambourg and Clermont, 1990) (Figure 1.1, B). Together, these form the membranous system called the 'Golgi ribbon', which is located in a perinuclear zone around the centrosome, and is maintained there through a microtubule (MT)-dependent mechanism (Rambourg and Clermont, 1990). There are three models for the biogenesis and inheritance of the Golgi complex: (i) *de-novo* synthesis, where a new copy of the organelle is generated in the absence of any existing copy of the organelle; (ii) template assembly/ growth; and (iii) growth followed by fission. The organelle inheritance during cell division depends on the number of copies of the organelle; indeed, multi-copy organelles can be shared, while a single copy organelle can be duplicated and then segregated into daughter cells or broken down into multiple pieces. However, a cell can switch from one model to another depending on the stage of its life cycle (Lowe and Barr, 2007). Mitotic inheritance of the Golgi apparatus involves the progressive and reversible disassembly of the Golgi ribbon into dispersed fragments (Figure 1.12), to allow the correct partitioning of the Golgi membranes between the two daughter cell (Colanzi et al., 2003, Persico et al., 2009).

During the cell cycle and in particular during G1 and S phase in mammalian cells, the Golgi membrane mass increases, probably because the pool of newly synthesised proteins increases in the ER, and these are then transported and deposited in the Golgi complex.

At late G2 and during mitosis, there are several structural reorganisations of the Golgi apparatus (Shorter et al., 2002) (Figure 1.13). First, at late G2/ early prophase, the tubules that interconnect the stacks are severed and this process leads to Golgi unlinking into individual or small clusters of stacks. At prometaphase, the Golgi stacks undergo unstacking and vesiculation, and mitotic Golgi clusters that comprise vesicular and tubular fragments are formed. At telophase, these fragments undergo a series of changes that lead to the reassembly of the stacks, and then to the Golgi ribbon formation in the two daughter cells.

Mitotic Golgi ribbon disassembly, and in particular the cleavage of the ribbon into stacks, is required for entry into mitosis. This is the reason why it is important to determine how Golgi fragmentation controls mitotic progression.

Two basic biochemical experimental approaches have been used during these years to reconstruct the molecular machinery of Golgi disassembly during mitosis: semi-intact cell assays and *in-vitro* disassembly/ reassembly assays. In the semi-intact cell assays, the cells are permeabilised with digitonin, washed with 1 M KCl to remove endogenous cytosolic proteins and peripheral membrane proteins, and incubated with cytosol prepared from interphase or mitosis-arrested cells. After incubation, the cells are fixed and analysed by light microscopy or EM. This technique has been useful for the identification of the following proteins involved in this Golgi breakdown: the fission-inducing protein CtBP1/BARS (Hidalgo Carcedo et al., 2004), the Golgi structural proteins GRASP65 (Sutterlin et al., 2002) and GRASP55 (Duran et al., 2008), the MEK1 kinase (Acharya et al., 1998) and Polo kinase 1 (Plk1; Sutterlin et al., 2002) (Figure 1.13).

The *in-vitro* Golgi disassembly/ reassembly assay consists of the incubation of purified rat liver Golgi stacks with mitotic cytosol. As a result of this incubation, the Golgi membranes are dispersed into mitotic Golgi fragments, which can then be reassembled into Golgi stacks upon incubation with interphase cytosol or purified components. This assay is useful because it is possible to follow, and thus to analyse the precise sequence of morphological events, by EM or biochemical analysis.

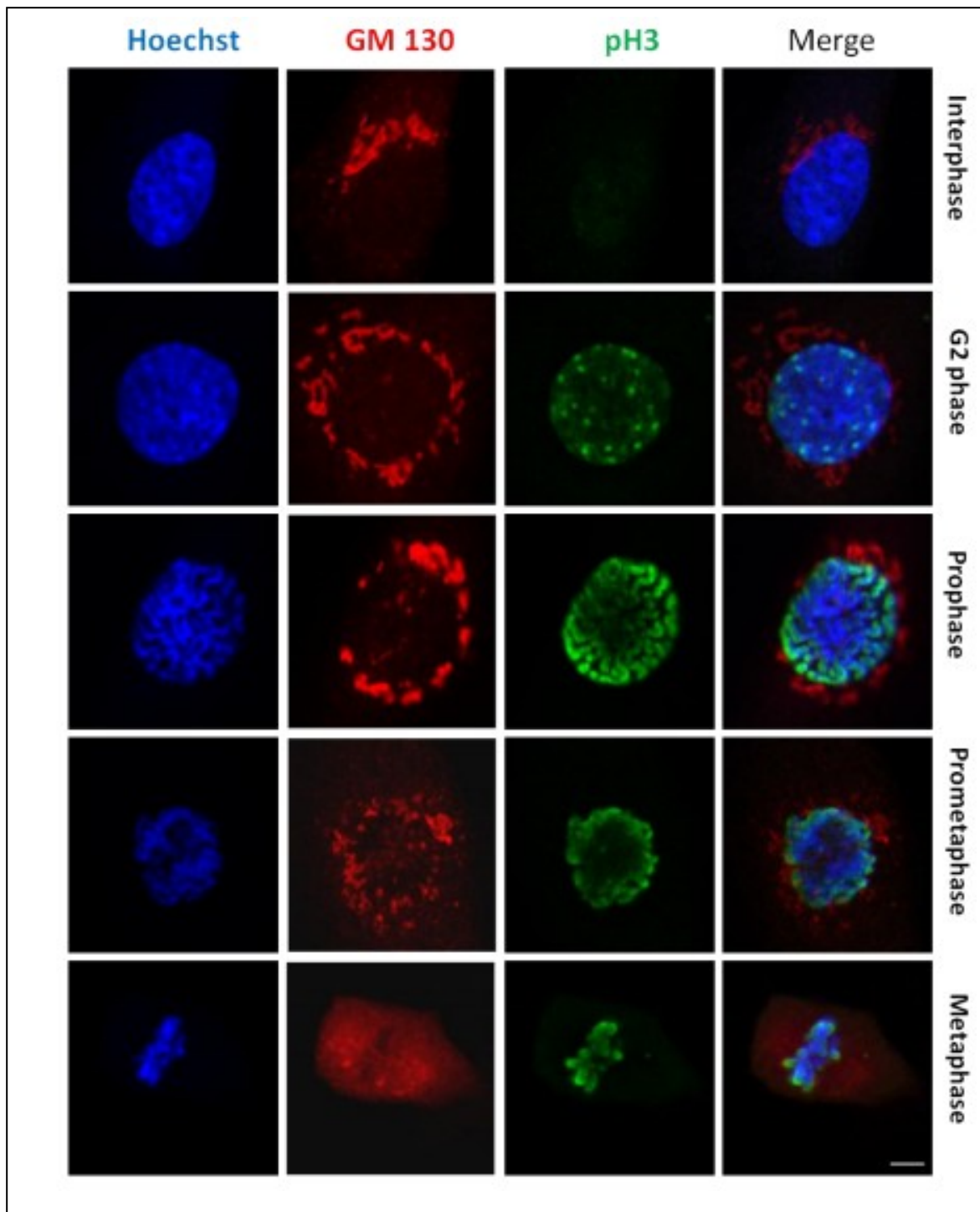


Figure 1.12. Golgi fragmentation begins during the G2 phase of the cell cycle. Confocal images of HeLa cells at different cell-cycle phases, grown on coverslips, fixed and labelled with Hoechst for DNA staining, with anti-phosphohistone-H3 antibody (pH3) to identify early and late G2 cells, and with an anti-GM130 antibody for Golgi morphology.

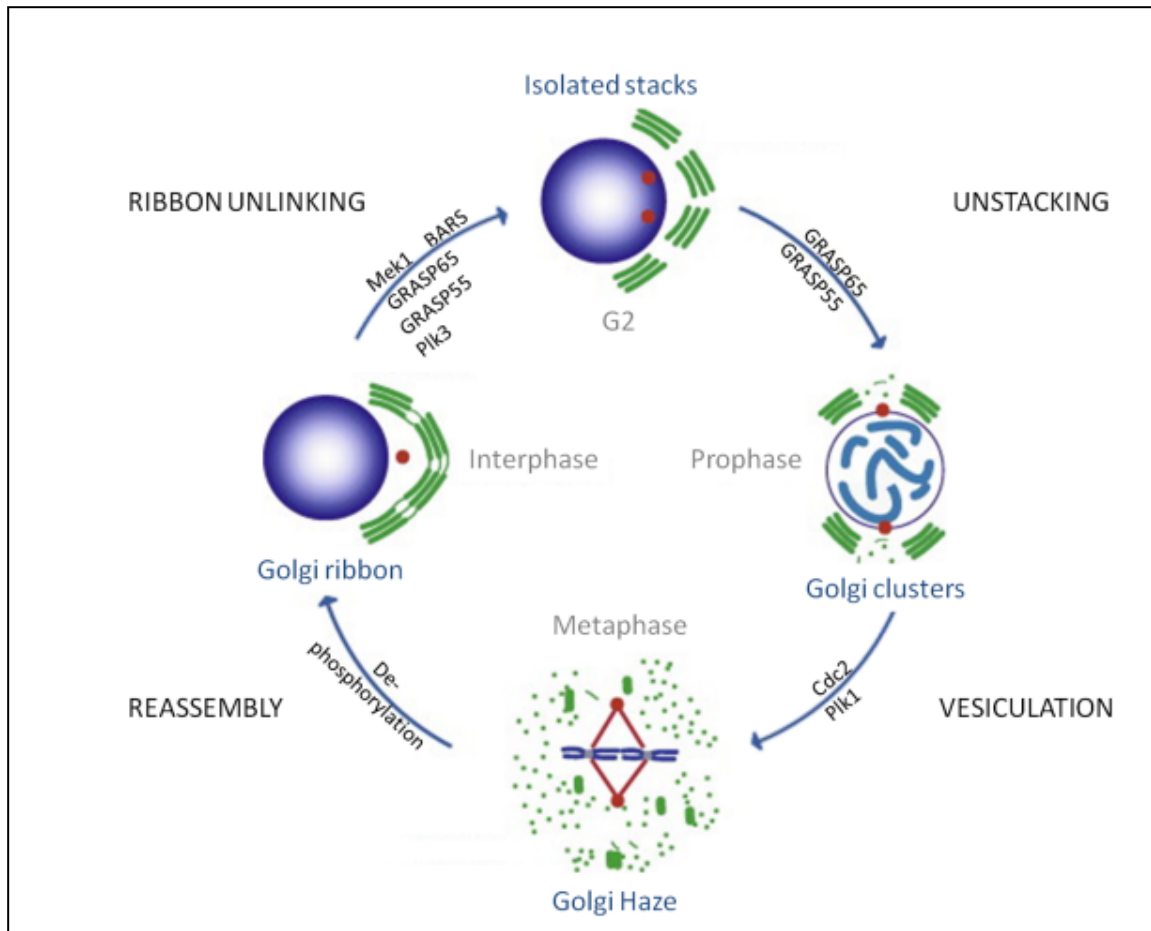


Figure 1.13 Golgi ribbon partitioning begins in G2, with the severing of the Golgi ribbon into isolated groups of stacks.

This first step of mitotic Golgi fragmentation (ribbon unlinking) controls G2/M transition and requires the activity of MEK1, BARS, GRASP55 and GRASP65. At the onset of mitosis, these isolated stacks undergo further disassembly in sequential steps: unstacking and vesiculation, leading to the so-called 'Golgi haze' during metaphase, where the Golgi membranes are completely fragmented. These processes require the activity of the kinases Plk1 and Cdc2, and their targets GRASP55 and GRASP65.

1.7 The role of proteins in Golgi partitioning during mitosis

The unlinking of the Golgi ribbon at late G2/ early prophase, and its subsequent unstacking and vesiculation, depend on the phosphorylation of Golgi-localised proteins by several kinases. A combination of a semi-intact cell assay and the use of specific inhibitors and RNA interference (RNAi) have demonstrated that activation of the MEK1/ ERK cascade is involved in Golgi fragmentation during G2/M (Acharya et al., 1998). MEK1 is recruited to the Golgi ribbon at G2/M, and its depletion or inhibition blocks Golgi ribbon unlinking and is responsible for delay of mitotic entry (Colanzi et al., 2003). Two ERK kinases have been identified as the strongest downstream MEK1 candidates: ERK1c and ERK2. The former localises on the Golgi ribbon at late G2/ early prophase. Its depletion inhibits mitotic Golgi fragmentation (Shaul and Seger, 2007). The latter, ERK2, is phosphorylated in mitosis by GRASP55, a protein that is required for the structural integrity of the Golgi apparatus

(Jesch et al., 2001). Moreover, MEK1 can be activated in mitosis by Raf1 (Colanzi et al., 2003). Indeed, inhibition of Raf1 inhibits Golgi fragmentation in cell-permeabilisation assays, whereas addition of the recombinant constitutively activated MEK1 rescues the failure in Golgi fragmentation. This suggests that specific Raf1-mediated activation of MEK1 is required for Golgi complex fragmentation by mitotic cytosol (Colanzi et al., 2003). Furthermore, the inhibition of Raf1 by injection of its autoinhibitory domain inhibits cell entry into mitosis by 50%. A further confirmation of the role of MEK1 in Golgi fragmentation is that activated MEK1 has been found on the Golgi apparatus in late prophase (Colanzi et al., 2003).

GRASP65 and GRASP55 are the two proteins that have roles in Golgi stacking. GRASP65 is phosphorylated during mitosis by two kinases, Plk1 and cyclin-dependent kinase 1 (Cdk 1); these phosphorylations mediate membrane unstacking both *in vitro* and *in vivo* (Wang et al., 2003). A model has been proposed according to which GRASP65 forms homodimers that can form *trans*-oligomers with molecules residing on adjacent cisternae, to hold them together. This model comes from the finding that the formation of oligomers by GRASP65 is regulated by phosphorylation (Figure 1.14) (Wang et al., 2005; Wang et al., 2003). The overexpression of the N-terminal of GRASP65 (which is not mitotically phosphorylated) inhibits Golgi unstacking, which results in the formation of more and larger Golgi clusters during mitosis (Wang et al., 2005). GRASP55 has complementary roles in Golgi cisternal stacking (Xiang and Wang, 2010).

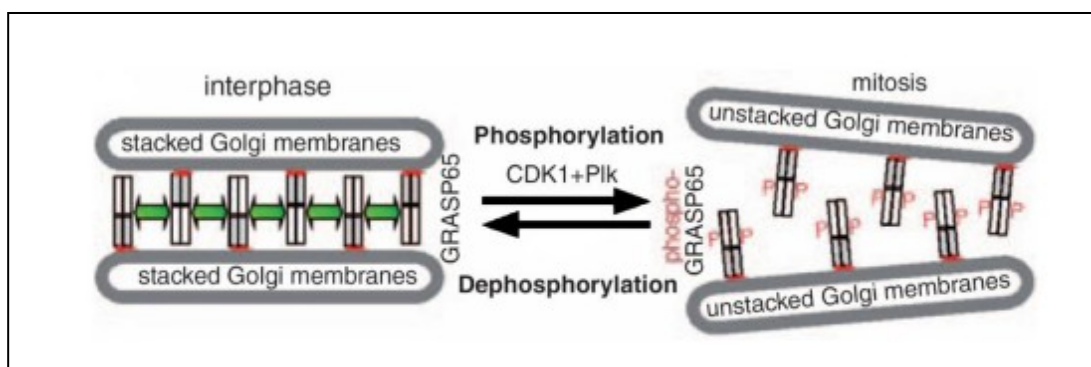


Figure 1.14 Model of mitotic Golgi cisternal unstacking.

Schematic representation of mitotic Golgi unstacking. During interphase, GRASP65 dimers form oligomers with GRASP65 dimers present on adjacent cisternal membranes; this mechanism holds the cisternae together (Golgi stacking). During mitosis, GRASP65 phosphorylation by the Cdk1/CycB complex and Plk1 kinase breaks the GRASP65 oligomers, causing unstacking of the cisternae. At the end of mitosis, dephosphorylation of GRASP65 restacks the cisternae (modified from Mironov et al., 2008).

In mitosis, the Golgi stacks undergo further fragmentation, which is controlled by Cdk1 and Plk1 (Ferrari et al., 2006). For mitotic Golgi disassembly, Cdk1 appears to act after MEK1/ ERK-mediated ribbon unlinking, to promote complete vesiculation of the Golgi stack (Colanzi et al., 2003). Moreover the depletion of Plk1 by RNAi was shown to be required for full Golgi stack vesiculation (Preisinger et al., 2005).

At the vesiculation step, the Golgi appears as the 'Golgi haze' (Misteli and Warren, 1995a). The mechanism of inheritance between the two daughter cells has been explained by two opposing views. The first suggested that the Golgi haze is Golgi

proteins that are redistributed into the ER, so the Golgi is inherited together with the ER (Zaal et al., 1999). The second view supports the idea that the Golgi apparatus is independent of the ER, and in this case the key mechanism of Golgi inheritance is the disruption of the membrane-tethering complexes, which is induced by the action of mitotic kinases (Shorter and Warren, 2002). These fragments contained in the Golgi haze are then partitioned between the two daughter cells through a process directed by the mitotic spindle (Shima et al., 1998). The final destination of the mitotic Golgi membranes is still not known, but it is clear that the Golgi apparatus is reassembled before cytokinesis. Thus, once divided between the daughter cells during telophase, the Golgi fragments reassemble and fuse into a fully functional Golgi stack.

1.7.1 GRASP65

GRASP65 is a peripheral membrane protein that is associated with Golgi membranes through its N-terminal myristic acid, which is known as the 'GRASP domain' (residues 1-197), and which includes two PDZ-like domains. The GRASP domain is important to form dimers, which associate in *trans* and links adjacent cisternae to form the stacked Golgi (Wang et al., 2005; Wang et al., 2003). The C-terminal portion of GRASP65 contains the serine-proline-rich (SPR) domain (residues 198-446) (Barr et al., 1997) (Figure 1.15), which is phosphorylated at multiple sites during mitosis (Preisinger et al., 2005).

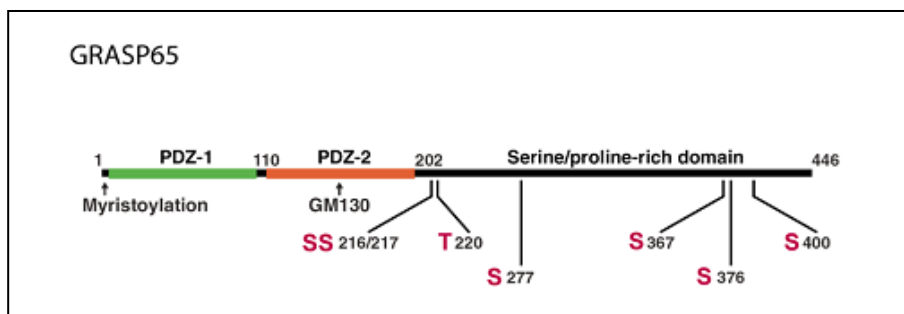


Figure 1.15 Schematic representation of the GRASP65 sequence.

The N-terminal domain, called the 'GRASP domain', comprises two PDZ-like domains and the GM130-binding region. The C-terminal domain is rich in phosphorylation sites, which are indicated in red.

It has been shown that the microinjection of a GRASP65-blocking antibody into mitotic cells blocks Golgi stack formation in the daughter cells. This suggests that GRASP65 is required for Golgi stacking (Wang et al., 2008). However, it was later demonstrated that GRASP65 might not have a role in cisternal stacking (Sutterlin et al., 2005), but in the formation and/or maintenance of the tubules that connect the stacks within the Golgi ribbon (Puthenveedu et al., 2006). The C-terminal SPR domain of GRASP65 can be phosphorylated by Cdk1 and Plk1 kinases on multiple sites. *In-vitro* experiments have suggested that Cdk1 targets GRASP65 at four serine/ threonine residues (S216/ Ser217, T220, S277, S376) (Barr et al., 1997; Lin et al., 2000; Wang et al., 2003), while Plk1 can be recruited to Golgi membranes and drives the fragmentation of the Golgi complex under mitotic conditions (Preisinger et al., 2005; Sengupta and Linstedt, 2010). Furthermore, GRASP65 could be a substrate of MEK1/ ERK also in mitosis, although this has not yet been demonstrated (Yoshimura et al., 2005). The role of GRASP65 in the Golgi checkpoint has been

extensively studied, but there is no clear model on how it regulates Golgi fragmentation and mitotic entry. This might either be an effect caused directly by the inhibition of GRASP65, or a secondary effect caused by the perturbation of the Golgi structure or by the disruption of the signalling cascades that control mitotic entry. Indeed, as described above, GRASP65 has a C-terminal domain that is phosphorylated at multiple sites during mitosis, which suggests its involvement in regulatory functions or structural functions (Preisinger et al., 2005). One of the phosphorylation site on GRASP65, serine 277 (S277), has been extensively studied. This residue is phosphorylated *in vitro* by Cdk1/ CycB during mitosis, and this has provided clarification of a hypothetical regulatory role of GRASP65 during G2/M transition (Yoshimura et al., 2005). However, there are still several points to address the role of GRASP65 in the Golgi-related mitotic checkpoint.

1.7.2 GRASP55

GRASP55 is the second mammalian GRASP homologue (Shorter and Warren, 1999). In contrast to GRASP65, GRASP55 has been shown to be mitotically phosphorylated *in vitro* by ERK2, a downstream target of MEK1 (Jesch et al., 2001). The overexpression of the two GRASP55 phosphorylation-defective mutants (T222, 225A) inhibit Golgi ribbon unlinking and blocks/ delays G2/M transition (Feinstein and Linstedt, 2007). The requirement for GRASP55 in Golgi fragmentation and mitotic entry was also demonstrated by Malhotra and colleagues (Duran et al., 2008). They showed that also T225 and T249 phosphorylation in the C-terminal of GRASP55 are required for both Golgi fragmentation and entry into mitosis. However, several parallel studies on the two GRASPs are needed to more fully address their roles in Golgi ribbon unlinking.

1.7.3 BARS

The involvement of BARS in mitotic Golgi partitioning was evaluated through a well-established assay that reconstitutes the process of Golgi fragmentation in permeabilised NRK cells incubated with mitotic cytosol (Acharya et al., 1998). Depletion of BARS from mitotic extracts inhibited Golgi fragmentation by more than 75%. Moreover, the addition of the two dominant-negative mutants of BARS, NBD or SBD, to mitotic cytosol resulted in inhibition of Golgi fragmentation. As confirmation that this inhibition of Golgi fragmentation was due to a failure in BARS activity, the re-addition of recombinant BARS to these extracts completely restored the fragmentation process (Hidalgo Carcedo et al., 2004).

The functional role of BARS has also been analysed in living cells, by microinjection of an anti-BARS antibody, or the purified recombinant SBD mutant. Both treatments inhibited Golgi fragmentation and mitotic entry. Using these inhibitory reagents (antibody and SBD) in combination with FRAP analysis, BARS was later shown to act through the severing of the tubules that interconnect the Golgi stacks in the Golgi ribbon in late G2 (Colanzi et al., 2007). Of note, although the BARS knock-out mouse is embryonically lethal, the derived embryonic fibroblasts divide normally.

However, interference with BARS activity in interphase does not lead to Golgi fragmentation (Hidalgo Carcedo et al., 2004), which indicates that the role of BARS in fission of Golgi tubules is mitotically regulated and probably acts in concert with other proteins. The above-described requirement for Golgi fragmentation for entry into mitosis is in agreement with a checkpoint that monitors Golgi fragmentation, to allow cell entry into mitosis.

1.7.4 PKD

As mentioned above, PKD is a protein that belongs to a family of serine/ threonine kinases. This family is composed of three members: PKD1, PKD2 and PKD3. In 2002, the involvement of PKD in the fission of vesicles directed to the plasma membrane was demonstrated by Baron and Malhotra. Indeed, PKD interacts with DAG and is recruited into the TGN, where it is involved in the fission of post-Golgi carriers (Liljedahl et al., 2001). Moreover, Kienzle and colleagues (2012) have demonstrated that PKD is required also for mitotic entry of HeLa cells, in particular in the cleavage of the Golgi interstack connections in late G2 phase of the cell cycle. Indeed the depletion of PKD1 and PKD2 by siRNA treatments leads to accumulation of cells in G2 phase. Additionally, it has been demonstrated that PKD is required for the cleavage of the non-compact zones of the Golgi membranes in G2 phase, which prevents cells from entering mitosis. Moreover, mitotic Raf-1 and MEK1 activation are blocked after PKD inhibition, which suggests that PKD is involved in Golgi partitioning during mitosis in a Raf-1/ MEK1–dependent manner.

CHAPTER 2

MATERIALS AND METHODS

2.1 Materials

DL-dithiothreitol (DTT), bovine serum albumin (BSA), saponin, Tris-[hydroxymethyl]-aminomethane (Tris), ethylene glycolbis(beta-aminoethyl ether)-N,N,N',N'-tetraacetic acid (EGTA), ethylenediaminetetraacetic acid (EDTA), H_2PO_4 , Na_2HPO_4 , NaH_2PO_4 , sucrose, brefeldin A (BFA) and reduced L-glutathione were all from Sigma–Aldrich (WI, USA). NaCl, HCl, NaOH, KOH, NH_4Cl , dimethylsulphoxide (DMSO), methanol and chloroform were all from Carlo Erba (Italy). 4-(2-Hydroxy-ethyl)-piperazine-1-ethanesulfonic acid (Hepes), glycerol, KCl, MgCl_2 and CaCl_2 were all from Merck (Germany). C-Mercaptoethanol was from Fluka (Switzerland). Mowiol was from Calbiochem (CA, USA). Paraformaldehyde was from Electron Microscopy Sciences (PA, USA). The sources of the other materials used are specified for each procedure.

2.2 Solutions

Phosphate-buffered saline (PBS): 1.5 mM KH_2PO_4 , 8 mM Na_2HPO_4 , 2.7 mM KCl, 137 mM NaCl, pH 7.4.

The blocking solution was prepared as follows: 0.5% BSA, 50 mM NH_4Cl in PBS, pH 7.4. Where needed, saponin was added to 0.05% to the preparation. Aliquots of this blocking solution were stored at $-20\text{ }^\circ\text{C}$.

The composition of the other solutions used are specified for each procedure.

2.3 Subcloning and mutation of DNA

2.3.1 Materials

Restriction enzymes were from Amersham Pharmacia Biotech (NJ, USA). T4 DNA ligase and DNA molecular size standards were from Gibco/BRL (NY, USA). The 'QIAprep Spin Miniprep' kits and the 'QIAGEN Plasmid Maxi' kits were from Qiagen (CA, USA). The 'QuikChange Site-Directed-Mutagenesis' kits were from Stratagene (La Jolla, CA, USA). Tryptone, peptone, yeast extract and agar were from Difco, Becton Dickinson (MD, USA). 3-Morpholino-propanesulfonic acid (MOPS), RbCl and MnCl_2 were from Sigma–Aldrich (WI, USA).

2.3.2 Solutions and media

Lysogeny broth (LB): 1% (w/v) tryptone peptone, 0.5% (w/v) yeast extract, 1% (w/v) NaCl; autoclaved 15 min at $121\text{ }^\circ\text{C}$.

LB-agar: LB plus 1.5% (w/v) agar; autoclaved 15 min at $121\text{ }^\circ\text{C}$.

TE (Tris/EDTA) buffer: 10 mM Tris-HCl, 1 mM EDTA, pH 8.

TAE (Tris/acetic acid/EDTA) buffer (50x, 1.0 l): 242 g Trizma base, 57.1 ml glacial acetic acid, 100 ml 500 mM EDTA.

2.3.3 DNA agarose gels

Agarose gels were prepared by dissolving agarose in TAE buffer and heating in a microwave oven. Ethidium bromide was added (to $0.5\text{ }\mu\text{g/ml}$), and the gels were poured and run on an agarose gel apparatus from Bio-Rad Laboratories (UK). DNA

standards (0.5 µg) were loaded and used as a reference for approximate estimations of the amounts of DNA in the samples.

2.3.4 PCR amplification of DNA inserts

To amplify specific regions of DNA inserts, PCR was performed by incubating 10 ng DNA plasmid as a template in 50 µl 20 mM Tris-HCl, pH 8.8, 10 mM KCl, 2 mM MgSO₄, 10 mM (NH₄)₂SO₄, 0.1% Triton X-100, 0.1 mg/ml nuclease-free BSA, 1 µM each oligonucleotide, 200 µM each dNTP, 2.5 U PFU Turbo DNA Polymerase. All of the reagents, except the DNA and the oligonucleotides, were from Stratagene (CA, USA). The oligonucleotides were from Sigma–Genosys.

The PCR reaction mixtures were layered with mineral oil (Sigma–Aldrich, WI, USA) and subjected to 25 temperature cycles in a programmable thermal cycler (MJ Research Inc.). The melting, annealing and elongation temperatures were adjusted according to the features of the template and primers. To facilitate the subsequent subcloning of the PCR products, the forward and reverse primers were provided with restriction sites at their 5' ends.

2.3.5 Restriction and ligation

DNA (vectors and inserts) were cut with 5 U/µg of the appropriate restriction enzymes in the buffer supplied with each enzyme by Amersham Pharmacia Biotech (NJ, USA). After restriction, the enzymes were usually inactivated by incubating them at 65 °C to 75 °C for 10 min to 20 min, according to the manufacturer instructions, and then the samples were loaded onto 1.0% to 1.4% agarose gels. The bands of interest were cut from the gels with a sterile scalpel, and the DNA was extracted from these gel samples with the 'Qiaex II' extraction kits (Qiagen, CA, USA), according to the manufacturer instructions. The DNA was eluted in 10 mM Tris-HCl, pH 8.0. To ligate the vector and the insert, ~100 ng of the vector and an ~3-fold molar amount of the insert were incubated with 1 U T4 DNA ligase in T4-DNA-ligase buffer (Gibco/BRL, UK) for 10 min at room temperature (RT).

2.3.6 DNA mutagenesis

The DNA (10 ng vector and insert) and 125 ng of the two synthetic oligonucleotide primers containing the desired mutations were amplified by PCR, according to the manufacturer instructions of the 'QIAprep Spin Miniprep' kits (Qiagen, CA, USA). The mutagenesis reaction mixtures were layered with mineral oil (Sigma–Aldrich, WI, USA), and subjected to 25 temperature cycles in a programmable thermal cycler (MJ Research Inc.). The melting, annealing, and elongation temperatures were adjusted according to the features of the template and primers. The oligonucleotides were from Sigma–Genosys. After the reaction, DpnI endonuclease was added to the mixture for 1 h at 37 °C, to digest the parental non-mutated DNA template. The products were analysed on agarose gels and the mutations were verified by DNA sequencing (BMR Genomics, CRIBI, Padova, Italy)

2.3.7 Transformation of bacteria

The DNA plasmid of interest (10 ng uncut plasmid, or half of a ligation reaction) was added to competent bacteria. After gentle mixing, the bacteria were left on ice for 30 min, and then heat shocked for 45 s at 42 °C. After the addition of 800 µl LB, the bacteria were incubated under continuous shaking (200 rpm) at 37 °C for 45 min. The bacteria were plated onto LB agar containing the appropriate selective antibiotic, and incubated overnight (O/N), at 37 °C. The next day, an isolated bacterial colony

was picked and used to inoculate 2 ml LB containing the appropriate antibiotic. The culture was incubated O/N at 37 °C. Sterile glycerol (300 µl; 50%; v/v) was added to 700 µl of the bacterial culture, which was then stored at -80 °C.

2.3.8 Small-scale preparation of plasmid DNA (minipreps)

The clones obtained after the transformation of the ligation reaction were usually screened using minipreps and subsequent restriction analysis. Isolated bacterial colonies were picked and inoculated into 5 ml LB containing the appropriate antibiotic. After O/N growth at 37 °C under continuous shaking (200 rpm), 700 µl of the cultures was mixed with 300 µl 50% (v/v) sterile glycerol and stored at -80 °C; the rest of each culture was chilled on ice and centrifuged 10 min at 4,000x g. The DNA was extracted using 'QIAprep Spin Miniprep' kits (Qiagen, CA, USA), according to the manufacturer instructions, and analysed by restriction analysis and separation on agarose gels.

2.3.9 Large-scale preparation of plasmid DNA (maxipreps)

A small amount of the bacteria transformed with the plasmid of interest was scraped from the glycerol stock, inoculated into 2 ml LB containing the appropriate selective antibiotic, and grown at 37 °C under continuous shaking (200 rpm) for 6 h to 8 h. This pre-culture was used to inoculate 200 ml LB containing the selective antibiotic. After an O/N incubation, the bacteria were collected by centrifugation at 6,000 rpm in a JA14 rotor (4,000x g) for 10 min at 4 °C, and processed according to the maxi-plasmid purification protocol of the 'Qiagen Plasmid Maxi' kits. The DNA obtained was resuspended in TE buffer and stored at -20 °C.

2.4 Expression and purification of recombinant proteins

2.4.1 Solutions

GST lysis buffer: 20 mM Tris-HCl, pH 8.0, 100 mM NaCl, 1 mM EDTA.

GST elution buffer: 100 mM Tris-HCl, pH 8.0, 20 mM glutathione, 5 mM DTT.

Protease inhibitor cocktail (Complete Mini EDTA-free; Roche).

His lysis buffer: 50 mM sodium phosphate buffer, pH 8.0, 300 mM NaCl, 10 mM imidazole.

His wash buffer: 50 mM sodium phosphate buffer, pH 8.0, 300 mM NaCl, 20 mM imidazole.

His elution buffer: 50 mM sodium phosphate buffer, pH 8.0, 300 mM NaCl, 250 mM imidazole.

2.4.2 Expression and purification of GST-tagged proteins

GST-BARS was purified as described in Valente et al., 2005.

2.4.3 Expression and purification of his-tagged proteins

His-BARS was purified as described in Valente et al., 2005.

2.5 General biochemical procedures

2.5.1 Materials

Sodium dodecyl sulphate (SDS), glycine, Trizma base, Ponceau red, polyoxyethylenesorbitan monolaurate (Tween-20), ammonium persulphate (APS) and N,N,N',N'-tetramethylethylenediamine (TEMED) were from Sigma–Aldrich

(WI,USA). The acrylamide stock solution, at 40% (w/v) acrylamide:bis-acrylamide (37.5:1), was from Eurobio (France). Acetic acid was from Carlo Erba (Italy). Secondary antibodies conjugated with horse radish peroxidase (HRP) and directed against mouse or rabbit IgGs were from Calbiochem (CA, USA). The ECL reagents were from Amersham Pharmacia Biotech (NJ, USA).

2.5.2 Solutions

Running buffer: 25 mM Trizma base, 200 mM glycine, 0.1% (w/v) SDS.

SDS sample buffer: 62.5 mM Tris-HCl, pH 6.8, 2% (w/v) SDS, 10% (v/v) glycerol, 5% (v/v) C-mercaptoethanol and 0.1% (w/v) bromophenol blue.

Transfer buffer: 25 mM Trizma base, 200 mM glycine, 20% (v/v) methanol.

TBS: 150 mM NaCl, 20 mM Tris-HCl, pH 7.5.

TTBS (TBS plus Tween 20): 0.05% (w/v) Tween 20, 150 mM NaCl, 20 mM Tris-HCl, pH 7.5.

Blocking solution for Western blotting: 1% (w/v) BSA in TTBS; 5% skimmed milk in TTBS.

2.5.2.1 Assembly of polyacrylamide gel

Two 16 cm x 18 cm plates were used for standard gels, while two 16 cm x 32 cm plates were used for long gels. The plates were assembled to form a chamber using two 1.5 mm plastic spacers aligned along the lateral edges of the plates. The plates were then fixed using two clamps and mounted onto a plastic base which sealed the bottom. All of the materials were from Hoefer Scientific Instruments (Germany). The 'running' polyacrylamide gel was prepared by mixing H₂O, 40% (w/v) acrylamide:bisacrylamide solution, 1.5 M Tris-HCl, pH 8.8, 10% (w/v) SDS, to have the selected concentration of acrylamide in 375 mM Tris-HCl, 0.1% (w/v) SDS. Then, 0.06% (w/v) APS and 0.06% (v/v) TEMED were added; the solution was mixed and poured into the gap between the plates, leaving ~5 cm for the stacking gel. Soon after pouring, the gel was covered with a layer of H₂O and left at RT for ~2 h. The H₂O layer was then removed. The 'stacking' polyacrylamide gel was prepared by mixing H₂O, 40% (w/v) acrylamide:bisacrylamide solution, 500 mM Tris-HCl, pH 6.8, 10% (w/v) SDS, to have 4% (w/v) acrylamide, 125 mM Tris-HCl, 0.1% (w/v) SDS. Then, 0.1% (w/v) APS and 0.07% (v/v) TEMED were added, and the solution was mixed and poured onto the running gel. Immediately, a 15-well or 10-well comb was inserted between the glass sheets and the apparatus was left for 1 h at RT.

2.5.2.2 Evaluation of protein concentration

Protein concentrations were evaluated using commercially available protein assay kits (Bio-Rad Laboratories, UK), according to the manufacturer instructions.

2.5.2.3 Sample preparation and running

Samples were prepared by adding SDS sample buffer, incubating at 100 °C for 5-10 min in a multi-block heater (Lab-Line, IL, USA), cooling to RT, briefly centrifuging, and finally loading onto the gel. One well was loaded with 5 µl Rainbow recombinant protein molecular weight markers (Amersham Pharmacia Biotech, NJ, USA) or with 5 µg Low Molecular Weight Standards (Bio-Rad Laboratories, UK). The gel was then transferred into the electrophoresis apparatus (Hoefer Scientific Instruments, NJ, USA), and the electrophoresis was carried out under constant current of 8 mA (for O/N runs) or 40 mA (for ~4-h runs).

2.5.3 Western blotting

2.5.3.1 Protein transfer onto nitrocellulose

The polyacrylamide gels were soaked for 15 min in transfer buffer, placed on a sheet of 3MM paper (Whatman, NJ, USA) and covered with a nitrocellulose filter (Schleicher & Schuell, Germany). The filter was covered with a second sheet of 3MM paper, to form a 'sandwich', which was subsequently assembled into the blotting apparatus (Hoefer Scientific Instruments, NJ, USA). The protein transfer was carried out at 500 mA for 4 h or at 125 mA O/N. At the end of the run, the sandwich was disassembled, and the nitrocellulose filter was soaked in 0.2% Ponceau red (Sigma-Aldrich, WI, USA) and 5% (v/v) acetic acid for 5 min, to appropriately visualise the protein bands, and then rinsed with 5% acetic acid, to remove excess unbound dye.

2.5.3.2 Probing the nitrocellulose with specific antibodies

The nitrocellulose filters were cut into strips with a razor blade. The strips containing the proteins of interest were incubated in the blocking solution for Western blotting plus 1% BSA or 5% milk powder (for ECL-based detection) for 1 h at RT, and then with the primary antibody diluted to its working concentration in the blocking solution for Western blotting (see Table 2.1, for list of antibodies used in the Western blotting). After a 2-3-h incubation at RT, or an O/N incubation at 4 °C, the antibody was removed and the strips were washed twice in TTBS, for 10 min each. The strips were next incubated for 1 h with the appropriate HRP-conjugated secondary antibody diluted in the blocking solution for Western blotting (antirabbit: 1:20,000; anti-mouse: 1:5,000) and washed twice in TTBS, for 10 min each, and once in TBS for 3 min. After washing, the strips were incubated with the ECL reagents, according to the manufacturer instructions for ECL-based detection.

2.6 Cell culture

2.6.1 Materials

African green monkey kidney (COS7), HeLa and HeLa CD8⁺ cells were from American Tissue Type Collection (ATTC, USA). HeLa shRNA TRCN0000154917 and HeLa shRNA TRCN0000127674 stable cell lines depleted for GRASP65 and GRASP55, respectively, were kindly provided by Dr Juan Duran from the Vivek Malhotra Laboratory. Dulbecco's modified Eagle's medium (DMEM), minimum essential medium (MEM), foetal calf serum (FCS), penicillin, streptomycin, trypsin-EDTA and L-glutamine were all from Gibco/BRL (NY, USA). All of the plastic cell culture materials were from Corning (NY, USA). Filters (0.45 µm, 0.20 µm) were from Amicon (MA, USA).

Table 2.1 List of antibodies used in the Western blotting.

Antibody target	Dilution	Animal source	Supplier source
BARS (BC3)	1:100	Mouse	Piccini D, IFOM-IEO Milan
BARS (p50 ₂)	1:1000	Rabbit	Lab Corda, Ibp, Naples
PI4KIIIβ	1:1000	Rabbit	De Matteis Lab, TIGEM, Naples
14-3-3γ	1:1000	Rabbit	De Matteis, TIGEM, Naples
GAPDH	1:70000	Mouse	Biogenesis
M2 Flag	1:5000	Mouse	Sigma,
GST	1:10000	Mouse	De Matteis, TIGEM, Naples
LPAATδ	1:1000	Rabbit	Abcam
LPAATγ	1:1000	Rabbit	Di Tullio, TIGEM, Naples
Penta-Histidine	1:1000	Mouse	Molecular Probes
GRASP65 C-20	1:5000	Goat	Santa-Cruz
GRASP55	1:1000	Mouse	BD Transduction
PKD2	1:1000	Rabbit	Bethyl
Myc	1:1000	Rabbit	Sigma
BFA	1:500	Rabbit	Covalab

2.6.2 Cell growth conditions

COS7, HeLa TRCN0000154917 and HeLa shRNA TRCN0000127674 cells were grown in DMEM supplemented with 4.5 g/l glucose, 2 mM L-glutamine, 1 U/ml penicillin and 1 mg/ml streptomycin, and 10% FCS.

HeLa and Hela CD8⁺ cells were grown in MEM supplemented with 2 mM L-glutamine, 50 U/ml penicillin and 50 µg/ml streptomycin, 10% FBS and 100 µM MEM non-essential amino-acids solution containing glycine, L-alanine, L-asparagine, L-aspartic acid, L-glutamic acid, L-proline and L-serine. Complete growth media were prepared by diluting stock solutions in DMEM or MEM, and filtering the resulting media through 0.2 µm filters. The cells were grown in flasks under a controlled atmosphere in the presence of 95% air/ 5% CO₂ at 37 °C, until they reached 90% confluence. For propagation, the medium was removed, the cells were washed with sterile PBS, and 0.25% trypsin solution was added for 2 min to 5 min. The medium was then added back to block the protease action of the trypsin, and the cells were collected in a plastic tube. After centrifugation for 5 min at 300x g, the pellet of cells was resuspended in fresh medium.

2.7 Immunoprecipitation and pull-down experiments

2.7.1 Immunoprecipitation procedures

2.7.1.1 Solutions

Lysis buffer: 20 mM Tris, pH 7.4, 150 mM KCl, 5 mM MgCl₂, 1 mM DTT, 1 mM EDTA, 1% (w/v) Triton X-100, protease inhibitor cocktail (Complete Mini EDTA-free, Roche) and phosphatase inhibitors (20 mM β-glycerophosphate, 1 mM sodium orthovanadate, 10 mM NaF).

2.7.1.2 Immunoprecipitation

All of the following steps were performed on ice or at 4 °C using ice-cold solutions, unless otherwise indicated. COS7 cells in 10-cm Petri dishes were transiently transfected with 7 µg of each DNA (BARS-pCDNA3, LPAATs-Flag) using 42 µl TransIT-LT1 per dish. Twenty-four hours after transfection, the cells were washed three times with PBS and lysed using 1 ml lysis buffer/ dish (25 mM Tris, pH 7.4, 150 mM NaCl, 5 mM EDTA, 5 mM MgCl₂, 10 mM NaF, 40 mM β-glycerophosphate, 1 mM Na₃VO₄, 1 mM DTT) supplemented with 1% (v/v) Triton X-100 and protease inhibitor mixture (30 min, 4 °C, shaking). The lysates were centrifuged (13,000× *g*, 10 min, 4 °C), and the supernatants were assayed for protein concentration (Bradford assay) and used fresh.

For BARS immunoprecipitation, 500 µg lysate protein from these COS7 cells was brought to 0.2% (v/v) Triton X-100 (final concentration), and incubated with 3 µg anti-BARS polyclonal antibody (overnight, 4 °C, shaking). Then 50 µl protein A Sepharose beads were added for a further 1 h of incubation (4 °C, shaking). For LPAAT immunoprecipitation, 1.2 mg lysate protein from the COS7 cells was brought to 0.2% (v/v) Triton X-100 (final concentration), and incubated with 40 µl anti-FLAG M2 affinity-gel-purified antibody (2 h, 4 °C, shaking).

For BARS immunoprecipitation in the presence of *Ec*LPAAT, 0.8 mg lysate protein from the COS7 cells was brought to 0.2% (v/v) Triton X-100 (final concentration) and incubated with 160 µg purified *Ec*LPAAT (2 h, 4 °C, shaking), and then incubated with 3 µg anti-BARS polyclonal antibody (overnight, 4 °C, shaking). The immune complexes were collected by centrifugation (500× *g*, 5 min, 4 °C). After three washes with lysis buffer with 0.2% Triton X-100, and twice with lysis buffer without Triton X-100, the bound protein was eluted from the protein A Sepharose beads or from anti-FLAG M2 affinity-gel-purified antibody by boiling (10 min) in 100 µl Laemmli buffer, separated by 10% SDS-PAGE, and subjected to Western blotting via transfer to nitrocellulose membranes (Millipore).

The BARS immunoprecipitation from HeLa (CD38+) cells treated with BFA/NAD was as described in Colanzi et al. 2013, with some modifications. The cells in 10-cm Petri dishes were transiently transfected with plasmids using 42 µl TransIT-LT1 and 7 µg of each DNA (BARS-YFP, LPAATδ-Flag) per dish. Sixteen hours after transfection, the cells were treated with vehicle alone (DMSO) as a control or with 80 µg/ml BFA in the presence of 5 mM NAD⁺ (2 h, 37 °C). The cells were then washed three times with PBS, lysed, and BARS immunoprecipitated.

COS7 cells (1 ×10⁶) in 10-cm Petri dishes were transiently transfected with plasmids using 42 µl TransIT-LT1 and 7 µg of each DNA per Petri dish. Twenty-four hours after transfection, the cells were washed with PBS, harvested by trypsinisation, pelleted and washed three times with PBS. Whole-cell extracts were obtained by resuspending and solubilising the cell pellets in lysis buffer on a shaker for 30 min at 4 °C. The lysates were centrifuged at 13,000× *g* for 10 min at 4 °C. Then, 500 µg of the lysate was incubated overnight with 5 µg mouse anti-Flag antibody, and 30 µl Protein-G Sepharose beads (Amersham) were added, with an incubation for an additional 1 h at 4 °C. After washing 3 times with lysis buffer and twice with lysis buffer without Triton X-100, the bound protein was eluted by boiling the samples for 10 min in 100 µl Laemmli buffer. The immunoprecipitated proteins and 30 µg total cell

lysate were separated on 10% SDS-PAGE gels (16 cm × 32 cm) and transferred onto nitrocellulose membranes (Millipore).

For BARS/GRASP55 co-immunoprecipitation, 500 µg lysate protein from HeLa cells transfected with 7 µg BARS pCDNA3 and synchronised in G2 or in M phase of the cell cycle, was brought to 0.2% (v/v) Triton X-100 (final concentration), and incubated with 3 µg anti-BARS polyclonal antibody (overnight, 4 °C, shaking). Then, 50 µl protein A Sepharose beads were added for a further 1 h of incubation (4 °C, shaking). The immune complexes were collected by centrifugation (500× g, 5 min, 4 °C). After three washes with lysis buffer with 0.2% Triton X-100, and twice with lysis buffer without Triton X-100, the bound protein was eluted from the protein A Sepharose beads by boiling (10 min) in 100 µl Laemmli buffer, separated by 10% SDS-PAGE, and subjected to Western blotting for GRASP55.

For GRASP65 immunoprecipitation, 500 µg lysate protein from HeLa cells synchronised in interphase or in G2 phase of the cell cycle was brought to 0.2% (v/v) Triton X-100 (final concentration), and incubated with 2 µg anti-GRASP65 antibody (overnight, 4 °C, shaking). Then 50 µl protein A Sepharose beads were added for a further 1 h of incubation (4 °C, shaking). The immune complexes were collected by centrifugation (500× g, 5 min, 4 °C). After three washes with lysis buffer with 0.2% Triton X-100, and twice with lysis buffer without Triton X-100, the bound protein was eluted from the protein A Sepharose beads by boiling (10 min) in 100 µl Laemmli buffer, separated by 10% SDS-PAGE, and subjected to Western blotting for GRASP65 and BARS.

2.7.2 GST and His pull-down assay

2.7.2.1 Solutions

GST incubation buffer: 20 mM Tris, pH 8.0, 100 mM KCl, 1 mM EDTA, 0.2% Triton X-100 and protease inhibitor cocktail (Complete Mini EDTA free, Roche).

GST elution buffer: 100 mM Tris, pH 8.0, 20 mM reduced glutathione, 5 mM DTT.

His lysis buffer: 50 mM sodium phosphate buffer, pH 8.0, 300 mM NaCl, 10 mM imidazole.

His wash buffer: 50 mM sodium phosphate buffer, pH 8.0, 300 mM NaCl, 20 mM imidazole.

His elution buffer: 50 mM sodium phosphate buffer, pH 8.0, 300 mM NaCl, 250 mM imidazole.

2.7.2.2 GST pull-down

Three micrograms *EclPAAT* was incubated with 3 µg GST as control or with 5 µg GST-BARS, in GST incubation buffer (20 mM Tris, pH 8.0, 1 mM EDTA, 0.2% Triton X-100, 100 mM KCl; overnight, 4 °C, shaking). Then, 30 µl glutathione Sepharose beads was added for a further incubation (1 h, 4 °C, shaking). The beads were then washed five times with GST incubation buffer, by centrifugation (500× g, 5 min). The bound protein was eluted from the glutathione Sepharose beads with GST elution buffer (100 mM Tris, pH 8.0, 20 mM glutathione, 5 mM dithiothreitol). The eluted protein was separated by 10% SDS-PAGE, and subjected to Western blotting via transfer to nitrocellulose membranes (Millipore).

For the GST pull-down with BAC-treated BARS, 5 µg GST-BARS was initially incubated with buffer alone (20 mM Tris, pH 7.4, 10 mM sucrose) or with 120 µM HPLC-purified BAC (Colanzi et al., 2013) (3 h, 37 °C), to allow binding of BAC to GST-BARS in the GST incubation buffer. For the GST pull-down with NAD-treated BARS, 5 µg GST-BARS was initially incubated with 50 µM NAD⁺ in GST incubation buffer (1 h, RT).

For the BARS-GST pull-down incubated with the GRASP65-myc (provided by the Vivek Malhotra Laboratory) overexpressing lysate blocked in G2 and M phase of the cell cycle, 1 mg lysate protein from GRASP65-myc tagged expressing cells in interphase or blocked in G2 phase of the cell cycle was incubated with GST alone or BARS-GST (2 h, 4 °C, shaking). Then, 30 µl glutathione Sepharose beads was added for a further incubation (1 h, 4 °C, shaking). The beads were then washed three times with GST incubation buffer, by centrifugation (500× *g*, 5 min). The bound protein was eluted from the glutathione Sepharose beads with GST elution buffer (100 mM Tris, pH 8.0, 20 mM glutathione, 5 mM DTT). The eluted proteins were separated by 10% SDS-PAGE, and subjected to Western blotting via transfer to nitrocellulose membranes (Millipore).

2.7.2.3 Histidine pull-down

His-BARS (20 µg) was incubated for 3 h at 37 °C with buffer alone (20 mM Tris, pH 7.4, 10 mM sucrose) or with 120 µM HPLC-purified BAC, to allow binding of BAC to His-BARS. The reaction mixture was stopped on ice, and 1 mg lysate protein from LPAATδ-Flag expressing cells was incubated with each sample (2 h, 4 °C, shaking). Then, 30 µl Ni-NTA agarose beads were added, and the samples were incubated (1 h, 4 °C, shaking). The beads were then washed three times with lysis buffer at pH 8.0 supplemented with 0.2% (v/v) Triton X-100 and 20 mM imidazole, by centrifugation (700× *g*, 5 min), and then twice with lysis buffer at pH 8.0 without Triton X-100 but supplemented with 20 mM imidazole. The bound protein was eluted from the Ni-NTA agarose beads by boiling (10 min) in 100 µl Laemmli buffer, separated by 10% SDS-PAGE, and subjected to Western blotting via transfer to nitrocellulose membranes (Millipore).

2.8 Cell transfection

2.8.1 Plasmids, chemicals and recombinant proteins

Human LPAAT cDNAs were from ImaGenes GmbH (for subcloning and mutations, see Extended Data Table 1); BARS-pCDNA3, BARS-YFP, BARS^{S147A}-YFP, BARS^{S147D}-YFP, and BARS^{D355A}-YFP were as previously described in Bonazzi et al. (2005), Liberali et al. (2008), Valente et al. (2012). LDLrY18A-GFP was provided by R. Polishchuk (TIGEM, Naples, Italy). CI-976 was from Tocris Bioscience, tannic acid and BFA from Fluka, protease inhibitors as Complete Mini EDTA-free from Roche, cycloheximide, Protein A Sepharose and anti-FLAG M2 affinity gel antibody beads from Sigma-Aldrich, oleoyl-LPA from Avanti Polar Lipids, oleoyl-1-[¹⁴C]-coenzymeA (specific activity, 60 mCi/mmol) and dioleoyl-1-[¹⁴C] phosphatidic acid (specific activity, 140 mCi/mmol) from PerkinElmer, siRNAs from Dharmacon, and TRICH-labelled dextran and FITC-labelled dextran from Molecular Probes. NAD⁺, BAC and HeLa (CD38+) cells were as previously described in Colanzi et al. (2013). Ni-NTA agarose and glutathione Sepharose beads were from Amersham, Protein A Gold was from Cell Microscopy Centre (University Medical Centre Utrecht). Recombinant purified

GST and GST-BARS proteins were prepared as described previously (Bankaitis et al., 2012), and His-plsC was from Cusabio.

2.8.2 TransIT-LT1-reagent-based cell transfection

The transfection mixture was prepared by diluting the TransIT-LT1 reagent in OptiMEM culture medium and incubating this at RT for 5 min. The DNA was then added to the transfection mixture, which was gently shaken, and kept at room temperature for another 20 min, to allow the DNA-TransIT-LT1 reagent complex to form. The cells were then incubated with the transfection mixture for 12 h to 48 h at 37 °C, in complete medium without antibiotics.

2.8.3 Lipofectamine LTX-based cell transfection

The transfection mixture was prepared by diluting the cDNA encoding VSVG-GFP (0.5 µg for a 24-well format) and the PLUS solution in OptiMEM medium and incubated at RT for 5 min. The Lipofectamine LTX was then added to the transfection mixture, which was gently shaken, and kept at RT for another 20 min, to allow the DNA-Lipofectamine LTX complex to form. The cells were then incubated with the transfection mixture for 1 h at 37 °C in complete medium without antibiotics and then shifted for 12 h at 40 °C.

2.8.4 siRNA transfection

2.8.4.1 Materials

SiRNAs were from Dharmacon (CO, USA), according to the following targets: 14-3-3 γ , D-008844-00; PI4KIII β , L-006777-00; BARS, M-008609-01; PAK1, D-003521-03; LPAAT3, J-008620-09; LPAAT4, D-009283-03; and si-control nontargeting siRNA pool, D-001206-13-20 (siRNA stocks, 20 µM). OptiMEM culture medium and Lipofectamine 2000 were from Invitrogen/Gibco (USA).

2.8.4.2 Procedures

Cells were plated in normal culture medium at a concentration suitable to have 25% confluence for transfection. One day later, a transfection mixture was prepared by diluting the siRNAs smart pool in OptiMEM medium, and Lipofectamine 2000 with the same medium in a separate tube, according to the manufacturer instructions. The tubes were gently shaken and incubated for 5 min at RT; after this, the diluted siRNAs smart pool was mixed with the diluted Lipofectamine 2000, which were then further incubated for 20 min at room temperature, to allow the siRNAs-Lipofectamine complex to form. The transfection mixture thus included the smart pool of the indicated siRNA sequences or the non-targeting siRNA (or mock transfection as control), and this was added to the cells in complete medium without antibiotics, with an incubation for an additional 48 h prior to the assays. The efficiency of interference was assessed by Western blotting.

In particular COS7 and HeLa cells were transfected with a non-targeting siRNA or with 150 nM of a Smart Pool of LPAAT δ /M-009283 or LPAAT γ /M-008620 siRNAs, for 72 h (except for BARS and 14-3-3s siRNAs, where 100 nM of a Smart Pool was used for 48 h) using Lipofectamine 2000, according to manufacturer instructions. The efficiency of interference was assessed by Western blotting. The treatment with Smart Pool siRNAs for LPAAT γ (M-008620) and for LPAAT δ (M-009283) specifically reduce the endogenous protein levels of LPAAT γ and LPAAT δ (by Western blotting) respectively, without affecting the levels of other tested LPAATs.

Alternatively, COS7 cells were transfected with the siRNAs (as above) in combination for the last 16 h with VSVG-GFP, LDLR^{Y18A}-GFP or p75-GFP, and then subjected to the specified Golgi-transport assay. For the rescue experiments, COS7 cells were transfected with siRNAs for LPAAT δ /D-009283-03 (5'-GCACACGGUUCACGGAGAA-3', Dharmacon) for 48 h, and transfected for a further 24 h (using TransIT-LT1) with Flag-LPAAT δ ^{wt} or Flag-LPAAT δ ^{H96V} (both encode an siRNA-resistant silent mutation), followed by infection with VSV for the TGN-exit assay.

2.9 Cell infection with vesicular stomatitis virus

2.9.1 Materials

For each infectious stock, the optimal working concentration was experimentally defined as the lowest that provided almost 100% infection of COS7 cells, as judged by staining for the viral membrane glycoprotein. Cycloheximide (Sigma Chemicals, WI, USA) was diluted in PBS to a concentration of 10 mg/ml (as 100 \times stock), and aliquots were stored at -20 °C.

2.9.2 Procedure

Cells were washed twice in serum-free culture medium and incubated with the diluted VSV infectious stock for 45 min at 32 °C. The virus was removed by replacing the infection medium with normal complete growth medium, and the cells were kept at 40 °C in a 95% air/ 5% CO₂ incubator for 2 h to allow VSV-G to accumulate in the endoplasmic reticulum (ER). After the incubation at 40 °C, the cells were kept at 20 °C for 2 h with 100 μ g/ml cycloheximide, to accumulate VSV-G in the Golgi complex, before shifting the temperature to 32 °C to follow Golgi-to-plasma membrane transport.

2.10 Electron microscopy

These procedures were performed by Gabriele Turacchio.

HeLa cells were transiently transfected with 8 μ g plasmid DNA encoding Flag-LPAAT δ for 24 h (using TransIT-LT1). The cells were then processed for cryo-immunogold EM. For cryo-immunoEM, the specimens were fixed, frozen, and cut using a ultramicrotome (Leica EM FC7). Cryo sections were double labelled for Golgin-97 (15-nm gold particles) and anti-LPAAT δ (10 nm gold particles). EM images were acquired using a FEI Tecnai-12 electron microscope.

2.11 Transport assays

2.11.1 VSVG transport from the TGN to the PM

For the TGN-exit assay of VSV-G, cells were transfected with VSV-G-GFP cDNA, or infected with VSV, or injected with the cDNA. The cells were then incubated for 2 h at 40 °C (12 h only when VSV-G was transfected), followed by 2 h at 20 °C (with 100 μ g/ml cycloheximide) to accumulate VSV-G in the Golgi complex. The temperature was then shifted to 32 °C, and the samples were fixed with 4% paraformaldehyde at the indicated times. To visualise VSV-G-containing carriers, 0.5% tannic acid was added to the VSV-G-infected or VSV-G-expressing cells just before the release of the 20 °C temperature block during the above TGN-exit assay (as described in Polishchuk et al., 2004). The cells were then shifted to 32 °C, fixed and labelled with the Cy3-conjugated P5D4 anti-VSVG antibody (for VSV infected cells). TGN-to-

plasma membrane transport carriers formed during the chase were counted using an LSM510 Zeiss confocal microscope.

The *trans*-Golgi network (TGN)-exit assay for p75-GFP-transfected, VSVG-GFP-transfected, and VSV-infected COS7 cells, microinjection, quantification of VSVG-containing post-Golgi carriers, and quantification of the Golgi-exit of p75 were all carried out as reported in Bonazzi et al. (2005) and in Valente et al. (2012). The COPI transport assay was performed as previously described in Yang et al. (2005). The transport of the endocytosis-defective LDL-GFP receptor (LDLrY18A) was performed as described previously in Peters et al. (2006). The CI-976 treatment was performed during the VSVG TGN-exit assay, at 50 μ M for 10 min, before the 32 °C temperature release block and during the 32 °C temperature release block. The anti-LPAAT δ antibody (1 mg/ml) was microinjected 1 h after the beginning of the 20 °C incubation in the VSVG transport assay and after 1 h of recovery the cells were then processed for wide-field microscopy. Wide-field microscopy was performed as described previously in Valente et al. (2012), with some modifications. COS7 cells were transfected with siRNAs for LPAAT δ (Smart Pool, Lipofectamine 2000), and after 48 h, the cells were transfected with VSVG-CFP (overnight, 40 °C) and then incubated with 100 μ g/ml cycloheximide (3 h, 20 °C). The cells were then shifted to 32 °C (with continued cycloheximide), and followed by fast videomicroscopy. For CI-976 treatment, COS7 cells were treated with 50 μ M CI-976 for 10 min before the shift to 32 °C.

2.12 Drug treatments

2.12.1 Ro3306 (*Cdk1 inhibitor IV*) treatment

HeLa cells were treated with 9 μ M Ro-3306 (Calbiochem) for 20 h, to block them in G2 phase of the cell cycle. The cells were then fixed or lysed, or the Ro-3306 was washed out, and the cells were left for 1 h in normal medium, to allow their entry into M phase.

2.12.2 CI-976 treatment

COS7 cells were treated with 50 μ M CI-976 (Tocris, USA) for 10 min before the release of 20 °C temperature block, and also during the chase at 32 °C. The cells were fixed after 0, 20 min or 40 min of chase, and assayed for VSV-G transport, or alternatively they were analysed by video microscopy.

2.13 LPAAT *in vitro* assays

2.13.1 Materials

OleoylLPA, was from Avanti Polar Lipids. [14 C]oleoylCoA was from Perkin Elmer. The dioleoyl-[14 C]PA standard was from Perkin Elmer. Thin layer chromatography (TLC) silica gel plates were purchased from Merck.

2.13.2 LPAAT *in-vitro* assays for BARS

2.13.2.1 Solutions

LPAAT reaction buffer: 75 mM Tris-HCl, pH 7.4, 4 mM MgCl₂, 1 mM DTT, 4 mM NaF, 1 mg/ml BSA fatty acid free, 200 μ M oleoylLPA, 20 μ M [14 C]oleoylCoA.

2.13.2.2 Preparation of oleoylLPA

OleoylLPA (10.9 mM, dissolved in chloroform/methanol, 1:1, v/v) was transferred to a glass tube, dried under a N₂ stream, resuspended in 20 mM Hepes, pH 7.4 (670 μM), and sonicated in a water bath.

2.13.2.3 Procedure

These procedures were performed by Carmen Valente.

Immunoprecipitated BARS (1.44 μg) or recombinant BARS (1.44 μg) was incubated in the LPAAT reaction buffer in a final volume of 100 μl, for 20 min at 25 °C. The reaction was stopped on ice by adding 5 μl cold CH₃OH/ 1 M HCl (1:1, v/v), vortexed, and then the lipids were extracted in 50 μl CHCl₃/CH₃OH (2:1, v/v). The lower organic phase was loaded onto oxalate pretreated TLC plates. The lipids were separated by running the TLC plates with CHCl₃/CH₃OH/NH₄OH/H₂O (54:42:2.9:9.1, v/v/v/v). The radiolabelled spots were quantified by gas ionisation counting (Instant Imager). [¹⁴C]PA was used as the standard.

2.13.3 LPAATδ *in-vitro* assay

2.13.3.1 Solutions

Lysis buffer: 100 mM Tris-HCl, pH 7.4, 5 mM NaCl, 3 mM MgCl₂, protease inhibitor cocktail (Complete Mini EDTA-free, Roche).

LPAAT reaction buffer: see section 2.13.2.1

2.13.3.2 Preparation of oleoylLPA

See section 2.13.2.2

2.13.3.3 Procedure

These procedures were performed by Carmen Valente.

All of the following steps were performed on ice or at 4 °C using ice-cold solutions, unless otherwise indicated. HeLa cells (1 × 10⁶) in 10-cm Petri dishes were transiently transfected with 8 μg plasmid DNA encoding Flag-LPAATδ^{wt} or Flag-LPAATδ^{H96V} for 48 h (using TransIT-LT1). Alternatively, the HeLa cells were transfected with siRNAs (as above) in combination with Flag-LPAATδ^{wt} for 48 h (using Lipofectamine 2000). The cells were washed three times with PBS, harvested as 250 μl/ dish in homogenisation buffer (100 mM Tris, pH 7.4, 5 mM NaCl, 3 mM MgCl₂) supplemented with the protease inhibitor mixture, and homogenised (6 pulses, 30% amplitude; Branson Digital Sonifier). The lysate was centrifuged at 600× *g* for 10 min at 4 °C. Two micrograms of this post-nuclear supernatant fraction was incubated with the LPAAT reaction buffer (75 mM Tris, pH 7.4, 4 mM MgCl₂, 1 mM DTT, 4 mM NaF, 1 mg/ml BSA fatty-acid free, 200 μM oleoylLPA, 20 μM [¹⁴C]oleoylCoA) in a final volume of 100 μl, for 20 min at 25 °C. The total lipids were extracted by adding 450 μl cold CHCl₃/CH₃OH (2:1, v/v). After 30 min on ice, the samples were centrifuged (10,000× *g*, 5 min). The lower, organic, phase was dried under a stream of nitrogen, resuspended in 50 μl CHCl₃, and loaded onto a oxalate-pretreated TLC plates. The lipids were separated by running the TLC plates with CHCl₃/ CH₃OH/ 33% NH₄OH/ H₂O (54:42:2.9:9.1; v/v/v/v). The radiolabelled spots were quantified by gas ionisation counting (Beta-Imager Systems, Biospace Laboratories). Dioleoyl [¹⁴C]PA was used as the standard.

For CI-976 treatment, the post-nuclear fraction from HeLa cells was incubated with 50 μM CI-976 for 30 min at 25 °C, followed by addition of LPAAT reaction buffer. For

anti-LPAAT δ antibody treatment, the post-nuclear fraction from HeLa cells was incubated with 50 ng anti-LPAAT δ affinity-purified polyclonal antibody for 30 min at 25 °C, followed by addition of LPAAT reaction buffer. For immunopurified BARS treatment, the post-nuclear fraction from HeLa cells was incubated with 500 ng immunoprecipitated BARS (purified from rat-brain cytosol with anti-BARS IgG cross-linked matrix for 30 min at 25 °C, followed by addition of LPAAT reaction buffer.

In these experiments, LPAAT δ -dependent activity (or LPAAT δ activity) is defined as the activity of LPAAT δ -overexpressing extracts minus the activity of LPAAT δ -depleted (or antibody-treated) extracts. In Figures 3.5-3.7, the LPAAT δ -independent activity (i.e., derived from LPAAT δ -depleted or antibody-treated extracts) is indicated with the dashed line. The LPAAT δ -independent activity was reproducibly 50% of the total activity in LPAAT δ -overexpressing extracts (as evaluated in more than 20 independent experiments).

2.14 Immunofluorescence

2.14.1 Materials

The Alexa 488-, Alexa 546- and Alexa 633-conjugated goat anti-rabbit and anti-mouse antibodies were from Molecular Probes (OR, USA).

2.14.2 Solutions

Samples on glass coverslips were mounted on glass microscope slides (Carlo Erba, Italy) using Mowiol (20 mg mowiol dissolved in 80 ml PBS, stirred O/N and centrifuged for 30 min at 12,000x g).

2.14.3 Sample preparation

Cells were fixed in 4% paraformaldehyde for 10 min at RT, washed three times in PBS, and incubated for 20 min at RT in blocking solution without or with saponin, as necessary. The cells were subsequently incubated with the specified antibodies diluted in blocking solution (see Table 2.2 for the list and dilutions of the antibodies used) for 1 h at RT or O/N at 4 °C. After incubation with the primary antibody, the cells were washed three times in PBS and incubated with a fluorescent-probe-conjugated secondary antibody directed against the constant region of the primary IgG molecule, for 45 min at RT. Commonly, Alexa 488-, Alexa 546- or Alexa 633-conjugated anti-rabbit or anti-mouse goat antibodies were used at a dilution of 1/400 in blocking solution. After immuno-staining, the cells were washed three times in PBS and twice in sterile water, to remove salts. The coverslips were then mounted on glass microscope slides (Carlo Erba, IT) with Mowiol.

Table 2.2 List of antibodies used in immunofluorescence experiments.

Antibody target	Dilution	Animal source	Supplier source
BARS (p50 ₂)	3 ng/μl	Rabbit	Corda, IBP, Naples
TGN46	1:1000	Sheep	AbDSerotec
M2 Flag	1:500	Mouse	Sigma
GM130	1:200	Mouse	BD Bioscience
VSVG	1:1000	Rabbit	Bethyl
VSVG P5D4 Cy3	1:400	Mouse	Sigma
LPAATδ	1:25	Rabbit	Sigma
14-3-3γ	1:100	Rabbit	De Matteis, TIGEM, Naples
PI4KIIIβ	1:100	Rabbit	De Matteis, TIGEM, Naples
GRASP65 C-20	1:50	Goat	Santa-Cruz
pS10H3 (06-570)	1:100	Rabbit	Millipore

2.14.4 Light and immunofluorescence analysis

Confocal images were acquired using a Zeiss LSM700 confocal microscope system (Carl Zeiss, Gottingen, Germany). Fixed cells were analysed using a 63× oil-immersion objective, maintaining the pinhole of the objective at 1 airy unit, with a resolution of 512 × 512 pixels or 1024 × 1024 pixels, and exported as .TIF files.

2.14.5 Fluorescence lifetime imaging microscopy measurements

This procedure was performed in collaboration with Fabio Formiggini. COS7 cells were transiently transfected with 0.5 μg BARS-YFP and 2 μg LPAATδ-CFP using LIPO LTX, according to manufacturer instructions. Sixteen hours after transfection, the cells were fixed at steady-state or subjected to the VSVG TGN-exit assay, and fixed after 2 h at the 20 °C temperature block. The fluorescence lifetime imaging microscopy measurements were performed as previously described in Valente et al., 2012.

2.15 Cell-cycle synchronisation

2.15.1. Materials

Thymidine was from Sigma–Aldrich (Milan, Italy). Dimethylsulfoxide (DMSO) was from Carlo Erba (Italy). RO-3306 was from Calbiochem.

2.15.2 HeLa-cell synchronisation

HeLa cells were grown on fibronectin-coated glass coverslips. As soon as they were attached to the coverslips, they were incubated in growth medium plus 2 mM thymidine for 16 h, and then rinsed and maintained in growth medium for 8 h. The cells were then incubated in medium with thymidine for an additional 16 h, before the final release of the cell-cycle arrest. At various times after this release (6 h to 13 h), the cells were fixed and the DNA was labelled with 2 μg/ml Hoechst 33342 and with the appropriate antibodies, depending on the experimental conditions. The mitotic index was estimated by measuring the number of cells showing clear mitotic (condensed chromosomes) and interphase (diffuse nuclear staining) features.

2.15.3 Preparation of mitotic and interphase extracts

The mitotic and interphase extracts were prepared by the method of Nakagawa et al. (1989). NRK cells were grown attached to 20 cm petri dishes and were incubated with 2 mM thymidine for 10 h to 12 h, to arrest the cells in S phase. The cells were then washed and incubated with 500 ng/ml nocodazole, O/N at 37 °C. This treatment arrested the cells in metaphase. The mitotic cells were rounded up by this treatment and were easily detached from the Petri dishes using a 'shake-off' procedure. The cells (95% mitotic index) were washed in PBS followed by mitotic extract buffer (MEB, see below), to remove the nocodazole. The cells were pelleted and resuspended in twice the packed cell volume with MEB. The cells were allowed to swell for 10 min on ice, and then homogenised by repeated passages through a 24 gauge needle. The homogenised cells were centrifuged in a table-top ultracentrifuge at 48,000 rpm for 45 min using a TLS55 rotor. The resulting high-speed supernatant (with an approximate protein concentration of 10-12 mg/ml) is termed the mitotic extract. This mitotic extract was aliquoted, frozen in liquid nitrogen, and stored at -80 °C. Interphase extract was prepared from untreated cells by scraping them with a rubber policeman. The buffer and homogenisation conditions were identical to those of mitotic extract.

The MEB contained 15 mM PIPES (pH 7.4), 50 mM KCl, 10 mM MgCl₂, 20 mM β-mercaptoethanol, 20 mM β-glycerophosphate, 15 mM EGTA, 0.5 mM spermidine, 0.2 mM spermine, 1 mM DTT, 0.1 mM phenylmethylsulphonyl fluoride, 0.2 mg/ml aprotinin, 0.2 mg/ml leupeptin, and 0.2 mg/ml pepstatin.

CHAPTER 3

RESULTS

3.1 Role of BARS in membrane trafficking

3.1.1 Introduction (Pagliuso et al. Manuscript under revision)

Membrane fission consists of a series of molecular rearrangements by which a tubular bilayer joining two membranous compartments undergoes constriction and splits in two parts without leakage of contents. It is required for the formation of transport vesicles during membrane traffic, organelle partitioning, cell division, and in general in the maintenance of the compartmental organisation of endomembranes. Fission has been studied intensely during the last decade, and it has been shown to be driven by diverse mechanisms (Kozlov, M. M., et al. 2010; Campelo, F et al. 2012; Pucadyil, T. J. et al. 2010; Johannes, L. et al. 2010), including membrane insertion of amphipathic protein domains (Campelo, F et al. 2012; Boucrot, E. et al 2012; Lee, M. C. et al. 2005; Adolf, F. et al 2013), constriction and destabilisation of membranes by the mechano-enzyme dynamin (Roux, A. 2013, Ferguson, S. M. & De Camilli, 2012; Schmid, S. L. & Frolov, V. A. 2011; Shnyrova, A. V. et al 2013; McMahon, H. T. & Boucrot, 2011; Daumke, O., et al 2014), and phase separation of lipid domains (Johannes, L. et al. 2010; Lenz, M., et al 2009). Nevertheless, the precise mechanics of fission remains elusive, and further analysis of the molecular steps leading to fission are still needed.

We have identified the protein CtBP1-S/BARS (henceforth, BARS) as a key player in the fission of post-Golgi tubular/ pleiomorphic carriers (Bonazzi, M. et al. 2005; Valente, C. et al 2012; Valente, C., et al 2013), macropinosomes (Liberali, P. et al 2008; Haga, Y., et al 2009) COPI-dependent transport vesicles (Yang, J. S. et al 2005; Yang, J. S. et al 2006; Yang, J. S. et al 2008), and the Golgi ribbon, during mitosis (Hidalgo Carcedo, C. et al 2004; Colanzi, A. et al. 2007). Structurally, BARS belongs to the D-hydroxyacid dehydrogenase family and includes a Rossmann fold (Nardini, M. et al, 2003) that regulates the interconversion of BARS between two (monomeric or dimeric) conformations, which depend on binding to NAD(H) or other ligands (Valente, C., et al 2013; Liberali, P. et al 2008; Nardini, M. et al, 2003; Nardini, M. et al., 2009; Colanzi, A. et al 2013). This conversion is critical because as a dual-function protein that controls fission in the cytoplasm and gene transcription in the nucleus (Valente, C., et al 2013; Corda, D., et al 2006; Chinnadurai, G. 2009), BARS can drive fission as a monomer, while it is fission-incompetent as a dimer (Liberali, P. et al 2008, Yang, J. S. et al 2005; Nardini, M. et al, 2003; Colanzi, A. et al 2013).

The mechanism of action of BARS in fission has been studied mostly in the context of the basolateral post-Golgi carrier formation process (Bonazzi, M. et al. 2005; Valente, C., et al 2013). Here, BARS assembles into a complex that includes Arf, frequenin, the phosphoinositide kinase PI4KIII β , 14-3-3 γ , and the kinases PKD and PAK, and this complex functions to coordinate the budding of carriers with fission (Valente, C. et al 2012; Valente, C., et al 2013). To induce fission, BARS must bind to 14-3-3 γ through a phosphorylated serine in its dimerisation surface (Ser147) (Valente, C. et al 2012; Valente, C., et al 2013) (see also below). This binding thus

locks BARS in its monomeric conformation. However, how 14-3-3 γ -bound BARS leads to the lipid rearrangements involved in fission remains unclear.

Previously, we proposed that BARS-dependent fission involves a lysophosphatidic acid (LPA) acyltransferase (LPAAT), based on the following observations: liver Golgi membranes contain an LPAAT(s), which upon addition of suitable substrates, generates phosphatidic acid (PA) (Weigert, R. et al 1999); PA production correlates with the fission of these Golgi membranes (Weigert, R. et al 1999); addition of BARS to the Golgi membranes stimulates both PA production and membrane fission (Weigert, R. et al 1999); and treatments that inhibit the formation of monomeric fission-competent BARS inhibit both LPAAT activity and membrane fission (Yang, J. S. et al 2005; Colanzi, A. et al 2013, Weigert, R. et al 1999). We have also reported that recombinant BARS is associated with a slow LPAAT activity (Weigert, R. et al 1999) (see below), which, however, was later shown not to be intrinsic to BARS (Gallop, J. L., et al 2005). Moreover, PA metabolism has been implicated in membrane transport by other groups, albeit generally based on indirect evidence (Liberali, P. et al 2008; Yang, J. S. et al 2008; Asp, L. et al 2009, Siddhanta, A., et al 2000; Stace, C. L. et al 2006; Baron, C. L et al 2002; Schwarz, K., et al 2011).

Based on these findings, here we examined whether BARS might bind to and stimulate an endogenous LPAAT, and how this can result in membrane fission. There are 11 known LPLATs, four of which have been cloned and shown to transfer fatty acids from acyl-CoA to the *sn*-2 position of LPA, to form PA (LPAAT α , β , γ , δ), while the others have mixed specificities for LPA and glycerol-phosphate (Yamashita, A. et al. 2014; Shindou, H., et al 2013). Here, I show that: BARS interacts with LPAAT type δ ; this LPAAT localises to the *trans*-Golgi and to post-Golgi carriers precursors; the catalytic activity of LPAAT δ is essential for Golgi carrier fission; BARS potently stimulates LPAAT δ , and this stimulation is essential for carrier fission; BARS needs to be incorporated in the PI4KIII β -14-3-3 γ -BARS complex (Valente, C. et al, 2012) to stimulate LPAAT δ and induce fission. BARS thus appears to behave as an 'active' scaffold that binds and stimulates LPAAT δ , inducing the LPA to PA conversion, and carrier fission. LPA and PA have unique biophysical properties that can strongly affect the organisation of lipid bilayers (Kooijman, E. E., et al 2003; Kooijman, E. E. et al. 2009, Kooijman, E. E. et al. 2005). Their interconversion might have a key role in several cellular fission events.

3.1.2 Results (Pagliuso et al. Manuscript under revision)

3.1.2.1 BARS interacts with a Golgi-localised protein, LPAAT δ (Pagliuso et al. Manuscript under revision)

To examine whether BARS interacts with an LPAAT, we first sought to identify the LPAATs that localise to the Golgi complex, as most of the BARS-dependent fission reactions occur in this organelle (Valente, C. et al. 2012; Valente, C. et al. 2013). We Flag-tagged and expressed the available mammalian LPAATs and inspected their localisation by immunofluorescence. LPAAT γ , LPAAT δ and LPAAT η localised to both the Golgi and the endoplasmic reticulum (ER) (Figure 3.1A), while LPAAT β and LPAAT ϵ localised to the ER and mitochondria (Figure 3.2; see also Asp, L. et al. 2009; Siddhanta, A., et al 2000). We thus investigated whether BARS interacts with the Golgi LPAATs, by co-expressing BARS with each of these transferases and testing for co-immunoprecipitation. BARS co-precipitated with LPAAT γ and LPAAT δ (and *vice-versa*), but not with LPAAT η (Figure 3.1B, C).

LPAAT γ has been shown to reside at the *cis*-Golgi and to regulate Golgi structure and retrograde transport to the ER (Schmidt, J. A. et al., 2009; Yang, J. S. et al., 2011), while LPAAT δ has no Golgi-related function that has been characterised to date. We examined whether the LPAAT δ location might be compatible with post-Golgi traffic, by studying the intra-Golgi location of this transferase using specific antibodies and immuno-electron microscopy (Figure 3.1D) as well as immunofluorescence (Figure 3.1E). LPAAT δ localised mostly to the *trans*-Golgi and *trans*-Golgi network (TGN) (Figure 3.1D,E) and to elongated tubules that emanated from the Golgi (Figure 3.1E).

Focusing further on LPAAT δ , we asked whether this transferase interacts selectively with the monomeric fission-competent form of BARS (Valente, C., et al 2013). As noted above, BARS shifts between these two conformations, depending on the ligand binding to its Rossmann fold. At steady-state, BARS is largely monomeric (Colanzi, A. et al 2013; Spanò, S. et al., 1999), while NAD(H) promotes dimerisation (Nardini, M. et al. 2003; Nardini, M. et al 2009; Colanzi, A. et al 2013; Birts, C. N. et al., 2013) and acyl-CoA promotes monomerisation (Yang, J. S. et al. 2005; Nardini, M. et al. 2003). Another BARS ligand is BAC (brefeldin-ADP-ribosylated conjugate), an ADP-ribosylated metabolite of brefeldin A that can also bind in the BARS Rossmann fold, which generates a covalent bond between its C3 atom and BARS Arg304 (Colanzi, A. et al 2013). This locks BARS in the dimeric inactive conformation very efficiently (Colanzi, A. et al 2013). BAC nearly abolished the association between BARS and LPAAT δ (Figure 3.1F,G), which indicated that BARS binds LPAAT δ in its monomeric form. Thus, an LPAAT isoform located in the *trans*-Golgi binds selectively with the fission-active form of BARS.

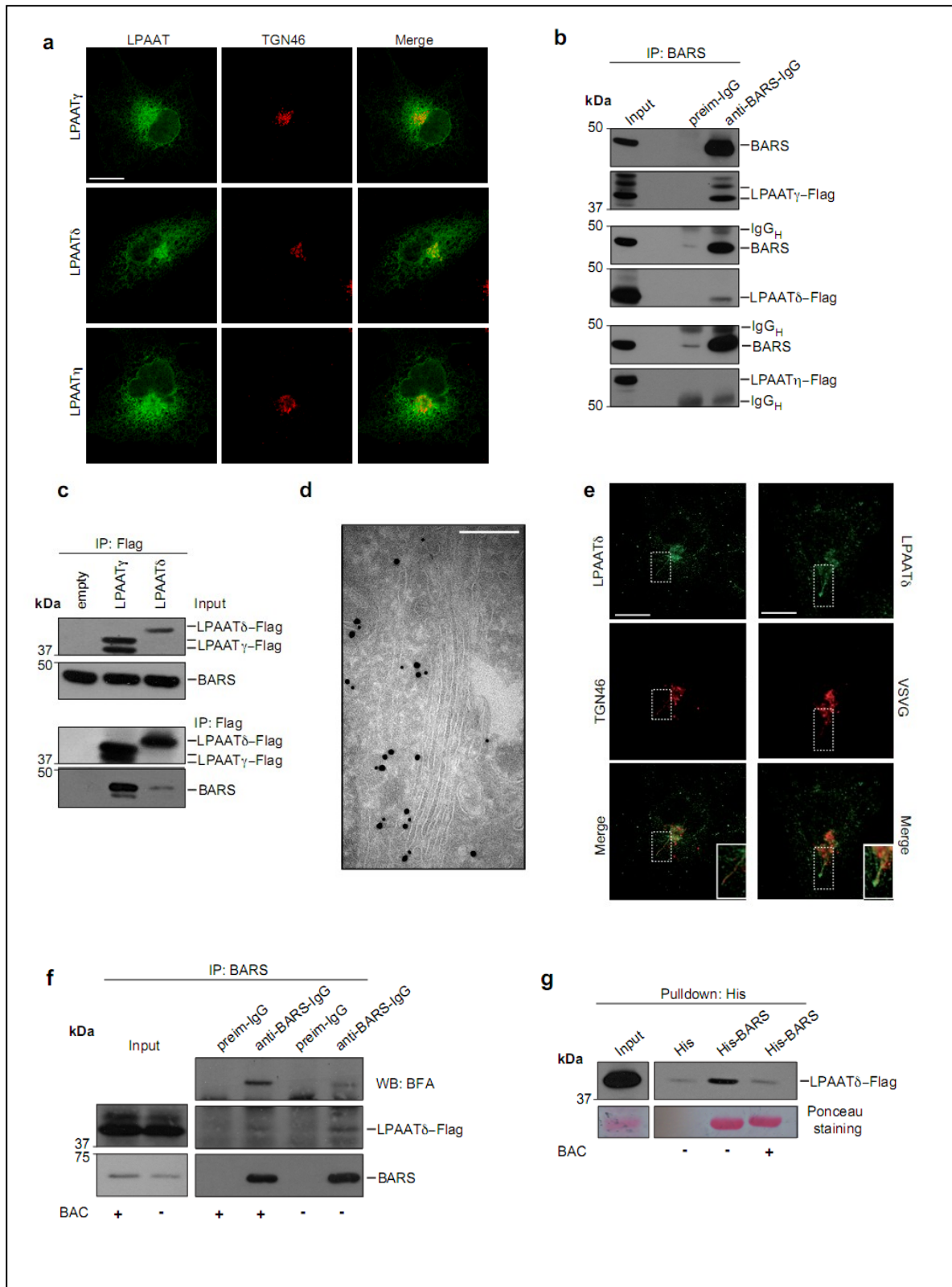


Figure 3.1 BARS interacts with the *trans*-Golgi localised LPAAT δ .

(A) Representative confocal microscopy images of COS7 cells transfected for Flag-tagged LPAAT γ , LPAAT δ and LPAAT η , and fixed and processed for immunofluorescence with a monoclonal anti-Flag antibody (green) and with a polyclonal anti-TGN46 antibody (red; as indicated). **(B)** BARS immunoprecipitation (IP: BARS) of lysate from COS7 cells co-expressing LPAAT γ -Flag, LPAAT δ -Flag or LPAAT η -Flag with BARS. Representative Western blotting (antibodies as indicated) of total lysate (input) and immunoprecipitated proteins with preimmune-IgG (preim-IgG) or anti-BARS-IgG (as indicated). IgG_H, IgG heavy chain. **(C)** Immunoprecipitation with an anti-Flag antibody (IP: Flag) of lysate from COS7 cells co-transfected with LPAAT γ -Flag, LPAAT δ -Flag or empty vector with BARS. Representative Western blotting of total lysate (input) and Flag-immunoprecipitated proteins with an anti-Flag monoclonal antibody or the anti-BARS polyclonal antibody (as indicated). **(D)** Representative electron microscopy image of HeLa cells transfected with Flag-tagged LPAAT δ for 24 h, and fixed and processed for cryo-immuno-electron microscopy with a monoclonal anti-Golgin 97 antibody (15-nm gold particles) and with a polyclonal anti-LPAAT δ antibody (10-nm gold particles). **(E)** Representative confocal microscopy images of COS7 cells at steady-state (left) or VSV-infected and subjected to the VSVG TGN-exit assay (right). Cells were fixed and labelled with a monoclonal anti-LPAAT δ antibody (green) and with a polyclonal anti-TGN46 antibody (red; left) or a polyclonal anti-VSVG antibody (red; right). Inset, right: Magnification of tubular carrier precursors. **(F)** BARS immunoprecipitation (IP: BARS) of control or BFA/ NAD⁺-treated lysates (\pm BAC) from HeLa (CD38+) cells with preimmune-IgG (preim-IgG) or anti-BARS-IgG. Representative Western blotting with anti-BFA polyclonal and anti-Flag monoclonal antibodies of total lysate (input) and BARS-immunoprecipitated proteins. The anti-BFA analysed blot (WB: BFA) was then reprobbed with an anti-BARS monoclonal antibody (as indicated). **(G)** Histidine pull-down for His or His-BARS beads of lysates from COS7 cells transfected with LPAAT δ -Flag. Beads were treated with buffer alone (-) or with HPLC-purified BAC (BAC +), and then incubated with the lysates. The eluted proteins were analysed by Western blotting using a monoclonal anti-Flag antibody (top), with the pulled-down His-BARS revealed by Ponceau staining (bottom). Molecular weight standards (kDa) in (b, c, f, g) are indicated on the left of each panel. Data are representative of three independent experiments. Scale bars: 10 μ m (a, e), 200 nm (d). (from Pagliuso *et al.* Manuscript under revision)

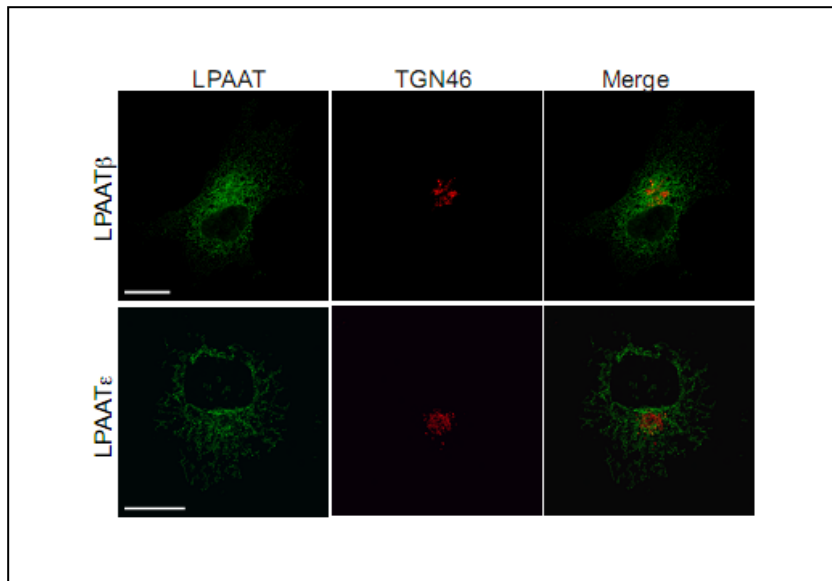


Figure 3.2 Localisation of LPAAT β and LPAAT ϵ

Representative confocal microscopy images of COS7 cells transfected with Flag-tagged LPAAT β and LPAAT ϵ (as indicated) for 24 h, and fixed and processed for immunofluorescence with a monoclonal anti-Flag antibody (green; LPAAT) and with a polyclonal anti-TGN46 antibody (red; TGN). Scale bars: 10 μ m. (from Pagliuso *et al.* Manuscript under revision)

3.1.2.2 *Escherichia coli* LPAAT binds to the fission-active BARS conformation and competes with LPAAT δ for BARS binding (Pagliuso *et al.* Manuscript under revision)

As noted, recombinant BARS purified from *Escherichia coli* is associated with low levels of LPAAT activity (Weigert, R. *et al.* 1999, Gallop, J. L., *et al.* 2005). We carried out a series of pull-down experiments to examine whether purified BARS and *E. coli* LPAAT bind in a specific fashion. His-tagged *E. coli* LPAAT (which can be prepared in a soluble form) (Coleman, J. *et al.*, 1992) showed strong binding with recombinant BARS (Figure 3.3A), and this binding was abolished by pretreatments with BAC or NAD(H), which indicated that *E. coli* LPAAT binds selectively to monomeric BARS (Figure 3.3B,C). We also asked whether *E. coli* LPAAT can compete with mammalian LPAAT δ for binding to BARS (Figure 3.3D), and found this to be the case, which indicated that the mammalian and bacterial LPAATs bind to the same BARS domain. These data suggest that the LPAAT δ and *E. coli* LPAAT BARS-binding surfaces are conserved. Considering the evolutionary distance between the two LPAATs, this is somewhat surprising. It is conceivable, however, that the evolutionary ancestors of LPAAT δ and BARS (namely, the bacterial LPAAT and 3-phospho-glycerate dehydrogenase, respectively) (Coleman, J. *et al.*, 1992; Nardini, M. *et al.* 2003), which are both metabolic enzymes, were interactors in an ancient metabolic multi-enzyme complex (Ovadì, J. & Srere, P. A., 2000), and that this interaction was maintained through evolution in different functional contexts.

These data thus explain our previous observation that BARS purified from *E. coli* associates with an LPAAT activity (Weigert, R. *et al.* 1999), and this provides a potentially useful tool (the soluble bacterial enzyme) for the *in-vitro* reconstitution of BARS-dependent fission (see below).

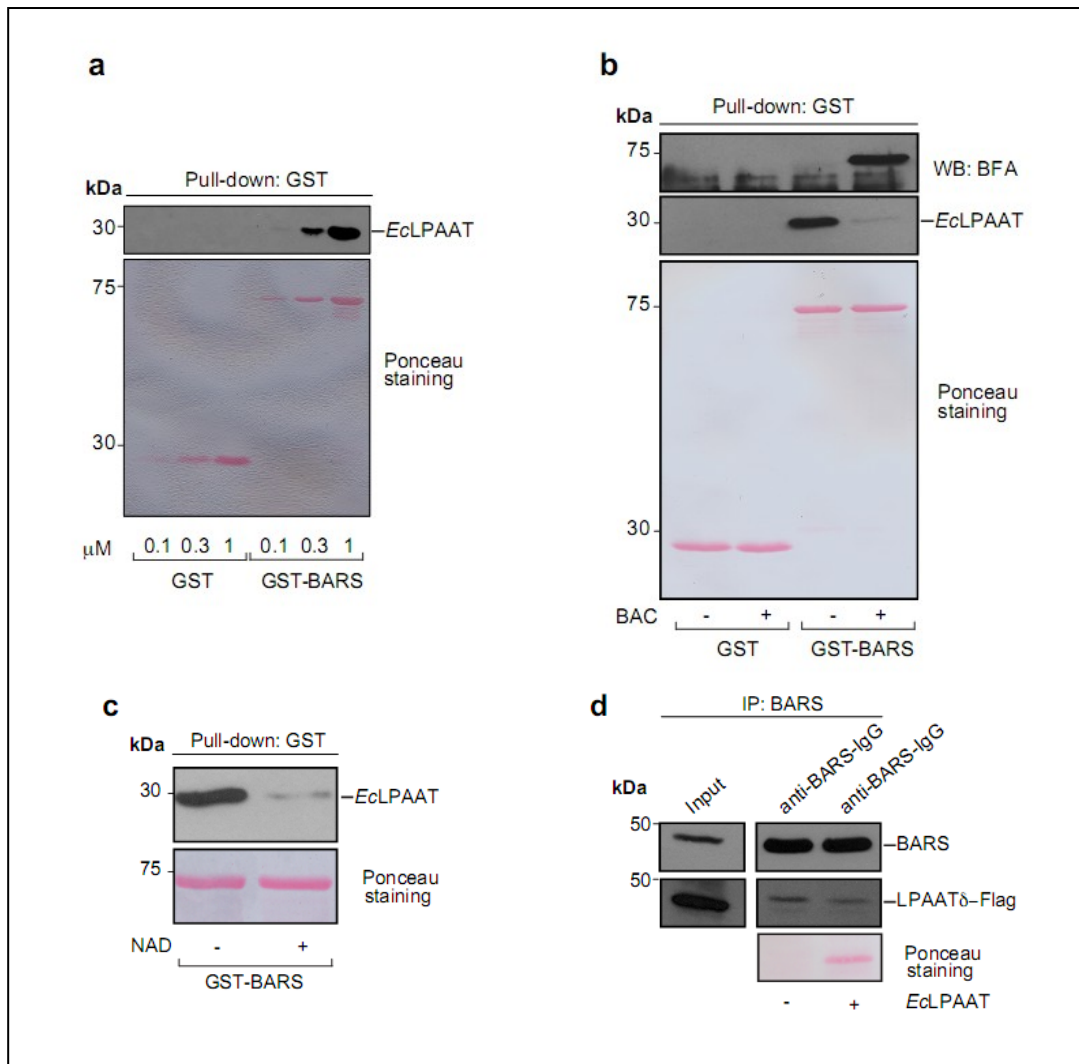


Figure 3.3 BARS binds *Escherichia coli* LPAAT in a conformation-dependent fashion.

Representative GST pull-down assays for GST and GST-BARS beads (as indicated). **(A)** Using recombinant His-tagged *E. coli* LPAAT (*EcLPAAT*). **(B)** Using buffer alone (-) or HPLC-purified BAC (BAC +), and then incubated with recombinant *EcLPAAT*. **(C)** Using buffer alone (-) or 50 mM NAD^+ (NAD +), and then incubated with recombinant *EcLPAAT*. The eluted proteins were analysed by Western blotting (top) using an anti-histidine antibody to monitor *EcLPAAT* in (a-c), and an anti-brefeldin A antibody (WB: BFA) to monitor ADP-ribosylation, in (b). The pulled-down proteins were revealed by Ponceau-S staining (bottom). **(D)** Representative Western blotting with anti-BARS and anti-Flag antibodies for BARS immunoprecipitation (IP: BARS) of lysate from COS7 cells transfected with LPAAT δ -Flag in the absence (-) or presence (*EcLPAAT* +) of recombinant purified *EcLPAAT* with anti-BARS IgG. Total lysate (input) and BARS-immunoprecipitated protein are shown. Molecular weight standards (kDa) are indicated on the left of each panel. (from Pagliuso *et al.* Manuscript under revision)

3.1.2.3 LPAAT δ is required for post-Golgi carrier fission (Pagliuso *et al.* Manuscript under revision)

The TGN localisation and the interaction of LPAAT δ with BARS prompted us to investigate the role of this enzyme in the BARS-dependent formation of post-Golgi carriers (Bonazzi, M. *et al.* 2005). LPAAT δ was silenced with specific small-interfering (si)RNAs, and the formation of carriers was monitored using the temperature-sensitive vesicular stomatitis virus G protein (ts045-VSVG; henceforth, VSVG) (Mironov, A. A. *et al.* 2001) as a traffic marker. The transport of VSVG out of the Golgi can be synchronised by accumulating VSVG in the TGN at 20 °C and then shifting to the permissive temperature of 32 °C (Bonazzi, M. *et al.* 2005). The formation and release of VSVG-containing tubular carriers from the TGN can then be visualised and quantified by immunofluorescence microscopy (Bonazzi, M. *et al.* 2005, Valente, C. *et al.* 2012; Polishchuk, R., *et al.* 2004). Depletion of LPAAT δ markedly reduced the formation of the VSVG-containing carriers (Figure 3.4A); whereas depletion of LPAAT γ , which is located at the *cis*-Golgi and is involved in Golgi-to-ER traffic (Schmidt, J. A. *et al.* 2009; Yang, J. S. *et al.* 2011), had no effect (Figure 3.4B). To determine whether the reduction in VSVG-containing carriers was due to inhibition of carrier budding or of fission, we monitored carrier formation in living cells expressing VSVG-GFP. LPAAT δ -depleted cells showed a large number of long (>10 μ m) tubular extensions that contained VSVG-GFP, which appeared to be carrier precursors. These elongated out of the Golgi but did not detach, and often retracted back into the Golgi area without forming free-moving intermediates. This phenotype was similar to that induced by expressing BARS dominant-negative mutants or by depleting BARS (we noted that BARS depletion also reduced the number of tubular precursors), or by depleting the PI4KIII β -14-3-3 γ dimer-BARS complex component 14-3-3 γ (Valente, C. *et al.* 2012, Valente, C. *et al.* 2013). Very similar effects were induced by microinjection of an affinity-purified antibody against LPAAT δ and by the general LPAAT inhibitor CI-976 (Drecktrah, D. *et al.*, 2003). These collective observations are consistent with an essential role for LPAAT δ in carrier fission from the Golgi complex.

We also determined the role of LPAAT δ in other traffic steps. We first examined retrograde traffic from the Golgi to the ER (which is known to require LPAAT γ) (Schmidt, J. A. *et al.* 2009; Yang, J. S. *et al.* 2011), by tracking the retrograde transport marker VSVG-KDEL (a fusion of VSVG with the KDEL receptor) (Cole, N. B., *et al.* 1998). Transport of VSVG-KDEL was not affected by LPAAT δ depletion (Figure 3.4C). Secondly, as BARS controls the fission of basolateral but not of apical carriers (Bonazzi, M. *et al.* 2005), we examined the role of LPAAT δ in Golgi export of p75 (an apical cargo) (Yeaman, C. *et al.*, 1997) in comparison with export of the low-density lipoprotein (LDL) receptor (a basolateral cargo, like VSVG) (Matter, K., *et al.*, 1992). Depletion of LPAAT δ inhibited export of the LDL receptor (Figure 3.4D), as with VSVG, but not that of p75 (Figure 3.4E). Therefore, LPAAT δ appears to be selectively required for fission of basolateral carriers.

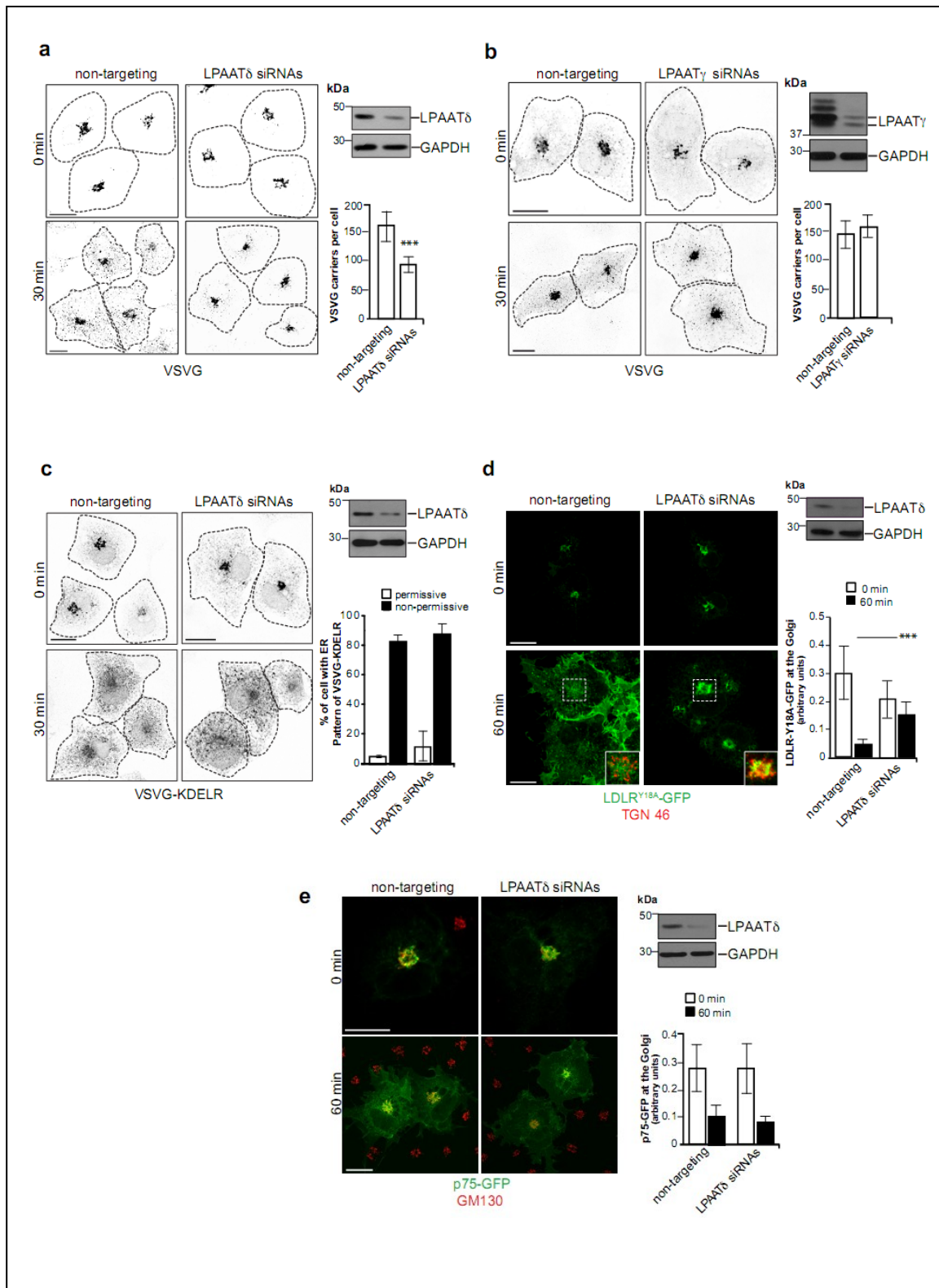


Figure 3.4 LPAAT δ is required for the fission of basolaterally directed carriers. (A, B) Representative images of COS7 cells treated with non-targeting and *LPAAT δ* siRNAs (a) or *LPAAT γ* siRNAs (b) before VSV infection and the TGN-exit assay with 0.5% tannic acid. The cells were fixed following a 20 °C block (0 min) or 30 min after the shift to 32 °C, and stained for VSVG-positive post-Golgi carriers. Quantification of

VSVG-containing carriers (right). **(c)** Representative images of COS7 cells treated with non-targeting and *LPAATδ* siRNAs before co-transfected for the last 16 h with VSVG-ts045-KDEL_R-myc. The cells were then examined for the distribution of the chimeric KDEL_R by immunofluorescence microscopy following the shift to the non-permissive temperature for 30 min. Quantification of ER distribution of the chimeric KDEL_R (right). **(A-C)** Dotted lines indicate cell borders. **(D, E)** Representative confocal microscopy of COS7 cells treated with non-targeting and *LPAATδ* siRNAs and co-transfected for the last 16 h with the endocytosis-defective LDLR-GFP receptor (LDLR^{Y18A}-GFP; green) **(D)** or with a plasmid encoding p75-GFP (green) **(E)**. **(D)** Following a 2 h at 20 °C transport block (0 min) and 60 min after the shift to the permissive temperature for transport (32 °C; with cycloheximide to inhibit protein synthesis), the cells were fixed and labelled with TGN46 (Golgi marker; red). Insets: Enlarged view of merged signals for the Golgi area. **(e)** Following the 3 h at 20 °C transport block (0 min) and 60 min after the shift to the permissive temperature for transport (32 °C; with cycloheximide), the cells were fixed and stained for GM130 (Golgi marker; red). **(D, E)** Quantification of LDLR^{Y18A}-GFP (d) and p75-GFP (e) in the Golgi area (right). **(A-E)** The efficiency of interference was monitored by Western blotting of the cell lysates using polyclonal anti-*LPAATδ* **(A, C-E)** or polyclonal anti-*LPAATγ* **(B)** antibodies. Glyceraldehyde 3-phosphate dehydrogenase (GAPDH) is shown for the internal protein levels and molecular weight standards (kDa) are indicated on the left of each panel **(A-E)**. Data are means ±s.d. of three independent experiments. ****P* <0.005 (Student's *t*-tests). Scale bars, 10 μm. (from Pagliuso et al. Manuscript under revision)

3.1.2.4 The enzymatic activity of *LPAATδ* is needed for post-Golgi carrier fission. (Pagliuso et al. Manuscript under revision)

In parallel Dr. Carmen Valente has examined whether the enzymatic activity of *LPAATδ* (Eto, M. et al., 2014) was required for fission, and she assessed *LPAATδ* activity and post-Golgi carrier fission in parallel experiments. To determine the *LPAAT* enzymatic activity, she prepared and incubated post-nuclear supernatants with the acyl donor [1-¹⁴C]oleoyl-CoA and the acyl acceptor oleoyl-LPA, with [1-¹⁴C]PA measured as the reaction product (see Section 2.13 and Figure 3.5A). Since attempts to purify *LPAAT* enzymes results in activity loss (Eto, M. et al., 2014; Chen, Y. Q. et al., 2008), these are the standard conditions used for *LPAAT* assays (Eto, M. et al., 2014; Chen, Y. Q. et al., 2008). Extracts from control cells showed a transferase activity that was suppressed by the general *LPAAT* inhibitor CI-976 (Figure 3.5B) (Yang, J. S. et al 2011; Chambers, K., et al. 2005) A difficulty with these extracts is that they contain multiple *LPAATs*. She therefore designed conditions to determine selectively the *LPAATδ* activity (Figure 3.5A) based on suppressing or overexpressing this enzyme. Extracts from *LPAATδ*-depleted cells (Figure 3.5A), or treatment of control extracts with a specific affinity-purified antibody against *LPAATδ* (Figure 3.5B) showed a reproducibly lower (25%) activity than in controls (Figure 3.5A,B), which indicated that *LPAATδ* is responsible for a small fraction of the total *LPAAT* activity. This is indeed in line with the presence of other *LPAATs* and in particular of the abundant glycerolipid synthetic enzymes *LPAATα* and *LPAATβ* (Yamashita, A. et al 2014; Leung, D. W. 2001). Extracts from *LPAATδ*-overexpressing cells showed a 40% increase in *LPAAT* activity over controls (Figure 3.5 A-C). This increase was completely inhibited by the antibodies against *LPAATδ*, which decreased the *LPAAT* activity (Figure 3.5B) to the levels found in the absence

of LPAAT δ (Figure 3.5A). LPAAT δ silencing or overexpression did not affect the cellular levels of other LPAATs. Similar data were obtained using [1- 14 C]palmitoyl-CoA as acyl donor and arachidonoyl-LPA as acyl acceptor. She thus defined the LPAAT δ -dependent activity (or LPAAT δ activity) as the activity of LPAAT δ overexpressing extracts (as measured using concentrations of substrates below the K_m values, see below), minus the activity of LPAAT δ depleted (or antibody-treated) extracts (Figure 3.5A, B, see dashed line). The V_{max} and K_m of this LPAAT δ activity were 38 ± 3 nmol/min/mg protein and 58 ± 18 μ M, respectively, for oleoyl-CoA, and 38 ± 1 nmol/min/mg protein and 29 ± 1 μ M, respectively, for oleoyl-LPA. These rates are comparable to those reported for LPAAT γ (see Yuki, K., et al 2003). Importantly, simple calculations show that they are potentially sufficient, depending on substrate availability, to change rapidly and substantially the PA concentrations in the TGN. Finally, she asked whether the LPAAT δ catalytic activity is required for post-Golgi carrier fission. She generated a single-point mutant (LPAAT δ^{H96V}) in the conserved acyltransferase catalytic site of LPAAT δ (NHX $_4$ D) (Yamashita, A. et al. 2014; Lewin, T. M., 1999). Overexpressed LPAAT δ^{H96V} was indeed devoid of LPAAT activity (Figure 3.5C) confirming that LPAAT δ is a canonical LPAAT. She then depleted cells of LPAAT δ , with the consequent inhibition of the post-Golgi transport of VSVG (see Figure 3.4A) and expressed either a siRNA-resistant variant of LPAAT δ or the catalytically dead LPAAT δ^{H96V} mutant. Only wild-type LPAAT δ rescued carrier formation, while LPAAT δ^{H96V} was completely inactive (Figure 3.5D). These data indicate that LPAAT δ has substantial catalytic activity and that this activity is necessary for post-Golgi carrier formation.

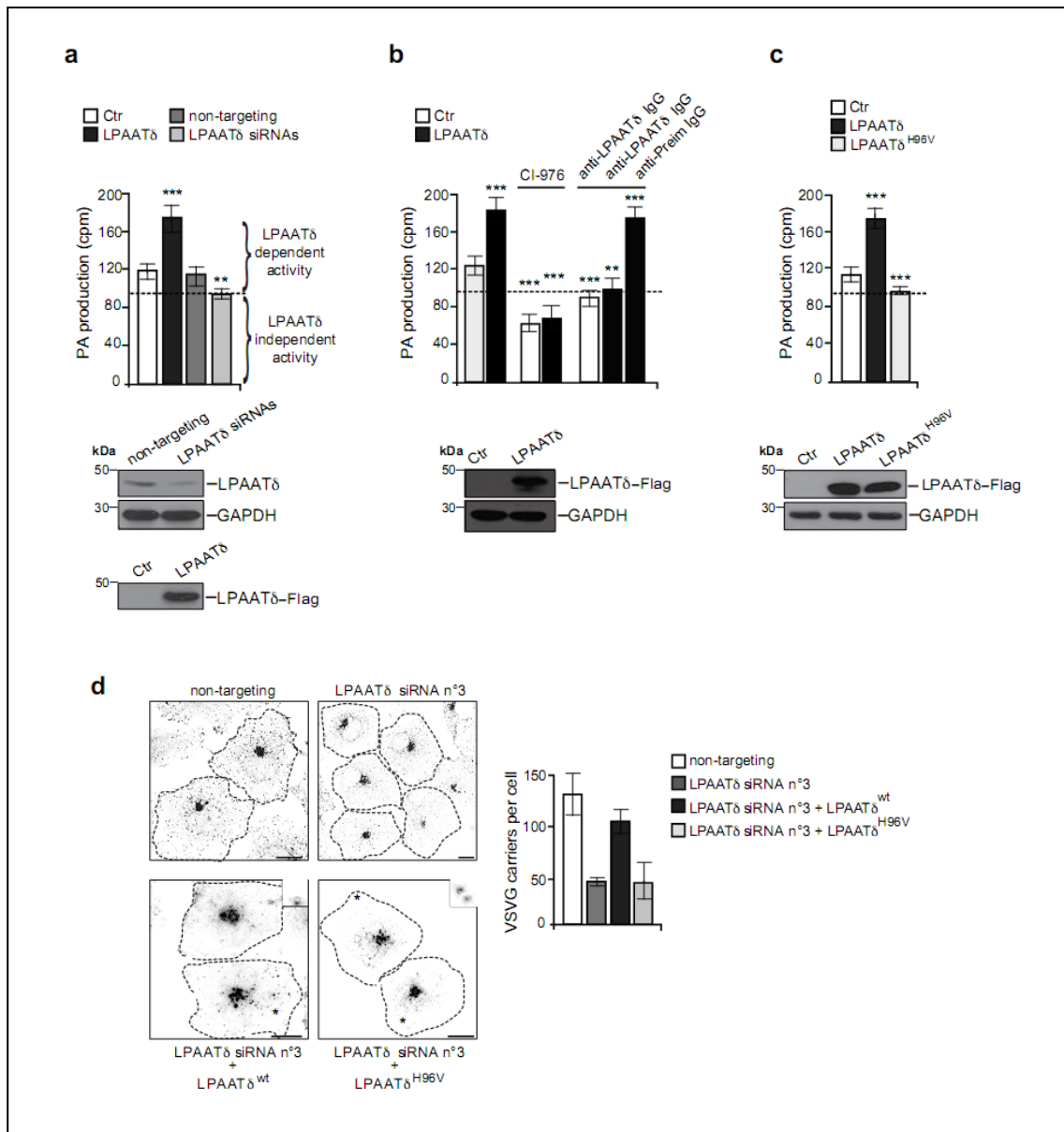


Figure 3.5 LPAAT δ is a canonical LPAAT and its activity is required for post-Golgi carrier formation.

(A) Quantification of phosphatidic acid (PA) production in the LPAAT assay for postnuclear supernatants from HeLa cells transfected for 48 h with an empty Flag-vector (Ctr) or with LPAAT δ -Flag (LPAAT δ), or for 72 h with non-targeting or LPAAT δ siRNAs. The parentheses indicate the LPAAT δ -dependent and independent activities. **(B)** Quantification as in (a), with the post-nuclear fractions also incubated with 50 μ M CI-976, or polyclonal anti-LPAAT δ antibody (anti-LPAAT δ IgG), or anti-preimmune IgG (anti-Preim IgG; as control) for 30 min at 25 °C before LPAAT assay. **(C)** Quantification as in (a), also in parallel with the LPAAT δ ^{H96V}-Flag (LPAAT δ ^{H96V}) catalytically inactive mutant. **(A-C)** The dashed line indicates the level of endogenous LPAAT activity not associated with LPAAT δ (see text for details). Bottom: representative Western blotting with an anti-Flag antibody, for the transfection efficiencies of these proteins used for the LPAAT assays. Glyceraldehyde 3-phosphate dehydrogenase (GAPDH) is shown for the internal protein levels.

Molecular weight standards (kDa) in (a-c) are indicated on the left of each panel. **(D)** Representative images of COS7 cells transfected with non-targeting or *LPAATδ* siRNA (duplex 3; *LPAATδ* siRNA n°3), and with *LPAATδ*^{wt}-Flag or the *LPAATδ*^{H96V}-Flag catalytically inactive mutant, and subjected to VSV infection and the TGN-exit assay with 0.5% tannic acid. The cells were fixed 30 min after the shift to the permissive temperature (32 °C) and processed for immunofluorescence with monoclonal anti-Flag and polyclonal anti-VSVG (p5D4) antibodies, to monitor formation of VSVG-containing carriers. Dotted lines show cell borders. Asterisks represent *LPAATδ*^{wt}-Flag and *LPAATδ*^{H96V}-Flag transfected cells (see inserts for staining with anti-Flag antibody; bottom images). Scale bars, 10 μm. Quantification of VSVG-positive carriers (right). Data are means ±s.d. of three independent experiments. ***P* <0.01, ****P* <0.005 versus control (Student's *t*-tests). (from Pagliuso et al. Manuscript under revision)

3.1.2.5 BARS activates *LPAATδ*, and this activation is required for carrier fission. (Pagliuso et al. Manuscript under revision)

As BARS and *LPAATδ* interact (Figure 3.1) and are required for post-Golgi carrier fission (see Bonazzi, M. et al. 2005; Valente, C. et al. 2012), Dr. Carmen Valente investigated whether BARS might regulate the enzymatic activity of *LPAATδ*, and whether this regulation might be required for carrier fission. She first silenced BARS and measured the *LPAATδ* activity in cell extracts. BARS depletion abolished this activity (Figure 3.6A). She then re-expressed BARS in BARS-silenced cells, using a siRNA-resistant replacement BARS construct. This nearly completely restored the *LPAATδ* activity (Figure 3.6A). As a specificity control, the above BARS manipulations did not affect the cellular levels of *LPAATδ* or of other *LPAAT*s. These results indicate that *LPAATδ* requires BARS to express its activity.

She then sought to manipulate the BARS levels acutely *in-vitro* to exclude transcriptional or compensatory effects that might arise in siRNA depletion experiments (Valente, C. et al. 2013; Corda, D., et al 2006; Chinnadurai, G. 2009). She prepared extracts from *LPAATδ*-expressing BARS-depleted cells, where *LPAATδ* is inactive (Figure 3.6A), and added immunopurified BARS to the assay mixture to reach a final BARS concentration of 5 μg/ml (comparable to the levels of endogenous BARS) (Bonazzi, M. et al. 2005; Haga, Y., et al 2009). Under these conditions, BARS completely restored the *LPAATδ*-dependent activity (Figure 3.6B) (notably, the *LPAAT* activity associated with the purified BARS was quantitatively negligible) (Weigert, R. et al, 1999; Gallop, J. L., et al 2005). She also added BARS to control *LPAATδ*-expressing extracts. This only slightly stimulated the *LPAATδ*-dependent activity (Figure 3.6B), which suggested that endogenous BARS is sufficient to activate *LPAATδ* nearly maximally, at least in preparations from quiescent cells (i.e., in cells not subjected to a traffic pulse; see below). As a further control, she used extracts from cells depleted of BARS and *LPAATδ* (Figure 3.6B). Here, added BARS had no effect on the *LPAAT* activity, suggesting that other *LPAAT* isoforms are not detectably stimulated by BARS. She also tested the effects of BARS on the activity of *LPAATγ*, a BARS interactor, in experiments similar to those designed for *LPAATδ* (Figure 3.1B,C). Perhaps surprisingly, BARS had no effect on this enzyme. These collective data indicate that the stimulatory effects of BARS are rapid and apparently selective for *LPAATδ*, at least under these experimental conditions. Notably, these effects correlate well with the ability of microinjected

purified BARS to activate the fission of post-Golgi carriers in live cells (Bonazzi, M. et al. 2005).

Further along this line, she sought to inhibit BARS by adding in the LPAAT δ assay mixture a characterised affinity-purified neutralising anti-BARS antibody that when microinjected into cells, inhibits carrier fission (Bonazzi, M. et al. 2005; Valente, C. et al., 2012; Valente, C., et al., 2005). This antibody inhibited the LPAAT δ -dependent activity, while preimmune-IgG addition had no effect (Figure 3.6C). Moreover, a BARS pre-treatment with BAC, which locks BARS in its dimeric fission-incompetent conformation and inhibits the fission of the Golgi ribbon (Colanzi, A. et al., 2013), reduced the LPAAT δ activity (Figure 3.6D), which indicates that monomeric BARS is required for LPAAT δ to express its enzymatic activity.

She further examined the relationship between LPAAT δ activity and carrier fission by expressing suitable BARS mutants. Previously, she had characterised two single-point mutants, BARS^{D355A} and BARS^{S147A}, that have dominant-negative effects on carrier fission in living cells (Bonazzi, M. et al 2005; Valente, C. et al. 2012). She tested these mutants in the LPAAT δ activity assay by co-expressing each of them with LPAAT δ . Both nearly completely inhibited the LPAAT δ -dependent activity (Figure 3.6E), again without affecting LPAAT δ expression levels. As a control, she tested the effects of overexpressing wild-type BARS (notably, wild-type BARS and the dominant negative mutants showed comparable expression levels in these experiments). Overexpressed BARS did not have significant effects on the LPAAT δ activity in extracts from 'quiescent' cells (Figure 3.6E). She noted, however, that BARS is recruited to the Golgi during a traffic pulse and activates carrier fission, which suggested that active traffic increases the requirement for BARS (Valente, C. et al. 2012). In extracts prepared during a traffic pulse, overexpressed BARS stimulated the LPAAT δ activity (Figure 3.6F). Further, again in traffic-stimulated extracts, expression of the fission-active BARS^{S147D} mutant that mimics the activatory phosphorylation of BARS on Ser147 (Valente, C. et al. 2012; Liberali, P. et al. 2008; Haga, Y., et al 2009) stimulated the LPAAT δ activity to an even greater extent (Figure 3.6F).

She finally tested the role of the BARS-14-3-3 γ -PI4KIII β complex in LPAAT δ activation. As noted, within this complex, 14-3-3 γ binds to phosphorylated S147 in the BARS dimerisation interface and is necessary for Golgi carrier fission (Valente, C. et al 2012; Valente, C. et al 2013). The LPAAT δ activity of cell extracts was markedly suppressed by 14-3-3 γ depletion (Figure 3.7A), while depletion of other 14-3-3 isoforms had no effect (Figure 3.7B). Moreover, addition to cell extracts of a characterised affinity-purified anti-14-3-3 γ antibody (Valente, C. et al 2012) also suppressed the LPAAT δ activity (Figure 3.7C). These data indicate that 14-3-3 γ is required for LPAAT δ activity, presumably because it stabilises BARS in its monomeric fission-competent conformation.

In summary, a number of treatments based on BARS silencing or overexpression, or on the use of BARS mutants as well as anti-BARS antibodies and inhibitors, or on manipulations of the BARS-containing complex, stimulated or inhibited LPAAT δ activity and Golgi carrier fission in completely parallel fashions. These data indicate a causal relationship between the BARS-induced LPAAT δ activation and membrane fission. The stimulation of LPAAT δ by BARS is very potent, and appears to occur rapidly, most likely via a physical interaction between BARS and LPAAT δ during assembly of the BARS protein complex required for carrier formation.

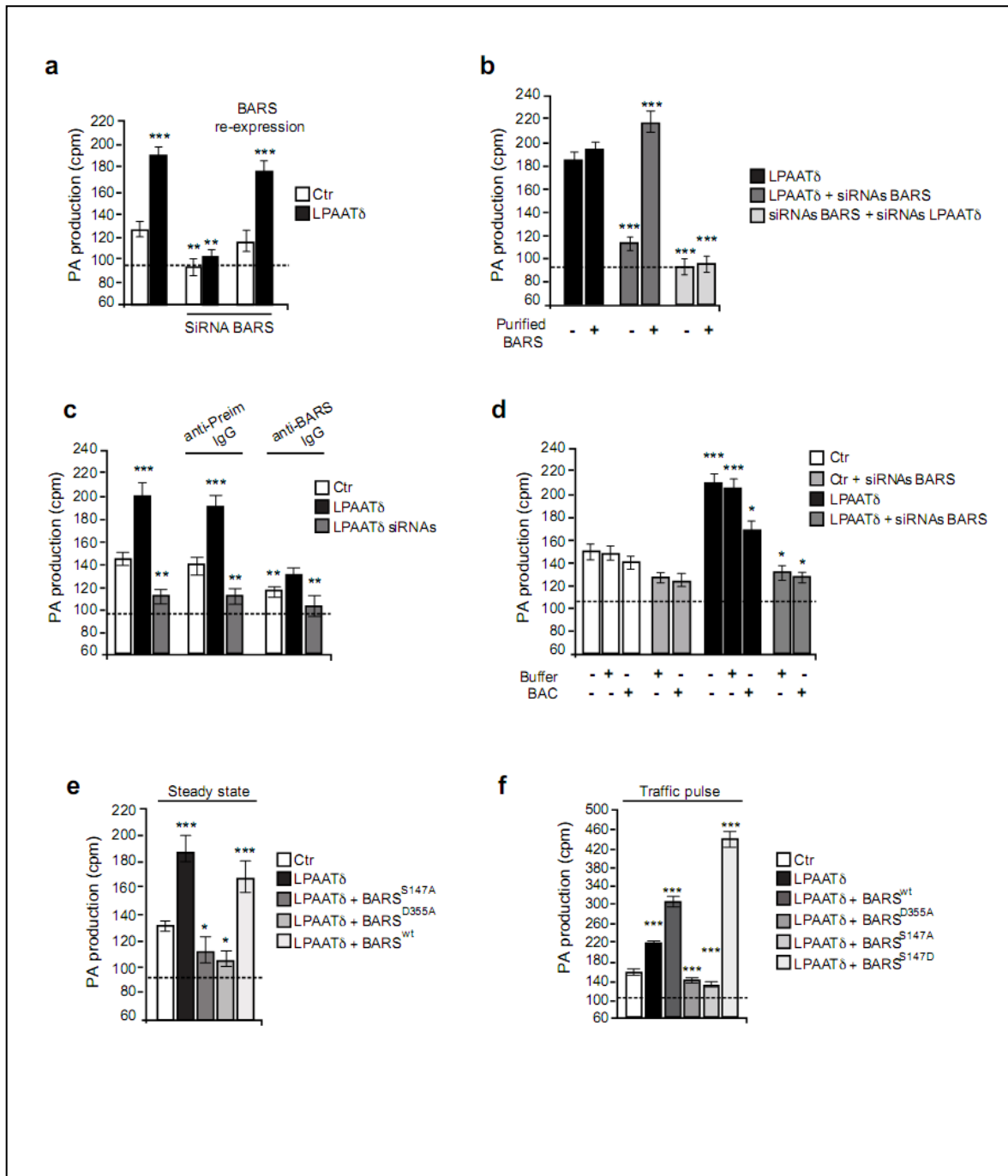


Figure 3.6 BARS activates LPAATδ and this activation is required for post-Golgi carrier formation.

(a) Quantification of phosphatidic acid (PA) production in the LPAAT assay for postnuclear supernatants from HeLa cells transfected with empty Flag-vector (Ctr) or LPAATδ-Flag (LPAATδ) and with *BARS* siRNAs for 48 h, and with the last 12 h with siRNA-resistant replacement BARS-YFP encoding vector (BARS re-expression). (b) Quantification of phosphatidic acid (PA) production in the LPAAT assay for postnuclear supernatants from HeLa cells transfected with empty Flag-vector (Ctr) or LPAATδ-Flag (LPAATδ) and with *BARS* siRNAs and/ or *LPAATδ* siRNAs. Post-nuclear fractions were incubated with immunopurified BARS (Purified BARS) for 30 min at 25 °C before LPAAT assay (as indicated). (c) Quantification of phosphatidic acid (PA) production in the LPAAT assay for postnuclear supernatants from HeLa

cells transfected with empty Flag-vector (Ctr) or LPAAT δ -Flag (LPAAT δ) for 48 h or with LPAAT δ siRNAs for 72 h. The anti-BARS polyclonal antibody (anti-BARS IgG) or anti-preimmune IgG (anti-Preim IgG, as control) were incubated with the indicated post-nuclear fraction for 30 min at 25 °C before the LPAAT assay. **(d)** Quantification of phosphatidic acid (PA) production in the LPAAT assay for postnuclear supernatants from HeLa cells transfected with empty Flag-vector (Ctr) or LPAAT δ -Flag (LPAAT δ) and with BARS siRNAs for 48 h. Post-nuclear fractions were incubated with HPLC-purified BAC (BAC +) or with buffer alone (Buffer -) for 30 min at 25 °C before the LPAAT assay (as indicated). **(e-f)** Quantification of phosphatidic acid (PA) production in the LPAAT assay for postnuclear supernatants from HeLa cells transfected with: **(e)** empty Flag-vector (Ctr) or LPAAT δ -Flag (LPAAT δ) for 48 h and the last 12 h with BARS^{S147A}-YFP, BARS^{D355A}-YFP or BARS^{wt}-YFP (as indicated); **(f)** empty Flag-vector (Ctr) or LPAAT δ -Flag (LPAAT δ) for 48 h and the last 12 h with BARS^{wt}-YFP, BARS^{D355A}-YFP, BARS^{S147A}-YFP or BARS^{S147D}-YFP (as indicated). Cells were infected with VSV, subjected to TGN-exit assay and post-nuclear fractionations were prepared 10 min after the shift to 32 °C temperature-block release. The dashed line indicates the level of endogenous LPAAT activity not associated with LPAAT δ (see text for details). Data are means \pm s.d of three independent experiments. **P* <0.05, ***P* <0.01, ****P* <0.005 versus control (Student's *t*-test). (from Pagliuso *et al.* Manuscript under revision)

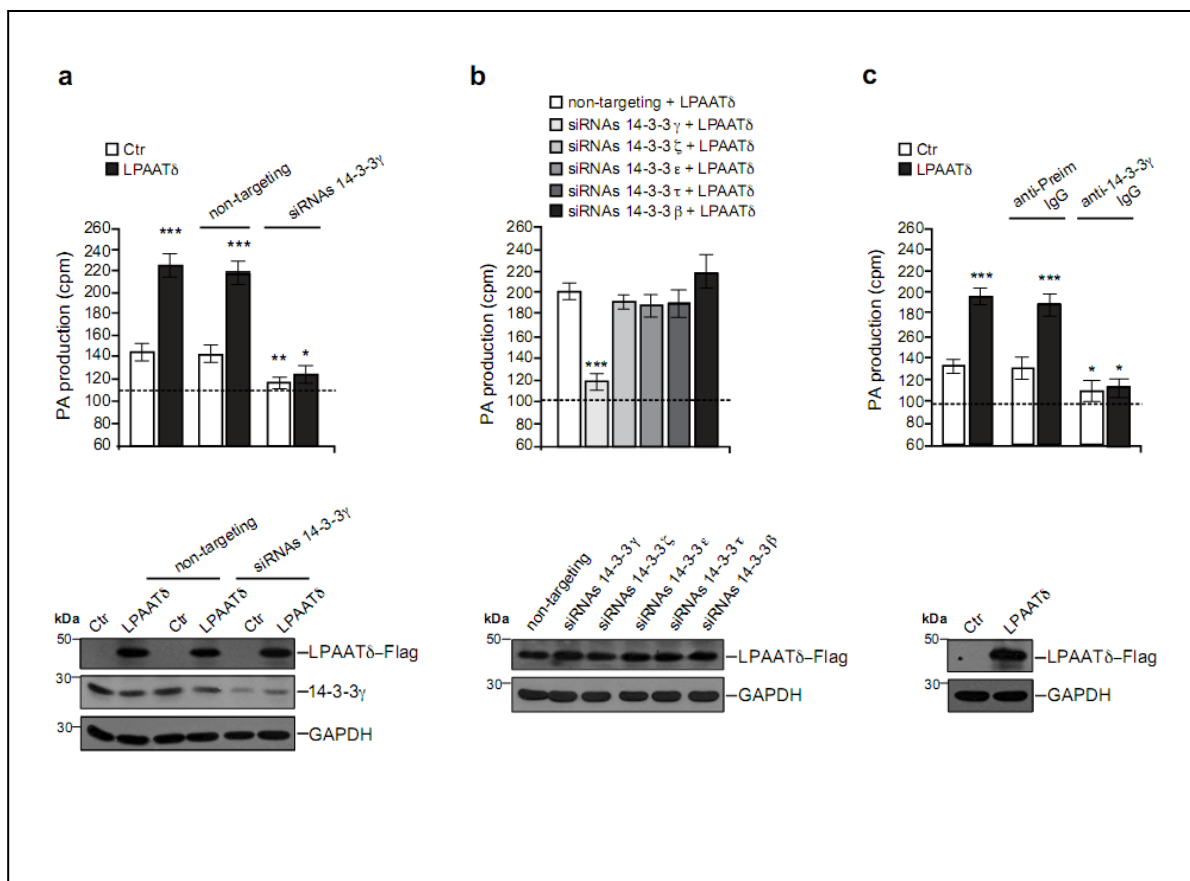


Figure 3.7 14-3-3 γ , but not other 14-3-3 isoforms, is required for LPAAT δ activity.

(A-C) Quantification of phosphatidic acid (PA) production in the LPAAT assay for postnuclear supernatants from HeLa cells transfected with the empty Flag-vector (Ctr) or LPAAT δ -Flag (LPAAT δ) plus: **(A)** transfection with non-targeting siRNAs or 14-3-3 γ siRNAs for 48 h (as indicated); **(B)** transfection with 14-3-3 γ , ζ , ϵ , τ and β siRNAs for 48 h (as indicated); **(C)** treatment of the post-nuclear supernatant with an anti-14-3-3 γ polyclonal antibody (anti-14-3-3 γ IgG) or anti-preimmune IgG (anti-Preim IgG, as control) for 30 min at 25 °C before the LPAAT assay. **(A-C)** The dashed line indicates the level of endogenous LPAAT activity not associated with LPAAT δ (see text for details). Bottom: representative Western blotting with an anti-Flag antibody (a-c) and with an anti-14-3-3 γ monoclonal antibody (a) to monitor the transfection of LPAAT δ and the depletion of 14-3-3 γ in the lysate used for LPAAT assay. Glyceraldehyde 3-phosphate dehydrogenase (GAPDH) is shown for the internal protein levels and molecular weight standards (kDa) are indicated on the left of each panel. Data are means \pm s.d. of three independent experiments. * P <0.05; ** P <0.01; *** P <0.005 versus control (Student's t -tests). (from Pagliuso *et al.* Manuscript under revision)

3.1.2.6 The BARS–LPAAT δ interaction occurs at the Golgi complex in live cells (Pagliuso *et al.* Manuscript under revision)

The effects of BARS and LPAAT δ on the fission of carriers emanating from the Golgi suggested that the BARS–LPAAT δ interaction occurs at this organelle. To confirm this concept directly, we first re-examined the localisation of BARS and of the other complex components, 14-3-3 γ and PI4KIII β , at high resolution. Similar to LPAAT δ (Figure 3.1D,E), these proteins were all seen to localise at the TGN (Figure 3.8A) as well as within the VSVG-containing tubular carrier precursors that form during synchronised exit from the TGN (Figure 3.8B). Secondly, we asked whether the interaction between BARS and LPAAT δ occurs *in vivo*, as expected. To this end, we used a Förster resonance energy transfer (FRET) approach with fluorescence lifetime imaging microscopy, which reveals the co-presence of donor and acceptor fluorophores within the same complex at a distance of \leq 8 nm. We expressed CFP-LPAAT δ as the FRET donor, and BARS-YFP as the acceptor, and monitored the FRET. A FRET signal was detected at the Golgi at steady-state (Figure 3.8C) and this was markedly increased during a VSVG traffic pulse (Figure 3.8C,D), which is consistent with the observation that BARS is recruited to the Golgi during traffic (Valente, C. *et al.* 2012). These results indicate that LPAAT δ is in a complex with BARS *in vivo*, and that it co-localises at the TGN with BARS, 14-3-3 γ and PI4KIII β , in agreement with the BARS–LPAAT δ co-precipitation data (Figure 3.1B, C).

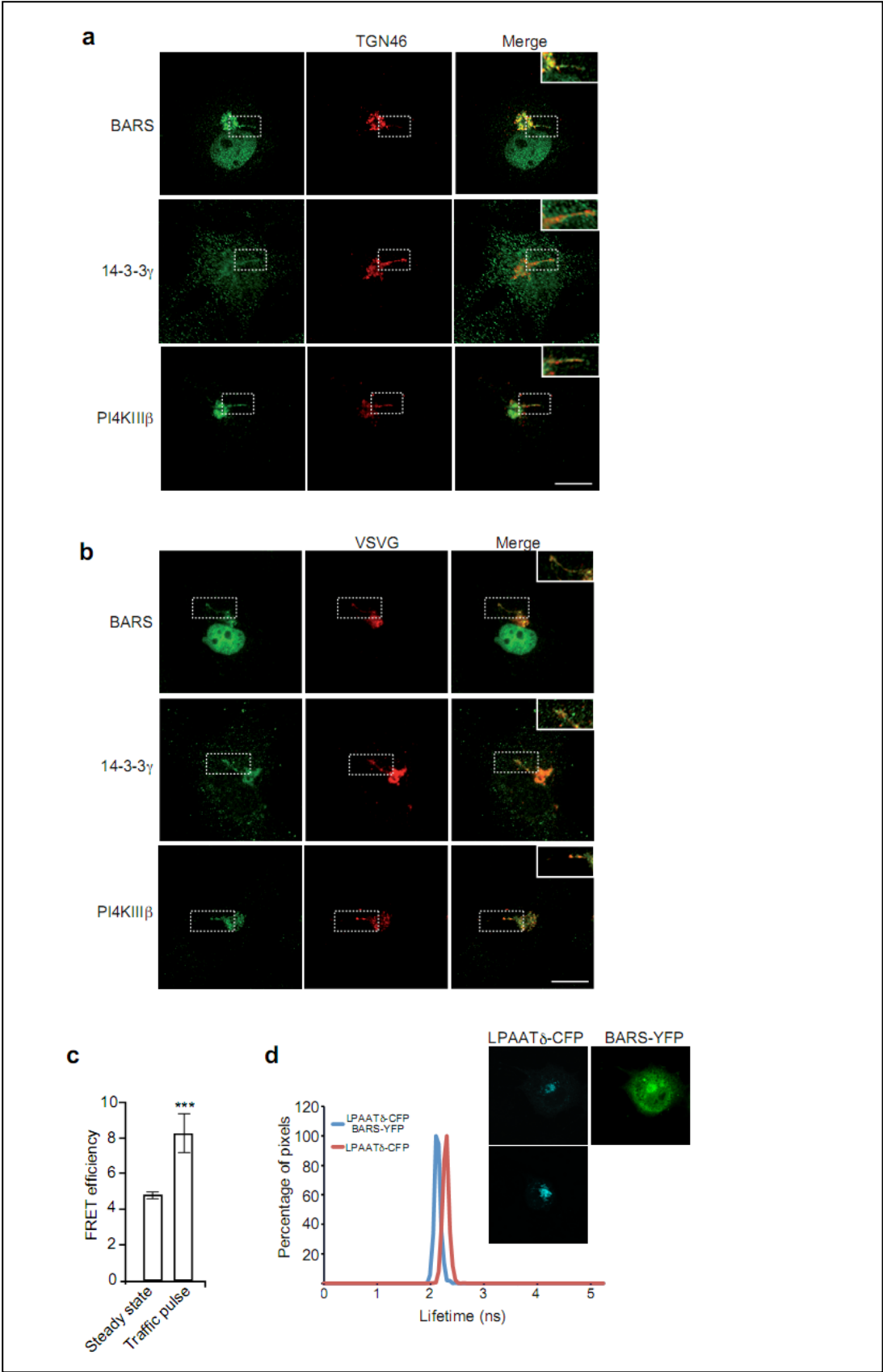


Figure 3.8 BARS colocalises with 14-3-3 γ and PI4KIII β at the TGN and in carrier precursors, and interacts with LPAAT δ at the Golgi.

(A, B) Representative images of COS7 cells at steady state **(A)** or VSV-infected and subjected to the VSVG TGN-exit assay **(B)**. The cells were fixed and labelled with polyclonal anti-BARS, anti-14-3-3 γ or anti-PI4KIII β (a-b; green) antibodies, and with an anti-TGN46 antibody (a; red) or a monoclonal anti-VSVG antibody (b; red). Insets, right: Magnification of the tubular carrier precursors in the Golgi area. Scale bars: 10 μ m (a, b). **(C, D)** FLIM-FRET of COS7 cells transfected with LPAAT δ -CFP and BARS-YFP. **(C)** Quantification of FLIM-FRET efficiency for the Golgi area at steady state and during a VSVG traffic pulse (as indicated). Data are means \pm s.d. (n = 20 cells/condition). *** P < 0.005 (Student's t -tests) versus steady-state. **(D)** Distribution of fluorescence lifetimes measured in the Golgi area for LPAAT δ -CFP alone (red) and with BARS-YFP (blue). Co-expression of BARS-YFP produces a shift towards shorter lifetimes (hence indicating FRET between LPAAT δ -CFP and BARS-YFP). The average fluorescence lifetime of LPAAT δ -CFP was 2.31 ns for LPAAT δ -CFP alone, and 2.10 ns for LPAAT δ -CFP with BARS-YFP. Inset: Representative FLIM-FRET images of cells (top: LPAAT δ -CFP, blue; BARS-YFP, green; bottom: LPAAT δ -CFP alone, blue). (from Pagliuso *et al.* Manuscript under revision)

3.2 Role of BARS in mitosis

3.2.1 Introduction

As indicated above, inhibition of Golgi fragmentation results in the arrest of the cell cycle at the G2 phase, which suggests that a 'Golgi checkpoint' monitors the mitotic partitioning of the Golgi membranes (Hidalgo Carcedo et al., 2004; Persico et al., 2010; Sutterlin et al., 2002).

The membrane fission factor BARS controls the disassembly of the Golgi stacks by severing the tubular networks of the non-compact zones (Colanzi et al., 2007). Interfering with BARS activity in a semi-intact Golgi fragmentation assay results in groups of large tubular-vesicular-saccular networks of Golgi membranes that are continuous and are localised in the pericentriolar region (Colanzi et al., 2007). As discussed in Chapter 1, section 1.5, BARS is required for several membrane-fission processes (Bonazzi et al., 2005; Valente et al., 2012; Yang et al., 2011). However, Golgi membranes are only fragmented in late G2, which indicates that BARS is specifically activated in G2 to promote Golgi-ribbon severing. Several molecules involved in the initial Golgi-ribbon unlinking during mitosis have been identified. In particular, Golgi fragmentation is inhibited by blocking the GRASP65 and GRASP55 proteins with a cell-cycle arrest at the G2 stage (Preisinger et al., 2005; Feinstein and Linstedt, 2007; Duran et al., 2008).

It has been demonstrated that GRASP55 is a mitogen-activated protein kinase (MAPK) substrate that is phosphorylated by ERK2 both *in vitro* and *in vivo* (Jesch et al., 2001). Moreover, GRASP55 is connected to the Raf-MEK1 pathway, although it is not clear whether this occurs through the ERK2 protein or its splice variant ERK1b/1c (1b in mouse; 1c in humans). ERK2 and ERK1b/1c have been demonstrated to be recruited to the Golgi membranes, to be activated by MEK1, and to be required for Golgi fragmentation and for cell entry into mitosis (Abershold et al., 2004; Shaul and Seger, 2006). Moreover, Kienzle (2012) and colleagues have recently demonstrated that PKD is an important player in Golgi mitotic checkpoint control. PKD can activate the Raf1-MEK1-ERK1c pathway during G2, and GRASP55 has been reported to be a putative downstream target of this pathway.

On the other hand, it has been demonstrated that GRASP65 can be phosphorylated by Cdk1 and Plk1 during mitosis, and that this phosphorylation changes the GRASP65 conformation, leads to its de-oligomerisation, and to Golgi cisternae unlinking (Wang et al., 2005). After mitosis, GRASP65 is dephosphorylated and reforms *trans*-oligomers and re-stacks Golgi cisternae.

With the aim to clarify the molecular mechanisms of BARS-dependent membrane fission in mitosis, my study also focussed on the identification of possible links between BARS and the two well-characterised GRASP55-dependent and GRASP65-dependent mitosis-activated pathways.

3.2.2 Results

To examine whether BARS interacts with GRASP55 and/or GRASP65, I first immunoprecipitated BARS from HeLa cells that were transfected with BARS pCDNA3 synchronised and blocked in G2 or in M phase of the cell cycle, using treatment with Ro3306, a Cdk1 specific inhibitor. The immunoprecipitated proteins were analysed by Western blotting with an anti-GRASP55 antibody. As shown in Figure 3.9A, endogenous GRASP55 specifically co-precipitated with BARS in both G2 and M-phase synchronised cells.

Conversely, using the same approach, upon GRASP65 immunoprecipitation, BARS did not co-precipitate, neither in G2 nor M-phase synchronised cells (Figure 3.9B). Similar data were obtained in pull-down experiments. Purified recombinant GST-BARS did not pull down GRASP65 from GRASP65-myc overexpressing cells lysates blocked in the G2 and M phases (Figure 3.9C).

Collectively, these data indicate that BARS interacts with GRASP55, but not with GRASP65.

To further understand the functional role of this interaction between GRASP55 and BARS, I first analysed whether the localisation of BARS at the Golgi complex is GRASP55-mediated, using immunofluorescence. Taking advantage of the use of HeLa cells that were under stable depletion of GRASP55 or GRASP65, I found that the Golgi localisation of BARS is neither GRASP55-mediated nor GRASP65-mediated (Figure 3.10A).

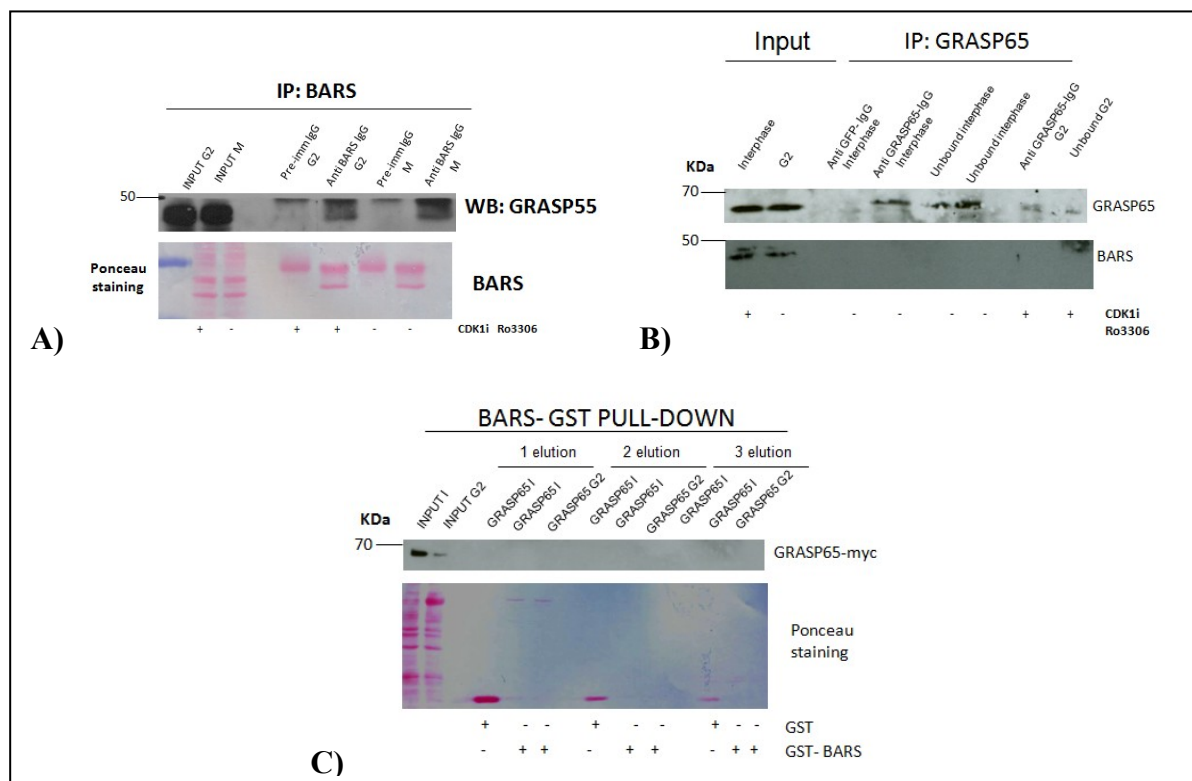


Figure 3.9 BARS interacts with GRASP55 but not with GRASP65.

(A) BARS immunoprecipitation (IP:BARS) of lysate from HeLa cells synchronised in G2 or M phase (as indicated). Ponceau staining or representative Western blotting (WB; antibodies as indicated) of total lysate (input) and co-immunoprecipitated protein (as indicated). **(B)** Immunoprecipitation with an anti-GRASP65 antibody (IP:GRASP65) of lysate from HeLa cells synchronised in interphase or G2 phase (as indicated). Representative Western blotting of total lysate (input) and GRASP65-immunoprecipitated proteins with an anti-GRASP65 antibody or the anti-BARS antibody (as indicated). **(C)** Pull-down assay of GST and GST-BARS (as indicated) with GRASP65 overexpressing cell lysate synchronised in interphase (I) or G2 (as indicated). Elution with reduced glutathione (1,2), or sample buffer (3) followed by Western blotting with an anti-GRASP65 antibody (top), with pulled-down proteins revealed by Ponceau-S staining (bottom).

However, based on the demonstrated of Kienzle and colleagues that PKD has a role in the activation of GRASP55, I investigated whether the Golgi localisation of BARS can be affected by PKD knock-down. Interestingly, as shown in Figure 3.10B, the Golgi pool of BARS was reduced in PKD knock-down cells, compared to non-targeting treated cells.

Additionally, I have shown that the Golgi localisation of BARS is also PtdIns4*P*-mediated. Indeed, treatment with PIK93, a PI4KIII β specific inhibitor, strongly reduced the Golgi localisation of BARS (Figure 3.10C). These data are in line with the ability of BARS to bind PtdIns4*P* *in vitro* (Yang et al., 2008) and with its co-localisation with a Golgi pool of PtdIns4*P* (data not presented in this thesis). I have also shown that the PI4KIII β -mediated PtdIns4*P* pool affects the interaction between BARS and LPAAT δ . As shown in (Figure 3.10D), cell treatment with PIK93 reduced the co-precipitation between LPAAT δ and BARS.

Collectively these results suggest a possible link between BARS and the PKD-Raf-MEK1-Erk-GRASP55 signalling pathway in mitosis. However, further studies are needed to clarify how BARS is specifically involved in this pathway, what is the molecular mechanism of BARS in mitosis, and whether a lipid metabolic enzyme and its product is involved in BARS-mediated membrane fission in mitosis.

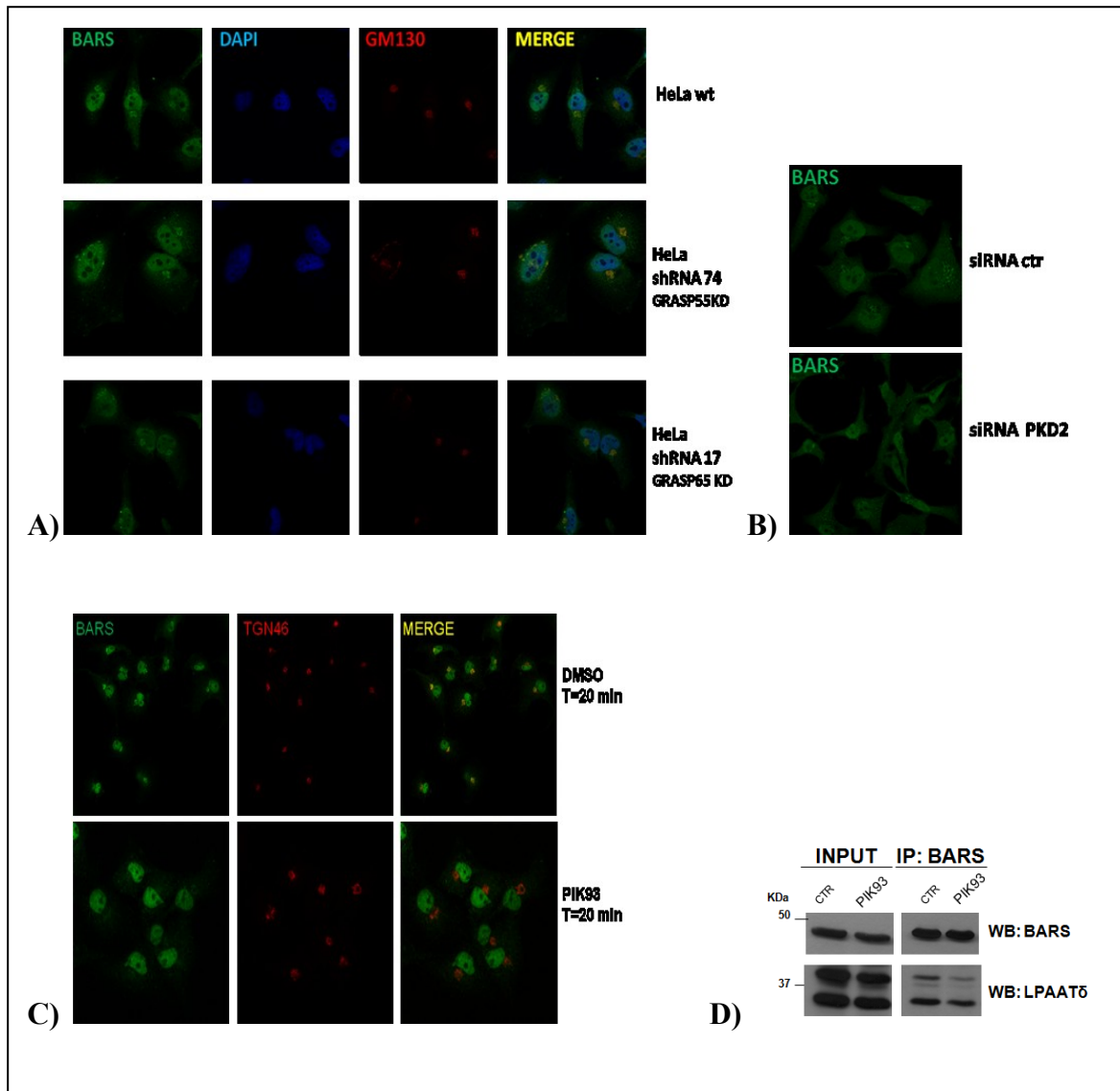


Figure 3.10 BARS localises at the Golgi complex in a PtdIns4P-dependent manner.

(A). Representative confocal microscopy images of HeLa wild-type (wt) cells, GRASP55 stable depleted cells (shRNA74), and GRASP65 stable depleted cells (shRNA17), fixed and processed for immunofluorescence with an anti-GM130 antibody (red), DAPI (blue), and an anti-BARS antibody (green; as indicated). **(B)** Representative confocal microscopy images of HeLa wt cells, treated with non-targeting (siRNA ctr) or PKD2 siRNA (lower panel), fixed and processed for immunofluorescence with an anti-BARS antibody (green; as indicated). **(C)** Representative confocal microscopy images of COS7 cells treated with 1 μ M PIK-93 or with DMSO (as control) for 20 min, fixed and labelled with an anti-BARS antibody (green) and an anti-TGN46 antibody (red) **(D)** BARS immunoprecipitation (IP:BARS) of lysates from COS7 cells transfected with LPAAT4-flag and BARS and incubated without (-) or with (+) PIK-93. Analysis by Western blotting (antibodies as indicated) of total lysate (input), and immunoprecipitated material (IP).

CHAPTER 4

DISCUSSION

In the first part of my PhD thesis, I demonstrated that BARS induces fission of basolaterally directed post-Golgi carriers through its interaction and activation of LPAAT δ , a member of the acyl-transferase family that converts LPA into PA. I also showed that this LPA-PA interconversion has a role in BARS-dependent fission.

Transport carriers have an essential role in intracellular membrane transport. These carriers shuttle from donor to acceptor compartments, through budding and fission from the former, and fusion with the latter. They can be divided in two main groups: small coated (or coat-dependent) vesicles (e.g., COPI or COPII vesicles, clathrin-dependent vesicles) and large pleiomorphic carriers or PGCs. BARS is required for the fission of these PGCs (Bonazzi et al., 2005; Valente et al., 2012), as well as for other fission events, including fission of the macropinocytic cup during EGF-stimulated macropinocytosis (Liberali et al., 2008), fission of COPI vesicles for retrograde trafficking from the Golgi to the ER (Yang et al., 2005), and also for the fission-fragmentation of the Golgi complex during mitosis (Hidalgo Carcedo et al., 2004). Even though the involvement of BARS in these pathways has been extensively characterised, the mechanism of action of BARS-induced membrane fission is still under investigation.

On the basis that we previously identified BARS as a key component of a protein complex that is required for post-Golgi carrier fission (Valente et al., 2012), in this thesis the question I wished to address was how BARS drives membrane fission, and if this function requires specific interaction/ regulation through an LPAAT enzyme.

Here, I have shown that BARS interacts with two Golgi-localised LPAATs, namely LPAAT γ and LPAAT δ , and in particular that LPAAT δ interacts with the monomeric fission-competent form of BARS. Indeed, LPAAT γ has been recently suggested to localise at the *cis*-side of the Golgi complex and to have a role in the retrograde membrane trafficking, whereas nothing is known about LPAAT δ . We have used immuno-electron microscopy studies to demonstrate that LPAAT δ localises mostly to the *trans*-Golgi and the TGN, so I have analysed its possible role in PGC formation. LPAAT δ depletion impairs both VSVG and LDLr transport from the TGN to the PM, while it does not affect p75 apical transport or retrograde transport from the Golgi to the ER. Therefore, LPAAT δ , like BARS, is selectively required for fission of basolateral carriers.

In agreement with published data (Eto et al., 2014), Dr. Valente has shown that LPAAT δ is an LPA acyltransferase, the activity of which can be abrogated by mutagenesis of three conserved amino acids in its catalytic core (Schmidt and Brown, 2009). The data reported here show that when LPAAT δ activity is blocked, the exit of the cargo reporter VSVG from the Golgi complex is heavily impaired. Indeed, when the LPAAT δ activity was reduced by either overexpression of a catalytically inactive mutant or by injection of an anti-LPAAT δ antibody, VSVG trafficking was inhibited, and a fission-defect phenotype was observed. Strikingly, when the LPAAT δ activity is inhibited using a general LPAAT inhibitor, CI976, there was massive tubulation of the Golgi complex, which suggests that LPAAT activity is involved in fission.

Collectively, these data show that LPAAT δ is involved in Golgi dynamics, with a clear role in fission at the TGN. However, Dr. Valente has also shown that BARS activates

LPAAT δ and that this activation is important for PGC fission. In particular, when BARS is inhibited by the addition in the LPAAT assay mixture of a well-characterised affinity-purified neutralising anti-BARS antibody, or by siRNA treatment, or by pre-treatment of BARS with BAC (which locks BARS in its dimeric fission-incompetent conformation and inhibits the fission of the Golgi ribbon), there was a reduction in the LPAAT δ activity. This indicates that monomeric BARS is required for LPAAT δ to express its enzymatic activity.

These studies have demonstrated that a new enzyme, LPAAT δ , and its product PA, have crucial roles in membrane trafficking, and specifically at the fission step.

In the second part of my PhD thesis I analysed the fission-inducing property of BARS in Golgi partitioning in mitosis. The molecular mechanism by which BARS acts in mitosis is still unclear. However, here I have provided evidence that BARS can interact with GRASP55 (but not with GRASP65), in both the G2 and M phases of the cell cycle. Moreover, I have also showed that the localisation of BARS at the Golgi complex is PKD-mediated and not GRASP55 or GRASP65 dependent.

PKD is required for mitotic fragmentation of Golgi membranes in late G2 phase of the cell cycle and for mitotic entry, through activation of the Raf1-MEK1-Erk1c pathway. A putative downstream target of this signalling pathway is the Golgi stacking protein GRASP55. Indeed, inhibition of GRASP55 resulted in inhibition of the severing of the Golgi ribbon and arrest of the cell cycle at the G2 stage. Moreover, it has been demonstrated that PKD phosphorylates PI4KIII β at the Golgi complex, which in turn is involved in post-Golgi carrier fission. Indeed, the PKD-mediated PI4KIII β phosphorylation increases the local production of PtdIns4P, which supports the budding of tubular carrier precursors, most likely through recruitment of PtdIns4P binding proteins. One of these PtdIns4P binding proteins might be BARS. Indeed, the PI4KIII β specific inhibitor, PIK93, reduces the localisation of BARS at the Golgi complex, and in turn, the interaction between BARS and LPAAT δ .

Collectively these data show the identification of key components, as proteins and a lipid metabolic enzyme, involved in the BARS-mediated fission process. Specifically, these data reveal the role of LPAAT δ in BARS-dependent post-Golgi carrier fission, and identify GRASP55 as a component of BARS-dependent Golgi-ribbon unlinking in mitosis.

CHAPTER 5

CONCLUSIONS

What is the relevant biotechnological approach of this study?

The CtBP proteins have been linked to tumorigenesis and tumour progression. As transcriptional co-repressors, the CtBPs can promote epithelial-mesenchymal transition and act as apoptosis antagonists, while as fission-inducing proteins, they control the Golgi checkpoint in mitosis, and thus cell-cycle progression.

To define the molecular mechanisms involved in the dual action of the CtBPs, and in particular of BARS in tumorigenesis and tumour progression, several molecules that can functionally modulate BARS are under investigation in our laboratories. However, a novel anti-cancer strategy might be developed based on the functional modulation of key BARS interactors.

I have contributed to the identification of a novel LPAAT family member, LPAAT δ , that localises at the Golgi complex, where it catalyses the acylation of LPA to form PA. BARS activates LPAAT δ , which results in an increase in PA production at the Golgi complex. PA is an important membrane remodelling metabolite that is involved in membrane transport, as well as a key second messenger that can modulate cell survival and proliferation, and tumour progression. Indeed, PA has been shown to bind Raf1 kinase and to activate the Ras-Raf signalling pathway, which in turn, regulates cell proliferation and apoptosis. Additionally, PA is required for mTOR activity, the mammalian target of rapamycin, which is implicated in signals that suppress apoptosis in cancer cells (Rizzo et al., 2000; Fang et al., 2001; Foster et al., 2001).

Among the several LPAATs isoforms, LPAAT β is the most well studied in cancer. It is overexpressed in several tumours (e.g., lung, breast, colon, prostate, leukaemia, lymphoma), and its activity is associated with more aggressive tumour phenotypes (Scott et al., 2014). The knock-down (by isoform-specific siRNAs) or inhibition (by small-molecule inhibitors) of LPAAT β induces a G2/M cell-cycle checkpoint block, followed by growth arrest and apoptosis. These data indicate that LPAAT β is a potential target for several tumours (Coon et al., 2003; Pagel et al., 2005; la Rosèe et al., 2006; Niesporek et al., 2005; Rastegar et al., 2010). Moreover, a specific LPAAT β inhibitor, CT-32228, was recently identified that can inhibit proliferation of several cancer cell lines. Unfortunately, *in vivo*, this compound induced higher toxicity, making it unsuitable for clinical development.

The data obtained in this study demonstrate the relevance of LPAAT δ -mediated PA production in membrane fission, a process that is required for membrane trafficking as well as for the Golgi partitioning in mitosis in the G2 phase of the cell cycle. Starting from these observations the role of the LPAAT δ enzyme can be investigated in mitosis and thus in cell-cycle regulation, with the aim to identify chemical inhibitors that can selectively target and inhibit it in cancer cells overexpressing LPAAT δ . Indeed, as well as LPAAT β , LPAAT δ is also highly expressed in several tumours.

LPAAT δ -specific inhibitors can be designed and synthesised based on the molecular analogy with LPAAT β and its specific inhibitors (e.g., CT-32228), and their role in BARS-mediated tumorigenesis and tumour progression will be analysed.

REFERENCES

- Acharya, U., Mallabiabarrena, A., Acharya, J.K., and Malhotra, V. (1998). Signaling via mitogen-activated protein kinase kinase (MEK1) is required for Golgi fragmentation during mitosis. *Cell* 92, 183-192.
- Adolf, F. et al. (2013). Scission of COPI and COPII vesicles is independent of GTP hydrolysis. *Traffic* 14, 922-932.
- Aebbersold, D. M., Shaul, Y. D., Yung, Y., Yarom, N., Yao, Z., Hanoch, T., Seger, R. (2004). Extracellular signal-regulated kinase 1c (ERK1c), a novel 42-kilodalton ERK, demonstrates unique modes of regulation, localization, and function. *Mol. Cell. Biol.* 24, 10000–10015.
- Alonso, R. et al. (2005). Diacylglycerol kinase alpha regulates the secretion of lethal exosomes bearing Fas ligand during activation-induced cell death of T lymphocytes. *J Biol Chem* 280, 28439-28450.
- Asp, L. et al. (2009). Early stages of Golgi vesicle and tubule formation require diacylglycerol. *Mol Biol Cell* 20, 780-790.
- Bannykh SI, Balch WE (1997). Membrane dynamics at the endoplasmic reticulum-Golgi interface. *J Cell Biol.* Jul 14;138(1):1-4.
- Bankaitis, V.A., Garcia-Mata, R., and Mousley, C.J. (2012). Golgi membrane dynamics and lipid metabolism. *Current biology : CB* 22, R414-424.
- Bard, F., and Malhotra, V. (2006). The formation of TGN-to-plasma-membrane transport carriers. *Annual review of cell and developmental biology* 22, 439-455.
- Baron, C.L., and Malhotra, V. (2002). Role of diacylglycerol in PKD recruitment to the TGN and protein transport to the plasma membrane. *Science* 295, 325-328.
- Barr, F.A., Puype, M., Vandekerckhove, J., and Warren, G. (1997). GRASP65, a protein involved in the stacking of Golgi cisternae. *Cell* 91, 253-262.
- Bechler, M. E., de Figueiredo, P. & Brown, W. J. (2012). A PLA1-2 punch regulates the Golgi complex. *Trends Cell Biol* 22, 116-124.
- Birts, C. N. et al. (2013). A cyclic peptide inhibitor of C-terminal binding protein dimerization links metabolism with mitotic fidelity in breast cancer cells. *Chem. Sci.* 4, 3046-3057.
- Bonazzi, M. et al. (2005). CtBP3/BARS drives membrane fission in dynamin-independent transport pathways. *Nat Cell Biol* 7, 570-580.
- Boucrot, E. et al. (2012). Membrane fission is promoted by insertion of amphipathic helices and is restricted by crescent BAR domains. *Cell* 149, 124-136.
- Boyd, J.M., Subramanian, T., Schaeper, U., La Regina, M., Bayley, S., and Chinnadurai, G. (1993). A region in the C-terminus of adenovirus 2/5 E1a protein is required for association with a cellular phosphoprotein and important for the negative modulation of T24-ras mediated transformation, tumorigenesis and metastasis. *The EMBO journal* 12, 469-478.
- Brindley DN, Waggoner DW. (1998). Mammalian lipid phosphate phosphohydrolases. *J. Biol.Chem.* 273:24281–84.
- Bruce Alberts, Alexander Johnson, Julian Lewis, Martin Raff, Keith Roberts, and Peter Walter (2007) *Molecular Biology of the Cell* Garland Science.
- Bruns JR, Ellis MA, Jeromin A, Weisz OA (2002) Multiple roles for phosphatidylinositol 4-kinase in biosynthetic transport in polarized Madin-Darby canine kidney cells. *J Biol Chem* 277(3): 2012–2018

- Burger, K.N. (2000). Greasing membrane fusion and fission machineries. *Traffic* 1, 605-613.
- Campelo, F. & Malhotra, V. (2012). Membrane fission: the biogenesis of transport carriers. *Annu Rev Biochem* 81, 407-427.
- Cao X, Coskun U, Rossle M, Buschhorn SB, Grzybek M, Dafforn TR, Lenoir M, Overduin M, Simons K (2009). Golgi protein FAPP2 tubulates membranes. *Proc Natl Acad Sci USA* 106(50): 21121–21125.
- Chambers, K., and Brown, W.J. (2004). Characterization of a novel CI-976-sensitive lysophospholipid acyltransferase that is associated with the Golgi complex. *Biochemical and biophysical research communications* 313, 681-686.
- Chambers, K., Judson, B. & Brown, W. J. (2005). A unique lysophospholipid acyltransferase (LPAT) antagonist, CI-976, affects secretory and endocytic membrane trafficking pathways. *J Cell Sci* 118, 3061-3071.
- Chen, Y.G., Siddhanta, A., Austin, C.D., Hammond, S.M., Sung, T.C., Frohman, M.A., Morris, A.J., and Shields, D. (1997). Phospholipase D stimulates release of nascent secretory vesicles from the trans-Golgi network. *The Journal of cell biology* 138, 495-504.
- Chen, Y. Q. et al. (2008). AGPAT6 is a novel microsomal glycerol-3-phosphate acyltransferase. *J Biol Chem* 283, 10048-10057
- Chernomordik, L.V., and Kozlov, M.M. (2003). Protein-lipid interplay in fusion and fission of biological membranes. *Annual review of biochemistry* 72, 175-207.
- Chernomordik, L.V., and Zimmerberg, J. (1995). Bending membranes to the task: structural intermediates in bilayer fusion. *Current opinion in structural biology* 5, 541-547.
- Chinnadurai, G. The transcriptional corepressor CtBP: a foe of multiple tumor suppressors. *Cancer Res* 69, 731-734 (2009).
- Chinnadurai, G. (2002). CtBP, an unconventional transcriptional corepressor in development and oncogenesis. *Molecular cell* 9, 213-224.
- Clermont, Y., Rambourg, A. and Hermo, L. (1995). Trans-Golgi network (TGN) of different cell types: three-dimensional structural characteristics and variability. *Anat Rec* 242, 289-301.
- Colanzi, A. et al. (2013).Molecular mechanism and functional role of brefeldin A-mediated ADP-ribosylation of CtBP1/BARS. *Proc Natl Acad Sci U S A* 110, 9794-9799.
- Colanzi, A. et al. (2007). The Golgi mitotic checkpoint is controlled by BARS-dependent fission of the Golgi ribbon into separate stacks in G2. *EMBO J* 26, 2465-2476.
- Colanzi, A., Sutterlin, C., and Malhotra, V. (2003). RAF1-activated MEK1 is found on the Golgi apparatus in late prophase and is required for Golgi complex fragmentation in mitosis. *J Cell Biol* 161, 27-32.
- Coon M, et al (2003). Inhibition of lysophosphatidic acid acyltransferase B disrupts proliferative and survival signals in normal cells and induces apoptosis of tumor cells *Mol Cancer Ther.* 2:1067–1078.
- Cole, N. B., Ellenberg, J., Song, J., DiEuliis, D. & Lippincott-Schwartz, J. (1998).Retrograde transport of Golgi-localized proteins to the ER. *J Cell Biol* 140, 1-15.
- Coleman, J. (1992).Characterization of the Escherichia coli gene for 1-acyl-sn-glycerol-3-phosphate acyltransferase (plsC). *Mol Gen Genet* 232, 295-303.
- Corda, D., Colanzi, A. & Luini, A. (2006). The multiple activities of CtBP/BARS proteins: the Golgi view. *Trends Cell Biol* 16, 167-173.

- Corda, D., Hidalgo Carcedo, C., Bonazzi, M., Luini, A., and Spano, S. (2002). Molecular aspects of membrane fission in the secretory pathway. *Cellular and molecular life sciences* : CMLS 59, 1819-1832.
- Cossart, P., and Sansonetti, P.J. (2004). Bacterial invasion: the paradigms of enteroinvasive pathogens. *Science* 304, 242-248.
- D'Angelo G, Polishchuk E, Di Tullio G, Santoro M, Di Campi A, Godi A, West G, Bielawski J, Chuang CC, van der Spoel AC, Platt FM, Hannun YA, Polishchuk R, Mattjus P, De Matteis MA (2007) Glycosphingolipid synthesis requires FAPP2 transfer of glucosyl-ceramide. *Nature* 449(7158):62–67.
- Dalton, A.J., and Felix, M.D. (1954). Cytologic and cytochemical characteristics of the Golgi substance of epithelial cells of the epididymis in situ, in homogenates and after isolation. *Am J Anat* 94, 171-207.
- Daumke, O., Roux, A. & Haucke, V. (2014). BAR domain scaffolds in dynamin-mediated membrane fission. *Cell* 156, 882-892.
- De Matteis M, Godi A, Daniela Corda (2002). Phosphoinositides and the golgi complex Aug;14(4):434-47 *Current opinion cell biology*.
- De Matteis MA, Luini A (2008). Exiting the Golgi complex. *Nat Rev Mol Cell Biol* 9(4):273–284.
- De Matteis, M.A., Di Girolamo, M., Colanzi, A., Pallas, M., Di Tullio, G., McDonald, L.J., Moss, J., Santini, G., Bannykh, S., Corda, D., et al. (1994). Stimulation of endogenous ADP-ribosylation by brefeldin A. *Proceedings of the National Academy of Sciences of the United States of America* 91, 1114-1118.
- Drecktrah, D., Chambers, K., Racoosin, E.L., Cluett, E.B., Gucwa, A., Jackson, B., and Brown, W.J. (2003). Inhibition of a Golgi complex lysophospholipid acyltransferase induces membrane tubule formation and retrograde trafficking. *Molecular biology of the cell* 14, 3459-3469.
- Duran, J.M., Kinseth, M., Bossard, C., Rose, D.W., Polishchuk, R., Wu, C.C., Yates, J., Zimmerman, T., and Malhotra, V. (2008). The role of GRASP55 in Golgi fragmentation and entry of cells into mitosis. *Mol Biol Cell* 19, 2579-2587.
- Eto M., et al (2014) A novel lysophosphatidic acid acyltransferase enzyme (LPAAT4) with a possible role for incorporating docosahexaenoic acid into brain glycerophospholipids. *Biochem Biophys Res* 10;443(2):718-24.
- Fang Y, et al (2001) Phosphatidic Acid-mediated mitogenic activation of mTOR signaling *SCIENCE* 294, 1942-1945.
- Farquhar, M.G., and Palade, G.E. (1998). The Golgi apparatus: 100 years of progress and controversy. *Trends Cell Biol* 8, 2-10.
- Feinstein, T.N., and Linstedt, A.D. (2007). Mitogen-activated protein kinase kinase 1-dependent Golgi unlinking occurs in G2 phase and promotes the G2/M cell cycle
- Ferguson, S. M. & De Camilli, P. (2012). Dynamin, a membrane-remodelling GTPase. *Nat Rev Mol Cell Biol* 13, 75-88
- Ferrari, S. (2006). Protein kinases controlling the onset of mitosis. *Cell Mol Life Sci* 63, 781-795.
- Foster D.A. (2009) Phosphatidic acid signaling to mTOR: Signals for the survival of human cancer cells *Biochimica et Biophysica Acta* 1791 949–955.
- Gallop, J. L., Butler, P. J. & McMahon, H. T. (2005). Endophilin and CtBP/BARS are not acyl transferases in endocytosis or Golgi fission. *Nature* 438, 675-678.

Gareth Griffiths, Stephen D. Fuller,* Ruth Back, Michael Hollinshead, Steve Pfeiffer, and Kai Simons (1989). The dynamic nature of the Golgi complex. *Journal cell biology* ;108(2):277-97.

Geuze, H. J. and Morre, D. J. (1991). Trans-Golgi reticulum. *J Electron Microscop Tech* 17, 24-34.

Godi A, Di Campli A, Konstantakopoulos A, Di Tullio G, Alessi DR, Kular GS, Daniele T, Marra P, Lucocq JM, De Matteis MA (2004). FAPPs control Golgi-to-cell-surface membrane traffic by binding to ARF and PtdIns(4)P. *Nat Cell Biol* 6(5):393-404.

Godi A, Pertile P, Meyers R, Marra P, Di Tullio G, Iurisci C, Luini A, Corda D, De Matteis MA (1999). ARF mediates recruitment of PtdIns-4-OH kinase-beta and stimulates synthesis of PtdIns(4,5)P₂ on the Golgi complex. *Nat Cell Biol* 1(5):280-287.

Godi, A. et al. (1999). ARF mediates recruitment of PtdIns-4-OH kinase-beta and stimulates synthesis of PtdIns(4,5)P₂ on the Golgi complex. *Nat Cell Biol* 1, 280-287.

Golgi, C. (1898). Sulla struttura della cellula nervosa dei gangli spinali. *Boll Soc Med Chir Pavia* 13, 60-70.

Goni FM, Alonso A. 1999. Structure and functional properties of diacylglycerols in membranes. *Prog. Lipid. Res.* 38:1-48

Griffiths, G. (2000). Gut thoughts on the Golgi complex. *Traffic* 1, 738-745.

Grooteclaes et al., (2003) C-terminal-binding protein corepresses epithelial and proapoptotic gene expression programs. *Proc Natl Acad Sci USA* 100(8):4568-73.

Ha, K. D., Clarke, B. A. & Brown, W. J. (2010). Regulation of the Golgi complex by phospholipid remodeling enzymes. *Biochim Biophys Acta* 1821, 1078-1088.

Haga, Y., Miwa, N., Jahangeer, S., Okada, T. & Nakamura, S. (2009). CtBP1/BARS is an activator of phospholipase D1 necessary for agonist-induced macropinocytosis. *Embo J* 28, 1197-1207.

Hausser A, Link G, Hoene M, Russo C, Selchow O, Pfizenmaier K (2006). Phospho-specific binding of 14-3-3 proteins to phosphatidylinositol 4-kinase III beta protects from dephosphorylation and stabilizes lipid kinase activity. *J Cell Sci* 119(Pt 17):3613-3621.

Haynes LP, Thomas GM, Burgoyne RD (2005). Interaction of neuronal calcium sensor-1 and ADP-ribosylation factor 1 allows bidirectional control of phosphatidylinositol 4-kinase beta and trans-Golgi network-plasma membrane traffic. *J Biol Chem* 280(7):6047-6054.

Hidalgo Carcedo, C., Bonazzi, M., Spano, S., Turacchio, G., Colanzi, A., Luini, A., and Corda, D. (2004). Mitotic Golgi partitioning is driven by the membrane-fissioning protein CtBP3/BARS. *Science* 305, 93-96.

Hinshaw et al., (2000) Dynamin and its role in membrane fission *Annu Rev Cell Dev* 16:483-519

Ichikawa S, Hirabayashi Y. (1998). Glucosylceramide synthase and glycosphingolipid synthesis. *Trends Cell Biol.* 8:198-202.

Jesch, S.A., Lewis, T.S., Ahn, N.G., and Linstedt, A.D. (2001). Mitotic phosphorylation of Golgi reassembly stacking protein 55 by mitogen-activated protein kinase ERK2. *Mol Biol Cell* 12, 1811-1817.

Johannes, L. & Mayor, S. (2010). Induced domain formation in endocytic invagination, lipid sorting, and scission. *Cell* 142, 507-510.

Kagey MH, Melhuish TA, Wotton D (2003) The polycomb protein Pc2 is a SUMO E3. *Cell* 113(1):127-137.

Katsanis, N., and Fisher, E.M. (1998). A novel C-terminal binding protein (CTBP2) is closely related to CTBP1, an adenovirus E1A-binding protein, and maps to human chromosome 21q21.3. *Genomics* 47, 294-299.

Keller P. and Simons K. (1997) Post-Golgi biosynthetic trafficking. *J Cell Sci* 110 (Pt 24):3001-9

Kent and Carman, (1999). Interactions among pathways for phosphatidylcholine metabolism, CTP synthesis and secretion through the Golgi apparatus. *24(4):146-50 Trends Biochem. Sci*

Kienzle C, Stephan A, Eislera, Julien Villeneuveb, Tilman Brummerc, Monilola A. Olayioyey, and Angelika Hausser (2012). PKD controls mitotic Golgi complex fragmentation through a Raf–MEK1 pathway *Molecular Biology of the Cell*.

Kim JH, Choi SY, Kang BH, Lee SM, Park HS, Kang GY, Bang JY, Cho EJ, Youn HD (2013). AMP-activated protein kinase phosphorylates CtBP1 and down-regulates its activity. *BiochemBiophys Res Commun* 431(1):8–13.

Kooijman, E. E. & Burger, K. N. (2009). Biophysics and function of phosphatidic acid: a molecular perspective. *Biochim Biophys Acta* 1791, 881-888.

Kooijman, E. E. et al. (2005). Spontaneous curvature of phosphatidic acid and lysophosphatidic acid. *Biochemistry* 44, 2097-2102.

Kooijman, E. E. et al. (2005). What makes the bioactive lipids phosphatidic acid and lysophosphatidic acid so special? *Biochemistry* 44, 17007-17015.

Kooijman, E. E., Chupin, V., de Kruijff, B. & Burger, K. N. (2003). Modulation of membrane curvature by phosphatidic acid and lysophosphatidic acid. *Traffic* 4, 162-174.

Kozlov, M. M., McMahon, H. T. & Chernomordik, L. V. (2010). Protein-driven membrane stresses in fusion and fission. *Trends Biochem Sci* 35, 699-706.

Kozlovsky, Y., and Kozlov, M.M. (2003). Membrane fission: model for intermediate structures. *Biophysical journal* 85, 85-96.

Kreitzer G, Marmorstein A, Okamoto P, Vallee R, Rodriguez-Boulan E (2000). Kinesin and dynamin are required for post-Golgi transport of a plasma-membrane protein. *Nat Cell Biol* 2(2):125–127.

Ktistakis, N.T., Brown, H.A., Waters, M.G., Sternweis, P.C., and Roth, M.G. (1996). Evidence that phospholipase D mediates ADP ribosylation factor-dependent formation of Golgi coated vesicles. *The Journal of cell biology* 134, 295-306.

Kumar, V., Carlson, J. E., Ohgi, K. A., Edwards, T. A., Rose, D. W., Escalante, C. R., Rosenfeld, M. G. and Aggarwal, A. K. (2002). Transcription corepressor CtBP is an NAD(+)-regulated dehydrogenase. *Mol Cell* 10, 857-69.

la Rosée P. et al. (2006). Antileukemic activity of lysophosphatidic acid acyltransferase-beta inhibitor CT32228 in chronic myelogenous leukemia sensitive and resistant to imatinib. *Clinical Cancer Res* 12 (21).

Lee, M. C. et al. (2005). Sar1p N-terminal helix initiates membrane curvature and completes the fission of a COPII vesicle. *Cell* 122, 605-617.

Lenz, M., Morlot, S. & Roux, A. (2009). Mechanical requirements for membrane fission: common facts from various examples. *FEBS Lett* 583, 3839-3846.

Leung, D. W. (2001). The structure and functions of human lysophosphatidic acid acyltransferases. *Front Biosci* 6, D944-953.

- Lewin, T. M., Wang, P. & Coleman, R. A. (1999). Analysis of amino acid motifs diagnostic for the sn-glycerol-3-phosphate acyltransferase reaction. *Biochemistry* 38, 5764-5771.
- Liberali, P., Kakkonen, E., Turacchio, G., Valente, C., Spaar, A., Perinetti, G., Bockmann, R.A., Corda, D., Colanzi, A., Marjomaki, V., et al. (2008). The closure of Pak1-dependent macropinosomes requires the phosphorylation of CtBP1/BARS. *The EMBO journal* 27, 970-981.
- Liljedahl M, Maeda Y, Colanzi A, Ayala I, Van Lint J, Malhotra V. (2001). Protein kinase D regulates the fission of cell surface destined transport carriers from the trans-Golgi network . *Cell* 9;104(3):409-20
- Lin X, Sun B, Liang M, Liang YY, Gast A, Hildebrand J, Brunicardi FC, Melchior F, Feng XH (2003) Opposed regulation of corepressor CtBP by SUMOylation and PDZ binding. *Mol Cell* 11(5):1389–1396.
- Lin, C.Y., Madsen, M.L., Yarm, F.R., Jang, Y.J., Liu, X., and Erikson, R.L. (2000). Peripheral Golgi protein GRASP65 is a target of mitotic polo-like kinase (Plk) and Cdc2. *Proc Natl Acad Sci U S A* 97, 12589-12594.
- Lippincott-Schwartz, J. (2001). *The Endoplasmic Reticulum and Golgi Complex in Secretory Membrane Transport* 4th edn (Philadelphia: Lippincott Williams & Wilkins).
- Lowe, M., and Barr, F.A. (2007). Inheritance and biogenesis of organelles in the secretory pathway. *Nat Rev Mol Cell Biol* 8, 429-439.
- Matter, K., Hunziker, W. & Mellman, I. (1992). Basolateral sorting of LDL receptor in MDCK cells: the cytoplasmic domain contains two tyrosine-dependent targeting determinants. *Cell* 71, 741-753.
- McMahon, H. T. & Boucrot, E. (2011). Molecular mechanism and physiological functions of clathrin-mediated endocytosis. *Nat Rev Mol Cell Biol* 12, 517-533.
- McNiven, M.A., and Thompson, H.M. (2006). Vesicle formation at the plasma membrane and trans-Golgi network: the same but different. *Science* 313, 1591-1594.
- Mellman, I. (1996). Endocytosis and molecular sorting. *Annual review of cell and developmental biology* 12, 575-625.
- Mellman, I., and Simons, K. (1992). The Golgi complex: in vitro veritas? *Cell* 68, 829-840.
- Merrill JC, Kagey MH, Melhuish TA, Powers SE, Zerlanko BJ, Wotton D (2010). Inhibition of CtBP1 activity by Akt-mediated phosphorylation. *J Mol Biol* 398(5):657–671.
- Mirnezami, A. H., Campbell, S. J., Darley, M., Primrose, J. N., Johnson, P. W. and Blaydes, J. P. (2003). Hdm2 recruits a hypoxia-sensitive corepressor to negatively regulate p53-dependent transcription. *Curr Biol* 13, 1234-9.
- Mironov, A.A., Weidman, P., and Luini, A. (1997). Variations on the intracellular transport theme: maturing cisternae and trafficking tubules. *The Journal of cell biology* 138, 481-484.
- Mironov, A. A. et al. Small cargo proteins and large aggregates can traverse the Golgi by a common mechanism without leaving the lumen of cisternae. *J Cell Biol* 155, 1225-1238 (2001).
- Miserey-Lenkei S, Chalancon G, Bardin S, Formstecher E, Goud B, Echard A (2010) Rab and actomyosin-dependent fission of transport vesicles at the Golgi complex. *Nat Cell Biol* 12(7):645–654.
- Misteli, T., and Warren, G. (1995). Mitotic disassembly of the Golgi apparatus in vivo. *J Cell Sci* 108 (Pt 7), 2715-2727.
- Nakagawa, J., Kitten, G.T., and Nigg, E.A. (1989). A somatic cell-derived system for studying both early and late mitotic events in vitro. *J. Cell. Sci.* 94, 449–462.

- Nakamura, N. (2005). Convergence of cell cycle regulation and growth factor signals on
- Nardini, M., Valente, C., Ricagno, S., Luini, A., Corda, D. and Bolognesi, M. (2009). CtBP1/BARS Gly172-->Glu mutant structure: impairing NAD(H)-binding and dimerization. *Biochem Biophys Res Commun* 381, 70-4.
- Nardini, M., Spano, S., Cericola, C., Pesce, A., Massaro, A., Millo, E., Luini, A., Corda, D., and Bolognesi, M. (2003). CtBP/BARS: a dual-function protein involved in transcription co-repression and Golgi membrane fission. *The EMBO journal* 22, 3122-3130.
- Niesporek S., et al (2005). Expression of lysophosphatidic acid acyltransferase beta in ovarian carcinoma: correlation with tumour grading and prognosis. *British Journal of Cancer* 92, 1729-1736
- Novikoff, A.B. (1976). The endoplasmic reticulum: a cytochemist's view (a review). *Proceedings of the National Academy of Sciences of the United States of America* 73, 2781-2787.
- Ovadi, J. & Srere, P. A. Macromolecular compartmentation and channeling *Int. rev. Cytol.* 192, 255-280 (2000).
- Pagel J.M. et al (2005). Induction of apoptosis using inhibitors of lysophosphatidic acid acyltransferase-B and anti-CD20 monoclonal antibodies for treatment of human Non-Hodgkin's Lymphomas *Clin Cancer Res*;11(13).
- Pelkmans, L., and Helenius, A. (2003). Insider information: what viruses tell us about endocytosis. *Current opinion in cell biology* 15, 414-422.
- Persico, A., Cervigni, R.I., Barretta, M.L., and Colanzi, A. (2009). Mitotic inheritance of the Golgi complex. *FEBS Lett* 583, 3857-3862.
- Persico, A., Cervigni, R.I., Barretta, M.L., Corda, D., and Colanzi, A. (2010). Golgi partitioning controls mitotic entry through Aurora-A kinase. *Mol Biol Cell* 21, 3708-3721.
- Peters, J. P., Bos, E. & Griekspoor, A. in *Current Protocols in Cell Biology* Ch. 4.7, (John Wiley & Sons, inc., (2006).
- Polishchuk, R., Di Pentima, A. & Lippincott-Schwartz, J. (2004). Delivery of raft-associated, GPI-anchored proteins to the apical surface of polarized MDCK cells by a transcytotic pathway. *Nat Cell Biol* 6, 297-307.
- Polishchuk, R.S., and Mironov, A.A. (2004). Structural aspects of Golgi function. *Cellular and molecular life sciences : CMLS* 61, 146-158.
- Polishchuk, E.V., Di Pentima, A., Luini, A., and Polishchuk, R.S. (2003). Mechanism of constitutive export from the golgi: bulk flow via the formation, protrusion, and en bloc cleavage of large trans-golgi network tubular domains. *Molecular biology of the cell* 14, 4470-4485.
- Polishchuk, R.S., Polishchuk, E.V., Marra, P., Alberti, S., Buccione, R., Luini, A., and Mironov, A.A. (2000). Correlative light-electron microscopy reveals the tubular-saccular ultrastructure of carriers operating between Golgi apparatus and plasma membrane. *The Journal of cell biology* 148, 45-58.
- Preisinger, C., Korner, R., Wind, M., Lehmann, W.D., Kopajtich, R., and Barr, F.A. (2005). Plk1 docking to GRASP65 phosphorylated by Cdk1 suggests a mechanism for Golgi checkpoint signalling. *EMBO J* 24, 753-765.
- Pucadyil, T. J. & Schmid, S. L. (2010). Supported bilayers with excess membrane reservoir: a template for reconstituting membrane budding and fission. *Biophys J* 99, 517-525
- Pusapati GV, Krndija D, Armacki M, von Wichert G, von Blume J, Malhotra V, Adler G, Seufferlein T (2010). Role of the second cysteine-rich domain and Pro275 in protein kinase D2 interaction with

ADP-ribosylation factor 1, trans-Golgi network recruitment, and protein transport. *Mol Biol Cell* 21(6):1011–1022.

Puthenveedu, M.A., Bachert, C., Puri, S., Lanni, F., and Linstedt, A.D. (2006). GM130 and GRASP65-dependent lateral cisternal fusion allows uniform Golgi-enzyme distribution.

Pyne S, Kong KC, Darroch PI. (2004). Lysophosphatidic acid and sphingosine 1-phosphate biology: the role of lipid phosphate phosphatases. *Semin. Cell Dev. Biol.* 15:491–501

Rambourg, A., and Clermont, Y. (1990). Three-dimensional electron microscopy: structure of the Golgi apparatus. *Eur J Cell Biol* 51, 189-200.

Rastegar F. et al (2010). Lysophosphatidic acid acyltransferase beta promotes the tumor growth of human osteosarcoma *PlosOne* 5 (12)

Reaves, B., and Banting, G. (1992). Perturbation of the morphology of the trans-Golgi network following Brefeldin A treatment: redistribution of a TGN-specific integral membrane protein, TGN38. *The Journal of cell biology* 116, 85-94.

Rhee SG. (2001). Regulation of phosphoinositide-specific phospholipase C. *Annu. Rev. Biochem.* 70:281–312

Rizzo M. A et al, (2000). The recruitment of Raf-1 to membranes is mediated by direct interaction with phosphatidic acid and is independent of association with Ras *J. Biol. Chem* 275:23911-23918.

Rothman, J.E. (2002). Lasker Basic Medical Research Award. The machinery and principles of vesicle transport in the cell. *Nature medicine* 8, 1059-1062.

Roux, A. (2014). Reaching a consensus on the mechanism of dynamin? *F1000Prime Rep* 6, 86

San Pietro, E. et al. (2009). Group IV phospholipase A(2)alpha controls the formation of inter-cisternal continuities involved in intra-Golgi transport. *PLoS Biol* 7.

Schmid, S.L. (1997). Clathrin-coated vesicle formation and protein sorting: an integrated process. *Annual review of biochemistry* 66, 511-548.

Schmid, S. L. & Frolov, V. A. (2011). Dynamin: functional design of a membrane fission catalyst. *Annu Rev Cell Dev Biol* 27, 79-105.

Schmidt, J.A., and Brown, W.J. (2009). Lysophosphatidic acid acyltransferase 3 regulates Golgi complex structure and function. *The Journal of cell biology* 186, 211-218.

Schmitz, F., Konigstorfer, A., and Sudhof, T.C. (2000). RIBEYE, a component of synaptic ribbons: a protein's journey through evolution provides insight into synaptic ribbon function. *Neuron* 28, 857-872.

Schwarz, K., Natarajan, S., Kassas, N., Vitale, N. & Schmitz, F. (2011). The synaptic ribbon is a site of phosphatidic acid generation in ribbon synapses. *J Neurosci* 31, 15996-16011.

Scott S.A. et al (2014). Chemical modulation of glycerolipid signaling and metabolic pathways *Biochimica et Biophysica Acta*

Sengupta, D., and Linstedt, A.D. (2010). Mitotic inhibition of GRASP65 organelle tethering involves Polo-like kinase 1 (PLK1) phosphorylation proximate to an internal PDZ ligand. *J Biol Chem* 285, 39994-40003.

Shaul, Y.D., and Seger, R. (2007). The MEK/ERK cascade: from signaling specificity to diverse functions. *Biochim Biophys Acta* 1773, 1213-1226.

Shaul, Y. D., and Seger, R. (2006). ERK1c regulates Golgi fragmentation during mitosis. *J. Cell Biol.* 172, 885–897

- Shemesh T, Luini A, Malhotra V, Burger KN, Kozlov MM. (2003). Prefission constriction of Golgi tubular carriers driven by local lipid metabolism: a theoretical model. *Biophys. J.* 85:3813–27
- Shima, D.T., Cabrera-Poch, N., Pepperkok, R., and Warren, G. (1998). An ordered inheritance strategy for the Golgi apparatus: visualization of mitotic disassembly reveals a role for the mitotic spindle. *J Cell Biol* 141, 955-966.
- Shindou, H., and Shimizu, T. (2009). Acyl-CoA:lysophospholipid acyltransferases. *The Journal of biological chemistry* 284, 1-5.
- Shindou, H., Hishikawa, D., Harayama, T., Eto, M. & Shimizu, T. (2013). Generation of membrane diversity by lysophospholipid acyltransferases. *J Biochem* 154, 21-28.
- Shorter, J., and Warren, G. (1999). A role for the vesicle tethering protein, p115, in the post-mitotic stacking of reassembling Golgi cisternae in a cell-free system. *J Cell Biol* 146,
- Shorter, J., and Warren, G. (2002). Golgi architecture and inheritance. *Annu Rev Cell Dev Biol* 18, 379-420.
- Shorter, J., Beard, M.B., Seemann, J., Dirac-Svejstrup, A.B., and Warren, G. (2002). Sequential tethering of Golgins and catalysis of SNARE in assembly by the vesicle-tethering protein p115. *J Cell Biol* 157, 45-62.
- Shnyrova, A. V. et al. (2013). Geometric catalysis of membrane fission driven by flexible dynamin rings. *Science* 339, 1433-1436.
- Siddhanta, A., Backer, J.M., and Shields, D. (2000). Inhibition of phosphatidic acid synthesis alters the structure of the Golgi apparatus and inhibits secretion in endocrine cells. *The Journal of biological chemistry* 275, 12023-12031.
- Spanò, S. et al. (1999). Molecular cloning and functional characterization of brefeldin A-ADP-ribosylated substrate. A novel protein involved in the maintenance of the Golgi structure. *J Biol Chem* 274, 17705-17710.
- Stace, C. L. & Ktistakis, N. T. (2006). Phosphatidic acid- and phosphatidylserine-binding proteins. *Biochim Biophys Acta* 1761, 913-926.
- Sutterlin, C., Hsu, P., Mallabiabarrena, A., and Malhotra, V. (2002). Fragmentation and dispersal of the pericentriolar Golgi complex is required for entry into mitosis in mammalian cells. *Cell* 109, 359-369.
- Sutterlin, C., Polishchuk, R., Pecot, M., and Malhotra, V. (2005). The Golgi-associated protein GRASP65 regulates spindle dynamics and is essential for cell division. *Mol Biol Cell* 16, 3211-3222.
- Sujoy Ghosh, Jay C. Strum, Vicki A. Sciorra, Larry Danieli, and Robert M. Bell. (1996) Raf-1 kinase possesses distinct binding domains for phosphatidylserine and phosphatidic Acid *THE JOURNAL OF BIOLOGICAL CHEMISTRY*, 274: 8472–8480.
- Swanson, J.A., and Watts, C. (1995). Macropinocytosis. *Trends in cell biology* 5, 424-428.
- Testerink and Munnik, (2005). Phosphatidic acid: a multifunctional stress signaling lipid in plants. *10(8):368-75. Trends Plant Sci*
- Tigyi and Parrill, (2003). Molecular mechanisms of lysophosphatidic acid action. *42(6):498-526 Proq Lipid Res*
- Valente, C., Luini, A. & Corda, D. (2013). Components of the CtBP1/BARS-dependent fission machinery. *Histochem Cell Biol* 140, 407-421

- Valente C, Turacchio G, Mariggio S, Pagliuso A, Gaibisso R, Di Tullio G, Santoro M, Formiggini F, Spano S, Piccini D, Polishchuk RS, Colanzi A, Luini A, Corda D (2012). A 14-3-3gamma dimer-based scaffold bridges CtBP1-S/BARS to PI(4)KIIIbeta to regulate post-Golgi carrier formation. *Nat Cell Biol* 14(4):343–354.
- Valente, C., Spano, S., Luini, A., and Corda, D. (2005). Purification and functional properties of the membrane fissioning protein CtBP3/BARS. *Methods in enzymology* 404, 296-316.
- Verger, A., Quinlan, K.G., Crofts, L.A., Spano, S., Corda, D., Kable, E.P., Braet, F., and Crossley, M. (2006). Mechanisms directing the nuclear localization of the CtBP family proteins. *Molecular and cellular biology* 26, 4882-4894.
- Wang, Y., Seemann, J., Pypaert, M., Shorter, J., and Warren, G. (2003). A direct role for GRASP65 as a mitotically regulated Golgi stacking factor. *EMBO J* 22, 3279-3290.
- Wang, Y., Satoh, A., and Warren, G. (2005). Mapping the functional domains of the Golgi stacking factor GRASP65. *J Biol Chem* 280, 4921-4928.
- Wang, Y., Wei, J.H., Bisel, B., Tang, D., and Seemann, J. (2008). Golgi cisternal unstacking stimulates COPI vesicle budding and protein transport. *PLoS One* 3, e1647
- Weigert, R. et al. (1999). CtBP/BARS induces fission of Golgi membranes by acylating lysophosphatidic acid. *Nature* 402, 429-433.
- Xiang, Y., and Wang, Y. (2010). GRASP55 and GRASP65 play complementary and essential roles in Golgi cisternal stacking. *J Cell Biol* 188, 237-251.
- Yamashita, A. et al. (2014). Glycerophosphate/Acylglycerophosphate acyltransferases. *Biology* 3, 801-830
- Yang, J.S., Valente, C., Polishchuk, R.S., Turacchio, G., Layre, E., Moody, D.B., Leslie, C.C., Gelb, M.H., Brown, W.J., Corda, D., et al. (2011). COPI acts in both vesicular and tubular transport. *Nature cell biology* 13, 996-1003.
- Yang, J.S., Gad, H., Lee, S.Y., Mironov, A., Zhang, L., Beznoussenko, G.V., Valente, C., Turacchio, G., Bonsra, A.N., Du, G., et al. (2008). A role for phosphatidic acid in COPI vesicle fission yields insights into Golgi maintenance. *Nature cell biology* 10, 1146-1153.
- Yang, J.S., Lee, S.Y., Spano, S., Gad, H., Zhang, L., Nie, Z., Bonazzi, M., Corda, D., Luini, A., and Hsu, V.W. (2005). A role for BARS at the fission step of COPI vesicle formation from Golgi membrane. *The EMBO journal* 24, 4133-4143.
- Yang, J. S. et al. (2005). A role for BARS at the fission step of COPI vesicle formation from Golgi membrane. *EMBO J* 24, 4133-4143
- Yang, J. S. et al. (2006). Key components of the fission machinery are interchangeable. *Nat Cell Biol* 8, 1376-1382
- Yeaman, C. et al. (1997). The O-glycosylated stalk domain is required for apical sorting of neurotrophin receptors in polarized MDCK cells. *J Cell Biol* 139, 929-940
- Yeaman, C., Ayala, M.I., Wright, J.R., Bard, F., Bossard, C., Ang, A., Maeda, Y., Seufferlein, T., Mellman, I., Nelson, W.J., et al. (2004). Protein kinase D regulates basolateral membrane protein exit from trans-Golgi network. *Nature cell biology* 6, 106-112.
- Yoshimura, S., et al (1999). Golgi membranes are absorbed into and reemerge from the ER during mitosis. *Cell* 99, 589-601.
- Yuki, K., Shindou, H., Hishikawa, D. & Shimizu, T. (2009). Characterization of mouse lysophosphatidic acid acyltransferase 3: an enzyme with dual functions in the testis. *J Lipid Res* 50, 860-869

AKNOWLEDGMENTS

I would like to thank all the people who have helped and supported me during these years.

First of all I would like to thank my supervisor, Dr.ssa Daniela Corda for giving me the opportunity to do my PhD; for her continuous scientific support and for giving me many opportunities to grow as a scientist and as a woman all over these years.

I want to thank also Dr Alberto Luini for all the precious and useful discussions on my project. I am also grateful to my tutor, Dr.ssa Carmen Valente for her constant patience and guidance and for teaching me how become a good scientist.

Many thanks go to Prof.re Giovanni Sannia, the coordinator of the PhD program and also to Chris Berrie for reading and correcting my thesis.

I would like to thank also Prof. Vivek Malhotra and all his lab, I spent almost two months in his laboratory with the aim to perform some experiments on the role of CtBP1-S/BARS in mitosis. It was a beautiful and exciting experience, I have worked in a beautiful atmosphere and I am sure I will always remember that period.

I would like to thank my lab colleagues (past and present) for the pleasant time spent together, a special thought goes to Alessandro for all the scientific and not discussions, he has passed to me all his experience, I think he is the most generous scientist I have ever met.

I want to thank my nice flatmates, Melissa, Valeria and Grazia for sharing with me all the best and worst moments during my PhD. They made my Neapolitan experience more beautiful and meaningful. I am sure that our friendship will never end despite the distance.

A big thank you goes to my family, my mum Anna, who has always supported me and encouraged me to do my best, my dad Domenico, who has always believed in me and my brother Giulio who loves me despite what he usually says.

I want to thank also my old and best friends Valentina, Rossana and Chiara who are always with me in every significant moment of my life, during these years they have always listened to me and supported me as only best friends can do.

Last but not least I want to thank Massimiliano for being my “sun after the storm”.

Appendix

List of Communications

Young Scientist's Forum, Paris, France 27- 30 August 2014

Lucia Laura Giordano, Carmen Valente, Alessandro Pagliuso, Alberto Luini, Daniela Corda.

"Molecular mechanisms of the CtBP1-S/BARS-dependent membrane fission processes".

FEBS-EMBO Paris, France 30 August- 4 September 2014

Lucia Laura Giordano, Carmen Valente, Alessandro Pagliuso, Alberto Luini, Daniela Corda.

"Molecular mechanisms of the CtBP1-S/BARS-dependent membrane fission processes".

Golgi Apparatus Symposium, Bad Ischl, Austria September 17-19, 2013.

Valente Carmen, Pagliuso Alessandro, **Giordano Lucia Laura**, Turacchio Gabriele, Circolo Diego, Corda Daniela and Luini Alberto.

"Lysophosphatidic acid acyltransferases 4 (LPAAT4) is activated by CtBP1/BARS and drives membrane fission during the formation of post-Golgi basolateral carriers."

PhD Student Conference, Vico Equense, Italy, 4-6 November 2012.

Giordano Lucia Laura, Valente Carmen, Pagliuso Alessandro, Luini Alberto, Corda Daniela.

"Molecular mechanisms of CtBP1-S/BARS-dependent membrane fission processes involved in membrane trafficking"

ABCD MEETING, Joint National PhD Meeting, Rimini, Italy, 11-13 October 2012.

Giordano Lucia Laura, Valente Carmen, Pagliuso Alessandro, Luini Alberto, Corda Daniela.

"Molecular mechanisms of CtBP1-S/BARS-dependent membrane fission processes involved in membrane trafficking"

FEBS Advanced Course, Lipid signalling and cancer. Vico Equense, Italy, 4-10 October 2012.

Giordano Lucia Laura, Valente Carmen, Pagliuso Alessandro, Luini Alberto, Corda Daniela.

"Molecular mechanisms of CtBP1-S/BARS-dependent membrane fission processes involved in membrane trafficking"

Oral Communication

Young Scientist's Forum, Paris, France 27- 30 August 2014

"Molecular mechanisms of the CtBP1-S/BARS-dependent membrane fission processes"

List of Abstracts

Young Scientist's Forum

Paris, France 27- 30 August 2014

Lucia Laura Giordano, Carmen Valente, Alessandro Pagliuso, Alberto Luini, Daniela Corda.

“Molecular mechanisms of the CtBP1-S/BARS-dependent membrane fission processes”.

FEBS-EMBO

Paris, France 30 August- 4 September 2014

Lucia Laura Giordano, Carmen Valente, Alessandro Pagliuso, Alberto Luini, Daniela Corda.

“Molecular mechanisms of the CtBP1-S/BARS-dependent membrane fission processes”.

EMBO Workshop: “Cellular imaging of lipids”

Vico Equense, Italy June 2014

Valente Carmen, Pagliuso Alessandro, **Giordano Lucia Laura**, Turacchio Gabriele, Circolo Diego, Corda Daniela and Luini Alberto.

“Molecular mechanisms of post-Golgi tubular carrier formation”.

Confèrence Jaques Monod: “Molecular basis for membrane remodelling and organization”

Roscoff, France November 2014

Valente Carmen, Pagliuso Alessandro, **Giordano Lucia Laura**, Turacchio Gabriele, Circolo Diego, Corda Diego and Luini Alberto.

“Molecular mechanisms of post-Golgi tubular carrier formation”

MTOB Molecular Trafficking and Organelle Biogenesis

Pesaro, Italy 4-5 April, 2014

Valente Carmen, Pagliuso Alessandro, **Giordano Lucia Laura**, Turacchio Gabriele, Circolo Diego, Luini Alberto, Corda Daniela.

“Molecular mechanisms of post-Golgi tubular carrier formation.”

9th Interational EMBO-Annaberg Conference

Goldegg am See, Austria, 14-19 January 2014

Valente Carmen, Pagliuso Alessandro, **Giordano Lucia Laura**, Turacchio Gabriele, Circolo Diego, Corda Daniela and Luini Alberto.

“Lysophosphatidic acid acyltransferases 4 (LPAAT4) is activated by CtBP1/BARS and drives membrane fission during the formation of post-Golgi basolateral carriers.”

Golgi Apparatus Symposium

Bad Ischl, Austria September 17-19, 2013

Valente Carmen, Pagliuso Alessandro, **Giordano Lucia Laura**, Turacchio Gabriele, Circolo Diego, Corda Daniela and Luini Alberto.

“Lysophosphatidic acid acyltransferases 4 (LPAAT4) is activated by CtBP1/BARS and drives membrane fission during the formation of post-Golgi basolateral carriers.”

PhD Student Conference

Vico Equense, Italy, 4-6 November 2012

Giordano Lucia Laura, Valente Carmen, Pagliuso Alessandro, Luini Alberto, Corda Daniela.

“Molecular mechanisms of CtBP1-S/BARS-dependent membrane fission processes involved in membrane trafficking”

ABCD MEETING, Joint National PhD Meeting

Rimini, Italy, 11-13 October 2012

Giordano Lucia Laura, Valente Carmen, Pagliuso Alessandro, Luini Alberto, Corda Daniela.

“Molecular mechanisms of CtBP1-S/BARS-dependent membrane fission processes involved in membrane trafficking”

FEBS Advanced Course, Lipid signalling and cancer

Vico Equense, Italy, 4-10 October 2012

Giordano Lucia Laura, Valente Carmen, Pagliuso Alessandro, Luini Alberto, Corda Daniela.

“Molecular mechanisms of CtBP1-S/BARS-dependent membrane fission processes involved in membrane trafficking”

Awards

14th YSF grant for:

- **Young Scientist’s Forum,**
Paris, France 27- 30 August 2014
- **FEBS-EMBO 2014 Conference.**
Paris, France 30 August- 4 September 2014

List of publications

Manuscript submitted to “ E-Life”

A.Pagliuso[#], C.Valente[#], **L.L.Giordano**, G. Li, D.Circolo, G.Turacchio, F.Forniggini, R. S. Polishuck, D.Corda and A. Luini.

“Golgi membrane fission requires the BARS-induced activation of lysophosphatidic acid acyltransferase δ ”

[#]These authors contributed equally to this work.

Experience in foreign laboratories

Stage at the **CRG (Centre for Genomic Regulation), Dr Aiguader 88, Barcelona, Spain** from 1 November 2014 to 21 December 2014.

Supervisor: Prof.re Vivek Malhotra, Cell and Developmental Biology Department.

Project: “Molecular mechanisms of the CtBP1-S/BARS-dependent membrane fission processes involved in mitosis”.



To whom it may concern

The **Centre for Genomic Regulation (CRG)** with fiscal number Identification G62426937 and addressed in Doctor Aiguader 88, Spain, Barcelona,

CERTIFIES:

That Ms. Lucia Laura Giordano, with identity number AO6346746, was a scientist visitant at CRG from 1st November 2014 until 19th December 2014.

That Ms. Lucia Laura Giordano joined at Dr. Vivek Malhotra lab, dedicated to "Intracellular Compartmentation" research. For more information on the research of Dr. Malhotra visit: <http://www.crg.eu/en/programmes-groups/intracellular-compartmentation>.

And it is on record, this document is issued in Barcelona on December 19th, 2014.



Ines Fonseca
Human Resources Department
Centre for Genomic Regulation (CRG)

C/ Dr. Aiguader, 88
08003 Barcelona
Tel. +34 93 316 01 00
Fax +34 93 316 00 99
www.crg.es



1 **Golgi membrane fission requires the BARS-induced activation of lysophosphatidic acid**
2 **acyltransferase δ .**

3

4 Alessandro Pagliuso^{1,2,3,4}, Carmen Valente^{1,2,5}, Lucia Laura Giordano¹, Guiling Li^{1,5}, Diego
5 Circolo¹, Gabriele Turacchio¹, Fabio Formiggini³, Roman S. Polishchuk², Daniela Corda^{1,6} and
6 Alberto Luini^{1,8}.

7

8 ¹Institute of Protein Biochemistry, National Research Council, Via Pietro Castellino 111,
9 80131 Naples, Italy.

10 ²Telethon Institute of Genetics and Medicine (TIGEM), Via Campi Flegrei 34, 80078
11 Pozzuoli, Italy.

12 ³Italian Institute of Technology, Center for Advanced Biomaterials for Health Care at CRIB,
13 Naples, Italy.

14

15 ⁴These authors contributed equally to this work and are listed in alphabetic order.

16

17 Current addresses:

18 ⁴Institute Pasteur, Unité des Interactions Bactéries-Cellules; Département de Biologie
19 Cellulaire et Infection; Paris, France

20 ⁵Institute of Genomic Medicine, Wenzhou Medical University, Wenzhou, Zhejiang Province
21 P.R. China, 325000.

22

23 ⁸Correspondence should be addressed to:

24 Daniela Corda

25 Institute of Protein Biochemistry, CNR

26 Via Pietro Castellino 111, 80131, Naples, Italy

27 e-mail: d.corda@ibp.cnr.it

28 Tel: +39-081-6132536

29 Fax: +39-081-6132277

30

31 Alberto Luini

32 Institute of Protein Biochemistry, CNR

33 Via Pietro Castellino 111, 80131, Naples, Italy

34 e-mail alberto.luini@cnr.it

35 Tel: +39-081-6132535

36 Fax: +39-081-6132277

37

38 Carmen Valente

39 Institute of Protein Biochemistry, CNR

40 Via Pietro Castellino 111, 80131, Naples, Italy

41 e-mail c.valente@ibp.cnr.it

42 Tel: +39-081-6132631

43 Fax: +39-081-6132277

44

Manuscript under revision

45

46 **Abstract**

47

48 Membrane fission is an essential cellular process by which continuous endomembranes divide
49 into separate parts. We have previously identified CtBP1-S/BARS (BARS) as a key
50 component of a protein complex that is required for the fission of several endomembranes
51 including basolateral post-Golgi transport carriers. At the Golgi, BARS binds to the
52 phosphoinositide kinase PI4KIII β through a 14-3-3 γ dimer, as well as to ARF and the PKD
53 and PAK kinases. We now report that 14-3-3 γ -bound BARS binds and activates a trans-Golgi
54 acyl-transferase type δ (LPAAT δ) that converts lysophosphatidic acid (LPA) into
55 phosphatidic acid (PA); and that this reaction is essential for carrier fission. Given the
56 biophysical properties of LPA/PA, these findings can provide new insight into the mechanics
57 of membrane fission.

58

Manuscript under revision

59

60 **Introduction**

61

62 Membrane fission consists of a series of molecular rearrangements by which a tubular bilayer
63 joining two membranous compartments undergoes constriction and splits in two parts without
64 leakage of contents. It is required for the formation of transport vesicles during membrane
65 traffic, organelle partitioning, cell division, and in general in the maintenance of the
66 compartmental organization of endomembranes. Fission has been studied intensely during the
67 last decade and shown to be driven by diverse mechanisms (Campelo and Malhotra, 2012;
68 Johannes and Mayor, 2010; Kozlov et al., 2010; Pucadyil and Schmid, 2010) including
69 membrane insertion of amphipathic protein domains (Adolf et al., 2013; Boucrot et al., 2012;
70 Campelo and Malhotra, 2012; Lee et al., 2005) constriction and destabilization of membranes
71 by the mechano-enzyme dynamin (Daumke et al., 2014; Ferguson and De Camilli, 2012;
72 McMahon and Boucrot, 2011; Roux, 2014; Schmid and Frolov, 2011; Shnyrova et al., 2013),
73 and phase separation of lipid domains (Johannes and Mayor, 2010; Lenz et al., 2009).
74 Nevertheless, the precise mechanics of fission remains elusive, and further analysis of the
75 molecular steps leading to fission are still needed.

76 We have identified the protein CtBP1-S/BARS (henceforth, BARS) as a key player in
77 the fission of post-Golgi tubular/ pleiomorphic carriers (Bonazzi et al., 2005; Valente et al.,
78 2013; Valente et al., 2012); macropinosomes (Haga et al., 2009; Liberali et al., 2008); COPI-
79 dependent transport vesicles (Yang et al., 2008; Yang et al., 2005; Yang et al., 2006); and of
80 the Golgi ribbon during mitosis (Colanzi et al., 2007; Hidalgo Carcedo et al., 2004).
81 Structurally, BARS belongs to the D-hydroxyacid dehydrogenase family and includes a
82 Rossmann fold (Nardini et al., 2003) which, depending on binding to NAD(H) or other ligands,
83 regulates the interconversion of BARS between two (monomeric or dimeric) conformations
84 (Colanzi et al., 2013; Liberali et al., 2008; Nardini et al., 2003; Nardini et al., 2009; Valente et
85 al., 2013). This conversion is critical because BARS (a dual-function protein that controls
86 fission in the cytoplasm and gene transcription in the nucleus) (Chinnadurai, 2009; Corda et
87 al., 2006; Valente et al., 2013) can drive fission as a monomer, while it is fission-incompetent
88 as a dimer (Colanzi et al., 2013; Liberali et al., 2008; Nardini et al., 2003; Yang et al., 2005).

89 The mechanism of action of BARS in fission has been studied mostly in the context of
90 the basolateral post-Golgi carrier formation process (Bonazzi et al., 2005; Valente et al.,
91 2013; Valente et al., 2012). Here, BARS assembles into a complex that includes ARF,

92 frequenin, the phosphoinositide kinase PI4KIII β , 14-3-3 γ and the kinases PKD and PAK, and
93 functions to coordinate the budding of carriers with fission (Valente et al., 2013; Valente et
94 al., 2012). To induce fission, BARS must bind to 14-3-3 γ through a phosphorylated serine
95 (Ser147) in its dimerization surface (Valente et al., 2013; Valente et al., 2012) (see also
96 below). This binding thus locks BARS in its monomeric conformation. However, how the 14-
97 3-3 γ -bound BARS leads to the lipid rearrangements involved in fission remains unclear.

98 Previously, we have proposed that BARS-dependent fission involves a
99 lysophosphatidic acid (LPA) acyltransferase (LPAAT), based on the following observations:
100 liver Golgi membranes contain an LPAAT(s) which, upon addition of suitable substrates,
101 generates phosphatidic acid (PA) (Weigert et al., 1999); PA production correlates with the
102 fission of these Golgi membranes (Weigert et al., 1999); addition of BARS to the Golgi
103 membranes stimulates both PA production and membrane fission (Weigert et al., 1999);
104 treatments that inhibit the formation of monomeric fission-competent BARS inhibit both
105 LPAAT activity and membrane fission (Colanzi et al., 2013; Weigert et al., 1999; Yang et al.,
106 2005). We have also reported that recombinant BARS is associated with a slow LPAAT
107 activity (Weigert et al., 1999) (see below) which, however, was later shown not to be intrinsic
108 to BARS (Gallop et al., 2005).

109 Moreover, PA metabolism has been implicated in membrane transport by other
110 groups, albeit generally based on indirect evidence (Asp et al., 2009; Baron and Malhotra,
111 2002; Haga et al., 2009; Schwartz et al.; Siddhanta et al., 2000; Stace and Ktistakis, 2006;
112 Yang et al., 2008).

113 Based on these findings, here we examined whether BARS might bind to and
114 stimulate an endogenous LPAAT, and this might result in membrane fission. There are 11
115 known LPLATs, 4 of which have been cloned and shown to transfer fatty acids from acyl-
116 CoA to the *sn*-2 position of LPA to form PA (LPAAT α , β , γ and δ) while others have mixed
117 specificities for LPA and glycerol-phosphate (Shindou et al., 2013; Yamashita et al., 2014).
118 We find that: BARS interacts with LPAAT type δ ; this LPAAT localizes to the *trans*-Golgi
119 and to post-Golgi carriers precursors; the catalytic activity of LPAAT δ is essential for Golgi
120 carrier fission; BARS potently stimulates LPAAT δ , and this stimulation is essential for
121 carrier fission; BARS needs to be incorporated in the PI4KIII β -14-3-3 γ -BARS complex
122 (Valente et al., 2012) to stimulate LPAAT δ and induce fission. BARS thus appears to behave
123 as an 'active' scaffold that binds and stimulates LPAAT δ , inducing LPA-PA conversion and
124 carrier fission. LPA and PA possess unique biophysical properties that can strongly affect the

125 organization of lipid bilayers (Kooijman and Burger, 2009; Kooijman et al., 2005a; Kooijman
126 et al., 2003; Kooijman et al., 2005b). Their interconversion may play a key role in several
127 cellular fission events.

128

129

130

131 **Results**

132

133 **LPAAT δ localizes at the Golgi and interacts with BARS**

134 To examine whether BARS interacts with an LPAAT, we first sought to identify the LPAATs
135 that localize to the Golgi, as most of the BARS-dependent fission reactions occur in this
136 organelle (Valente et al., 2013; Valente et al., 2012). We Flag-tagged and expressed the
137 available mammalian LPAAT and inspected their localization by immunofluorescence.
138 LPAAT γ , LPAAT δ and LPAAT η localized to both the Golgi and the Endoplasmic Reticulum
139 (ER) (Figure 1A), while LPAAT β and LPAAT ϵ localized to the ER and mitochondria (Figure
140 1-figure supplement 1; see also Shindou et al., 2013, Yamashita et al., 2014). We thus asked
141 whether BARS interacts with the Golgi LPAATs by co-expressing BARS with each of these
142 transferases and testing for co-immunoprecipitation. BARS co-precipitated with LPAAT γ and
143 LPAAT δ (and *vice-versa*), but not with LPAAT η (Figure 1B,C). LPAAT γ has been shown to
144 reside at the *cis*-Golgi and to regulate Golgi structure and retrograde transport to the ER
145 (Schmidt and Brown, 2009; Yang et al., 2011), while LPAAT δ has no characterized, Golgi-
146 related function to date. We examined if the LPAAT δ location might be compatible with
147 post-Golgi traffic by studying the intra-Golgi location of this transferase using specific
148 antibodies and immuno-electron microscopy (Figure 1D) as well as immunofluorescence
149 (Figure 1E). LPAAT δ localized mostly to the *trans*-Golgi and *trans*-Golgi network (TGN)
150 (Figure 1D,B) and to elongated tubules that emanated from the Golgi (Figure 1E).

151 Focusing further on LPAAT δ , we asked whether this transferase interacts selectively
152 with the monomeric fission-competent form of BARS (Valente et al., 2013). As noted above,
153 BARS shifts between these two conformations depending on ligand binding to its Rossman
154 fold. At steady state, BARS is largely monomeric (Colanzi et al., 2013; Spanò et al., 1999),
155 while NAD(H) promotes dimerization (Birts et al., 2013; Colanzi et al., 2013; Nardini et al.,
156 2003; Nardini et al., 2009) and acyl-CoA promotes monomerization (Nardini et al., 2003;
157 Yang et al., 2005). Another ligands is BAC, an ADP-ribosylated metabolite of brefeldin A
158 (Brefeldin-ADP-ribosylated Conjugate) which also fits in the BARS Rossman fold and

159 generates a covalent bond between its C3 atom and BARS Arg304 (Colanzi et al., 2013). This
160 locks BARS in the dimeric inactive conformation very efficiently (Colanzi et al., 2013). BAC
161 nearly abolished the association between BARS and LPAAT δ (Figure 1F,G), indicating that
162 BARS binds LPAAT δ in its monomeric form.

163 Thus, an LPAAT isoform located in the *trans*-Golgi binds selectively with the fission-
164 active form of BARS.

165

166 **The *E. Coli* LPAAT binds to the fission-active BARS conformation and competes with** 167 **LPAAT δ for BARS binding**

168 As noted, recombinant BARS purified from *E. Coli* is associated with low levels of LPAAT
169 activity (Gallop et al., 2005; Weigert et al., 1999) (see also Figure 1-figure supplement 2).
170 We carried out a series of pull-down experiments to examine whether purified BARS and *E.*
171 *Coli* LPAAT bind in a specific fashion. His-tagged *E. coli* LPAAT (which can be prepared in
172 soluble form) (Coleman, 1992) showed strong binding with recombinant BARS (Figure 1-
173 figure supplement 3A), and this binding was abolished by pretreatments with BAC or
174 NAD(H), indicating that *E. coli* LPAAT binds selectively to monomeric BARS (Figure 1-
175 figure supplement 3B,C). We also asked whether *E. coli* LPAAT might compete with
176 mammalian LPAAT δ for binding to BARS (Figure 1-figure supplement 3D), and found this
177 to be the case, indicating that the mammalian and bacterial LPAATs bind to the same BARS
178 domain. These results suggest that the LPAAT δ and *E. coli* LPAAT BARS-binding surfaces
179 are conserved. Considering the evolutionary distance between the two LPAATs, this is
180 somewhat surprising. It is conceivable, however, that the evolutionary ancestors of LPAAT δ
181 and BARS (namely, the bacterial LPAAT and 3-phospho-glycerate dehydrogenase,
182 respectively) (Coleman, 1992; Nardini et al., 2003), which are both metabolic enzymes, were
183 interactors in an ancient metabolic multi-enzyme complex (Ovadi and Sreere, 2000), and that
184 this interaction was maintained through evolution in different functional contexts.

185 Regardless, these data explain our previous observation that BARS purified from *E.*
186 *coli* associates with an LPAAT activity (Weigert et al., 1999) and provide a potentially useful
187 tool (the soluble bacterial enzyme) for the *in vitro* reconstitution of BARS-dependent fission
188 (see below).

189

190 **LPAAT δ is required for post-Golgi carrier fission**

191 The TGN localization and the interaction of LPAAT δ with BARS prompted us to investigate
192 the role of this enzyme in the BARS-dependent formation of post-Golgi carriers (Bonazzi et

193 al., 2005). LPAAT δ was silenced with specific (si)RNAs, and the formation of carriers was
194 monitored using the temperature-sensitive vesicular stomatitis virus G protein (ts045-VSVG;
195 henceforth, VSVG) (Mironov et al., 2001) as a traffic marker. The transport of VSVG out of
196 the Golgi can be synchronized by accumulating this protein in the TGN at 20°C and then
197 shifting to the permissive temperature of 32°C (Bonazzi et al., 2005). The formation and
198 release of VSVG-containing tubular carriers from the TGN can then be visualized and
199 quantified by immunofluorescence microscopy (Bonazzi et al., 2005; Polishchuk et al., 2004;
200 Valente et al., 2012). Depletion of LPAAT δ markedly reduced the formation of the VSVG-
201 containing carriers (Figure 2A); whereas depletion of LPAAT γ , which is located to the *cis*-
202 Golgi and is involved in Golgi-to-ER traffic (Schmidt and Brown, 2009; Yang et al., 2011),
203 had no effect (Figure 2B).

204 To determine whether the reduction in VSVG-containing carriers was due to inhibition
205 of carrier budding or of fission, we monitored carrier formation in living cells expressing
206 VSVG-GFP. LPAAT δ -depleted cells showed a large number of long (>10 μ m) tubular
207 extensions that contained VSVG-GFP, which appeared to be carrier precursors. These
208 elongated out of the Golgi but did not detach, and often retracted back into the Golgi area
209 without forming free-moving intermediates (Videos 1 and 2). This phenotype was similar to
210 that induced by expressing BARS dominant negative mutants or by depleting BARS (we
211 noted that BARS depletion also reduced the number of tubular precursors; see Bonazzi et al.,
212 2005; Valente et al., 2012 and our unpublished data), or by depleting the PI4KIII β -14-3-3 γ
213 dimer-BARS complex component 14-3-3 γ (Valente et al., 2013; Valente et al., 2012). Very
214 similar effects were induced by microinjection of an affinity-purified antibody against
215 LPAAT δ (Video 3; see also Video 3-figure supplement 1) and by the general LPAAT
216 inhibitor CI-976 (Drecktrah et al., 2003) (Video 4). These collective observations are
217 consistent with an essential role for LPAAT δ in carrier fission from the Golgi complex.

218 We also determined the role of LPAAT δ in other traffic steps. We first examined
219 retrograde traffic from Golgi to ER (which is known to require LPAAT γ) (Schmidt and
220 Brown, 2009; Yang et al., 2011), by tracking the retrograde transport marker VSVG-KDEL
221 (a fusion of VSVG with the KDEL receptor) (Cole et al., 1998). Transport of VSVG-KDEL
222 was not affected by LPAAT δ depletion (Figure 2C). Secondly, as BARS controls the fission
223 of basolateral but not of apical carriers (Bonazzi et al., 2005), we examined the role of
224 LPAAT δ in Golgi export of p75 (an apical cargo) (Yeaman et al., 1997) in comparison with
225 export of the LDL receptor (a basolateral cargo, like VSVG) (Matter et al., 1992). Depletion
226 of LPAAT δ inhibited export of the LDL receptor (Figure 2D), as with VSVG, but not that of

227 p75 (Figure 2E). Therefore, LPAAT δ appears to be selectively required for fission of
228 basolateral carriers.

229

230 **The enzymatic activity of LPAAT δ is needed for post-Golgi carrier fission**

231 To examine whether the enzymatic activity of LPAAT δ (Eto et al., 2014) was required for
232 fission, we assessed LPAAT δ activity and post-Golgi carrier fission in parallel experiments.

233 To determine the LPAAT enzymatic activity, we prepared and incubated post-nuclear
234 supernatants with the acyl donor (1-¹⁴C)-oleoyl-CoA and the acyl acceptor oleoyl-LPA, with

235 (1-¹⁴C)-PA measured as the reaction product (see Methods and Figure 3A). Since attempts to
236 purify LPAAT enzymes results in activity loss (Chen et al., 2008; Eto et al., 2014) these are

237 standard conditions used for LPAAT assays (Chen et al., 2008; Eto et al., 2014). Extracts
238 from control cells showed a transferase activity that was suppressed by the general LPAAT

239 inhibitor CI-976 (Figure 3B) (Chambers et al., 2005; Yang et al., 2011). A difficulty with
240 these extracts is that they contain multiple LPAATs. We therefore designed conditions to

241 determine selectively the LPAAT δ activity (Figure 3A) based on suppressing or
242 overexpressing this enzyme. Extracts from LPAAT δ -depleted cells (Figure 3A), or treatment

243 of control extracts with a specific affinity-purified antibody against LPAAT δ (Figure 3B) (see
244 Methods for antibody characterization) showed a reproducibly lower (25%) activity than in

245 controls (Figure 3A,B), indicating that LPAAT δ is responsible for a small fraction of the total
246 LPAAT activity. This is indeed in line with the presence of other LPAATs and in particular of

247 the abundant glycerolipid synthetic enzymes LPAAT α and LPAAT β (Leung, 2001;
248 Yamashita et al., 2014). Extracts from LPAAT δ -overexpressing cells showed a 40% increase

249 in LPAAT activity over controls (Figure 3A-C). This increase was completely inhibited by
250 the antibodies against LPAAT δ , which, in fact, decreased the LPAAT activity (Figure 3B) to

251 the levels found in the absence of LPAAT δ (Figure 3A). LPAAT δ silencing or
252 overexpression did not affect the cellular levels of other LPAATs (our unpublished data).

253 Similar data were obtained using (1-¹⁴C)-palmitoyl-CoA as acyl donor and arachidonoyl-LPA
254 as acyl acceptor (not shown). We thus define the LPAAT δ -dependent activity (or LPAAT δ

255 activity) as the activity value of LPAAT δ overexpressing extracts (as measured using
256 concentrations of substrates below the K_m values, see below) minus the activity value of

257 LPAAT δ depleted (or antibody-treated) extracts (Figure 3A,B, see dashed line and Methods).

258 The V_{max} and K_m of this LPAAT δ activity were 38 ± 3 nmol/min/mg proteins and 58 ± 18 μ M,
259 respectively, for oleoyl-CoA, and 38 ± 1 nmol/min/mg proteins and 29 ± 1 μ M, respectively,

260 for oleoyl-LPA. These rates are comparable to those reported for LPAAT γ (see Yuki et al.,

261 2009; our unpublished data). Importantly, simple calculations show that they are potentially
262 sufficient, depending on substrate availability, to change rapidly and substantially the PA
263 concentrations in the TGN.

264 Finally, we asked whether the LPAAT δ catalytic activity is required for post-Golgi
265 carrier fission. We generated a single-point mutant (LPAAT δ^{H96V}) in the conserved
266 acyltransferase catalytic site of LPAAT δ (NHX₂D) (Lewin et al., 1999; Yamashita et al.,
267 2014). Overexpressed LPAAT δ^{H96V} was indeed devoid of LPAAT activity (Figure 3C)
268 confirming that LPAAT δ is a canonical LPAAT. We then depleted cells of LPAAT δ , with
269 the consequent inhibition of the post-Golgi transport of VSVG (see Figure 2A and Video 2)
270 and expressed either a siRNA-resistant variant of LPAAT δ or the catalytically-dead
271 LPAAT δ^{H96V} mutant. Only wild-type LPAAT δ rescued carrier formation, while LPAAT δ^{H96V}
272 was completely inactive (Figure 3D). These data indicate that LPAAT δ possesses substantial
273 catalytic activity and that this activity is necessary for post-Golgi carrier formation.

274

275 **BARS activates LPAAT δ and this activation is required for carrier fission**

276 Since BARS and LPAAT δ interact (Figure 1) and are required for post-Golgi carrier fission
277 (see Bonazzi et al., 2005; Valente et al., 2012 and Videos 2 and 3, respectively), we asked
278 whether BARS might regulate the enzymatic activity of LPAAT δ , and whether this regulation
279 might be required for carrier fission. We first silenced BARS and measured the LPAAT δ
280 activity in cell extracts. BARS depletion abolished this activity (Figure 4A). We then re-
281 expressed BARS in BARS-silenced cells, using a siRNA-resistant replacement BARS
282 construct (Figure 4-figure supplement 1A). This nearly completely restored the LPAAT δ
283 activity (Figure 4A). As a specificity control, the above BARS manipulations did not affect
284 the cellular levels of LPAAT δ (Figure 4-figure supplement 1A) or of other LPAATs (our
285 unpublished data). These results indicate that LPAAT δ requires BARS to express its activity.

286 We then sought to manipulate the BARS levels acutely *in-vitro* to exclude
287 transcriptional or compensatory effects that might arise in siRNA depletion experiments
288 (Chinnadurai, 2009; Corda et al., 2006; Valente et al., 2013). We prepared extracts from
289 LPAAT δ -expressing BARS-depleted cells, where LPAAT δ is inactive (Figure 4A), and
290 added immunopurified BARS to the assay mixture to reach a final BARS concentration of 5
291 μ g/ml (comparable to the levels of endogenous BARS) (Bonazzi et al., 2005; Haga et al.,
292 2009). Under these conditions, BARS completely restored the LPAAT δ -dependent activity
293 (Figure 4B) (notably, the LPAAT activity associated with the purified BARS was

294 quantitatively negligible) (Gallop et al., 2005; Weigert et al., 1999). We also added BARS to
295 control LPAAT δ -expressing extracts. This only slightly stimulated the LPAAT δ -dependent
296 activity (Figure 4B), suggesting that endogenous BARS is sufficient to activate LPAAT δ
297 nearly maximally, at least in preparations from quiescent cells (i.e., in cells not subjected to a
298 traffic pulse; see below). As a further control, we used extracts from cells depleted of BARS
299 and LPAAT δ (Figure 4B). Here, added BARS had no effect on the LPAAT activity,
300 suggesting that other LPAAT isoforms are not detectably stimulated by BARS. We also tested
301 the effects of BARS on the activity of LPAAT γ , a BARS interactor (Figure 1B,C), in
302 experiments similar to those designed for LPAAT δ . Perhaps surprisingly, BARS had no
303 effect on this enzyme (our unpublished data). These collective data indicate that the
304 stimulatory effects of BARS are rapid and apparently selective for LPAAT δ , at least under
305 our experimental conditions. Notably, these effects correlate well with the ability of
306 microinjected purified BARS to activate the fission of post-Golgi carriers in live cells
307 (Bonazzi et al., 2005).

308 Further along this line, we sought to inhibit BARS by adding in the LPAAT assay
309 mixture a characterized affinity-purified neutralizing anti-BARS antibody which, when
310 microinjected into cells, inhibits carrier fission (Bonazzi et al., 2005; Valente et al., 2005;
311 Valente et al., 2012). This antibody inhibited the LPAAT δ -dependent activity, while
312 preimmune-IgG addition had no effect (Figure 4C). Moreover, a BARS pre-treatment with
313 BAC, which locks BARS in its dimeric fission-incompetent conformation and inhibit the
314 fission of the Golgi ribbon (Colanzi et al., 2013), reduced the LPAAT δ activity (Figure 4D),
315 indicating that monomeric BARS is required for LPAAT δ to express its enzymatic activity.

316 We further examined the relationship between LPAAT δ activity and carrier fission by
317 expressing suitable BARS mutants. Previously, we have characterized two single-point
318 mutants, BARS^{S35N} and BARS^{S147A} that exert a dominant-negative effect on carrier fission in
319 living cells (Bonazzi et al., 2005; Valente et al., 2012). We tested these mutants in the
320 LPAAT δ activity assay by co-expressing each of them with LPAAT δ . Both nearly
321 completely inhibited the LPAAT δ -dependent activity (Figure 4E), again without affecting
322 LPAAT δ expression levels (Figure 4-figure supplement 1B). As a control, we tested the
323 effect of overexpressing wild-type BARS (notably, wild-type BARS and the dominant
324 negative mutants showed comparable expression levels in these experiments; see Figure 4-
325 figure supplement 1B). Overexpressed BARS did not have significant effects on the LPAAT δ
326 activity in extracts from 'quiescent' cells (Figure 4E). We noted, however, that BARS is
327 recruited to the Golgi during a traffic pulse and activates carrier fission, suggesting that active

328 traffic increases the requirement for BARS (Valente et al., 2012). In extracts prepared during
329 a traffic pulse, overexpressed BARS stimulated the LPAAT δ activity (Figure 4F). Further,
330 again in traffic-stimulated extracts, expression of the fission-active BARS^{S147D} mutant that
331 mimics the activatory phosphorylation of BARS on Ser147 (Haga et al., 2009; Liberali et al.,
332 2008; Valente et al., 2012) stimulated the LPAAT δ activity to an even greater extent (Figure
333 4F).

334 We finally tested the role of the BARS-14-3-3 γ -PI4KIII β complex in LPAAT δ
335 activation. As noted, within this complex, 14-3-3 γ binds to phosphorylated S147 in the BARS
336 dimerization interface and is necessary for Golgi carrier fission (Valente et al., 2013; Valente
337 et al., 2012). The LPAAT δ activity of cell extracts was markedly suppressed by 14-3-3 γ
338 depletion (Figure 5A), while depletion of other 14-3-3 isoforms had no effect (Figure 5B and
339 see also Figure 5-figure supplement 1). Moreover, addition to cell extracts of a characterized
340 affinity-purified anti-14-3-3 γ antibody (Valente et al., 2012) also suppressed the LPAAT δ
341 activity (Figure 5C). These data indicate that 14-3-3 γ is required for LPAAT δ activity,
342 presumably because it stabilizes BARS in its monomeric fission-competent conformation.

343 In sum, a number of treatments based on BARS silencing or overexpression, or on the
344 use of BARS mutants as well as anti-BARS antibodies and inhibitors, or on manipulations of
345 the BARS-containing complex, stimulate or inhibit LPAAT δ activity and Golgi carrier fission
346 in completely parallel fashions. These results indicate a causal relationship between the
347 BARS-induced LPAAT δ activation and membrane fission. The stimulation of LPAAT δ by
348 BARS is very potent, and appears to occur rapidly, most likely via a physical interaction
349 between BARS and LPAAT δ during assembly of the BARS protein complex required for
350 carrier formation.

351

352 **The BARS-LPAAT δ interaction occurs at the Golgi complex in live cells**

353 The effects of BARS and LPAAT δ on the fission of carriers emanating from the Golgi
354 suggest that the BARS-LPAAT δ interaction occurs at this organelle. To confirm this notion
355 directly, we first re-examined the localization of BARS and of the other complex components,
356 14-3-3 γ and PI4KIII β at high resolution. Similar to LPAAT δ (Figure 1D,E), these proteins
357 were all seen to localize at the TGN (Figure 6A) as well as within the VSVG-containing
358 tubular carrier precursors that form during synchronized exit from the TGN (Figure 6B).
359 Secondly, we asked whether the interaction between BARS and LPAAT δ occurs *in vivo*, as
360 expected. To this end, we used a Förster resonance energy transfer (FRET) approach with
361 fluorescence lifetime imaging microscopy, which reveals the co-presence of donor and

362 acceptor fluorophores within the same complex at a distance of ≤ 8 nm. We expressed CFP-
363 LPAAT δ as the FRET donor, and BARS-YFP as the acceptor and monitored FRET. A FRET
364 signal was detected at the Golgi at steady state (Figure 6C) and markedly increased during a
365 VSVG traffic pulse (Figure 6C,D), consistent with the observation that BARS is recruited to
366 the Golgi during traffic (Valente et al., 2012). These results indicate that LPAAT δ is in
367 complex with BARS *in vivo*, and that it co-localizes at the TGN with BARS, 14-3-3 γ and
368 PI4KIII β , in agreement with the BARS–LPAAT δ co-precipitation data (Figure 1B,C).

369

370

371 Discussion

372 The main finding of this study is that BARS induces fission of post-Golgi basolateral carriers
373 by interacting with and activating LPAAT δ , a member of the acyl-transferase family that
374 converts LPA into PA; and hence, that the LPA-PA interconversion plays a role in BARS-
375 dependent fission.

376 Based on these results, we propose the following working model for basolateral carrier
377 formation: ARF initiates the process by recruiting and activating PI4KIII β at the Golgi. This
378 produces a local increase in phosphatidylinositol 4-phosphate (PtdIns4P) (Godi et al., 1999),
379 which supports the budding of tubular carrier precursors, most likely through recruitment of
380 PtdIns4P binding proteins (Valente et al., 2013). Carrier budding is assisted also by
381 phospholipase A₂ (PLA₂) via production of positively curved lysolipids, including LPA, which
382 facilitate the bending of membranes into tubules (Alonso et al., 2005; Bankaitis et al., 2012;
383 Bechler et al., 2012; Campelo and Malhotra, 2012; Ha et al., 2010; San Pietro et al., 2009;
384 Schmidt and Brown, 2009; Siddhanta et al., 2000; Yang et al., 2011). Concomitantly, BARS
385 and 14-3-3 γ assemble with PI4KIII β (possibly facilitated by their affinity for PtdIns4P) (Roth
386 et al., 1994; Yang et al., 2008), resulting in the binding of 14-3-3 γ to the dimerization surface
387 of BARS, and thus keeping BARS in a fission competent conformation (Valente et al., 2013;
388 Valente et al., 2012). BARS can then activate LPAAT δ at the TGN and in the elongating
389 tubular carrier precursors, where the PLA₂-generated LPA is converted into PA, leading to
390 fission.

391 LPA and PA possess biophysical properties that might be relevant for fission. PA is
392 endowed with a highly charged headgroup close to the glycerol backbone; a tendency to form
393 intramolecular and intermolecular hydrogen bonds and segregate into microdomains; the
394 ability to translocate across bilayers and induce fusion between interacting membranes,

395 possibly due to the formation of neutral complexes with cations and to headgroup dehydration
396 at a mildly acidic pH. Moreover, LPA and PA have strongly positive and negative
397 spontaneous curvatures, respectively (Faraudo and Travesset, 2007; Garidel et al., 1997;
398 Kooijman and Burger, 2009; Kooijman et al., 2005a; Kooijman et al., 2003; Kooijman et al.,
399 2005b; Kooijman et al., 2007); their interconversion is therefore likely to induce large shifts
400 in local membrane curvature. Additionally, PA microdomains might mediate the membrane
401 insertion of PA-binding proteins bearing amphipathic/ hydrophobic domains (Kooijman et al.,
402 2007; Stace and Ktistakis, 2006), which might be conducive to fission (Boucrot et al., 2012).
403 Notably, both BARS itself and ARF have been reported to bind PA and insert into membranes
404 (Manifava et al., 2001; Yang et al., 2008). These properties of LPA/PA can play a role in the
405 lipid rearrangements that lead to fission; moreover, further potential fission mechanisms
406 might relate to the property of PA to generate DAG (Asp et al., 2009; Baron and Malhotra,
407 2002; Fernandez-Ulibarri et al., 2007; Freyberg et al., 2003).

408 There is thus more than one way at this stage in which the LPA-PA interconversion
409 can be envisaged to induce membrane fission. The exact role of these lipids must now be
410 defined. Many of the key protein and lipid components involved in BARS-dependent fission
411 are available in pure form, and the possibility to reconstitute this fission pathway in artificial
412 membranes using known components appears to be within reach.

413
414
415
416
417
418
419
420
421
422
423
424
425
426
427
428

429

430 **Material and methods**

431

432 **Reagents**

433 Plasmids, chemicals and recombinant proteins: Human LPAAT cDNAs were from ImaGenes
434 GmbH (for subcloning and mutations, see Supplementary Table 1); BARS-pCDNA3, BARS-
435 YFP, BARS^{S147A}-YFP, BARS^{S147D}-YFP, and BARS^{D355A}-YFP were as previously described
436 (Bonazzi et al., 2005; Liberali et al., 2008; Valente et al., 2012); LDLRY18A-GFP was
437 provided by R. Polishchuk (TIGEM, Naples, Italy). CI-976 was from Tocris Bioscience,
438 tannic acid and BFA from Fluka, protease inhibitors as Complete Mini EDTA free from
439 Roche, cycloheximide, Protein A Sepharose and anti-FLAG M2 affinity gel antibody beads
440 from Sigma-Aldrich, oleoyl-LPA from Avanti Polar Lipids, oleoyl-1-(¹⁴C)-coenzymeA
441 (specific activity, 60 mCi/mmol) and dioleoyl-1-(¹⁴C) phosphatidic acid (specific activity, 140
442 mCi/mmol) from PerkinElmer, siRNAs from Dharmacon, and TRICH-labelled dextran and
443 FITC-labelled dextran from Molecular Probes. NAD⁺, BAC and HeLa (CD38+) cells were as
444 previously described (Colanzi et al., 2013). Ni-NTA agarose and glutathione Sepharose beads
445 were from Amersham, Protein A Gold was from Cell Microscopy Center (University Medical
446 Center Utrecht). Recombinant purified GST and GST-BARS proteins were prepared as
447 described previously (Valente et al., 2005), and His-plsC was from Cusabio.

448 Antibodies: All of the individually sourced antibodies for Western blotting,
449 immunofluorescence and the LPAAT assay were obtained as detailed in (Valente et al.,
450 2012), unless otherwise stated. The rabbit polyclonal anti-LPAAT δ antibody (for WB use)
451 was from Abcam; the mouse polyclonal anti-LPAAT δ antibody (for microinjection and
452 LPAAT assay use) was from Abnova; the rabbit polyclonal anti-LPAAT δ antibody (for IF
453 use) was from Sigma-Aldrich, and the anti-GM130 monoclonal antibody (for IF use) was
454 from BD Transduction Laboratories. The anti-LPAAT δ polyclonal antibodies from Abcam
455 and Abnova recognize specifically LPAAT δ and not other LPAATs by Western blot analysis
456 (our unpublished data).

457

458 **Immunoprecipitations and pull-downs**

459 COS7 cells in 10-cm Petri dishes were transiently transfected with 7 μ g of each DNA (BARS-
460 pCDNA3 and LPAATs-Flag) using 42 μ l TransIT-LT1 per dish. Twenty-four hours after
461 transfection, the cells were washed three times with phosphate-buffered saline (PBS) and
462 lysed using 1 ml lysis buffer/ dish (25 mM Tris, pH 7.4, 150 mM NaCl, 5 mM EDTA, 5 mM

463 MgCl₂, 10 mM NaF, 40 mM β-glycerophosphate, 1 mM Na₃VO₄, 1 mM dithiothreitol)
464 supplemented with 1% Triton X-100 and protease inhibitor mixture (30 min, 4 °C, shaking).
465 The lysates were centrifuged (13,000× g, 10 min, 4 °C), with the supernatants assayed for
466 protein concentration (Bradford assay) and used fresh.

467 For BARS immunoprecipitation, 500 μg lysate protein from these COS7 cells was
468 brought to 0.2% (v/v) Triton X-100 (final concentration), and incubated with 3 μg anti-BARS
469 polyclonal antibody (overnight, 4 °C, shaking) (Valente et al., 2005). Then 50 μl protein A
470 Sepharose beads were added for a further 1 h of incubation (4 °C, shaking). For LPAAT
471 immunoprecipitation, 1.2 mg lysate protein from the COS7 cells was brought to 0.2% (v/v)
472 Triton X-100 (final concentration), and incubated with 40 μl anti-FLAG M2 affinity-gel-
473 purified antibody (2 h, 4 °C, shaking). For BARS immunoprecipitation in the presence of
474 *Ec*LPAAT, 0.8 mg lysate protein from the COS7 cells was brought to 0.2% (v/v) Triton X-
475 100 (final concentration) and incubated with 160 μg purified *Ec*LPAAT (2 h, 4 °C, shaking),
476 and then incubated with 3 μg anti-BARS polyclonal antibody (overnight, 4 °C, shaking). The
477 immune complexes were collected by centrifugation (500× g, 5 min, 4 °C). After three
478 washes with lysis buffer with 0.2% Triton X-100, and twice with lysis buffer without Triton
479 X-100, the bound protein was eluted from the protein A Sepharose beads or from anti-FLAG
480 M2 affinity-gel-purified antibody by boiling (10 min) in 100 μl Laemmli buffer, separated by
481 10% SDS-PAGE, and subjected to Western blotting via transfer to nitrocellulose membranes
482 (Millipore).

483 The BARS immunoprecipitation from HeLa (CD38+) cells treated with BFA/NAD
484 was as described previously (Colanzi et al., 2013), with some modifications. The cells in 10-
485 cm Petri dishes were transiently transfected with plasmids using 42 μl TransIT-LT1 and 7 μg
486 of each DNA (BARS-YFP, LPAATδ-Flag) per dish. Sixteen hours after transfection, the cells
487 were treated with vehicle alone (DMSO) as a control or with 80 μg/ml BFA in the presence of
488 5 mM NAD₊ (2 h, 37 °C). The cells were then washed three times with PBS, lysed (see
489 above), and BARS immunoprecipitated (see above).

490 Histidine pull-down: His-BARS (20 μg) was incubated for 3 h at 37 °C with buffer alone (20
491 mM Tris, pH 7.4, 10 mM sucrose) or with 120 μM HPLC-purified BAC, to allow binding of
492 BAC to His-BARS. The reaction mixture was stopped on ice, and 1 mg lysate protein from
493 LPAATδ-Flag expressing cells was incubated with each sample (2 h, 4 °C, shaking). Then, 30
494 μl Ni-NTA agarose beads were added, and the samples were incubated (1 h, 4 °C, shaking).
495 The beads were then washed three times with lysis buffer at pH 8.0 supplemented with 0.2%
496 (v/v) Triton X-100 and 20 mM imidazole, by centrifugation (700× g, 5 min), and then twice

497 with lysis buffer at pH 8.0 without Triton X-100 but supplemented with 20 mM imidazole.
498 The bound protein was eluted from the Ni-NTA agarose beads by boiling (10 min) in 100 μ l
499 Laemmli buffer, separated by 10% SDS-PAGE, and subjected to Western blotting via transfer
500 to nitrocellulose membranes (Millipore).

501 GST pull-down: Three micrograms of *Ec*LPAAT were incubated with 3 μ g GST as control or
502 with 5 μ g GST-BARS in GST incubation buffer (20 mM Tris, pH 8.0, 1 mM EDTA, 0.2%
503 Triton X-100, 100 mM KCl) (overnight, 4 °C, shaking). Then, 30 μ l glutathione Sepharose
504 beads was added for a further incubation (1 h, 4 °C, shaking). The beads were then washed
505 five times with GST incubation buffer, by centrifugation (500 \times g, 5 min). The bound protein
506 was eluted from the glutathione Sepharose beads with GST elution buffer (100 mM Tris, pH
507 8.0, 20 mM glutathione, 5 mM dithiothreitol). The eluted proteins were separated by 10%
508 SDS-PAGE, and subjected to Western blotting via transfer to nitrocellulose membranes
509 (Millipore). For the GST pull-down with BAC-treated BARS, 5 μ g GST-BARS was initially
510 incubated with buffer alone (20 mM Tris, pH 7.4, 10 mM sucrose) or with 120 μ M HPLC-
511 purified BAC (Colanzi et al., 2013) (3 h, 37 °C), to allow binding of BAC to GST-BARS in
512 the GST incubation buffer. For the GST pull-down with NAD-treated BARS, 5 μ g GST-
513 BARS was initially incubated with 50 μ M NAD in GST incubation buffer (1 h, room
514 temperature).

515

516 **Transport protocols, microinjection, light and wide-field microscopies**

517 The *trans*-Golgi network (TGN)-exit assay for p75-GFP-transfected, VSVG-GFP-transfected,
518 and VSV-infected COS7 cells, microinjection, quantification of VSVG-containing post-Golgi
519 carriers, and quantification of the Golgi-exit of p75 were all carried out as reported
520 previously (Bonazzi et al., 2005; Valente et al., 2012). The COPI transport assay was
521 performed as previously described (Yang et al., 2005). The transport of the endocytosis-
522 defective LDL-GFP receptor (LDLrY18A) was performed as described previously (Giannotta
523 et al.). The CI-976 treatment was performed during the VSVG TGN-exit assay, at 50 μ M for
524 10 min, before the 32 °C temperature release block and during the 32 °C temperature release
525 block. The anti-LPAAT δ antibody (1 mg/ml) was microinjected 1 h after the beginning of the
526 20 °C incubation in the VSVG transport assay and after 1 h of recovery the cells were then
527 processed for wide-field microscopy. Wide-field microscopy was performed as described
528 previously (Valente et al., 2012), with some modifications. COS7 cells were transfected with
529 siRNAs for LPAAT δ (Smart Pool, Lipofectamine 2000), and after 48 h, the cells were

530 transfected with VSVG-CFP (overnight, 40 °C) and then incubated with 100 µg/ml
531 cycloheximide (3 h, 20 °C). The cells were then shifted to 32 °C (with continued
532 cycloheximide), and followed by fast videomicroscopy (see Valente et al., 2012). For CI-976
533 treatment, COS7 cells were treated with 50 µM CI-976 for 10 min before the shift to 32 °C.

534

535 **Fluorescence lifetime imaging microscopy measurements**

536 COS7 cells were transiently transfected with 0.5 µg BARS-YFP and 2 µg LPAATδ-CFP
537 using LIPO LTX, according to manufacturer instructions. Sixteen hours after transfection, the
538 cells were fixed at steady-state or subjected to the VSVG TGN-exit assay, and fixed after 2 h
539 at the 20 °C temperature block. The fluorescence lifetime imaging microscopy measurements
540 were performed as previously described (Valente et al., 2012).

541

542 **Electron microscopy**

543 HeLa cells were transiently transfected with 8 µg plasmid DNA encoding Flag-LPAATδ for
544 24 h (using TransIT-LT1). The cells were then processed for cryo-immunogold electron
545 microscopy, as described previously (Peters et al., 2006). For cryo-immunoelectron
546 microscopy, specimens were fixed, frozen, and cut using Leica EM FC7 ultramicrotome.
547 Cryo sections were double labeled for Golgin-97 (15 nm Gold particles) and anti- LPAATδ
548 (10 nm Gold particles). Electron microscopy images were acquired using FEI Tecnai-12
549 electron microscope.

550

551 **Transfections with siRNAs**

552 COS7 and HeLa cells were transfected with a non-targeting siRNA or with 150 nM of a
553 Smart Pool of *LPAATδ*/M-009283 or *LPAATγ*/M-008620 siRNAs, for 72 h (except for *BARS*
554 and *14-3-3s* siRNAs, where 100 nM of a Smart Pool was used for 48 h, as previously
555 described in (Valente et al., 2012)) using Lipofectamine 2000, according to manufacturer
556 instructions. The efficiency of interference was assessed by Western blotting. The treatment
557 with Smart Pool siRNAs for *LPAATγ* (M-008620) and for *LPAATδ* (M-009283) specifically
558 reduce the endogenous protein levels of *LPAATγ* and *LPAATδ* (by Western blotting)
559 respectively, without affecting the levels of other tested LPAATs (our unpublished data).
560 Alternatively, COS7 cells were transfected with the siRNAs (as above) in combination for the
561 last 16 h with VSVG-CFP, VSVG-GFP, VSVG-ts045-KDEL^R-myc, LDLR^{Y18A}-GFP or p75-
562 GFP, and then subjected to the specified Golgi-transport assay (Bonazzi et al., 2005;

563 Giannotta et al.; Valente et al., 2012). For the rescue experiments, COS7 cells were
564 transfected with siRNAs for LPAAT δ /D-009283-03 (5'-GCACACGGUUCACGGAGAA-3',
565 Dharmacon) for 48 h, and transfected for a further 24 h (using TransIT-LT1) with Flag-
566 LPAAT δ^{wt} or Flag-LPAAT δ^{H96V} (both encode an siRNA-resistant silent mutation), followed
567 by infection with VSV for the TGN-exit assay.

568

569 ***In-vitro* acyltransferase assay**

570 HeLa cells (1×10^6) in 10-cm Petri dishes were transiently transfected with 8 μ g plasmid DNA
571 encoding Flag-LPAAT δ^{wt} or Flag-LPAAT δ^{H96V} for 48 h (using TransIT-LT1). Alternatively,
572 the HeLa cells were transfected with siRNAs (as above) in combination with Flag-LPAAT δ^{wt}
573 for 48 h (using Lipofectamine 2000). The cells were washed three times with PBS, harvested
574 as 250 μ l/ dish in homogenisation buffer (100 mM Tris, pH 7.4, 5 mM NaCl, 3 mM MgCl₂)
575 supplemented with the protease inhibitor mixture, and homogenised (6 pulses, 30%
576 amplitude; Branson Digital Sonifier). The lysate was centrifuged at 600 \times g for 10 min at 4 $^{\circ}$ C.
577 Two micrograms of this post-nuclear supernatant fraction was incubated with the LPAAT
578 reaction buffer (75 mM Tris, pH 7.4, 4 mM MgCl₂, 1 mM dithiothreitol, 4 mM NaF, 1 mg/ml
579 bovine serum albumin fatty acid free, 50 μ M oleoylLPA, 20 μ M [¹⁴C]oleoylCoA) in a final
580 volume of 100 μ l for 20 min at 25 $^{\circ}$ C. The total lipids were extracted by adding 450 μ l cold
581 CHCl₃/CH₃OH (2:1). After 30 min on ice, the samples were centrifuged (10,000 \times g, 5 min).
582 The lower, organic, phase was dried under a stream of N₂, resuspended in 50 μ l CHCl₃, and
583 loaded onto an oxalate-pretreated TLC plate (Valente et al., 2005). The lipids were separated
584 by running the TLC plates with CHCl₃/ CH₃OH/ 33% NH₄OH/ H₂O (54:42:2.9:9.1; v/v/v/v).
585 The radiolabelled spots were quantified by gas ionisation counting (Beta-Imager Systems,
586 Biospace Laboratories). Dioleoyl (¹⁴C)-PA was used as the standard.

587 For CI-976 treatment, the post-nuclear fraction from HeLa cells was incubated with 50 μ M
588 CI-976 for 30 min at 25 $^{\circ}$ C, followed by the addition of the LPAAT reaction buffer (as
589 above). For anti-LPAAT δ antibody treatment, the post-nuclear fraction from HeLa cells was
590 incubated with 50 ng anti-LPAAT δ affinity-purified polyclonal antibody for 30 min at 25 $^{\circ}$ C,
591 followed by addition of the LPAAT reaction buffer (as above). For immunopurified BARS
592 treatment, the post-nuclear fraction from HeLa cells was incubated with 500 ng
593 immunoprecipitated BARS (purified from rat-brain cytosol with anti-BARS IgG crosslinked
594 matrice, as described in Valente et al., 2012, for 30 min at 25 $^{\circ}$ C, followed by addition of the
595 LPAAT reaction buffer (as above).

596 In these experiments LPAAT δ -dependent activity (or LPAAT δ activity) is defined as the
597 activity value of LPAAT δ overexpressing extracts minus the activity value of LPAAT δ
598 depleted (or antibody-treated) extracts (see also Figure 3a). In figures 3-5 the LPAAT δ -
599 independent activity (i.e, derived from LPAAT δ depleted or antibody-treated extracts) is
600 indicated with a dashed line. The LPAAT δ -independent activity was reproducibly 50% of the
601 total activity in LPAAT δ overexpressing extracts (as evaluated in more than 20 independent
602 experiments).

603

604

605 **Chromatographies**

606 Size-exclusion chromatography: For the fast protein liquid chromatography, 600 μ g purified
607 recombinant GST or GST-BARS was applied to a Sephacryl S-200 High Resolution HiPrep
608 16/60 (Amersham Pharmacia) gel filtration column equilibrated with PBS buffer (4 °C; flow
609 rate, 0.3 ml/min), with 1 ml fractions collected using an AKTA FPLC system. The eluted
610 protein was detected by monitoring absorbance at 280 nm, and 10 μ l of the collected fractions
611 were separated on 10% SDS-PAGE gels, and analysed by silver staining. Eighty microlitres
612 of each of these fractions was then subjected to the LPAAT assay.

613 Ion-exchange chromatography: For the fast protein liquid chromatography, 600 μ g purified
614 recombinant GST-BARS was applied to a MonoQ column (HR5/5 Pharmacia LKB)
615 equilibrated with buffer A (25 mM Tris, pH 8.00, 50 mM KCl) (4 °C; flow rate, 1 ml/min),
616 with 0.5 ml fractions collected using an AKTA FPLC system. After washing the MonoQ
617 column with buffer A, the protein was eluted with a 20 ml gradient of 0.05 M to 1 M KCl,
618 and 10 μ l of the collected fractions were separated on 10% SDS-PAGE gels, and analyzed by
619 silver staining. Eighty microlitres of each of these fractions was then subjected to the LPAAT
620 assay.

621

622 **Statistical analysis**

623 Two-tailed Student *t*-tests were applied to the data. Significance is indicated as **P* <0.05, ***P*
624 <0.01 and ****P* <0.005.

625

626

627

628

629 **Acknowledgments**

630 The authors would like to thank all colleagues who kindly provided them with antibodies and
631 reagents (as listed under `Reagents`); Dr. D. Barneda for very preliminary experiments, Dr
632 C.P. Berrie for editorial assistance; the BioImaging Facility at the Institute of Protein
633 Biochemistry and the Laboratory of Ultrastructure at the Italian Institute of Technology of
634 Naples, for support in imaging microscopy, data processing and analysis; the Italian
635 Association for Cancer Research (to D.C. IG4664 and IG10341, to A.L. IG4700), Telethon
636 Italia (to A.L. GGPO8231), grant FIT DM 24/09/2009 from MEF, projects PON01-00117 and
637 PON01-00862 from MIUR, and PNR-CNR Aging Program 2012-2014 and FaReBio di
638 Qualità, for financial support. A.P. and C.V. were recipients of Italian Foundation for Cancer
639 Research Fellowships (FIRC, Milan, Italy).

640

641

642 **Author Contributions**

643 A.P. and C.V. designed, carried out and analyzed all of the experiments. L.L.G. and G.L.
644 carried out immunofluorescence, immunoprecipitation and pull-down experiments. D.Circolo
645 carried out in-vitro acyltransferase assays and immunofluorescence experiments. G.T. carried
646 out in-vitro acyltransferase assays, immunofluorescence and electron microscopy
647 experiments. F.F. carried out FLIM experiments. R.S.P. carried out time-lapse microscopy.
648 C.V., D.Corda, and A.L. conceived and supervised the project, discussed and analyzed the
649 data and co-wrote the manuscript.

650

651

652

653

654

655

656

657

658

659

660

661

662

663 **References**

- 664 **Adolf F**, Herrmann A, Hellwig A, Beck R, Brugger B, Wieland FT. 2013. Scission of COPI
665 and COPII vesicles is independent of GTP hydrolysis. *Traffic* **14**:922-32.
- 666 **Alonso R**, Rodriguez MC, Pindado J, Merino E, Merida I, Izquierdo M. 2005. Diacylglycerol
667 kinase alpha regulates the secretion of lethal exosomes bearing Fas ligand during activation-
668 induced cell death of T lymphocytes. *J Biol Chem* **280**:28439-50.
- 669 **Asp L**, Kartberg F, Fernandez-Rodriguez J, Smedh M, Elsner M, Laporte F, Barcena M,
670 Jansen KA, Valentijn JA, Koster AJ, Bergeron JJ, Nilsson T. 2009. Early stages of Golgi
671 vesicle and tubule formation require diacylglycerol. *Mol Biol Cell* **20**:780-90.
- 672 **Bankaitis VA**, Garcia-Mata R, Mousley CJ. 2012. Golgi membrane dynamics and lipid
673 metabolism. *Curr Biol* **22**:R414-24.
- 674 **Baron CL**, Malhotra V. 2002. Role of diacylglycerol in PKD recruitment to the TGN and
675 protein transport to the plasma membrane. *Science* **295**:325-8.
- 676 **Bechler ME**, de Figueiredo P, Brown WJ. 2012. A PLA1-2 punch regulates the Golgi
677 complex. *Trends Cell Biol* **22**:116-24.
- 678 **Birts CN**, Nijjar SK, Mardle CA, Hoakwie F, Duriez PJ, Blaydes JP, Tavassoli A. 2013. A
679 cyclic peptide inhibitor of C-terminal binding protein dimerization links metabolism with
680 mitotic fidelity in breast cancer cells. *Chem. Sci.* **4**:3046-3057.
- 681 **Bonazzi M**, Spano S, Turacchio G, Cericola C, Valente C, Colanzi A, Kweon HS, Hsu VW,
682 Polishchuck EV, Polishchuck RS, Sallèse M, Pulvirenti T, Corda D, Luini A. 2005.
683 CtBP3/BARS drives membrane fission in dynamin-independent transport pathways. *Nat*
684 *Cell Biol* **7**:570-80.
- 685 **Boucrot E**, Pick A, Candere G, Liska N, Evergren E, McMahon HT, Kozlov MM. 2012.
686 Membrane fission is promoted by insertion of amphipathic helices and is restricted by
687 crescent BAR domains. *Cell* **149**:124-36.
- 688 **Campelo F**, Malhotra V. 2012. Membrane fission: the biogenesis of transport carriers. *Annu*
689 *Rev Biochem* **81**:407-27.
- 690 **Chambers K**, Judson B, Brown WJ. 2005. A unique lysophospholipid acyltransferase
691 (LPAT) antagonist, CI-976, affects secretory and endocytic membrane trafficking pathways.
692 *J Cell Sci* **118**:3061-71.
- 693 **Chen YQ**, Kuo MS, Li S, Bui HH, Peake DA, Sanders PE, Thibodeaux SJ, Chu S, Qian YW,
694 Zhao Y, Bredt DS, Moller DE, Konrad RJ, Beigneux AP, Young SG, Cao G. 2008.
695 AGPAT6 is a novel microsomal glycerol-3-phosphate acyltransferase. *J Biol Chem*
696 **283**:10048-57.

697 **Chinnadurai G.** 2009. The transcriptional corepressor CtBP: a foe of multiple tumor
698 suppressors. *Cancer Res* **69**:731-4.

699 **Colanzi A,** Grimaldi G, Catara G, Valente C, Cericola C, Liberali P, Ronci M, Lalioti VS,
700 Bruno A, Beccari AR, Urbani A, De Flora A, Nardini M, Bolognesi M, Luini A, Corda D.
701 2013. Molecular mechanism and functional role of brefeldin A-mediated ADP-ribosylation
702 of CtBP1/BARS. *Proc Natl Acad Sci U S A* **110**:9794-9.

703 **Colanzi A,** Hidalgo Carcedo C, Persico A, Cericola C, Turacchio G, Bonazzi M, Luini A,
704 Corda D. 2007. The Golgi mitotic checkpoint is controlled by BARS-dependent fission of
705 the Golgi ribbon into separate stacks in G2. *EMBO J* **26**:2465-76.

706 **Cole NB,** Ellenberg J, Song J, DiEuliis D, Lippincott-Schwartz J. 1998. Retrograde transport
707 of Golgi-localized proteins to the ER. *J Cell Biol* **140**:1-15.

708 **Coleman J.** 1992. Characterization of the Escherichia coli gene for 1-acyl-sn-glycerol-3-
709 phosphate acyltransferase (plsC). *Mol Gen Genet* **232**:295-303.

710 **Corda D,** Colanzi A, Luini A. 2006. The multiple activities of CtBP/BARS proteins: the
711 Golgi view. *Trends Cell Biol* **16**:167-73.

712 **Daumke O,** Roux A, Haucke V. 2014. BAR domain scaffolds in dynamin-mediated
713 membrane fission. *Cell* **156**:882-92.

714 **Drecktrah D,** Chambers K, Racoosin EL, Cluetz EB, Gucwa A, Jackson B, Brown WJ. 2003.
715 Inhibition of a Golgi complex lysophospholipid acyltransferase induces membrane tubule
716 formation and retrograde trafficking. *Mol Biol Cell* **14**:3459-69.

717 **Eto M,** Shindou H, Shimizu T. 2014. A novel lysophosphatidic acid acyltransferase enzyme
718 (LPAAT4) with a possible role for incorporating docosahexaenoic acid into brain
719 glycerophospholipids. *Biochem Biophys Res Commun* **443**:718-24.

720 **Faraudo J,** Travesset A. 2007. Phosphatidic acid domains in membranes: effect of divalent
721 counterions. *Biophys J* **92**:2806-18.

722 **Ferguson SM,** De Camilli P. 2012. Dynamin, a membrane-remodelling GTPase. *Nat Rev Mol*
723 *Cell Biol* **13**:75-88.

724 **Fernandez-Ulibarri I,** Vilella M, Lazaro-Dieguez F, Sarri E, Martinez SE, Jimenez N, Claro
725 E, Merida I, Burger KN, Egea G. 2007. Diacylglycerol is required for the formation of COPI
726 vesicles in the Golgi-to-ER transport pathway. *Mol Biol Cell* **18**:3250-63.

727 **Freyberg Z,** Siddhanta A, Shields D. 2003. "Slip, sliding away": phospholipase D and the
728 Golgi apparatus. *Trends Cell Biol* **13**:540-6.

729 **Gallop JL,** Butler PJ, McMahon HT. 2005. Endophilin and CtBP/BARS are not acyl
730 transferases in endocytosis or Golgi fission. *Nature* **438**:675-8.

731 **Garidel P**, Johann C, Blume A. 1997. Nonideal mixing and phase separation in
732 phosphatidylcholine-phosphatidic acid mixtures as a function of acyl chain length and pH.
733 *Biophys J* **72**:2196-210.

734 **Giannotta M**, Ruggiero C, Grossi M, Cancino J, Capitani M, Pulvirenti T, Consoli GM,
735 Geraci C, Fanelli F, Luini A, Sallese M. The KDEL receptor couples to Galphaq/11 to
736 activate Src kinases and regulate transport through the Golgi. *EMBO J* **31**:2869-81.

737 **Godi A**, Pertile P, Meyers R, Marra P, Di Tullio G, Iurisci C, Luini A, Corda D, De Matteis
738 MA. 1999. ARF mediates recruitment of PtdIns-4-OH kinase-beta and stimulates synthesis
739 of PtdIns(4,5)P2 on the Golgi complex. *Nat Cell Biol* **1**:280-7.

740 **Ha KD**, Clarke BA, Brown WJ. 2010. Regulation of the Golgi complex by phospholipid
741 remodeling enzymes. *Biochim Biophys Acta* **1821**:1078-88.

742 **Haga Y**, Miwa N, Jahangeer S, Okada T, Nakamura S. 2009. CtBP3/BARS is an activator of
743 phospholipase D1 necessary for agonist-induced macropinocytosis. *Embo J* **28**:1197-207.

744 **Hidalgo Carcedo C**, Bonazzi M, Spano S, Turacchio G, Colanzi A, Luini A, Corda D. 2004.
745 Mitotic Golgi partitioning is driven by the membrane-fissioning protein CtBP3/BARS.
746 *Science* **305**:93-6.

747 **Johannes L**, Mayor S. 2010. Induced domain formation in endocytic invagination, lipid
748 sorting, and scission. *Cell* **142**:507-10.

749 **Kooijman EE**, Burger KN. 2009. Biophysics and function of phosphatidic acid: a molecular
750 perspective. *Biochim Biophys Acta* **1791**:881-8.

751 **Kooijman EE**, Carter KM, van Laar EG, Chupin V, Burger KN, de Kruijff B. 2005a. What
752 makes the bioactive lipids phosphatidic acid and lysophosphatidic acid so special?
753 *Biochemistry* **44**:17007-15.

754 **Kooijman EE**, Chupin V, de Kruijff B, Burger KN. 2003. Modulation of membrane
755 curvature by phosphatidic acid and lysophosphatidic acid. *Traffic* **4**:162-74.

756 **Kooijman EE**, Chupin V, Fuller NL, Kozlov MM, de Kruijff B, Burger KN, Rand PR.
757 2005b. Spontaneous curvature of phosphatidic acid and lysophosphatidic acid. *Biochemistry*
758 **44**:2097-102.

759 **Kooijman EE**, Tieleman DP, Testerink C, Munnik T, Rijkers DT, Burger KN, de Kruijff B.
760 2007. An electrostatic/hydrogen bond switch as the basis for the specific interaction of
761 phosphatidic acid with proteins. *J Biol Chem* **282**:11356-64.

762 **Kozlov MM**, McMahon HT, Chernomordik LV. 2010. Protein-driven membrane stresses in
763 fusion and fission. *Trends Biochem Sci* **35**:699-706.

764 **Lee MC**, Orci L, Hamamoto S, Futai E, Ravazzola M, Schekman R. 2005. Sar1p N-terminal
765 helix initiates membrane curvature and completes the fission of a COPII vesicle. *Cell*
766 **122**:605-17.

767 **Lenz M**, Morlot S, Roux A. 2009. Mechanical requirements for membrane fission: common
768 facts from various examples. *FEBS Lett* **583**:3839-46.

769 **Leung DW**. 2001. The structure and functions of human lysophosphatidic acid
770 acyltransferases. *Front Biosci* **6**:D944-53.

771 **Lewin TM**, Wang P, Coleman RA. 1999. Analysis of amino acid motifs diagnostic for the sn-
772 glycerol-3-phosphate acyltransferase reaction. *Biochemistry* **38**:5764-71.

773 **Liberali P**, Kakkonen E, Turacchio G, Valente C, Spaar A, Perinetti G, Bockmann RA,
774 Corda D, Colanzi A, Marjomaki V, Luini A. 2008. The closure of Pak1-dependent
775 macropinosomes requires the phosphorylation of CtBP1/BARS. *Embo J* **27**:970-81.

776 **Manifava M**, Thuring JW, Lim ZY, Packman L, Holmes AB, Ktistakis NT. 2001.
777 Differential binding of traffic-related proteins to phosphatidic acid- or phosphatidylinositol
778 (4,5)- bisphosphate-coupled affinity reagents. *J Biol Chem* **276**:8987-94.

779 **Matter K**, Hunziker W, Mellman I. 1992. Basolateral sorting of LDL receptor in MDCK
780 cells: the cytoplasmic domain contains two tyrosine-dependent targeting determinants. *Cell*
781 **71**:741-53.

782 **McMahon HT**, Boucrot E. 2011. Molecular mechanism and physiological functions of
783 clathrin-mediated endocytosis. *Nat Rev Mol Cell Biol* **12**:517-33.

784 **Mironov AA**, Beznoussenko GV, Nicoziani P, Martella O, Trucco A, Kweon HS, Di
785 Giandomenico D, Polishchuk RS, Fusella A, Lupetti P, Berger EG, Geerts WJ, Koster AJ,
786 Burger KN, Luini A. 2001. Small cargo proteins and large aggregates can traverse the Golgi
787 by a common mechanism without leaving the lumen of cisternae. *J Cell Biol* **155**:1225-38.

788 **Nardini M**, Spano S, Cericola C, Pesce A, Massaro A, Millo E, Luini A, Corda D, Bolognesi
789 M. 2003. CtBP/BARS: a dual-function protein involved in transcription co-repression and
790 Golgi membrane fission. *Embo J* **22**:3122-30.

791 **Nardini M**, Valente C, Ricagno S, Luini A, Corda D, Bolognesi M. 2009. CtBP1/BARS
792 Gly172-->Glu mutant structure: impairing NAD(H)-binding and dimerization. *Biochem*
793 *Biophys Res Commun* **381**:70-4.

794 **Ovadi J**, Srere PA. 2000. Macromolecular compartmentation and channeling *Int. rev. Cytol.*
795 **192**:255-80.

796 **Peters JP**, Bos E, Griekspoor A. 2006. Cryo-Immunogold Electron microscopy editors.
797 Current Protocols in Cell Biology. John Wiley & Sons, inc.

798 **Polishchuk R**, Di Pentima A, Lippincott-Schwartz J. 2004. Delivery of raft-associated, GPI-
799 anchored proteins to the apical surface of polarized MDCK cells by a transcytotic pathway.
800 *Nat Cell Biol* **6**:297-307.

801 **Pucadyil TJ**, Schmid SL. 2010. Supported bilayers with excess membrane reservoir: a
802 template for reconstituting membrane budding and fission. *Biophys J* **99**:517-25.

803 **Roth D**, Morgan A, Martin H, Jones D, Martens GJ, Aitken A, Burgoyne RD. 1994.
804 Characterization of 14-3-3 proteins in adrenal chromaffin cells and demonstration of
805 isoform-specific phospholipid binding. *Biochem J* **301** (Pt 1):305-10.

806 **Roux A**. 2014. Reaching a consensus on the mechanism of dynamin? *F1000Prime Rep* **6**:86.

807 **San Pietro E**, Capestrano M, Polishchuk EV, DiPentima A, Trucco A, Zizza F, Mariggio S,
808 Pulvirenti T, Sallese M, Tete S, Mironov AA, Leslie CC, Corda D, Luini A, Polishchuk RS.
809 2009. Group IV phospholipase A(2)alpha controls the formation of inter-cisternal
810 continuities involved in intra-Golgi transport. *PLoS Biol* **7**:e1000194.

811 **Schmid SL**, Frolov VA. 2011. Dynamin: functional design of a membrane fission catalyst.
812 *Annu Rev Cell Dev Biol* **27**:79-105.

813 **Schmidt JA**, Brown WJ. 2009. Lysophosphatidic acid acyltransferase 3 regulates Golgi
814 complex structure and function. *J Cell Biol* **186**:211-8.

815 **Schwarz K**, Natarajan S, Kassas N, Vitale N, Schmitz F. The synaptic ribbon is a site of
816 phosphatidic acid generation in ribbon synapses. *J Neurosci* **31**:15996-6011.

817 **Shindou H**, Hishikawa D, Harayama T, Eto M, Shimizu T. 2013. Generation of membrane
818 diversity by lysophospholipid acyltransferases. *J Biochem* **154**:21-8.

819 **Shnyrova AV**, Bashkirov PV, Akimov SA, Pucadyil TJ, Zimmerberg J, Schmid SL, Frolov
820 VA. 2013. Geometric catalysis of membrane fission driven by flexible dynamin rings.
821 *Science* **339**:1433-6.

822 **Siddhanta A**, Backer JM, Shields D. 2000. Inhibition of phosphatidic acid synthesis alters the
823 structure of the Golgi apparatus and inhibits secretion in endocrine cells. *J Biol Chem*
824 **275**:12023-31.

825 **Spanò S**, Silletta MG, Colanzi A, Alberti S, Fiucci G, Valente C, Fusella A, Salmona M,
826 Mironov A, Luini A, Corda D. 1999. Molecular cloning and functional characterization of
827 brefeldin A-ADP-ribosylated substrate. A novel protein involved in the maintenance of the
828 Golgi structure. *J Biol Chem* **274**:17705-10.

829 **Stace CL**, Ktistakis NT. 2006. Phosphatidic acid- and phosphatidylserine-binding proteins.
830 *Biochim Biophys Acta* **1761**:913-26.

831 **Valente C**, Luini A, Corda D. 2013. Components of the CtBP1/BARS-dependent fission
832 machinery. *Histochem Cell Biol* **140**:407-21.

833 **Valente C**, Spano S, Luini A, Corda D. 2005. Purification and functional properties of the
834 membrane fissioning protein CtBP3/BARS. *Methods Enzymol* **404**:296-316.

835 **Valente C**, Turacchio G, Mariggio S, Pagliuso A, Gaibisso R, Di Tullio G, Santoro M,
836 Formiggini F, Spano S, Piccini D, Polishchuk RS, Colanzi A, Luini A, Corda D. 2012. A
837 14-3-3gamma dimer-based scaffold bridges CtBP1-S/BARS to PI(4)KIIIbeta to regulate
838 post-Golgi carrier formation. *Nat Cell Biol* **14**:343-54.

839 **Weigert R**, Silletta MG, Spano S, Turacchio G, Cericola C, Colanzi A, Senatore S, Mancini
840 R, Polishchuk EV, Salmona M, Facchiano F, Burger KN, Mironov A, Luini A, Corda D.
841 1999. CtBP/BARS induces fission of Golgi membranes by acylating lysophosphatidic acid.
842 *Nature* **402**:429-33.

843 **Yamashita A**, Hayashi Y, Matsumoto N, Nemoto-Sasaki Y, Oka S, Tanikawa T, Sugiura T.
844 2014. Glycerophosphate/Acylglycerophosphate acyltransferases. *Biology* **3**:801-30.

845 **Yang JS**, Gad H, Lee SY, Mironov A, Zhang L, Beznoussenko GV, Valente C, Turacchio G,
846 Bonsra AN, Du G, Baldanzi G, Graziani A, Bourgoin S, Frohman MA, Luini A, Hsu VW.
847 2008. A role for phosphatidic acid in COPI vesicle fission yields insights into Golgi
848 maintenance. *Nat Cell Biol* **10**:1146-53.

849 **Yang JS**, Lee SY, Spano S, Gad H, Zhang L, Nie Z, Bonazzi M, Corda D, Luini A, Hsu VW.
850 2005. A role for BARS at the fission step of COPI vesicle formation from Golgi membrane.
851 *EMBO J* **24**:4133-43.

852 **Yang JS**, Valente C, Polishchuk RS, Turacchio G, Layre E, Branch Moody D, Leslie CC,
853 Gelb MH, Brown WJ, Corda D, Luini A, Hsu VW. 2011. COPI acts in both vesicular and
854 tubular transport. *Nat Cell Biol* **13**:996-1003.

855 **Yang JS**, Zhang L, Lee SY, Gad H, Luini A, Hsu VW. 2006. Key components of the fission
856 machinery are interchangeable. *Nat Cell Biol* **8**:1376-82.

857 **Yeaman C**, Le Gall AH, Baldwin AN, Monlauzeur L, Le Bivic A, Rodriguez-Boulan E.
858 1997. The O-glycosylated stalk domain is required for apical sorting of neurotrophin
859 receptors in polarized MDCK cells. *J Cell Biol* **139**:929-40.

860 **Yuki K**, Shindou H, Hishikawa D, Shimizu T. 2009. Characterization of mouse
861 lysophosphatidic acid acyltransferase 3: an enzyme with dual functions in the testis. *J Lipid*
862 *Res* **50**:860-9.

Figure 1 Pagliuso et al.

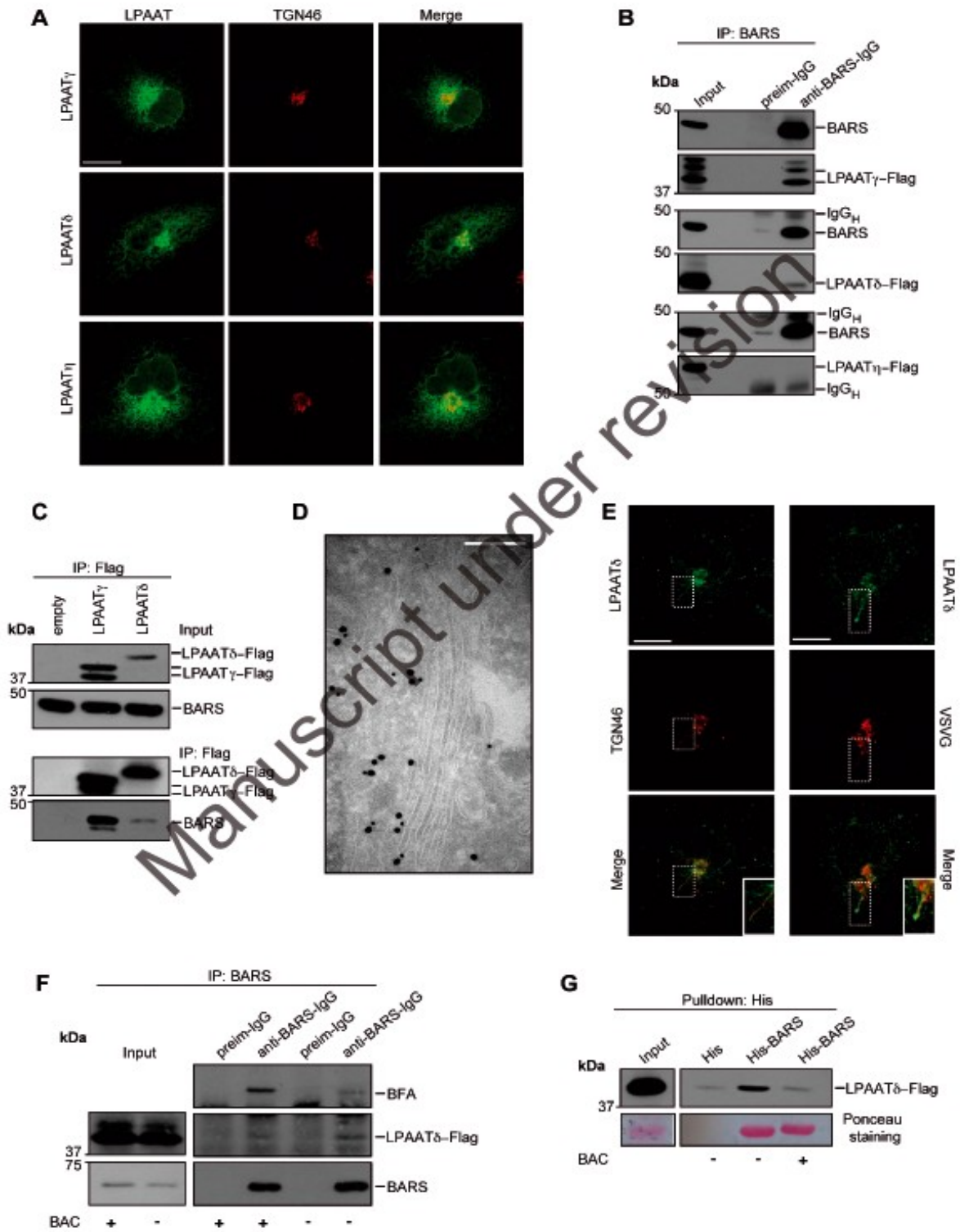


Figure 1. BARS interacts with the *trans*-Golgi localized LPAAT δ .

(A) Representative confocal microscopy images of COS7 cells transfected for Flag-tagged LPAAT γ , LPAAT δ and LPAAT η , and fixed and processed for immunofluorescence with a monoclonal anti-Flag antibody (green) and with a polyclonal anti-TGN46 antibody (red; as indicated). (B) BARS immunoprecipitation (IP:BARS) of lysate from COS7 cells co-expressing LPAAT γ -Flag, LPAAT δ -Flag or LPAAT η -Flag with BARS. Representative Western blotting (antibodies as indicated) of total lysate (input) and immunoprecipitated proteins with preimmune-IgG (preim-IgG) or anti-BARS-IgG (as indicated). IgG_H, IgG heavy chain. (C) Immunoprecipitation with an anti-Flag antibody (IP:Flag) of lysate from COS7 cells co-transfected with LPAAT γ -Flag, LPAAT δ -Flag or empty vector with BARS. Representative Western blotting of total lysate (input) and Flag-immunoprecipitated proteins with an anti-Flag monoclonal antibody or the anti-BARS polyclonal antibody (as indicated). (D) Representative electron microscopy image of HeLa cells transfected with Flag-tagged LPAAT δ for 24 h, and fixed and processed for cryo-immuno-electron microscopy with a monoclonal anti-Golgin-97 antibody (15 nm gold particles) and with a polyclonal anti-LPAAT δ antibody (10 nm gold particles). (E) Representative confocal microscopy images of COS7 cells at steady state (left) or VSV-infected and subjected to the VSVG TGN-exit assay (right). Cells were fixed and labelled with a monoclonal anti-LPAAT δ antibody (green) and with a polyclonal anti-TGN46 antibody (red; left) or a polyclonal anti-VSVG antibody (red; right). Inset, right: Magnification of tubular carrier precursors. (F) BARS immunoprecipitation (IP:BARS) of control or BFA/NAD₂-treated lysates (\pm BAC) from HeLa (CD38+) cells with preimmune-IgG (preim-IgG) or anti-BARS-IgG. Representative Western blotting with anti-BFA polyclonal and anti-Flag monoclonal antibodies of total lysate (input) and BARS-immunoprecipitated proteins. The anti-BFA analyzed blot (WB:BFA) was then reprobed with an anti-BARS monoclonal antibody (as indicated). (G) Histidine pull-down for His or His-BARS beads of lysates from COS7 cells transfected with LPAAT δ -Flag. Beads were treated with buffer alone (-) or with HPLC-purified BAC (BAC +), and then incubated with the lysates. The eluted proteins were analyzed by Western blotting using a monoclonal anti-Flag antibody (top), with the pulled-down His-BARS revealed by Ponceau staining (bottom). Molecular weight standards (kDa) in **B,C,F,G** are indicated on the left of each panel. Data are representative of three independent experiments. Scale bars: 10 μ m in **A,E**, 200 nm in **D**.

Figure 1 – figure supplement 1
Pagliuso et al.

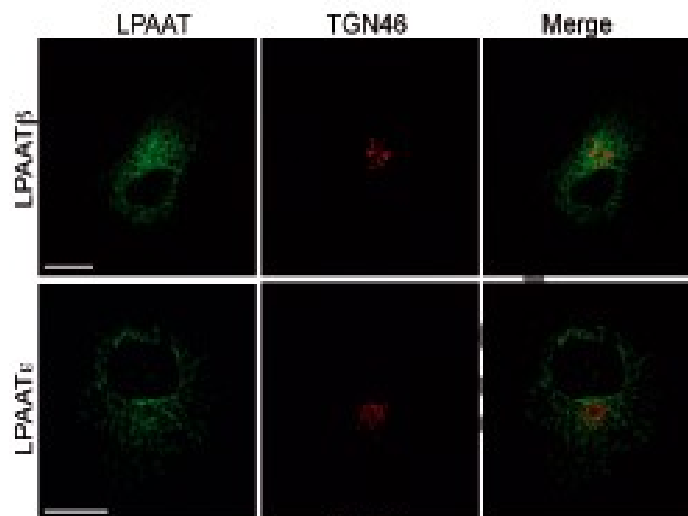


Figure 1-figure supplement 1. Localization of LPAAT β and LPAAT ϵ

Representative confocal microscopy images of COS7 cells transfected with Flag-tagged LPAAT β and LPAAT ϵ (as indicated) for 24 h, and fixed and processed for immunofluorescence with a monoclonal anti-Flag antibody (green; LPAAT) and with a polyclonal anti-TGN46 antibody (red; TGN). Scale bars: 10 μ m.

Manuscript under revision

Figure 1 – figure supplement 2
Pagliuso et al.

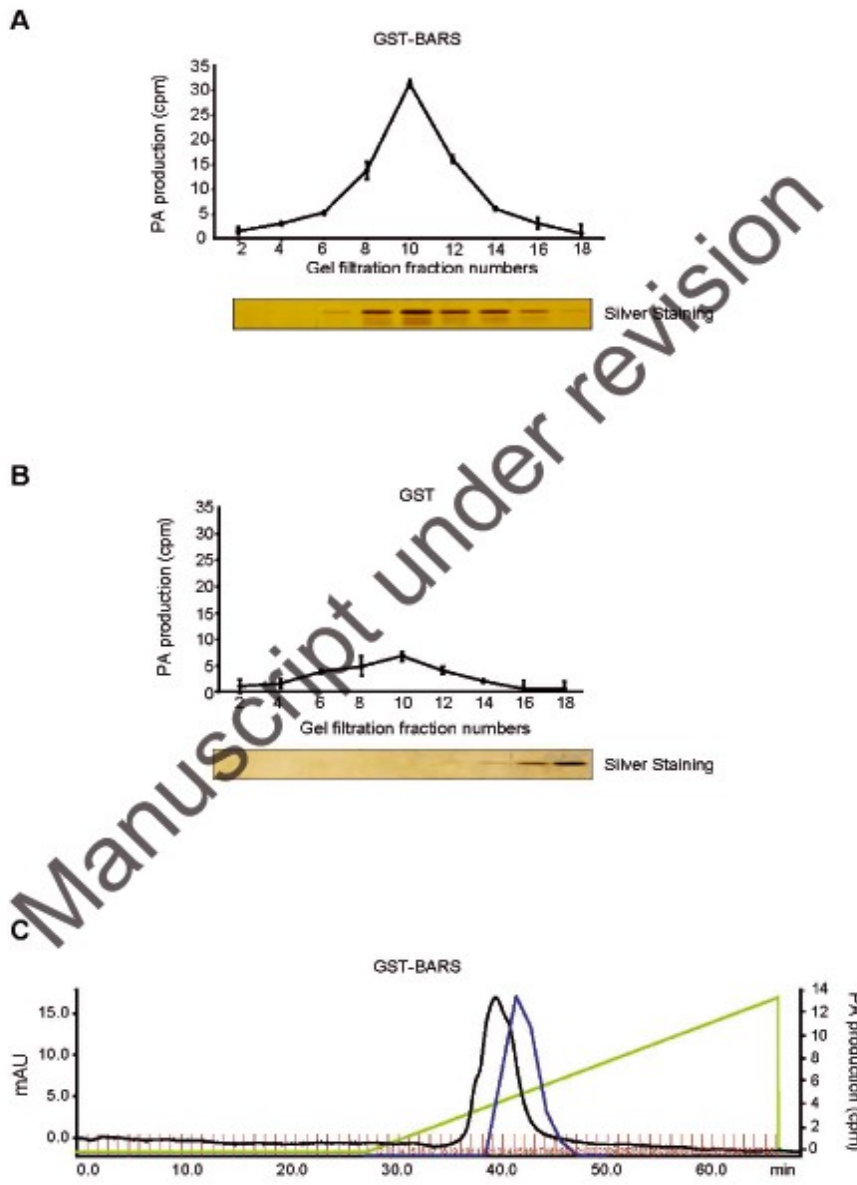


Figure 1-figure supplement 2. Purified recombinant BARS is associated with an LPAAT activity.

(A,B) Quantification of phosphatidic acid (PA) production in the LPAAT assay for purified recombinant GST-BARS in **A** and GST in **B** fractions (as indicated) with PBS elution from the size-exclusion chromatography column (Sephacryl S-200 column), at 0.3 ml/min at 4 °C. Aliquots of each fraction were subjected to the LPAAT assay and the production of PA was analyzed and quantified. Bottom: Silver staining analysis of the protein elution pattern of GST-BARS in **A** and GST in **B** in the fractions after size-exclusion chromatography. **(C)** Representative monoQ ion-exchange chromatography profiles of purified recombinant GST-BARS, monitoring absorbance at 280 nm (mAU; black line), as eluted with an NaCl gradient (green line). Aliquots of each fraction (as indicated in red) were subjected to the LPAAT assay, and the PA production is indicated by the blue line.

Manuscript under revision

Figure 1 – figure supplement 3
Pagliuso et al.

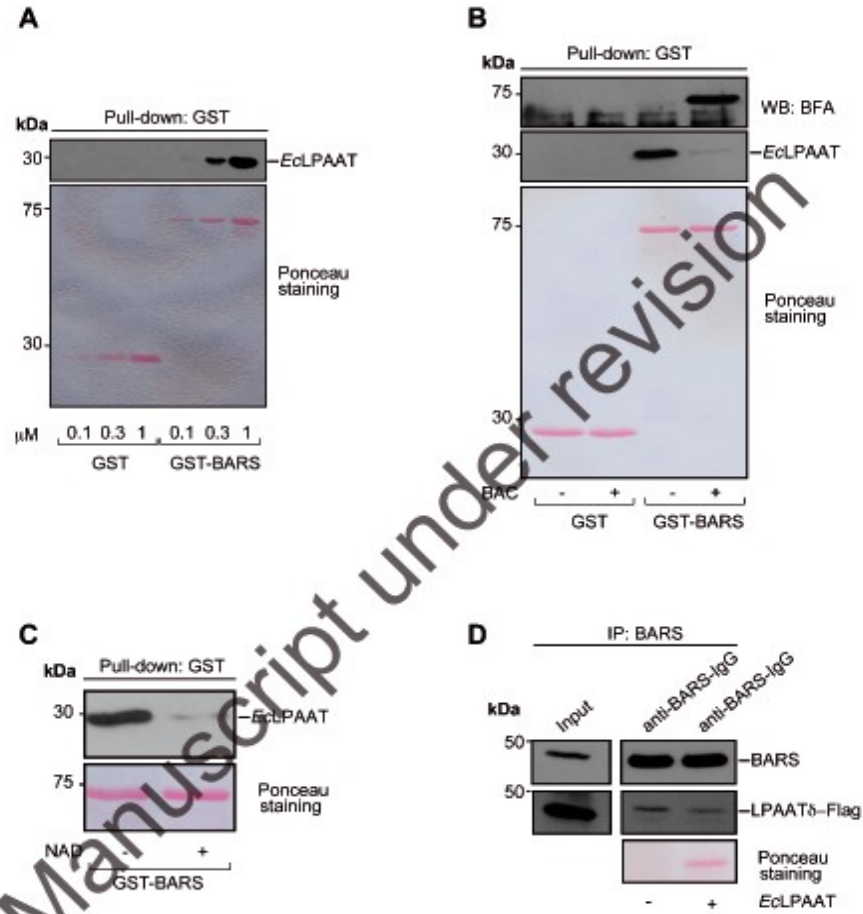


Figure 1-figure supplement 3. BARS binds *Escherichia coli* LPAAT in a conformation-dependent fashion.

Representative GST pull-down assays for GST and GST-BARS beads (as indicated). **(A)** Using recombinant His-tagged *E. coli* LPAAT (*EcLPAAT*). **(B)** Using buffer alone (-) or HPLC-purified BAC (BAC +), and then incubated with recombinant *EcLPAAT*. **(C)** Using buffer alone (-) or 50 mM NAD⁺ (NAD +), and then incubated with recombinant *EcLPAAT*. The eluted proteins were analysed by Western blotting (top) using an anti-histidine antibody to monitor *EcLPAAT* in **A-C**, and an anti-brefeldin A antibody (WB:BFA) to monitor ADP-rybosylation, in **B**. The pulled-down proteins were revealed by Ponceau-S staining (bottom). **(D)** Representative Western blotting with anti-BARS and anti-Flag antibodies for BARS immunoprecipitation (IP: BARS) of lysate from COS7 cells transfected with LPAAT δ -Flag in the absence (-) or presence (*EcLPAAT* +) of recombinant purified *EcLPAAT* with anti-BARS IgG. Total lysate (input) and BARS-immunoprecipitated protein are shown. Molecular weight standards (kDa) are indicated on the left of each panel.

Manuscript under revision

Figure 2 Pagliuso et al.

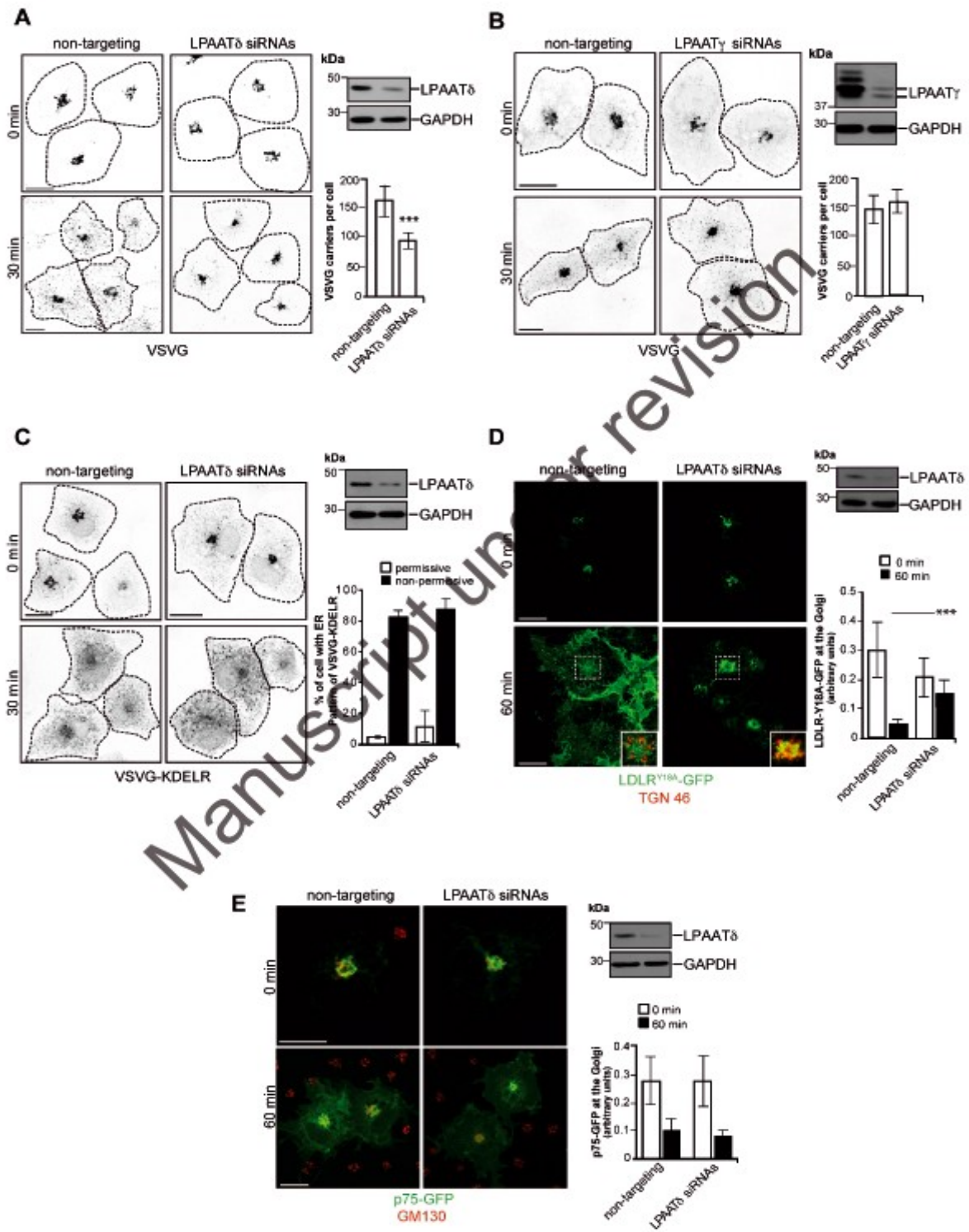


Figure 2. LPAAT δ is required for the fission of basolaterally directed carriers.

(**A,B**) Representative images of COS7 cells treated with non-targeting and *LPAAT δ* siRNAs in **A** or *LPAAT γ* siRNAs in **B** before VSV infection and the TGN-exit assay with 0.5% tannic acid. The cells were fixed following a 20 °C block (0 min) or 30 min after the shift to 32 °C, and stained for VSVG-positive post-Golgi carriers. Quantification of VSVG-containing carriers (right). (**C**) Representative images of COS7 cells treated with non-targeting and *LPAAT δ* siRNAs before co-transfected for the last 16 h with VSVG-ts045-KDEL-myc. The cells were then examined for the distribution of the chimeric KDEL by immunofluorescence microscopy following the shift to the non-permissive temperature for 30 min. Quantification of ER distribution of the chimeric KDEL (right). **A-C**, Dotted lines indicate cell borders. (**D,E**) Representative confocal microscopy of COS7 cells treated with non-targeting and *LPAAT δ* siRNAs and co-transfected for the last 16 h with the endocytosis-defective LDLR-GFP receptor (LDLR^{Y18A}-GFP, green) in **D**, or with a plasmid encoding p75-GFP (green) in **E**. (**D**) Following a 2 h at 20 °C transport block (0 min) and 60 min after the shift to the permissive temperature for transport (32 °C, with cycloheximide to inhibit protein synthesis), the cells were fixed and labelled with TGN46 (Golgi marker, red). Insets: Enlarged view of merged signals for the Golgi area. (**E**) Following the 3 h at 20 °C transport block (0 min) and 60 min after the shift to the permissive temperature for transport (32 °C; with cycloheximide), the cells were fixed and stained for GM130 (Golgi marker, red). (**D,E**) Quantification of LDLR^{Y18A}-GFP in **D** and p75-GFP in **E** in the Golgi area (right). (**A-E**) The efficiency of interference was monitored by Western blotting of the cell lysates using polyclonal anti-LPAAT δ in **A, C-E**, or polyclonal anti-LPAAT γ in **B** antibodies. Glyceraldehyde 3-phosphate dehydrogenase (GAPDH) is shown for the internal protein levels and molecular weight standards (kDa) are indicated on the left of each panel in **A-E**. Data are means \pm s.d. of three independent experiments. *** $P < 0.005$ (Student's *t*-tests). Scale bars, 10 μ m.

Figure 3

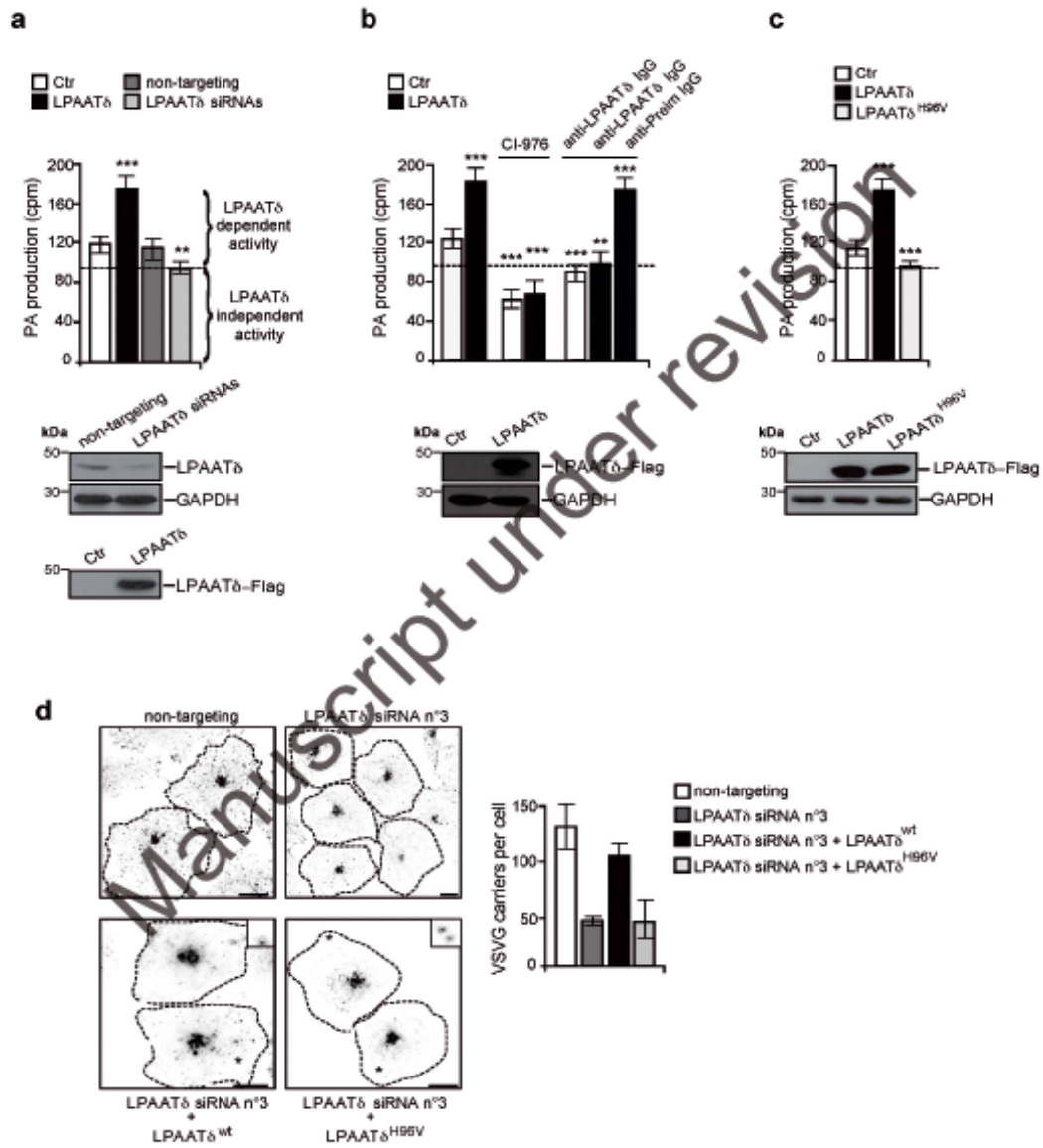


Figure 3. LPAAT δ is a canonical LPAAT and its activity is required for post-Golgi carrier formation.

(A) Quantification of phosphatidic acid (PA) production in the LPAAT assay for postnuclear supernatants from HeLa cells transfected for 48 h with an empty Flag-vector (Ctr) or with LPAAT δ -Flag (LPAAT δ), or for 72 h with non-targeting or LPAAT δ siRNAs. The parentheses indicate the LPAAT δ -dependent and independent activities, as defined under Methods. (B) Quantification as in A, with the post-nuclear fractions also incubated with 50 μ M CI-976, or polyclonal anti-LPAAT δ antibody (anti-LPAAT δ IgG), or anti-preimmune IgG (anti-Preim IgG; as control) for 30 min at 25 °C before LPAAT assay. (C) Quantification as in A, also in parallel with the LPAAT δ^{H96V} -Flag (LPAAT δ^{H96V}) catalytically inactive mutant. (A-C) The dashed line indicates the level of endogenous LPAAT activity not associated with LPAAT δ (see text for details). Bottom: representative Western blotting with an anti-Flag antibody, for the transfection efficiencies of these proteins used for the LPAAT assays. Glyceraldehyde 3-phosphate dehydrogenase (GAPDH) is shown for the internal protein levels. Molecular weight standards (kDa) in A-C, are indicated on the left of each panel. (D) Representative images of COS7 cells transfected with non-targeting or LPAAT δ siRNA (duplex 3; LPAAT δ siRNA n°3), and with LPAAT δ^{wt} -Flag or the LPAAT δ^{H96V} -Flag catalytically inactive mutant, and subjected to VSV infection and the TGN-exit assay with 0.5% tannic acid. The cells were fixed 30 min after the shift to the permissive temperature (32 °C) and processed for immunofluorescence with monoclonal anti-Flag and polyclonal anti-VSVG (p5D4) antibodies, to monitor formation of VSVG-containing carriers. Dotted lines show cell borders. Asterisks represent LPAAT δ^{wt} -Flag and LPAAT δ^{H96V} -Flag transfected cells (see insert for staining with anti-Flag antibody; bottom images). Scale bars, 10 μ m. Quantification of VSVG positive carriers (right). Data are means \pm s.d. of three independent experiments. ** $P < 0.01$, *** $P < 0.005$ versus control (Student's *t*-tests).

Figure 4 Pagliuso et al.

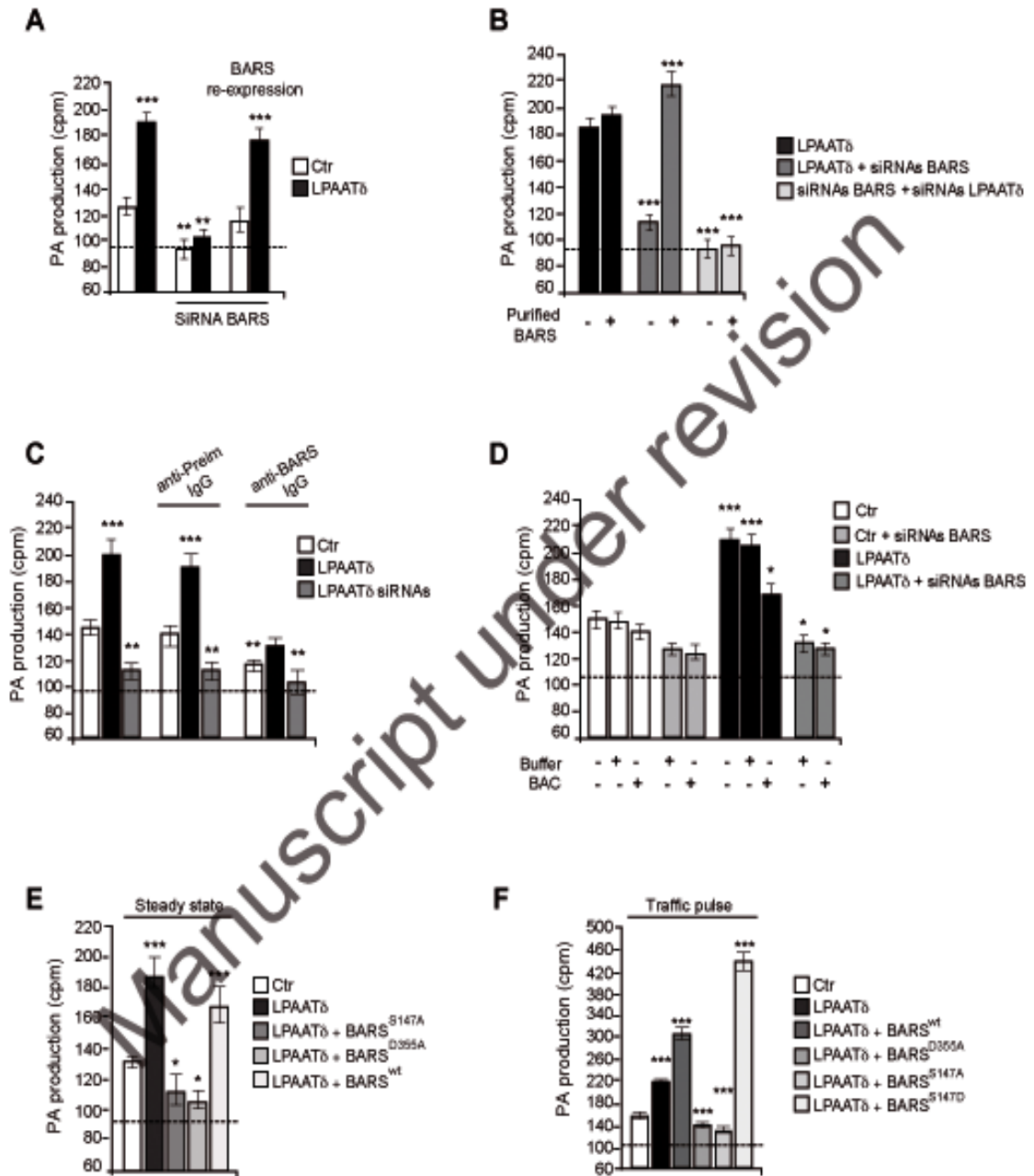


Figure 4. BARS activates LPAAT δ and this activation is required for post-Golgi carrier formation.

(A) Quantification of phosphatidic acid (PA) production in the LPAAT assay for postnuclear supernatants from HeLa cells transfected with empty Flag-vector (Ctr) or LPAAT δ -Flag (LPAAT δ) and with *BARS* siRNAs for 48 h, and with the last 12 h with siRNA-resistant replacement BARS-YFP encoding vector (BARS re-expression). (B) Quantification of phosphatidic acid (PA) production in the LPAAT assay for postnuclear supernatants from HeLa cells transfected with empty Flag-vector (Ctr) or LPAAT δ -Flag (LPAAT δ) and with *BARS* siRNAs and/or *LPAAT δ* siRNAs. Post-nuclear fractions were incubated with immunopurified BARS (Purified BARS) for 30 min at 25 °C before LPAAT assay (as indicated). (C) Quantification of phosphatidic acid (PA) production in the LPAAT assay for postnuclear supernatants from HeLa cells transfected with empty Flag-vector (Ctr) or LPAAT δ -Flag (LPAAT δ) for 48h or with *LPAAT δ* siRNAs for 72h. The anti-BARS polyclonal antibody (anti-BARS IgG) or anti-preimmune IgG (anti-Preim IgG, as control) were incubated with the indicated post-nuclear fraction for 30 min at 25 °C before LPAAT assay. (D) Quantification of phosphatidic acid (PA) production in the LPAAT assay for postnuclear supernatants from HeLa cells transfected with empty Flag-vector (Ctr) or LPAAT δ -Flag (LPAAT δ) and with *BARS* siRNAs for 48h. Post-nuclear fractions were incubated with HPLC-purified BAC (BAC +) or with buffer alone (Buffer -) for 30 min at 25 °C before LPAAT assay (as indicated). (E-F) Quantification of phosphatidic acid (PA) production in the LPAAT assay for postnuclear supernatants from HeLa cells transfected with: (E) empty Flag-vector (Ctr) or LPAAT δ -Flag (LPAAT δ) for 48h and the last 12h with BARS^{S147A}-YFP, BARS^{D355A}-YFP or BARS^{WT}-YFP (as indicated). (F) empty Flag-vector (Ctr) or LPAAT δ -Flag (LPAAT δ) for 48h and the last 12h with BARS^{WT}-YFP, BARS^{D355A}-YFP, BARS^{S147A}-YFP or BARS^{S147D}-YFP (as indicated). Cells were infected with VSV, subjected to TGN-exit assay and post-nuclear fractionations were prepared 10 min after the shift to 32 °C temperature release-block. The dashed line indicates the level of endogenous LPAAT activity not associated with LPAAT δ (see text for details). Data are means \pm s.d. of three independent experiments. * P < 0.05, ** P < 0.01, *** P < 0.005 versus control (Student's *t*-test). See Figure 4-figure supplement 1 for LPAAT δ and BARS (wild type and mutants) expression levels.

Figure 4 – figure supplement 1
Pagliuso et al.

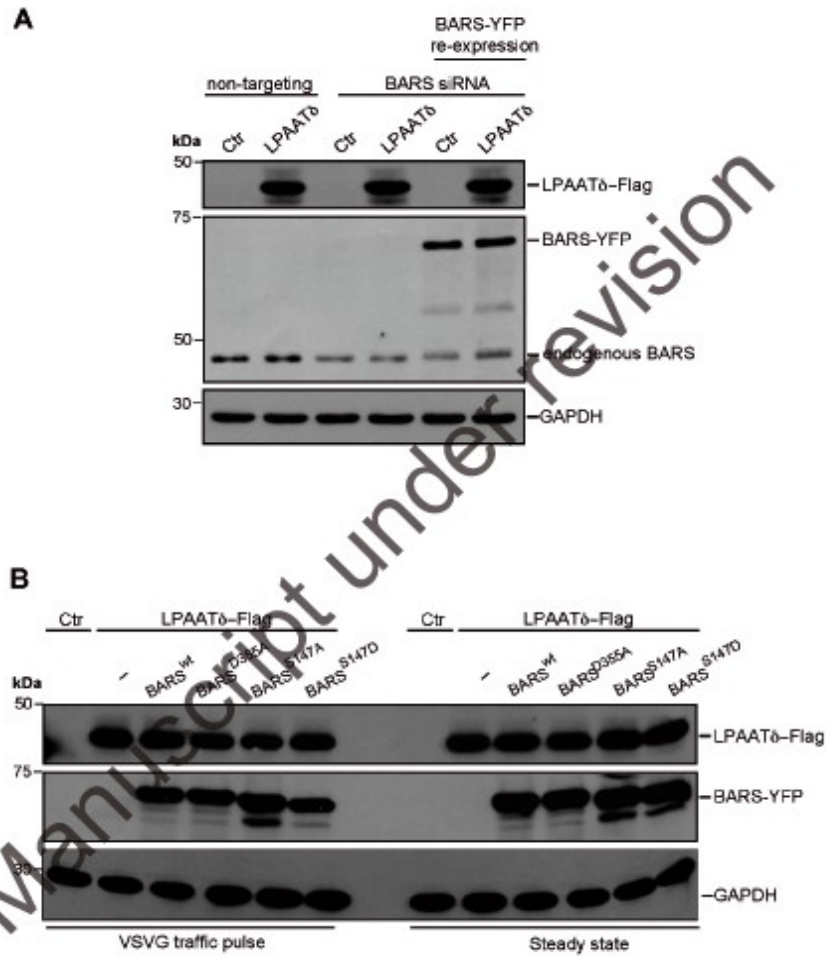


Figure 4-figure supplement 1. Depletion and overexpression of BARS in LPAAT δ -expressing HeLa cells.

(A) Representative Western blotting with anti-Flag, anti-BARS, and anti-GAPDH antibodies (as indicated) of HeLa cells transfected with empty Flag-vector (Ctr) or LPAAT δ -Flag (LPAAT δ) and with non-targeting (non-targeting) or *BARS* siRNA (duplex n°2) for 48 h, and with the last 12 h with a siRNA-resistant replacement BARS-YFP-encoding vector (BARS-YFP re-expression). (B) Representative Western blotting with anti-Flag, anti-BARS and anti-GAPDH antibodies (as indicated) of HeLa cells transfected with empty Flag-vector (Ctr) or LPAAT δ -Flag (LPAAT δ) for 48 h, and with the last 12 h with BARS^{wt}-YFP, BARS^{D355A}-YFP, BARS^{S147A}-YFP or BARS^{S147D}-YFP, at steady-state (right) or after a VSVG traffic pulse (left) (as indicated). Molecular weight standards (kDa) are indicated on the left of each panel.

Manuscript under revision

Figure 5 Pagliuso et al.

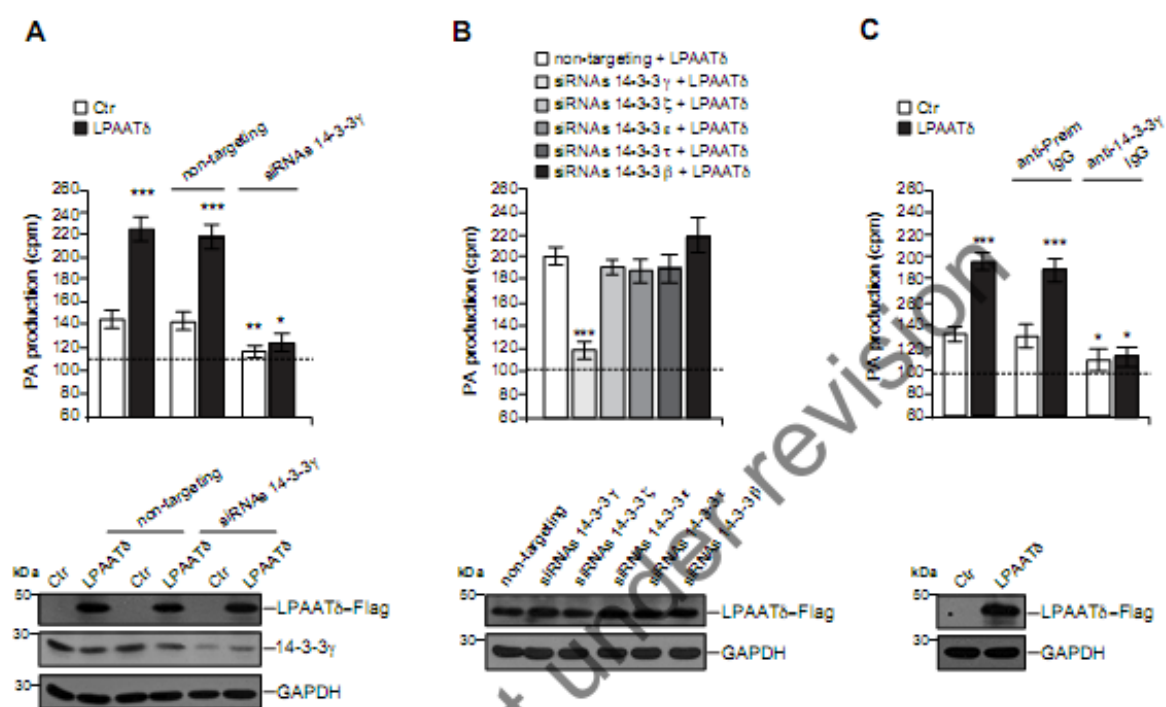
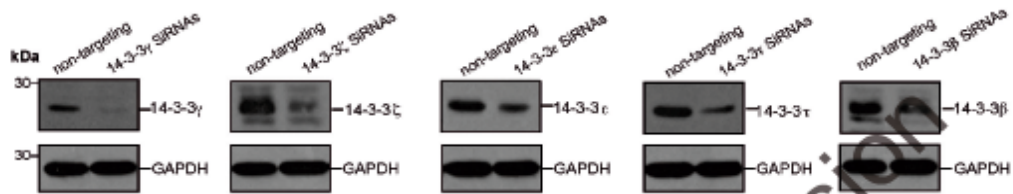


Figure 5. 14-3-3 γ , but not other 14-3-3 isoforms, is required for LPAAT δ activity.

(A-C) Quantification of phosphatidic acid (PA) production in the LPAAT assay for postnuclear supernatants from HeLa cells transfected with the empty Flag-vector (Ctr) or LPAAT δ -Flag (LPAAT δ) plus: (A) transfection with non-targeting siRNAs or 14-3-3 γ siRNAs for 48 h (as indicated); (B) transfection with 14-3-3 γ , ζ , ϵ , τ and β siRNAs for 48 h (as indicated); (C) treatment of the post-nuclear supernatant with an anti-14-3-3 γ polyclonal antibody (anti-14-3-3 γ IgG) or anti-preimmune IgG (anti-Preim IgG, as control) for 30 min at 25 °C before the LPAAT assay. (A-C) The dashed line indicates the level of endogenous LPAAT activity not associated with LPAAT δ (see text for details). Bottom: representative Western blotting with an anti-Flag antibody in A-C, and with an anti-14-3-3 γ monoclonal antibody in A to monitor the transfection of LPAAT δ and the depletion of 14-3-3 γ in the lysate used for LPAAT assay. Glyceraldehyde 3-phosphate dehydrogenase (GAPDH) is shown for the internal protein levels and molecular weight standards (kDa) are indicated on the left of each panel. Data are means \pm s.d. of three independent experiments. * P < 0.05; ** P < 0.01; *** P < 0.005 versus control (Student's t -tests). See Figure 5-figure supplement 1 for 14-3-3s expression levels.

Manuscript under revision

Figure 5 – figure supplement 1
Pagliuso et al.



Manuscript under revision

Figure 5-figure supplement 1. Depletion of 14-3-3s in LPAAT δ -expressing HeLa cells.

Representative immunoblotting of HeLa cells transfected with non-targeting siRNA or *14-3-3 γ* , ζ , ϵ , τ and β siRNAs (as indicated) for 48 h with isoform-specific 14-3-3 antibodies and an anti-GAPDH antibody (for internal protein levels). Note that the HeLa cells transfected with both non-targeting siRNA and *14-3-3s* siRNAs were co-transfected in combination with LPAAT δ -Flag. Representative Western blotting with an anti-Flag antibody is shown in Figure 5B.

Manuscript under revision

Figure 6 Pagliuso et al.

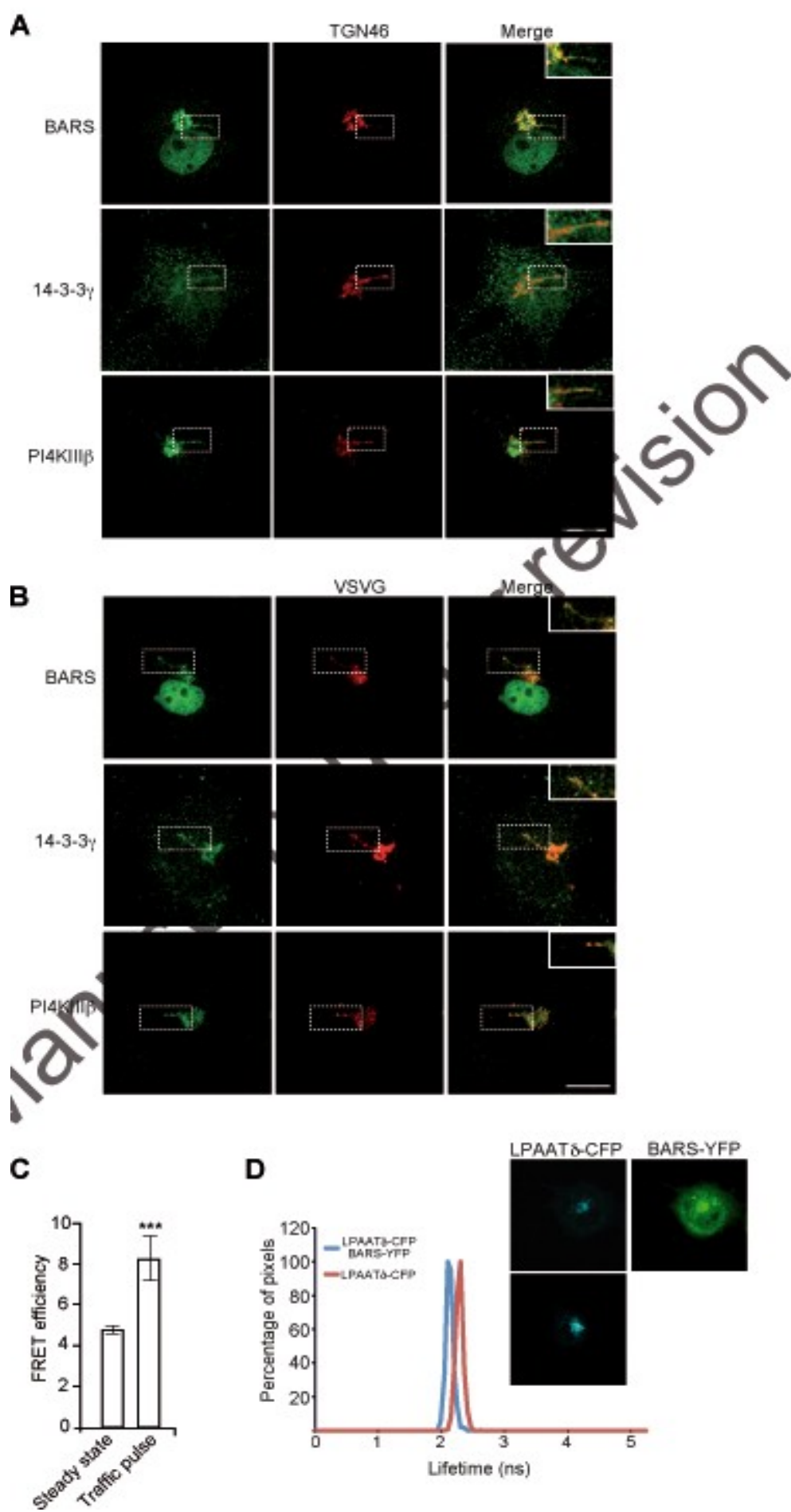


Figure 6. BARS colocalizes with 14-3-3 γ and PI4KIII β at the TGN and in carrier precursors, and interacts with LPAAT δ at the Golgi.

(A,B) Representative images of COS7 cells at steady state in **A**, or VSV-infected and subjected to the VSVG TGN-exit assay in **B**. The cells were fixed and labelled with polyclonal anti-BARS, anti-14-3-3 γ or anti-PI4KIII β (**A-B**; green) antibodies, and with an anti-TGN46 antibody (**A**; red) or a monoclonal anti-VSVG antibody (**B**; red). Insets, right: Magnification of the tubular carrier precursors in the Golgi area. Scale bars: 10 μ m in **A,B**. (**C,D**) FLIM-FRET of COS7 cells transfected with LPAAT δ -CFP and BARS-YFP. (**C**) Quantification of FLIM-FRET efficiency for the Golgi area at steady state and during a VSVG traffic pulse (as indicated). Data are means \pm s.d. ($n = 20$ cells/condition). *** $P < 0.005$ (Student's t -tests) *versus* steady state. (**D**) Distribution of fluorescence lifetimes measured in the Golgi area for LPAAT δ -CFP alone (red) and with BARS-YFP (blue). Co-expression of BARS-YFP produces a shift towards shorter lifetimes (hence indicating FRET between LPAAT δ -CFP and BARS-YFP). The average fluorescence lifetime of LPAAT δ -CFP was 2,31 ns for LPAAT δ -CFP alone, and 2,10 ns for LPAAT δ -CFP with BARS-YFP. Inset: Representative FLIM-FRET images of cells (top: LPAAT δ -CFP, blue; BARS-YFP, green; bottom: LPAAT δ -CFP alone, blue).

Manuscript under revision

TEMPLATE	OLIGONUCLEOTIDES	DIGESTIONS OF AMPLIFIED INSERTS	DESTINATION VECTOR
Human LPAAT β cDNA from Imagenes GmbH as the pOTB7 vector	5'-cggaaatc atggagctgtggcogtgtct-3' and 5'-gtggatccocctgggcoggtgcaogcc-3'	BamH1 and EcoR1	BamH1/EcoR1-digested p3xFLAG-CMV plasmid (SIGMA)
Human LPAAT γ cDNA from Imagenes GmbH as the pBluescriptR	5'-gtagaattcaccatgggactgtct-3' and 5'-cgcatatoccttctctttttcttaaacctcttggt-3'	EcoR1 and EcoR5	EcoR1/EcoR5-digested p3xFLAG-CMV plasmid (SIGMA)
Human LPAAT δ cDNA from Imagenes GmbH as the pOTB7 vector	5'-cggaaatc atggacctggcgggactg-3' and 5'-cgagatctggctcatcagttctgtctg-3'	EcoR1 and Bgl2	EcoR1/BamH1-digested p3xFLAG-CMV plasmid (SIGMA)
Human LPAAT ϵ cDNA from Imagenes GmbH as the pSPORT1 vector	5'-cggaaatc atgtgtgtgtccctggtg-3' and 5'-gtggatccctgctttaatagaaaccacag-3'	EcoR1 and BamH1	EcoR1/BamH1-digested p3xFLAG-CMV plasmid (SIGMA)
Human LPAAT ζ cDNA from Imagenes GmbH as the pOTB7 vector	5'-cggaaatc atgttccctgtctgctgcctttt-3' and 5'-cgagatctggagcggctcctgtcctt-3'	EcoR1 and Bgl2	EcoR1/BamH1-digested p3xFLAG-CMV plasmid (SIGMA)
Human LPAAT η cDNA from Imagenes GmbH as the pCMV-SPORT6 vector	5'-cggaaatc atgagccaggggaagtccgg-3' and 5'-cgagatctggctctcccttctgttgggt-3'	EcoR1 and Bgl2	EcoR1/Bgl2-digested p3xFLAG-CMV plasmid (SIGMA)

C-terminally Flag-tagged LPAAT δ encoding the silent mutation	5'- oatgattcaactgtgagggcaagaggttcaactgaaaagaagcat gagatcagca-3' and 5'- tgatgatotoatgotttttcaagtgaacotogtgcocotoaca gtgaatcagg-3'		
C-terminally Flag-tagged LPAAT δ^{S90V}	5'- goccatogtggttctcaaacgtcaagttgaaattgaottttotgt g-3' and 5'- cacagaaagtcatttcaaacotgacgttgagaaccacgatgg c-3'		
C-terminally Flag-tagged LPAAT δ^{S90V} encoding the silent mutation	5'- oatgattcaactgtgagggcaagaggttcaactgaaaagaagcat gagatcagca-3' and 5'- tgatgatotoatgotttttcaagtgaacotogtgcocotacaa gtgaatcagg-3'		
C-terminally CFP-tagged LPAAT δ	5'-cggaattcatggacctggcgggactg-3' 5'-ttaggtacctggtcattcagttctctctttg-3'	EcoRI-KpnI	EcoRI/KpnI-digested pECFPN1
N-terminally YFP-tagged BARS wt and mutants encoding the silent mutation	5'- tcaatgacttcacagtcacaacaaatgaggcaaggagccttct ggtga-3' and 5'- tcaccaggaaggctccttgcoctcaatttttgaactgtgaagtc attga-3'		

Table 1: List of the oligonucleotide sequences for amplification of the templates, and of the restriction enzymes used in the cloning of the listed expression vectors.

Manuscript under revision

Supplementary Videos

Video 1. Export of VSVG-GFP from the Golgi complex in COS7 cells following non-targeting siRNAs.

Following 48 h of non-targeting siRNAs treatment, COS7 cells were transfected for 24 h with VSVG-GFP, subjected to the TGN-exit assay, and observed at 32 °C *in vivo* under confocal microscopy. Several VSVG-GFP-containing carriers can be seen to be formed from the Golgi complex and to move across the cell toward the plasma membrane.

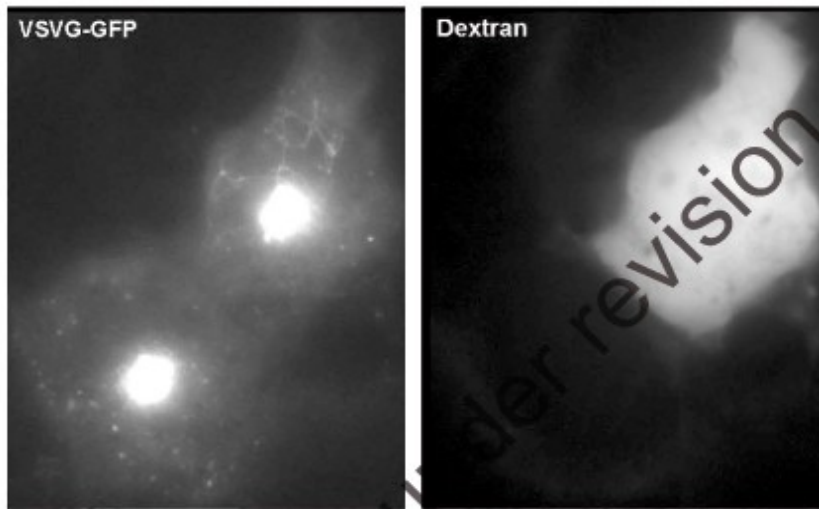
Video 2. Export of VSVG-GFP from the Golgi complex in COS7 cells following LPAAT δ -targeting siRNAs.

Following 48 h of LPAAT δ -targeting siRNAs treatment, COS7 cells were transfected for 24 h with VSVG-GFP, subjected to the TGN-exit assay, and observed at 32 °C *in vivo* under confocal microscopy. Several post-Golgi carrier precursors can be seen to extend from the Golgi complex, but they do not undergo fission, resulting in long tubular carrier precursors. The arrowheads indicate some VSVG-GFP-containing carriers with aberrantly extended tubular shapes.

Video 3. Post-Golgi carrier formation in VSVG-GFP expressing COS7 cells following anti-LPAAT δ antibody injection.

VSVG-GFP-expressing COS7 cells were subjected to the TGN-exit assay, and after 1 h at 20 °C the cells were microinjected with an anti-LPAAT δ antibody and incubated for a further 1 h at 20 °C. The cells were then observed at 32 °C *in vivo* under confocal microscopy. The microinjected cell shows long tubular carrier precursors (top right: indicated by the arrowhead; see also Video 3-figure supplement 1).

Video 3 – figure supplement 1
Pagliuso et al.



Video 3-figure supplement 1. Post-Golgi carrier formation in VSVG-GFP expressing COS7 cells following anti-LPAAT δ antibody injection.

Snapshot of Video 3 for post-Golgi carrier formation in VSVG-GFP-expressing COS7 cells (VSVG-GFP; left) after microinjection with an anti-LPAAT δ antibody mixed with TRICH-dextran (dextran; right).

Manuscript under revision

Video 4. Post-Golgi carrier formation in VSVG-GFP-expressing COS7 cells following CI-976 treatment.

VSVG-GFP-expressing COS7 cells were subjected to the TGN-exit assay and treated with the general LPAAT inhibitor CI-976 (50 μ M, 15 min) before the 32 °C temperature-block release. The cells were then observed *in vivo* under confocal microscopy. The CI-976 treatment dramatically reduces the fission of post-Golgi tubular carrier precursors, and increases the lengths of the fissioned post-Golgi carriers.

Manuscript under revision